DOE/ID/01523--T1

DE85 011780

# STABILITY ANALYSIS OF DIRECT CONTACT HEAT EXCHANGERS SUBJECT TO SYSTEM PERTURBATIONS

FINAL REPORT - TASK 2
U.S. Department of Energy
Contract DE-AS07-76ID0 1523
Modification A014

Submitted to:

Hydroelectric Project Manager
Advanced Technology Division
Idaho Operations Office
U.S. Department of Energy
550 Second Street
Idaho Falls, Idaho 83401

Submitted by:

Harold R. Jacobs, Ph.D., P.E.
Professor and Head
Department of Mechanical Engineering
The Pennsylvania State University
207 Mechanical Engineering Building
University Park, Pennsylvania 16802

## DISCLAIMER

## ABSTRACT

This report includes a project summary, copies of two papers resulting from the work and the Ph.D. Dissertation of Dr. Mehdi Golafshani entitled, "Stability of a Direct Contact Heat Exchanger". Specifically, the work deals with the operational stability of a spray column type heat exchanger subject to disturbances typical of those which can occur for geothermal applications. A computer program was developed to solve the one-dimensional transient two-phase flow problem and it was applied to the design of a spray column.

The operation and design of the East Mesa 500$Kw_e$ direct contactor was assessed. It is shown that the heat transfer is governed by the internal resistance of the dispersed phase. In fact, the performance is well-represented by diffusion of heat within the drops.

# SUMMARY

## i. Justification for Modeling Technique

The design of a direct contact heat exchanger prior to the present work was based entirely upon empirical correlations. These design methods predicted the size of heat exchanger necessary to meet given requirements for steady state operation; however, they could not be used to evaluate potential transient behavior.

In the use of direct contact heat exchangers for geothermal applications, one must be aware of potential destabilizing influences. Many geothermal fields are gassy and must be depressurized to release the dissolved gas. This is done in a flash tank. Thus, if the geothermal well burps a large amount of gas, it may be necessary to lower the delivery pressure. In addition, there may be variations in brine flow rate, brine temperature, etc., or even changes in working fluid conditions. It is possible that any of the above may have negative effects on the operation of the direct contactor which is run close to the flooding point at some location within the column. Thus, it is desirable to have a model to predict the column's transient behavior.

The solution of heat transfer problems for multiphase flows are extremely difficult. The prediction of the performance of a direct contact heat exchanger is no exception. In a direct contact heat exchanger operating without a phase change, one fluid is a continuous phase and the other immiscible fluid is a dispersed phase. Ideally, the two fluids flow in a counter-current manner due to a difference in density. However, due to difficulties in designing the continuous fluid injector large recirculation regions can occur. If the dispersed phase injector plate is large, there also may be a dead flow area above it. This dead flow region may result in a fraction of the total column volume where no heat transfer can take place. Ideally, however, one strives for counter-current flow. When the height to diameter ratio for a column exceeds eight, the literature indicates that recirculation regions are decreased. For geothermal applications, current practice has been to design systems fitting this length requirement. For situations where larger diameters are needed due to throughput requirements, it is possible to utilize internal vertical baffles so as to, in fact, maintain an equivalent 8:1 ratio to provide for the needed hydrodynamics.

At present, the state-of-the-art of solving problems of multiphase flow is such that two and three-dimensional problems cannot be solved unless the distributed phase merely travels along the streamlines for the continuous phase. While this is a reasonable assumption for modeling extremely small loading of the dispersed phase and is reasonable for co-current flows, it is not appropriate for counter-current flows. Thus, at present, counter-current, multi-dimensional, multiphase flow problems are intractable. This is especially true for high dispersed phase loadings.

Unfortunately, the problems we wish to consider, those of density driven multiphase flows are ones where the flow is counter current. Further, we wish to deal with high density loadings of the dispersed phase yet avoid flooding. (In this way, we can obtain close approach temperatures between the two streams.) For these situations, there can be a strong interaction between the flows of the two media. Thus, the problem is not tractable unless a super computer is used and the problem is posed in terms of Lagrangian coordinates. For these reasons, our problem of transient performance of a d.c.h.x. has not been dealt with previously. However, for geothermal applications, the length of the preheater is normally fairly long when using light organics such as isobutane, or pentane with moderate temperature brines. For this application, then, the assumption of a one-dimensional model should be reasonable.

## ii. Results

The two papers and thesis in the Appendix present the work carried out under this contract. The work has concentrated on the analysis of the preheater section of a spray column. Results are presented which are compared with experimental data from the $500KW_e$ facility at East Mesa.

In order to develop the transient model, it was important to understand the steady-state operation of a direct contact liquid-liquid spray column. Unfortunately, nearly all such work is based on empirical correlations to predict either volumetric heat transfer coefficients or heat transfer to single drops with the latter also being primarily empirical.

The best correlation to describe volumetric heat transfer coefficients for organic droplets in a continuous brine or water phase is that due to Plass, Jacobs and Boehm[1] which was developed under this contract. Heat transfer coefficients for single drops are described by Sideman in a survey article.[2] He presents the results for external heat transfer coefficients, and internal heat transfer coefficients for single drops as well as correlations for volumetric heat transfer coefficients for some of the data used for the P-J-B correlation.[1]

In carrying out the analyses reported in the Appendix, we studied situations where the drops were internally perfectly mixed and perfectly rigid as well as using the volumetric correlations of Reference 1. It was easily clear that the drops were not perfectly mixed, since then, the heat transfer should be well-represented by the heat transfer coefficient external to the drops. This drastically under-predicted the required heat exchanger length.

The heat transfer was reasonably well-represented by the early correlation developed in our laboratory. However, significant differences in the accuracy of predicting the experimental results from the East Mesa $500KW_e$ facility indicated that alternate means of describing the heat transfer needed to be examined.

When a liquid is injected from a nozzle into a second immiscible liquid the liquid can enter as either discrete drops or jets. The jets later break down to form drops. The drop diameters can vary depending upon the nozzle size and construction, the interfacial tension between the two liquids, the jet velocity, difference in the two fluids' densities, etc. The drops may remain spherical, be ellipsoidal or take on a hemispherical cap geometry. In designing a direct contact heat exchanger it is desirable for the drop shapes to be predictable. Thus, when designing the 500KW$_e$ d.c.h.x. for East Mesa, experiments were carried out to insure that the injector plate produced the type and size of drops for which they were designed. The experiments were carried out in the laboratory at the University of Utah using pentane and water. At the design flow conditions, pentane drops of 3.2 mm diameter ±10% were produced. These drops were spherical and showed no tendency toward wobbling. This is consistent with the behavior of drops with little or no internal circulation. However, it is inconsistent with the behavior predicted by the mapping of drop shape regimes presented by J. R. Grace[3] in his recent survey article on the hydrodynamics of liquid drops in immiscible liquids.

Grace's map is based on the work of Wairegi[4] and Bhagi and Weber.[5] Wairegi dealt with both liquid-liquid and gas-liquid systems whereas Bhagi and Weber studied only air bubbles in liquids. "The regimes are, of course, somewhat arbitrary because the transitions tend to be gradual, rather than sharp," states Grace. The regime map from Grace is shown in Figure 1. As can be seen the regime mapping depends upon the drop Reynolds number, $Re = \frac{\rho_c d_e U_D}{\mu_c}$ and the EoTmos number, $E_o = \frac{\Delta\rho g d_e^2}{\sigma}$ and the M-group, $M = \frac{g\mu_c^4 \Delta\rho}{\rho_c^2 \sigma^3}$.

For isobutane in water, $.6 \leq E_o \leq 1.1$, $500 \leq Re \leq 1500$ and log $M = 10^{-10}$ to $10^{-12}$. Thus, the map would indicate that the drops for the 500KW$_e$ facility would be in the wobbling ellipsoidal regime. However, our experiments indicated otherwise. Thus, one would expect that the map should not be taken to be exact as was indicated by Grace. Nonetheless, it is clear that slightly larger drops could well be in the wobbling regime as $E_o \propto d_e^2$.

The heat transfer model assuming transient conduction within the droplets and accounting for drop growth due to density changes gave very good agreement with the experimental data under all steady-state operating conditions. It was thus argued, heuristically, that the conduction heat transfer model of rigid drops should be used. It was this model that was, thus, used to carry out the stability analyses.

As examples, the stability analyses were carried out for typical operating conditions for the 500KW$_e$ facility at East Mesa. The results indicated that modest fluctuations in input conditions could cause the preheater length to change by as much as 1.1 meters

(3.5 ft.) and that the time constant for reaching a new steady-state was three minutes.

It is clear that if larger drop sizes had been generated in the $500KW_e$ facility that a shorter preheater length could have resulted and thus, a lower time constant. Larger circulating spheres not only would have reduced internal resistance to heat transfer, but could have reduced drag[3] resulting in a higher rise velocity. This would also reduce the response time to changes in operating parameters.

iii. Recommendations and Conclusions

The program developed in this work is readily altered to accept different drag coefficients and heat transfer models. Further studies are warranted to evaluate such models. In particular, studies should be carried out for ellipsoidal drops which are fluctuating. The hydrodynamics from Reference 3 and internal heat transfer coefficients from Reference 2 for fluctuating ellipsoidal drops could be used to ascertain the expected results. Such a study could result in an optimization of drop sizes. However, care would have to be taken as increasing the drop diameters could result in unstable behavior and enhance secondary circulations in the column itself. These, of course, could lead to degraded performance of the d.c.h.x.

Although the present work is not directly applicable to other types of direct contact heat exchangers, much of the work could be adapted. For example, the work is applicable to sieve tray towers directly only in terms of determining a drop heat transfer model. For drops of the same size range, the basic heat transfer model of a non-circulating drop should describe the heat transfer between trays. The hydrodynamics, of course, are different. Thus, for a sieve tray column, one would have to analyze the heat transfer in such a way as to depict the hydrodynamics. Such a device would be idealized as a cross-flow heat exchanger for each tray. The buildup of the dispersed phase below each tray would be modeled as an isothermal process above each heat transfer zone. Thus, a tray model composed of two parts could be made. One part would describe the heat transfer, the second a mass conservation to depict the mass buildup. This would have to be done for each tray. Such a model is being developed for the continuing work under Contract DE-AS07-84ID12552 at The Pennsylvania State University.

## REFERENCES

1. Plass, S. B., H. R. Jacobs, R. F. Boehm. "Operational Characteristics of a Spray Column Type Direct Contact Preheater." AIChE Symposium Series, No. 189, pp. 227-234 (1979).

2. Sideman, S. "Direct Contact Heat Transfer Between Immiscible Liquids." Advances in Chemical Engineering, Vol. 6, Academic Press, New York City, NY, pp. 207-286 (1966).

3. Grace, J. R. "Hydrodynamics of Liquid Drops in Immiscible Liquids." Handbook of Fluids in Motion, Chapter 38, Ann Arbor Science, The Butterworth Group, Ann Arbor, MI, pp. 1003-1025 (1983).

4. Wairegi, T. "The Mechanics of Large Drops in Immiscible Liquids." Ph.D. Thesis, McGill University, Montreal, Quebec (1974).

5. Bhagi, D. and M. E. Weber. "Bubbles in Viscous Liquids: Shapes, Wakes and Velocities." ASME Journal of Fluid Mechanics, 105, pp. 61-85 (1981).

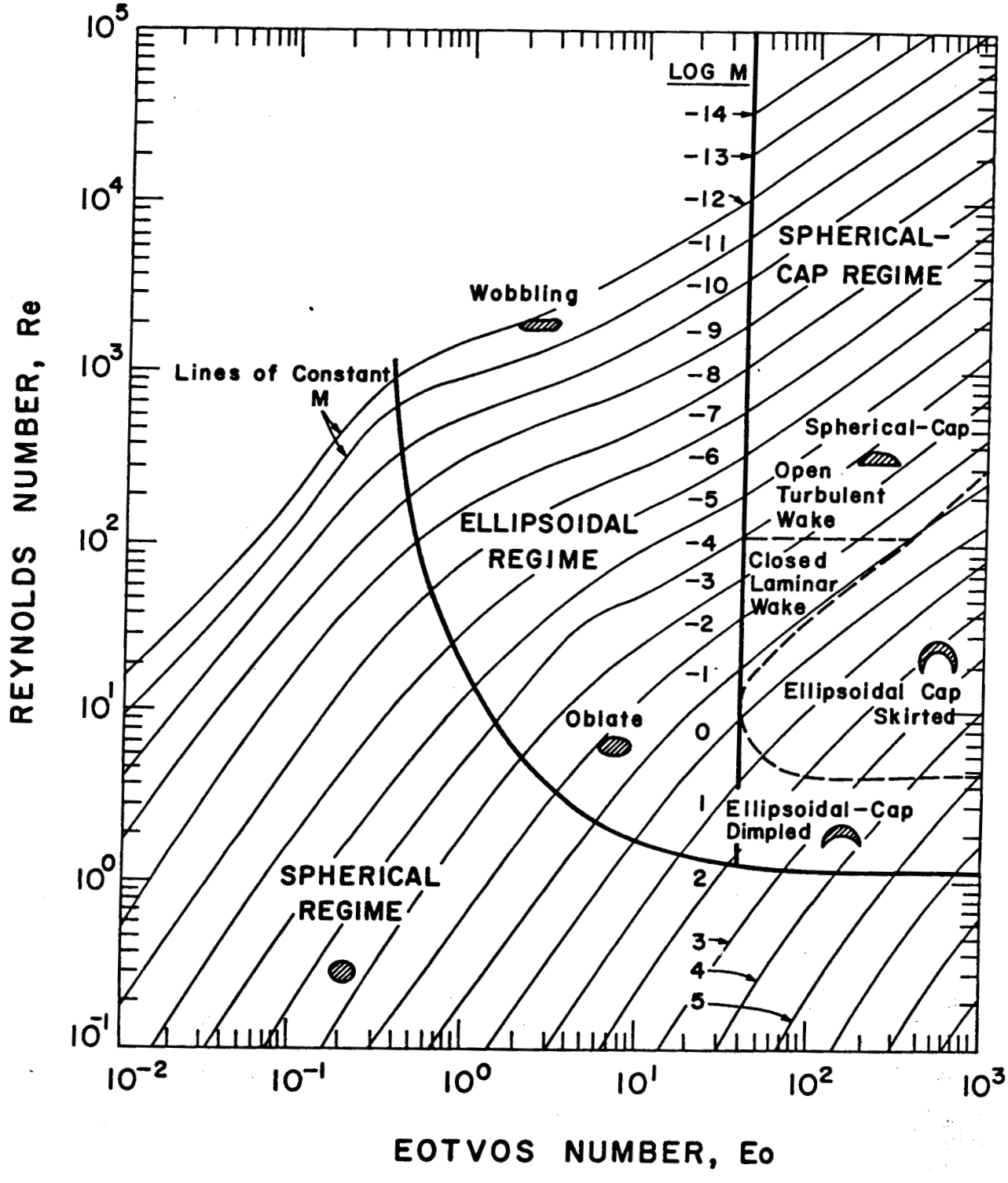


Figure 1. Regime plot for liquid drops and gas bubbles in free motion through an immiscible liquid. Curves are for constant values of M. Boundaries between the major regimes are shown as heavy black lines. Boundaries of subregimes are shown as dashed lines. (Taken from Reference 3.)

# A HEURISTIC EVALUATION OF THE GOVERNING MODE OF HEAT TRANSFER IN A LIQUID-LIQUID SPRAY COLUMN

Harold R. Jacobs
The Pennsylvania State University
Department of Mechanical Engineering
University Park, Pennsylvania

Mehdi Golafshani
Thiokol Corporation
Brigham City, Utah

## ABSTRACT

A steady state one-dimensional multi-phase flow model is developed to describe the characteristics of a spray column type direct contact liquid-liquid heat exchanger. Several models are assumed to describe the interphase heat exchange between water as the continuous phase and organic liquids as the dispersed phase. For small diameter droplets, it is shown that existing experimental data is best described by a model which assumes the heat transfer is controlled by conduction within the drops.

## NOMENCLATURE

| | |
|---|---|
| $C_D$ | Drag Coefficient |
| $C_p$ | Specific heat |
| G | Volumetric flow rate |
| g | Gravity |
| h | Enthalpy |
| $\bar{h}_m$ | Mean surface heat transfer coefficient |
| k | Thermal conductivity |
| $\bar{K}$ | Interphase friction factor |
| LMTD | Log mean temperature difference |
| m | Mass flow rate |
| $Nu_D$ | Average Surface Nusselt Number |
| $N_d$ | Number of droplets of dispersed phase |
| P | Pressure |
| Pr | Prandtl Number |
| Q | Heat transfer rate |
| r | Radial coordinate |
| $R_d$ | Radius of droplets |
| $Re_{D_C}$ | Reynolds number $\rho_c \mid (V_c - V_d) \mid D/\mu_c$ |
| t | Time |
| $t_1$ | Time for a droplet to rise through the column, $X/V_d$ |
| T | Temperature |
| $U_v$ | Volumetric heat transfer coefficient |
| V | Velocity in X direction |
| Vol | Volume |
| x | Vertical coordinate measured from the bottom of the column |
| $\phi$ | Holdup, fraction of volume occupied by the dispersed phase |
| $\rho$ | Density |
| $\mu$ | Dynamic viscosity |
| $\alpha$ | Thermal diffusivity |

Subscripts

| | |
|---|---|
| c | Continuous phase |
| d | Disperse phase |
| i | At the interface between the droplets and continuous phase |
| o | At entrance conditions |

## INTRODUCTION

Direct contact heat exchangers of the spray column type have many potential uses in industry.

Among them is the extraction of heat from low temperature sources such as geothermal brines. Since the 1960's, a number of investigators have proposed correlations to predict the volumetric heat transfer rate in such devices.

Spray column liquid-liquid heat exchanger experiments have been conducted in laboratory scale equipment for the following fluids as the dispersed phase with water as the continuous phase: benzene[1], toluene[2], $CCl_4$[3], Shell Oil A and spray base and kerosene[4], mercury[5], isobutane[6], hexane[7], R-113 and insulating oil[8] and also pentane in recent design studies carried out at the University of Utah. Defining a volumetric heat transfer coefficient as

$$U_v = \frac{Q/Vol}{LMTD} \qquad (1)$$

several different correlations have been proposed based on moderate temperature changes and overall column heat transfer. These correlations for $U_v$ have generally been written as a function of holdup, $\phi$, and the ratio of the volumetric flow rates of the dispersed and continuous phases, $G_D/G_C$.[1,4,8] In many of the experiments the actual holdup was not measured, but was instead calculated based on drop size, and relative bouyancy as well as flow rates and ratios for a given column.[9] This was due to the difficulty in making actual holdup measurements.

Garwin and Smith[1] presented two correlations for their experiments for benzene dispersed in water. For the benzene being heated their data showed

$$U_v = 1.09 \times 10^4 \phi \ \frac{Btu}{hrft^3\ °F} \qquad (2)$$

and for benzene being cooled

$$U_v = 1.67 \times 10^4 \phi \ \frac{Btu}{hrft^3\ °F} \qquad (3)$$

However, their experiments were conducted with two different size drops. For the benzene being heated the drops were 7.34 mm in diameter and for the benzene being cooled the diameter of the drops was 6.71 mm. Rosenthal's[2] data for toluene shows a similar trend. Rosenthal used two different orifice diameters for his injection plates, 7.2 mm and 3 mm. Higher heat transfer was achieved with the smaller drops.

Woodward's[4] data for Shell Oil A, spray base and kerosene was accumulated for a single volumetric flow ratio, $G_D/G_C = 2.5$ and a single drop size, 3.5 mm. For this condition, the data correlates as

$$U_v = 1.2 \times 10^4 \phi \ \frac{Btu}{hrft^3\ °F} \qquad (4)$$

In 1979, a research team at the University of Utah carried out a study of liquid-liquid heat transfer characteristics of a 6' x 6" diameter spray column using water as the continuous phase and insulating oil as the dispersed phase.[8] An orifice plate was chosen which yielded 3.5 - 4.0 mm diameter drops. Data was acquired for very small holdups up to near the flooding limit. Using their data and all of the existing data for organic liquids, they arrived at the following correlations

$$U_v = 1.2 \times 10^4 \phi \ \frac{Btu}{hrft^3\ °F} \qquad (5)$$

$$(\text{for } \phi < 0.05)$$

and

$$U_v = [4.5 \times 10^4 (\phi - 0.05) e^{-0.57 G_D/G_C} + 600] \ \frac{Btu}{hrft^3\ °F} \qquad (6)$$

$$(\text{for } \phi > 0.05)$$

The above correlations yielded conservative results and appeared to be accurate to within ±20% not only for those organic fluids lighter than water, but also for the data for R-113 which is 1.4 times as heavy as water. No attempt was made to use the correlations for the existing liquid metal-water system.[5]

Attempts to rationalize the organic liquid data on the basis of single drop studies even for low hold-up proved unsuccessful, thus Letan and Kehat[10] tried to develop a model based upon hydrodynamic observations in a glass column. They pointed out that when a drop is first released it undergoes a wake forming phase, then a wake shedding phase and finally an agglomeration phase at the top of the column where the drops coalesce. Since it is generally necessary to have a tall column in order to prevent back mixing[9] the heat transfer is generally dominated by the wake-shedding regime. If this were true, Letan and Kehat argued that a constant value of $U_v$ would be achieved through most of the column. This would, it appeared, justify the use of experimentally determined $U_v$ correlations.

In 1980, Barber-Nichols Engineering, under U.S. Department of Energy funding, began construction of a direct contact geothermal demonstration power plant at East Mesa, California. The direct contact heat exchanger for this system was designed by the first author. The column (see Figure 1) combined a boiler section at the top of the column with a liquid-liquid preheater section. Isobutane was injected at the bottom of the column as the dispersed phase and the geothermal brine at the top. For operation at 90% of flooding with a pinch point temperature of 5°F (2.8°C), Eq. (6) indicated a preheater (liquid-liquid) length of about 22 feet (6.7 m) above the isobutane distributor plate assuming 3.5 mm diameter drops. The nature of the potential drop behavior was studied using a small distributor plate in a glass column with normal pentane as the working fluid instead of isobutane. This was done so that the experiments could be conducted near atmospheric pressure. Drops of 3.2 mm diameter ±0.2 mm were formed. They maintained a nearly spherical shape with no fluctuation or oscillation which is contrary to the empirical curve of J. R. Grace.[11] The column was successfully operated over a 2.5 year period. However, temperature profiles measured in the preheater section appeared to be anomalous from that expected for a constant value of $U_v$.

In order to gain some insight into the operational characteristics of the East Mesa Column, the largest spray column yet constructed, the U.S. Department of Energy funded the present authors to

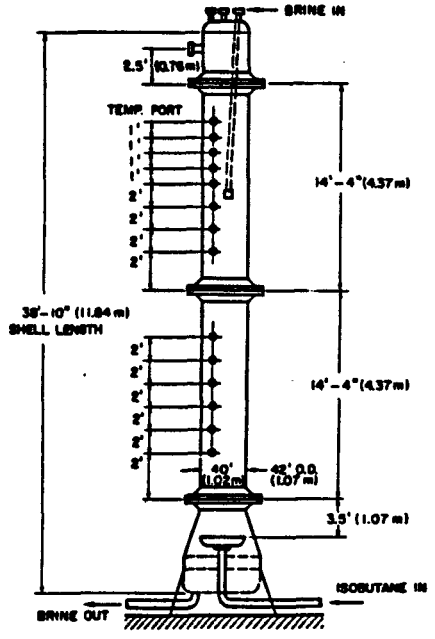


Figure 1. Schematic of 500KW$_e$ direct contact heat exchanger.

carry out the study described herein. In this paper, we concentrate on the preheater section of the column. Rather than using the simple correlation equations that have normally been used for design for both the hydrodynamics and heat transfer we have formulated the problem in terms of the basic conservation equations for multiphase flows. We then investigate several models for the interphase heat transfer.

## MATHEMATICAL MODELING

In a spray column, where the column diameter is very much larger than the droplet size, and if the continuous phase does not have significant recirculation zones, the flow can be assumed to be effectively one dimensional.

Assuming steady state, the one dimensional continuity equations for the continuous phase and dispersed phase are respectively,

$$\frac{d}{dx}\left((1-\phi)\rho_c V_c\right) = 0 \tag{7}$$

and

$$\frac{d}{dx}\left(\phi\rho_d V_d\right) = 0 \tag{8}$$

The conservation of momentum equations for a two-component system of immiscible fluids can be written in terms of the conservation of momentum of one fluid and for the mixture as a whole. Thus, we have for the dispersed phase

$$\frac{d}{dx}\left(\phi\rho_d V_d^2\right) = -\phi\frac{dP}{dx} - \bar{K}(V_c - V_d) - \phi\rho_d g \tag{9}$$

and for the mixture as a whole

$$\frac{d}{dx}\left((1-\phi)\rho_c V_c^2\right) + \frac{d}{dx}\left(\phi\rho_d V_d^2\right) = -\frac{d}{dx} - \left((1-\phi)\rho_c + \phi\rho_d\right)g \tag{10}$$

where $\bar{K}$ is the interphase friction factor. Note that the interphase friction factor does not occur in the mixture equation as it acts with equal magnitude but opposite direction on each of the two phases.

The energy equation for the droplets is

$$\frac{d}{dx}\left(\phi\rho_d V_d h_d\right) = -Qi/Vol \tag{11}$$

and for the mixture

$$\frac{d}{dx}\left((1-\phi)\rho_c V_c h_c\right) + \frac{d}{dx}\left(\phi\rho_d V_d h_d\right) = 0 \tag{12}$$

where $Q_i$ is the rate of interfacial heat transfer per unit volume. As was the case for the interfacial friction, no interfacial heat transfer term occurs in the mixture equation.

The set of differential equations given in Eqs. (7-12) has to be solved in conjuction with observance of variables represented by algebraic relations. The density and temperature for each fluid must be represented by an equation of state written in terms of that fluid's enthalpy and pressure.[12,13]

The interfacial friction factor, $\bar{K}$, may be written as

$$\bar{K} = N_d \pi R_d^2 C_d \, 1/2\rho_c \left| V_d - V_c \right| \tag{13}$$

where the number of droplets per unit volume, $N_d$, is

$$N_d = \frac{\phi}{\frac{4\pi}{3} R_d^3} \tag{14}$$

Substituting Eq. (13) into Eq. (14) yields

$$\bar{K} = \frac{3\phi}{8R_d} C_D \rho_c \left| V_d - V_c \right| \tag{15}$$

The drag coefficient, $C_D$, is in general a function of the Reynolds number of the droplet, which in turn is a function of the droplet radius, kinematic viscosity of the continuous phase and the relative velocity between phases. However, in the present analysis, the drag coefficient can be assumed to be of a constant value of 0.4 which is approximately valid for a droplet Reynolds number in the range of $10^3$ - $10^5$. This range is typical of that calculated for the rise of hydrocarbon liquid droplets in water or geothermal brine.

There are several ways of establishing the interfacial heat transfer per unit volume, $Q_i$/Vol. Utilizing the concept of a volumetric heat transfer coefficient, $U_v$, we could write

$$\frac{Q_i}{Vol} = U_v(T_d - T_c) \tag{16}$$

in Eq. (11). In so doing, we would be able to utilize any of the correlations found in the literature. The correlations most representative of all existing data are those given in Eqs. (5) and (6). As these correlations were not based on actually measured values of holdup, but rather on empirical correlation, we could use that correlation instead of the calculated values of $\phi$ from the governing equations.

A third possible way to evaluate $U_v$ is to assume that the heat transfer to the working fluid droplets is controlled by the convective heat transfer outside of the drop. This is essentially the same as assuming no internal to the drop resistance to heat transfer. (While this may be accurate for liquid metal drops, organic liquids such as refrigerants, oils or hydrocarbons normally have very low thermal conductivity, and thus, such an assumption is suspect.) If we were to use such a model, Sideman[14] recommends the following correlation for the surface heat transfer coefficient $\bar{h}$.

$$\bar{Nu}_D = 2.0 + 0.6\ Re_{D_C}^{1/2}\ Pr_{D_C}^{1/3} \tag{17}$$

The relationship between $U_v$ and $\bar{h}_m$ can be shown to be

$$U_v = 4N_d\ \pi\ R_d^2 \bar{h}_m \tag{18}$$

A final method for establishing $Q_i/Vol$ which we will consider for establishing the mechanism of heat transfer between the phases is to assume that the outside heat transfer coefficient is large and that the heat transfer inside the drop is the controlling mechanism. Since the droplets remain spherical as noted earlier, the internal circulation should be small. For such fluids as refrigerants and hydrocarbons which are notoriously poor conductors, a small radius could well cause conduction to dominate at $Re_{D_C}$ above 500. (Note: This would require only a small shift in the boundary of the empirical curves of Grace[11] which are used to define drop behavior.) In order to facilitate the use of this idea, one could use the one-dimensional transient spherical conduction equation with a time dependent boundary condition. This equation is

$$\frac{\partial(\rho C_p T)_d}{\partial t_1} = \frac{1}{r^2}\ \frac{\partial r^2 k_d \frac{\partial T}{\partial r}}{\partial r} \tag{19}$$

Here $t_1$ is defined as the elapsed time from the point of origin to x which is equal to $x/V_d$. The associated initial and boundary conditions are

$$\begin{aligned} &T_d = T_{do} \text{ at } t_1 = 0 \\ &T_d \text{ is finite at } r = 0 \\ &\text{and} \quad T_d = T_c \text{ at } r = R_d \end{aligned} \tag{20}$$

$T_{do}$ is the temperature of the droplets at the injection point.

In order to solve Eq. (19) subject to the conditions given in Eq. (20), one may assume two differential approaches. If $\rho_d$, $Cp_d$ and $k_d$ do not change significantly there would result an analytical solution for the mean temperature of the droplet utilizing the Duhammel superposition integral

$$T_{dm}(t_1) = T_{do} + \frac{6\alpha_d}{R_d^2}\left(\sum_{n=1}^{\infty} e^{\frac{-\alpha_d n^2 t_1}{Rd^2}}\right) \cdot \left(\int_0^{t_1} e^{\frac{\alpha_d n^2 \pi^2 s}{R_d^2}} (T_c - T_{do})ds\right) \tag{21}$$

Obtaining the solution of Eq. (19) in this manner precludes the solution of Eq. (11). However, Eq. (19) must be solved subject to simultaneously satisfying Eqs. (7, 8, 9, 10, and 12).

If the integration is done along sufficiently small steps in time, $t_1$, then $T_c$ could be considered constant during each of these intervals and the resulting expression for $T_{dm}$ would be

$$T_{dm} = T_{do} + \frac{\partial}{\pi^2}\ \sum_{n=1}^{\infty} \frac{1}{n^2}\ e^{\frac{-\alpha_d n^2 \pi^2 t_1}{Rd^2}}\ \sum_{t=1}^{M} (T_c - T_{do}) \left(e^{\frac{\alpha_d n^2 \pi^2}{R_d^2}} (\Delta t_i - \Delta t_{i-1})\right), \tag{22}$$

where $\Delta t$ = time step equal to $\Delta x/V_w$ and M = number of time steps to reach time $t_1$.

The second method for solving Eq. (19) subject to the conditions of Eq. (20) is to account for the change of the dispersed phase properties $\rho_d$, $Cp_d$ and $k_d$ as the droplet traverses the height of the column. When this is required due to a density change, then the droplet radius also changes.

$$R_d = R_{d_o} \left(\frac{\rho_{do}}{\rho_d}\right)^{1/3} \tag{23}$$

The change in radius leads to changes in drag, holdup, and phase velocity along the length of the column resulting in a computationally much more difficult problem.

Typically in carrying out an analysis for the design of a direct contact liquid-liquid heat exchanger, the two fluids, their mass flow rates and their temperatures as they enter the column are specified as well as the pressure at the top of the column. The column diameter is also specified in such a way as to insure that flooding would not take place in an isothermal column. Next one can specify the exit temperature of one of the fluids or the length of the column. This is, of course, analogous to the procedures used in designing shell and tube heat exchangers. For the case of the latter, one must worry about excessive pressure drop; however, for direct contact heat exchangers one must concern himself with flooding. If such a condition exists, one must either change the

flow rates or the column diameter. Although in an isothermal column it is only necessary to check the flooding condition at one axial location, in a column with heat exchange the holdup may change anywhere along its length. Thus, one does not design at the flooding point although the correlations for $U_v$ would indicate the higher the value of holdup the higher the heat transfer. Typically, one designs for 90% of holdup as a maximum with the column.

For steady state operation of a spray column with inlet and outlet temperatures specified the unknowns are the length of the column and the holdup, temperature distributions and pressure along the length of the column.

## NUMERICAL SOLUTION

In carrying out the numerical solutions the governing equations are first converted into a set of algebraic equations using an upwind differencing technique. As the finite difference equations are strongly coupled and non-linear they have to be solved by an iterative guess and correct technique. The method used closely follows that of Spalding and coworkers.[15,16,17] An outline of the procedure follows. Details of the programming may be found in the dissertation of the second author.[18]

(1) Determine the boundary conditions at the upper and lower limits of the solution domain. Estimate a length for the exchanger.

(2) Select appropriate guesses for all dependent variables.

(3) Determine the pressure distribution which is appropriate to the finite difference equation of the mixture momentum equation.

(4) Solve the energy equations for the dispersed phase and the mixture and update the densities of the fluids.

(5) Using the pressure distribution, solve for the velocity of the working fluid droplets.

(6) Check for continuity of the two fluids. Assume any error is due to pressure. The net error when the two fluid continuity equations are added together is a "source term". This term is used to modify the pressure so that continuity is assured.

(7) Corrections are made to the velocities and densities using the pressure corrections and the two momentum equations.

(8) Using the corrected densities and velocities the holdup is calculated along the column using the continuity equation for the dispersed phase.

(9) A second phase of correction is introduced by using the continuous phase continuity equation to find $V_c(x)$.

(10) Steps (3)-(9) are repeated until the continuity errors computed at step (6) are sufficiently small.

The finite difference equations for a given variable, over the integration domain, at a given stage of the whole solving procedure are solved using a tridiagonal algorithm.

## RESULTS AND DISCUSSION

In order to evaluate the five methods of predicting the heat transfer in a direct contact preheater discussed in this paper, it is necessary to compare the predictions with experimental data. The final report on the operation of the $500KW_e$ facility at East Mesa[19] provides such information.

The $500KW_e$ direct contact heat exchanger, shown schematically in Figure 1 is a 40 inch inside diameter spray column. The East Mesa brine contains typically less than 2000ppm dissolved solids and a small amount of $CO_2$ gas. The brine was preflashed to drive off most of the $CO_2$ prior to entering the heat exchanger. The perforated plate distributor was designed to deliver the isobutane as 3.2 mm diameter drops. Laboratory experiments using pentane indicated that for a range of ±10% of design flow rates that this diameter was obtained for virtually all of the droplets.

The column was operated as a combined preheater--boiler. Inlet and outlet temperatures for the two fluids as well as flow rates and pressure were reported. In addition, temperatures were recorded using resistance thermometers along the length of the column. An adequate heat transfer model should be able to predict these temperatures as well as heights of the preheater using only the inlet parameters.

Figures 2-4 show data from three different operating conditions of the $500KW_e$ direct contact heat exchanger. Figure 2 compares the three possible methods described earlier for calculating $U_v$. Method I utilizes Eqs. (5 and 6) with the holdup calculated from

$$0.81(m+1)((1-\phi)V_c-\phi V_d)\phi + 0.09(m+2)V_d\phi-V_d = 0 \qquad (24)$$

where $m = 1.39$ for droplet $Re_{D_C} > 500$, while method II utilizes Eqs. (5 and 6) with the holdup as calculated from the multiphase flow equations. Method III results from the use of Eqs. (17 and 18) and is applicable to a perfectly mixed drop. It is clear from Figure 2 that the latter model is unacceptable as it overpredicts the heat transfer. This is illustrated by the fact that the ebullition temperature is reached far below the length required experimentally. Thus, Model III was eliminated from further consideration.

If one looked only at Figures 2 and 3 he would think that the entirely empirical Model I would best describe the heat transfer; however, Figure 4 indicates that Model II best fits the data. The primary difference between the operating conditions for Figures 2 and 3 as opposed to Figure 4 is in the flow rate.

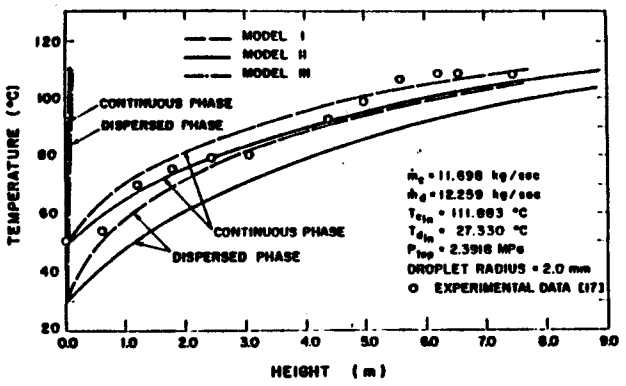


Figure 2. Temperature profile of the brine and the working fluid along the length of the column for comparison of models I, II and III.

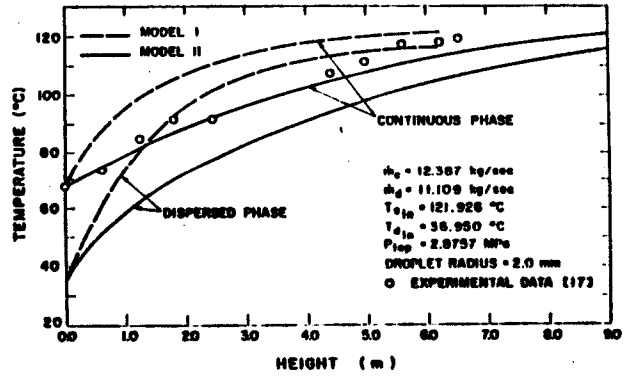


Figure 3. Temperature profile of the brine and the working fluid along the length of the column for comparing models I and II, $\dot{m}c$ = 12.387 Kg/sec, $\dot{m}d$ = 11.109 Kg/sec.

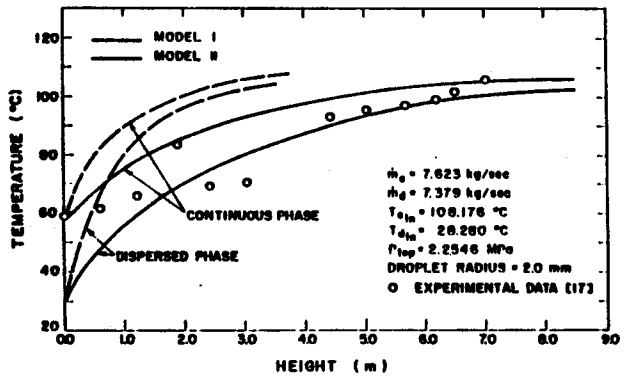


Figure 4. Temperature profile of the brine and the working fluid along the length of the column for comparing models I and II, $\dot{m}c$ = 7.623 Kg/sec, $\dot{m}d$ = 7.379 Kg/sec.

As the heat transfer was clearly not governed by the external heat transfer coefficient, at least as described by Eqs. (17 and 18), a fourth model was introduced. If one postulates that the dispersed phase was made up of droplets which had no internal circulation, then the heat transfer could be dominated by internal conduction. The heat transfer would then be described by a transient conduction model such as the one described by Eqs. (19 and 20). Initially such a model was developed by assuming the droplets would be of constant diameter even though it was known that a considerable change in density would be experienced by the isobutane for the operating conditions of the 500KW$_e$ direct contact heat exchanger. The reason for this assumption was to cut down on the computer time of the solution, since an analytical solution was available as indicated by Equations 21 and 22. In Reference 16, more than nine different experiments were analyzed assuming constant drop radii of 1.6 mm and 2.0 mm. Figures 5 and 6 illustrate typical results. It is clear that to approach duplicating all of the data neither choice of constant radius is always acceptable. Figure 7 illustrates a clear example where the heat transfer near the bottom of the column was well represented by the smaller radius, yet the total preheater length and temperature distribution at the top was better represented by the larger radius. Since both the higher temperature and lower pressure which occur as the isobutane droplets approach the top might explain this behavior, the fifth model tried was the variable property, variable radius conduction model. Figures 8-10 are the same cases as presented in Figures 5-7. It is clear that this latter model accurately predicts the preheater length as well as the temperature except for the depression of temperature near the three meter location. This depression appears in all of the East Mesa 500KW$_e$ direct contactor data. It could be due to recirculation within the column or temperature depression due to the massive central flange located just above it. In order to ascertain which, it would be necessary to carry out two-dimensional multiphase analyses.

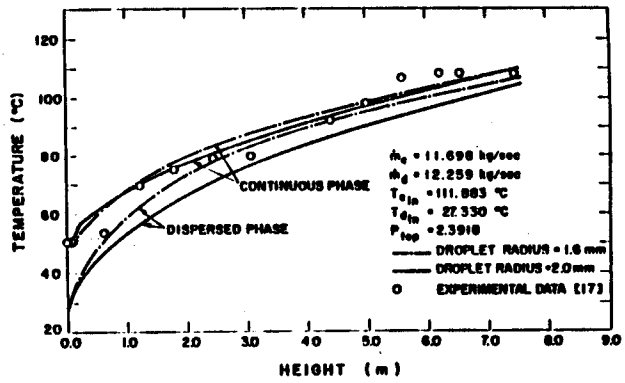


Figure 5. Temperature profile of the brine and the working fluid along the length of the column using constant diameter model, $\dot{m}c$ = 11.698 Kg/sec, $\dot{m}d$ = 12.259 Kg/sec.

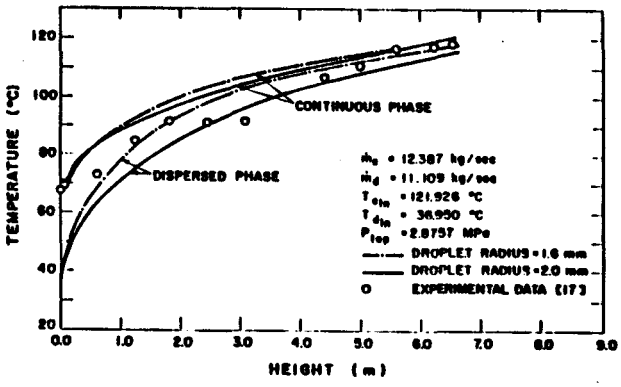


Figure 6. Temperature profile of the brine and the working fluid along the length of the column using constant diameter model, $\dot{m}c$ = 12.387 Kg/sec, $\dot{m}d$ = 11.109 Kg/sec.

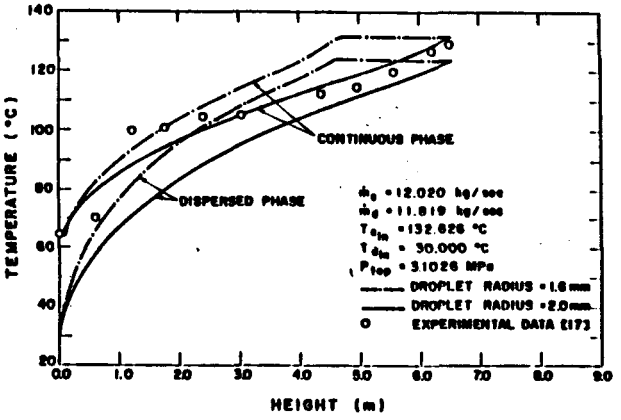


Figure 7. Temperature profile of the brine and the working fluid along the length of the column using constant diameter model, $\dot{m}c$ = 12.02 Kg/sec, $\dot{m}d$ = 11.819 Kg/sec.

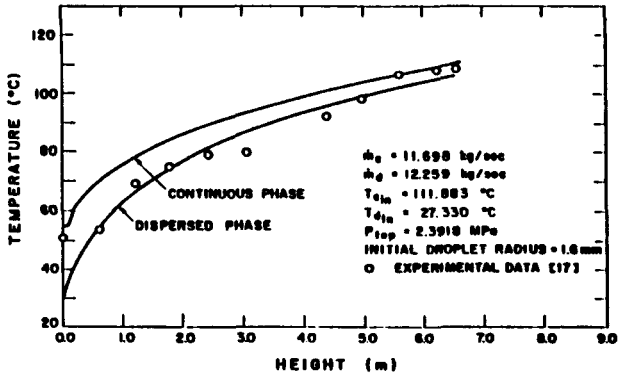


Figure 8. Temperature profile of the brine and the working fluid along the length of the column using variable radius model, $\dot{m}c$ = 11.698 Kg/sec, $\dot{m}d$ = 12.259 Kg/sec.

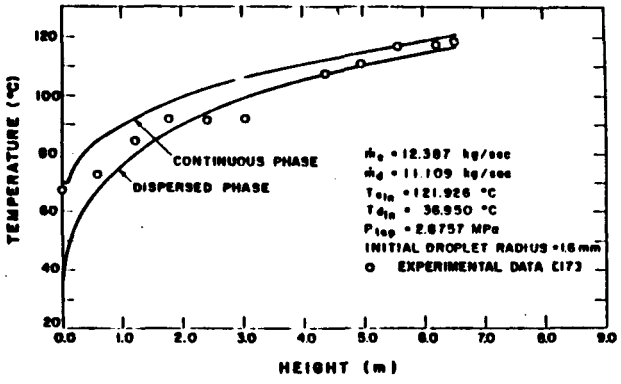


Figure 9. Temperature profile of the brine and the working fluid along the length of the column using variable radius model, $\dot{m}c$ = 12.387 Kg/sec, $\dot{m}d$ = 11.109 Kg/sec.

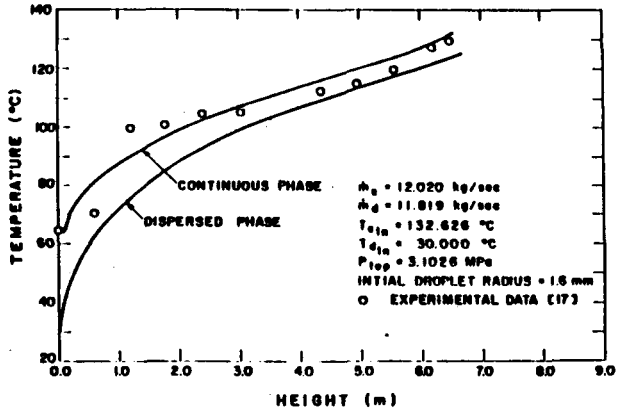


Figure 10. Temperature profile of the brine and the working fluid along the length of the column using variable radius model, $\dot{m}c$ = 12.02 Kg/sec, $\dot{m}d$ = 11.819 Kg/sec.

## CONCLUSIONS

Previous investigators, including the first author, have attempted to argue that the rate of heat transfer from water to dispersed organic liquids or visa-versa in a spray column was governed primarily by flow phenomena. The current study, however, clearly indicates that the controlling mechanism for small diameter drops is the internal transfer of heat. For drops which remain spherical little circulation takes place. Thus, the mechanism is probably controlled by conduction. Variable properties as a function of temperature and pressure must be accounted for in order to accurately predict preheater length in isobutane systems.

Since in large drops internal circulation can take place, it may be possible to reduce the preheater length in spray columns by going to larger drop sizes than the 3-4 mm diameter currently being used in the design of direct contactors for geothermal or solar applications. Care would have to be taken to insure

that drop integrity is maintained. Continued studies of internal drop heat transfer are warranted.

Further studies using two-dimensional multiphase modeling are recommended so as to investigate the prevalent temperature depression in the middle of the East Mesa 500KW$_e$ direct contact heat exchanger. Such a model should investigate the role of the mass of the direct contactor, and the external environment as well as potential internal recirculation and droplet agglomeration and redivision as possible sources of the anomaly.

ACKNOWLEDGEMENT

This work was carried out under contract with the U.S. Department of Energy, Contract Number DE-AS07-76ID01523. The data supplied by Mr. Robert Olander of Barber-Nichols Engineering was appreciated as was the technical encouragement of Mr. Judson Whitbeck of EG&G-Idaho, Inc.

REFERENCES

1. Garwin, L. and Smith, B. D. "Liquid-Liquid Spray Tower Operation in Heat Transfer," Chemical Engineering Progress, Vol. 49, No. 11 (1985), pp. 591-601.

2. Treybal, R. E. Liquid Extraction (1st Edition), McGraw-Hill, New York (1953).

3. Johnson, A. I., Mirand, G. W., Huang, C. J., Hansuld, J. H. and McNamara, V. M. "Spray Extraction Tower Studies," AICHE J., Vol. 3 (1957), pp. 101-110.

4. Woodward, T. "Heat Transfer in a Spray Column," Chemical Engineering Progress, Vol. 57 (1961), pp. 52-57.

5. Pierce, R. D., Dwyer, O. E. and Martin, J. J. "Heat Transfer and Fluid Dynamics in Mercury--Water Spray Columns," AICHE J., Vol. 5 (1959), pp. 257.

6. Suratt, W. B. and Hart, G. K. "Study and Testing of Direct Contact Heat Exchangers for Geothermal Brines," DSS Engineers, Fort Lauderdale, Florida, ERDA Report No. ORO-4893-1, (January 1977).

7. Holt, B. "A Preliminary Study of Direct Contact Heat Exchangers for Geothermal Power Production," a report submitted to ERDA (1977) by the Ben Holt Company, Pasadena, California.

8. Plass, S.B., Jacobs, H.R. and Boehm, R. F. "Operational Characteristics of a Spray Column Type Direct Contact Preheater," AICHE Symposium Series, No. 189 (1979), pp. 227-234.

9. Jacobs, H. R. and Boehm, R. F. "Direct Contact Binary Cycles," Section 426, Sourcebook on the Production of Electricity from Geothermal Energy, J. Kestin, Editor, DOE/RA/4051-1, Washington, D.C. (March 1980).

10. Letan, R. and Kehat, E. "The Mechanism of Heat Transfer in a Spray Column Heat Exchanger," AICHE J., Vol. 14, No. 3 (1968), pp. 398-405.

11. Grace, J.R. "Hydrodynamics of Liquid Drops in Immiscible Liquids," Chapter 38, Handbook of Fluids in Motion, N. P. Cheremisinoff and R. Gupta, Editors, Ann Arbor Science, The Butterfield Group, Ann Arbor, Michigan (1983), pp. 1003-1025.

12. Riemer, D. H., Jacobs, H. R., Boehm, R. F. and Cook, D. S. "A Computer Program for Determining the Thermodynamic Properties of Light Hydrocarbons," University of Utah, U.S.D.O.E. Report IDO/1549-3 (1976).

13. Riemer, D. H., Jacobs, H. R. and Boehm, R. F. "A Computer Program for Determining the Thermodynamic Properties of Water," University of Utah, U.S.D.O.E. Report IDO/1549-2 (1976).

14. Sideman, S. "Direct Contact Heat Transfer Between Immiscible Liquids," Advances in Chemical Engineering, Vol. 6, Academic Press, New York (1966), pp. 207-286.

15. Spalding, D. B. "The Calculation of Free Convection Phenomena in Gas-Liquid Mixtures," Lecture at ICHMT Seminar, Dubrovnik, Yugoslavia (1976).

16. Spalding, D. B. Numerical Computation of Multiphase Fluid Flow and Heat Transfer," Recent Advances in Numerical Methods in Fluids, Editors: C. Taylor and K. Morgan, Pineridge Press, Swansea, Wales (1980), pp. 139-167.

17. Kurosaki, Y. and Spalding, D. B. "One Dimensional Two-Phase Flows," 2nd Multiphase Flow and Heat Transfer Symposium Workshop, "Multiphase Transport: Fundamentals, Reactor Safety, Application," Hemisphere Publishing, Washington, D.C., Vols. 1-5 (1979).

18. Golafshani, Mehdi. "Stability of a Direct Contact Heat Exchanger," Ph.D. Dissertation, University of Utah, Salt Lake City, Utah (1984).

19. Olander, R., Oshmyansku, S., Nichols, K., and Werner, D. "Final Phase Testing and Evaluation of the 500KW$_e$ Direct Contact Pilot Plant at East Mesa," U.S.D.O.E. Report DOE/SF/11700-T1, Arvada, Colorado (Dec. 1983).

# STABILITY OF A DIRECT CONTACT SPRAY COLUMN HEAT EXCHANGER

Mehdi Golafshani
Thiokol Corporation
Brigham City, Utah

Harold R. Jacobs
The Pennsylvania State University
Department of Mechanical Engineering
University Park, Pennsylvania

## ABSTRACT

The governing equations for the transient multiphase flow in a liquid-liquid spray column are developed. Using the model, numerical calculations are presented which represent typical fluctuations observed in the operation of the direct contact tower of the U.S. Department of Energy's 500KW$_e$ geothermal power plant at East Mesa, California. The time constant is determined for the column and conditions leading to local flooding are determined.

## NOMENCLATURE

| | |
|---|---|
| $C_D$ | Drag Coefficient |
| $C_p$ | Specific heat |
| G | Volumetric flow rate |
| g | Gravity |
| h | Enthalpy |
| k | Thermal conductivity |
| $\overline{K}$ | Interphase friction factor |
| LMTD | Log mean temperature difference |
| $\dot{m}$ | Mass flow rate |
| $N_d$ | Number of droplets of dispersed phase |
| P | Pressure |
| Pr | Prandtl Number |
| Q | Heat transfer rate |
| r | Radial coordinate |
| $R_d$ | Radius of droplets |
| $Re_{D_C}$ | Reynolds number $\rho_c \mid (V_c-V_d) \mid D/\mu_c$ . |
| t | Time |
| $t_f$ | Time for a droplet to rise through the column, $X/V_d$ |
| T | Temperature |
| V | Velocity in X direction |
| Vol | Volume |
| x | Vertical coordinate measured from the bottom of the column |
| $\phi$ | Holdup, fraction of volume occupied by the disperse phase |
| $\rho$ | Density |
| $\mu$ | Dynamic viscosity |
| $\alpha$ | Thermal diffusivity |

Subscripts

| | |
|---|---|
| b | Brine |
| c | Continuous phase |
| d | Disperse phase |
| f | Conditions at flooding |
| i | At the interface between the droplets and continuous phase |
| o | At entrance conditions |
| w | Working fluid |

## INTRODUCTION

The design of direct contact heat exchange (dchx) equipment has been a subject of increased interest

since the mid-1960's. This interest orginated in the need for low-cost systems for the desalination of sea water.[1,2,3] In the 1970's, Jacobs and Boehm,[4,5] at the University of Utah initiated investigations into their use as primary heat exchangers for recovering heat from high scaling, high salinity geothermal brines. More recently dchx's have been proposed for use with solar ponds[6] and waste heat recovery systems.[7] Today, they are even being considered for use in space power systems; although, the latter requires the development of an artificial gravity as a means of separating the two immiscible fluids which would be used.[8]

A spray column is a type of direct contact heat exchanger that has attracted considerable interest. This device is made up of an injector for a continuous phase and an injector for either a less or greater density dispersed phase in an otherwise open vertical column having exit ports as shown in Figure 1. This type of device first received attention for mass transfer applications. The continuous phase for example might contain a substance soluble in both it and the disperse phase which is immiscible with the continuous phase. Reduction of the solute in the continuous phase solvent is achieved by absorption into the dispersed phase.[9] Early interest in heat transfer attempted to utilize the heat transfer - mass transfer analogies.[9] Studies of mass transfer equipment for use as heat transfer equipment clearly indicated the preference of a spray column when the continuous phase was either highly scaling or corrosive as might be the case with some geothermal brines. Prior to the work of Letan and Kehat,[10] however, all studies of direct contact heat exchange using spray columns were carried out with only small laboratory equipment (3" - 6" diameter), 7.6 to 15.2 cm diameter columns.[5,10] The work pointed out that

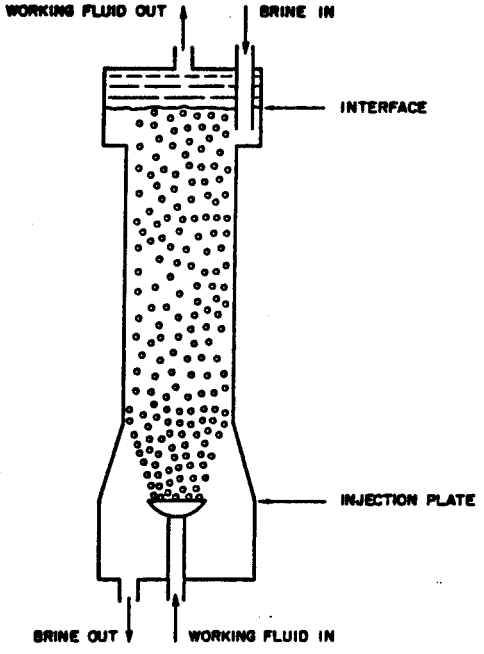


Figure 1. Schematic of a counter current spray column heat exchanger.

to eliminate back-mixing that column height to diameter ratios of greater than eight were required and that even with this ratio, care must be taken in designing the injectors. Elimination of back-mixing is of course, necessary if one wishes to achieve near counter current operation.

As noted in the paper by Plass et al.[11], experimental data exists for a variety of fluids including benzene, toluene, $CCl_4$, kerosene, Shell Oil A, spray base, hexane, isobutane insulating oil, R-113 and mercury as the dispersed phase with water as the continuous phase. Plass et al. were able to correlate the preponderence of data to ±20% in terms of a volumetric heat transfer coefficient for liquid-liquid operation. In their work they define the volumetric heat transfer coefficient as

$$U_v = \frac{Q/Vol}{LMTD} \qquad (1)$$

where Q is the total heat transferred per unit time, Vol is the volume of the column between injector plates, and LMTD is the log mean temperature difference based on exit and entrance temperatures of the fluids to the column.

The correlation of Plass et al. is

$$U_v = 1.2 \times 10^4 \, \phi \, \frac{Btu}{hrft^3 \, °F} \qquad (2)$$

for $\phi < 0.05$

and

$$U_v = [4.5 \times 10^4(\phi - 0.05)e^{-.57G_D/G_C} + 600] \, \frac{Btu}{hrft^3 \, °F} \qquad (3)$$

for $\phi > 0.05$)

where $\phi$ is the holdup.

When using the correlation, it was recommended that $\phi$ be selected as some fraction of the holdup at flooding. The holdup at flooding $\phi_f$ can be calculated from the experimentally derived correlation [12]

$$(m+1)\,(1-G_D/G_C)\,\phi_f^2 + (m+2)\,\frac{G_D}{G_C}\,\phi_f - \frac{G_D}{G_C} = 0 \qquad (4)$$

where $m = 1.39$ for $Re_{D_C} > 500$.

Although it is clear that the heat transfer would be at a maximum for operation near the flooding limit, the uncertainty in the experimentally derived relationship demands that a spray column be operated at a lower value. Thus, $\phi = 0.9\phi_f$ has been recommended where $\phi_f$ is calculated from Eq. (4).[5]

Using Eqs. (2, 3, and 4), the second author carried out the preheater sizing for the East Mesa DCHX Binary Cycle Geothermal Facility for Barber-Nichols Engineering. This heat exchanger, the schematic of which is shown in Figure 2, combined a preheater and boiler in a single column. The boiler volume was sized using the simple correlation

$U_v = 45{,}000\ \phi\ \frac{Btu}{hrft^3\ °F}$, given in Reference 5.

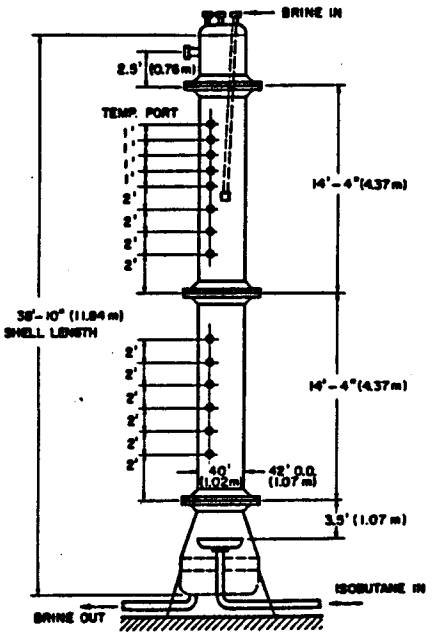


Figure 2. Schematic of 500KW$_e$ direct contact heat exchanger.

The dchx is the largest such device that has been built. It was constructed and operated for nearly three years by Barber-Nichols Engineering for the U.S Department of Energy.[13] The column was designed to operate with a minimum approach temperature between the low salinity geothermal brine (< 2000 ppm) and the isobutane working fluid of 5°F (-2.8°C). This minimum approach temperature occurred within the preheater. Data acquired during the operation of the system indicated that its performance was equal to or greater than expected. However, the temperature profiles along the length of the column did not follow closely those predicted from the correlations used in its design. Due to this it was recommended that research be conducted to better understand the actual mechanisms of heat transfer within the column.

In an attempt to better understand the operation of a direct contact liquid-liquid spray column, it was decided to formulate the problem in terms of the governing equations for multiphase flow. This was done assuming steady state operation in a companion paper.[14] The results of the steady state analysis indicated that for the East Mesa column the heat transfer to the small drops (3.2 - 4.0 mm diameter) was controlled by the conduction within the drops. As the organic fluid/water systems used in the correlation of Plass et al.[11], all had similar properties and were of approximately the same size (3.0 - 7.0 mm diameter) it was not surprising that they could thus be correlated as a function of only flow parameters.

Attempts to determine a physical model to describe the heat transfer during direct contact boiling have not met with much success.[5] In fact, a recent Ph.D. dissertation[15] concludes, "There appears to be no way to calculate a heat transfer coefficient." Thus, the simple correlation of Reference 5 remains the best available, at least for boiling of an organic liquid in water or brine.

Since dchx's are designed to operate near flooding conditions, it is important to determine how changes in operating conditions might influence the column's performance. This is particularly true in geothermal systems where changes in the well head conditions are beyond the control of the operator. Fluctuations in brine flow rate, pressure and temperature can all occur. Adjustments must be made before the column goes unstable. In addition, for a combined preheater-boiler spray column such as at East Mesa, it is necessary to ascertain how such changes affect the needed length of the preheater so that carryover of liquid brine with the working fluid vapor does not occur as this could damage the working fluid turbine. Based on this need to understand the transient operation, the present study was undertaken utilizing a transient multiphase model.

In modeling the direct contact preheater-boiler combination used at East Mesa, we note that the boiler volume is very small compared to that of the preheater. This is, of course, due to the intensity of the heat transfer in the boiler as compared to the preheater and the large temperature increase that is required across the preheater. Typically the vaporization process is completed in less than a meter of column height while the preheating takes nearly seven meters. Thus, as a first approximation, it is reasonable to assume a rapid adjustment in the boiler while the preheater provides the major time delay. (It should be noted that for solar pond applications, the low temperature increase across the preheater would make the boiler and preheater sections nearly identical in length.) In the present study, we restrict ourselves to a situation where the boiler section adjusts nearly instantaneously to the conditions of the fluids entering it. Thus, we can concentrate on the response of the preheater section.

## MATHEMATICAL MODELING

Consider the column shown in Figure 1. It is of constant diameter and ideally the dispersed phase, which we assume is lighter than the continuous phase, rises in continuous streams from the injector nozzles. Unless strong recirculation regions occur due to improper design of the continuous phase inlet, it is clear that the flow is essentially one-dimensional. However, for our problem there is the possibility of time dependence. Thus, the continuity equations for the continuous phase and dispersed phase are respectively,

$$\frac{\partial[(1-\phi)\rho_c]}{\partial t} + \frac{\partial[(1-\phi)\rho_c V_c]}{\partial x} = 0 \qquad (5)$$

and

$$\frac{\partial \rho_d \phi}{\partial t} + \frac{\partial \rho_d \phi V_d}{\partial x} = 0 \qquad (6)$$

For each phase the conservation of momentum can be written; however, in a two-component system it is only necessary to write the momentum equation for one phase and for the mixture. Thus, for the dispersed phase

$$\frac{\partial \rho_d \phi V_d}{\partial t} + \frac{\partial \rho_d \phi V_d^2}{\partial x} = -\phi \frac{\partial P}{\partial x} - \bar{K}(V_d - V_c) - \phi \rho_d g \qquad (7)$$

where $\bar{K}$ is the interphase friction factor.

For the mixture as a whole, we have

$$\frac{\partial[(1-\phi)\rho_c V_c]}{\partial t} + \frac{\partial[(1-\phi)\rho_c V_c^2]}{\partial x} + \frac{\partial \rho_d \phi V_d}{\partial t} + \frac{\partial \rho_d \phi V_d^2}{\partial x} = -\frac{\partial P}{\partial x} - [(1-\phi)\rho_c + \phi \rho_d]g \qquad (8)$$

Note in Eq. (8), that the interphase friction term disappears as the interphase forces on each phase are equal and opposite. Note also that we write the presure gradient as a partial derivative. This is due to the fact that during a transient the amount of mass of each fluid can vary in the column and thus the hydrostatic pressure can vary with time as well as axial location. As the continous phase flows downward, $V_c$ is a negative value.

The energy equations also need only be written for the dispersed phase and the mixture as a whole, thus for the dispersed phase

$$\frac{\partial \rho_d \phi h_d}{\partial t} + \frac{\partial \rho_d \phi h_d V_d}{\partial x} = \frac{\partial (\phi P)}{\partial t} - \frac{Qi}{Vol} \qquad (9)$$

and for the mixture

$$\frac{\partial[(1-\phi)\rho_c h_c]}{\partial t} + \frac{\partial[(1-\phi)\rho_c V_c h_c]}{\partial x} + \frac{\partial \phi \rho_d h_d}{\partial t} + \frac{\partial \phi \rho_d V_d h_d}{\partial x} = \frac{\partial P}{\partial t} \qquad (10)$$

The set of partial differential equations given in Eqs. (5-10) has to be solved in conjunction with equations of state for the two fluids and using appropriate relations for the interphase friction factor, $\bar{K}$, and the interfacial heat transfer, Qi/Vol. Reference 14 gives for $\bar{K}$,

$$\bar{K} = \frac{3}{8} \frac{\phi}{R_d} C_D \rho_C |V_d - V_c| \qquad (11)$$

For an organic fluid as a dispersed phase in water or brine, Jacobs and Golafshani[14] have shown that for droplets of ~3.0 - 4.0 mm in diameter that the heat transfer is governed by conduction within the drops and that, at least for isobutane, drop growth due to decreased density when the drops are being heated must be taken into account. Thus, for the droplets, it is also required to solve the transient conduction problem

$$\frac{\partial (\rho_c T)_d}{\partial t_1} = \frac{1}{r^2} \frac{\partial r^2 k_d \frac{\partial T_d}{\partial r}}{\partial r} \qquad (12)$$

where here $t_1$ is defined as the elapsed time from the point of origin of the drop to x, or

$$t_1 = \int_0^x \frac{dx}{V_d} \qquad (13)$$

The associated initial and boundary conditions are

$$T_d = T_{do} \text{ at } t_1 = 0$$

$$T_d \text{ is finite at } r = 0 \qquad (14)$$

and $$T_d = T_c \text{ at } r = R_d$$

It should be noted that since the density of the drops changes that

$$R_d = R_{do} \left(\frac{\rho_{do}}{\rho_d}\right)^{1/3} \qquad (15)$$

It is clear that even for steady state operation that the above described equations must be solved numerically since $T_c$ varies with x as does $V_d$. For transient behavior of the column, we have a doubly complex problem. However, for a given system of droplets released at a specified time, the problem is in fact no worse in regards to solving Eqs. (12-15).

At each location along the column the droplets' mean temperature is found after solving Eqs. (12-15). From this the value of the dispersed phase enthalpy can be obtained, and from the mixture energy equation, Eq. (10), the enthalpy of the continuous phase. Eq. (9), therefore, is only used to check convergence. Thus, the actual governing equations for solution of the problem are Eqs. (5-8) and Eqs. (10-15) subject to the constraints of the equations of state for the two fluids and the imposed boundary conditions.

## NUMERICAL SOLUTION

In carrying out the numerical solutions, the governing equations are first converted into a set of algebraic equations using a spacewise upwind differencing technique with the exception of the droplet conduction equations where central differencing is used. The transients are expressed in an implicit formulation. As the finite difference equations are strongly coupled and nonlinear they have to be solved by an iterative guess and correct

technique at each time step. The method used closely follows that of Spalding[16] and is described in detail in the dissertation of the first author.[17] Details of the programming can be found there as well.

Typically in carrying out an analysis, due to the added complexity of having to solve the droplet conduction problem simultaneously, we initiated our analyses by first solving for a steady state solution around which we wished to study a transient response. In carrying out an analysis for the design of a spray column, the two fluids, their mass flow rates and their temperatures as they enter the column are specified as well as the pressure at the top of the column. The column diameter is also specified in such a way as to insure that flooding would not take place in an isothermal column. This is normally done utilizing Eq. (4) or a similarly defined empirical formula. Next one can specify the exit temperature desired for one of the fluids or the column length. It is, of course, much easier to do the latter since defining one exit temperature in fact defines the other. However, the length would be unknown. Thus, initially a length would be guessed. Such a guess could be obtained by using an empirical expression for a volumetric heat transfer coefficient such as given in Reference 11. In this case, Eq. (9) could be used in place of Eqs. (12-14) in solving the problem. Even greater simplification could result by assuming the fluid properties $\rho$ and $C_p$ constant at inlet conditions; however, for many systems such as isobutane-water the results could be quite erroneous and lead to a long iteration time to converge to the actual length required for the variable property conduction model.

After obtaining a steady state solution for the column operation, the transient behavior can be obtained by imposing a change in one of the input variables or in the column pressure. In the work presented in Reference 17, changes in mass flow rates, pressure and temperature were considered.

## RESULTS AND DISCUSSION

The transient response analyses reported herein correspond to operating conditions reported by Olander et al.[13] for the 500KW$_e$ Direct Contact Geothermal Power Plant at East Mesa, California. The spray column, as shown in Figure 2, is a combined preheater-boiler arrangement. The design is such that liquid level is controlled primarily by adjusting flow rates. The boiling section is relatively short, in the range of 1.0 - 1.5 m (3-5 ft.) with the greater portion of the length being the preheater. Fluctuations in flows, temperatures and column pressure can occur as the continuous phase is brine and the dispersed phase is isobutane. Although the system ideally should operate in a steady state mode, the geothermal wells at East Mesa produce time varying amounts of $CO_2$ as well as hot brine. The $CO_2$ needs to be purged by flashing which can induce changes in brine temperature and flow rate and even pressure although the wells are pumped. Carryover of $CO_2$ to the condenser can also cause fluctuations in isobutane inlet temperature. Thus, at least small fluctuations can occur at regular intervals and the column must adjust to them. Since the column operation attempts to control fluid height, and the preheater required length can vary, it is possible to cause buildup of isobutane in the boiler section of the column since as the preheater lengthens, there may not be sufficient boiler length or contact time between the saturated isobutane drops and the brine. This can cause a drop in column pressure as less vapor is generated. Adjustments would thus have to be made to the turbine controls, etc., until the column re-equilibriated. It is thus necessary to determine the time constant for the column as well as changes in holdup and required preheater length to reach the saturation conditions for the isobutane.

Figures 3 and 4 present the steady state preheater temperature, void fraction or holdup and the velocities predicted throughout the 500KW$_e$ spray column. In Figure 3, there are also presented temperature measurements made with resistance thermometers located in the column.[13] The higher temperature curve is for the brine and the lower temperature curve is for the isobutane. The experimental data appear to represent the isobutane drops in this case, except at x = 0 which is the extraction temperature of the brine. This was not always the case, however. Usually the experimental data lies between the two curves indicating that normally some sort of weighted average is measured.

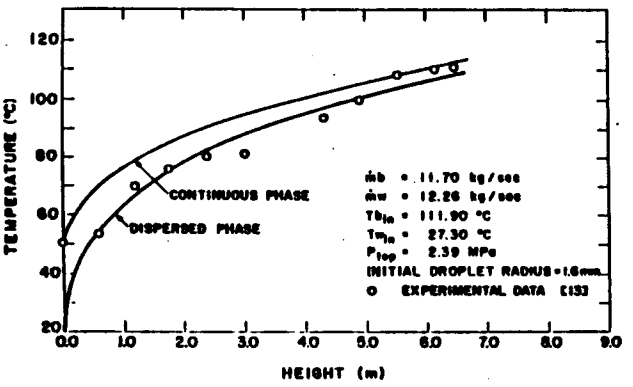


Figure 3. Temperature Profile of the brine and the working fluid along the length of the column using variable radius model, $\dot{m}b$ = 11.70 Kg/sec, $\dot{m}w$ = 12.26 Kg/sec.

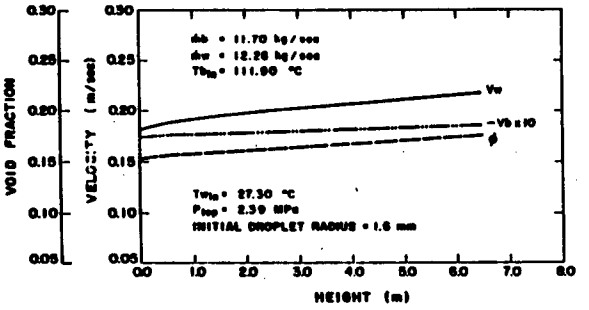


Figure 4. Variation of velocity of the brine and the working fluid as well as holdup along the length of the column, $\dot{m}b$ = 11.70 Kg/sec, $\dot{m}w$ = 12.26 Kg/sec.

Figures 5-7 indicate changes observed after 180 seconds for the brine temperature, isobutane temperature and holdup for step changes in mass flow rates or column pressure. It is clear that the preheater is relatively insensitive to pressure whereas changes in the mass flow rates as low as ±1kg/sec can yield temperature variations within the column of ±2°C. Figure 8 shows the effect of a 5°C decrease in brine inlet temperature. Near the bottom of the column the temperatures remain unchanged, but near the top changes of each fluid are seen. For the East Mesa column, all such changes in flow rates and brine inlet temperature can occur, and they can occur rapidly as the controllers were not sufficiently sensitive to respond. Thus, it is impossible to state that steady state operation is ever really achieved. Due to this, it was remarkable that Jacobs and Golafshani[14] were able to achieve the comparison shown in Figure 3 and better in many cases[17] between their model and measured temperatures. Table 1 indicates how each variation discussed influences the preheater length requirement.

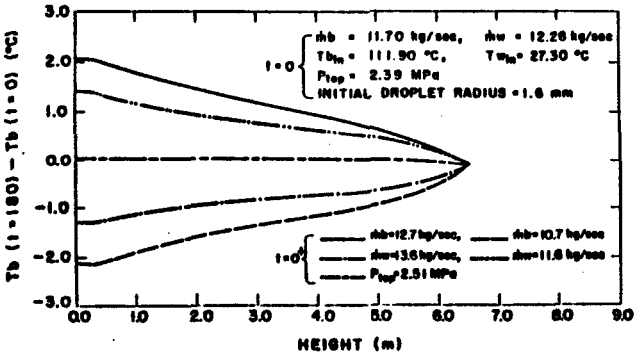


Figure 5. Effect of change in mass flow rate and column pressure on the brine temperature $\dot{m}b$ = 11.70 Kg/sec, $\dot{m}w$ = 12.26 Kg/sec.

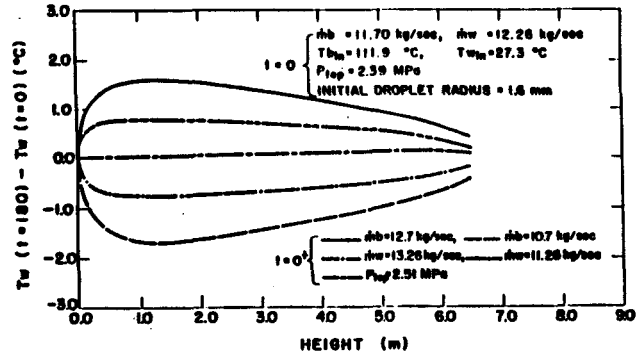


Figure 6. Effect of change in mass flow rate and column pressure on the working fluid temperature $\dot{m}b$ = 11.70 Kg/sec, $\dot{m}w$ = 12.26 Kg/sec.

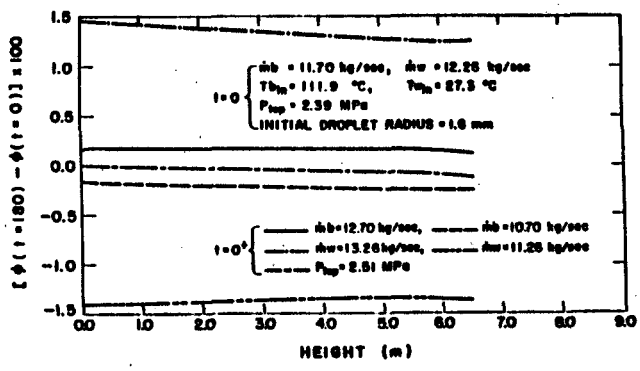


Figure 7. Effect of change in mass flow rate and column pressure on holdup $\dot{m}b$ = 11.70 Kg/sec, $\dot{m}w$ = 12.26 Kg/sec.

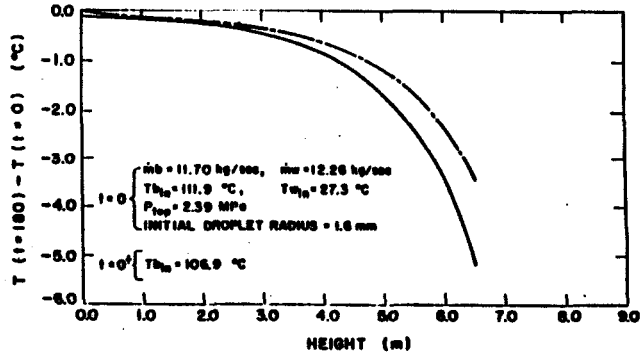


Figure 8. Effect of change in the brine inlet temperature on temperature profile at the brine and the working fluid, $\dot{m}b$ = 11.698 Kg/sec, $\dot{m}w$ = 12.259 Kg/sec.

Table 1

Changes in column height afater a sudden change in input characteristic of the column. Steady stated conditions are: $\dot{m}b$ = 11.70 kg/sec, $\dot{m}w$ = 12.26 kg/sec, $Tb_{in}$ = 111.9°C, $Tw_{in}$ = 27.3°C, $P_{top}$ = 2.39 Mpa and initial droplet radius = 1.6 mm.

| Change in Input Characteristic | H(t=180) - H(t=0) (m) |
|---|---|
| $\dot{m}b$ increased by 1 kg/sec | -0.87 |
| $\dot{m}b$ decreased by 1 kg/sec | 0.1 |
| $\dot{m}w$ increased by 1 kg/sec | 0.04 |
| $\dot{m}w$ decreased by 1 kg/sec | -0.04 |
| $P_{top}$ increased by 5% | 0.9 |
| $Tb_{in}$ decreased by 5°C | 1.04 |

Figures 9 and 10 illustrate another steady state calculation for an additional operating condition. Figures 11-15 show the response of Tw to changes in mass flows and inlet brine temperature as a function of time. The trends are all as expected except for the increase in working fluid flow rate. The early time response indicates an increase in temperature at the bottom of the column. This is due to the time that it takes the mass flux wave to traverse the column height. At 45 seconds the increased number of droplets per unit volume wil be occupying a greater fraction, i.e., $\phi$ will be higher and the drag on the drops greater. There will be a longer exposure to a hotter brine. However, as the higher mass flux works its way up the column there will be a cooling of the continuous fluid approaching the bottom and the temperatures will be depressed. It is clear that a longer preheater length will be required to bring the isobutane up to its saturation temperature as was indicated by the previous case studied.

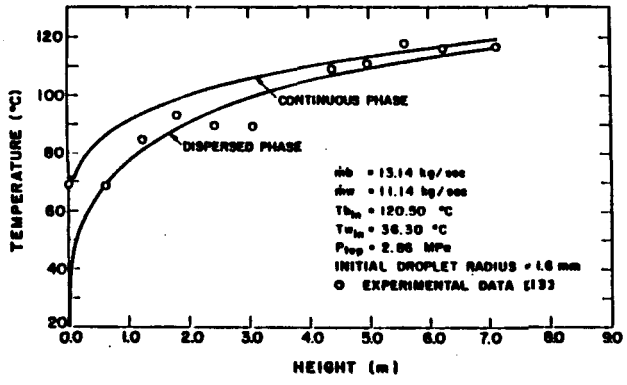


Figure 9. Temperature profile of the brine and the working fluid along the length of the column using variable radius model, $\dot{m}b$ = 13.14 Kg/sec, $\dot{m}w$ = 11.14 Kg/sec.

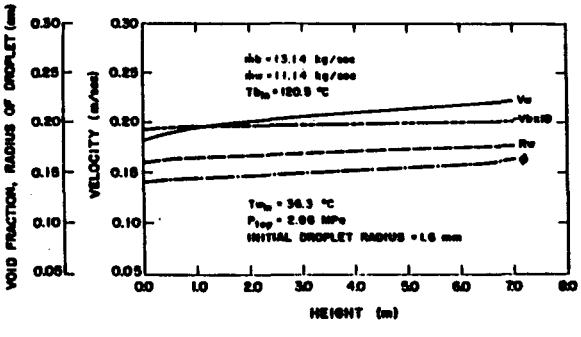


Figure 10. Variation of velocity of the brine and the working fluid as well as holdup and drop radius along the length of the column.

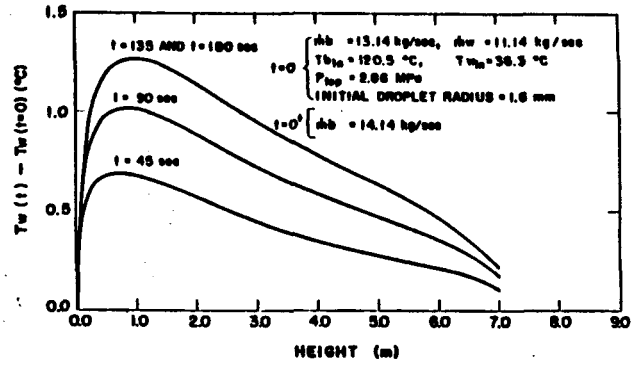


Figure 11. Transient response of the working fluid temperature after an increase in mass flow rate of the brine.

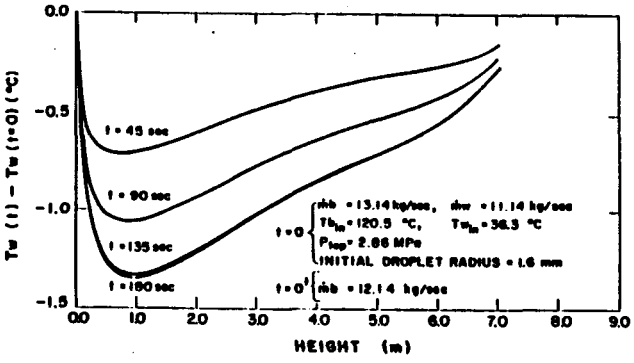


Figure 12. Transient response of the working fluid temperature after a decrease in mass flow rate of the brine.

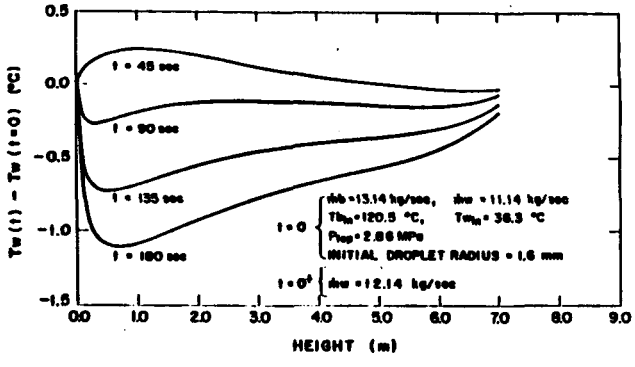


Figure 13. Transient response of the working fluid temperature after an increase in mass flow rate of the working fluid.

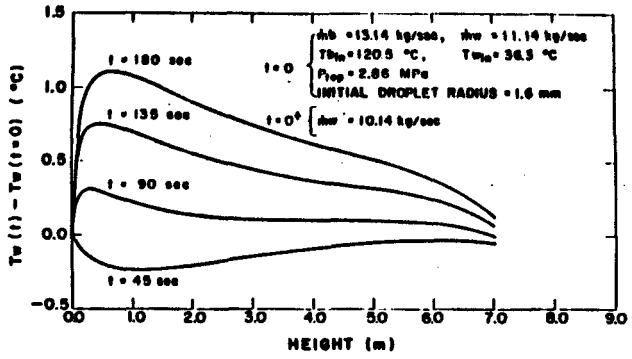


Figure 14. Transient response of the working fluid temperature after a decrease in mass flow rate of the working fluid.

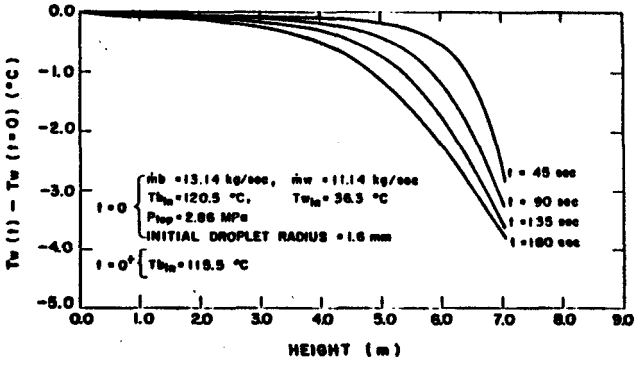


Figure 15. Transient response of the working fluid temperature after a decrease in the brine inlet temperature.

For all cases studied, a new equilibrium-steady state was achieved after approximately 180 seconds. Thus, the analysis indicates that this is the effective time constant for the preheater section of the column. As the boiler section is always very short for the East Mesa facility, this is a good approximate value for the column itself.

## CONCLUSIONS

A one-dimensional transient multiphase model appears to be adequate to describe the performance of a spray column such as that at the East Mesa 500KW$_e$ Direct Contact Binary Cycle Power Plant. Changes in preheater length of up to one meter can easily occur due to modest changes in the input conditions. The time constant for the direct contactor is of the order of 180 seconds. For changes occurring in shorter times than this, there should be a lag time such that a true equilibrium steady state is not achieved. Thus, observed temperature measurements in the column are not necessarily steady state. For small changes in various input parameters which are likely to occur, the long time constant, of 180 seconds, should allow for reasonable control if adequate space is provided for the boiler and a vapor accumulator. As this was the case for the 500KW$_e$ facility spray column, there occurred no adverse operational effects to the power plant due to the direct contactor.

## ACKNOWLEDGEMENT

This work was carried out under contract with the U.S. Department of Energy, Contract No. DE-AS07-76ID01523. The data supplied by Mr. Robert Olander of Barber-Nichols Engineering was appreciated as was the technical encouragement of Mr. Judson Whitbeck of EG&G-Idaho, Inc.

## REFERENCES

1. Kern, D. Q. "Evaluation of Liquid-Liquid Heat Transfer for Large Scale Desalination," Office of Saline Water, Research and Development Progress Report No. 261 (1967).

2. M. W. Kellogg Company. Saline Water Conversion Engineering Data Handbook, 2nd Edition, Office of Saline Water, Washington, D.C., U.S. Government Printing Office (Nov. 1971).

3. Sukhatine, S. P. and Hurwitz, M. "Heat Transfer in the Liquid-Liquid Spray Tower," Office of Saline Water, Washington, D.C., U.S. Government Printing Office (Nov. 1971).

4. Jacobs, H. R., Boehm, R. F. and Hansen, A. C. "Application of Direct Contact Heat Exchangers to Geothermal Power Production Cycles - Project Review 1974-1977," U.S. ERDA Report IDO/1549-8 (May 1977).

5. Jacobs, H. R. and Boehm, R. F. "Direct Contact Binary Cycles," Section 4.26, Sourcebook on the Production of Electricity from Geothermal Energy, J. Kestin, Editor, DOE/RA/4051-1, Washington, D.C. (March 1980).

6. Wright, J.D. "Selection of a Working Fluid for an Organic Rankine Cycle Coupled to a Salt Gradient Solar Pond by Direct-Contact Heat Exchange," ASME Journal of Solar Energy Engineering, Vol. 104 (Nov. 1982), pp. 286-291.

7. Goldstick, R. J. and KVB, Inc. "Survey of Flue Gas Condensation Heat Recovery Systems," Final Report No. GRI 80/0152, The Gas Research Institute, Chicago, Illinois.

8. Bruckner, A. P. and A. Hertzberg. "Direct Contact Droplet Heat Exchangers for Thermal Management in Space," Proceedings of the 17th IECEC (Aug. 1982), pp. 107-111.

9. Treybal, R. E. Liquid Extraction, 1st Edition, McGraw-Hill Book Company, New York, New York (1953).

10. Letan, R. and Kehat, E. "The Mechanism of Heat Transfer in a Spray Column Heat Exchanger," AIChE Journal, Vol. 14, No. 3 (1968), pp. 398-405.

11. Plass, S. B., Jacobs, H. R. and Boehm, R. F. "Operational Characteristics of a Spray Column Type Direct Contact Preheater," AIChE Symposium Series, No. 189 (1979), pp. 227-234.

12. Minard, G. W. and Johnson, A. I. "Limiting Flow and Holdup in a Spray Extraction Column," Chemical Engineering Progress, Vol. 48, No. 2 (Feb. 1952), pp. 62-74.

13. Olander, R., Oshmyansku, S., Nichols, K., and Werner, D. "Final Phase Testing and Evaluation of the 500KW$_e$ Direct Contact Heat Exchange Pilot Plant at East Mesa," ERDA Report/DOE/SF/11700-T1, Arcada, Colorado (Dec. 1983).

14. Jacobs, H. R. and Golafshani, M. "A Heuristic Evaluation of the Governing Mode of Heat Transfer in a Liquid-Liquid Spray Column," ASME/AIChE 1985 National Heat Transfer Conference, Denver, Colorado, August 5-9, 1985.

15. Walter, D. B. "An Experimental Investigation of Direct Contact Three Phase Boiling Heat Transfer," Ph.D. Dissertation, The University of Tennessee, Knoxville, Tennessee, 1981.

16. Spalding, D. B. "Numerical Computation of Multiphase Fluid Flow and Heat Transfer," Recent Advances in Numerical Methods in Fluids, Editors: C. Taylor and K. Morgan, Pineridge Press, Swansea, Wales (1980), pp. 139-167.

17. Golafshani, M. "Stability of a Direct Contact Heat Exchanger," Ph.D. Dissertation, University of Utah, Salt Lake City, Utah (1984).

# STABILITY OF A DIRECT CONTACT HEAT EXCHANGER

by

Mehdi Golafshani

A dissertation submitted to the faculty of
The University of Utah
in partial fulfillment of the requirements for the degree of

Doctor of Philosophy

in

Mechanical Engineering

Department of Mechanical and Industrial Engineering

University of Utah

December 1984

## ABSTRACT

Direct contact heat exchangers have received considerable attention in recent years for application in alternate energy systems. One version of a direct contact heat exchanger is a spray column. This device brings into contact a higher temperature fluid with cooler immiscible liquid.

Fluctuations in the input characteristics of either fluid can upset the operation of the column and affect the overall system design. This dissertation formulates the two-phase flow and heat transfer equations to describe the dynamics of a spray column direct contact heat exchanger. Further, the protocol is developed for numerically solving the governing equations and example results are presented. The solution demonstrates the effects of mass flow rate, and incoming temperature of either fluid as well as the operating pressure on the overall performance of the column.

The dissertation also focuses attention to the mechanism of heat transfer in such a device. Various models of heat transfer are incorporated into the solution routine and the validity of each model is examined by comparison to experimental data.

TABLE OF CONTENTS

## NOMENCLATURE

| | |
|---|---|
| A | Cross sectional area of the heat exchanger |
| Cd | Drag coefficient |
| Cpb | Specific heat of brine |
| Cpw | Specific heat of working fluid |
| $G_c$ | Volumetric flow rate of continuous phase |
| $G_d$ | Volumetric flow rate of dispersed phase |
| g | Vertical field acceleration |
| Hb | Thermodynamic enthalpy of brine |
| Hw | Thermodynamic enthalpy of working fluid |
| $\bar{h}m$ | Mean heat transfer coefficient |
| Kb | Thermal conductivity of brine |
| Kw | Thermal conductivity of working fluid |
| $\bar{k}$ | Interphase friction factor |
| LMTD | Log mean temperature difference |
| $\dot{m}b$ | Inlet mass flow rate of brine |
| $\dot{m}w$ | Inlet mass flow rate of working fluid |
| $\overline{NuD}$ | Average Nusselt number |
| Nw | Number of working fluid droplets per unit volume |
| P | Pressure |
| Prb | Prandtl number of brine |
| $P_{top}$ | Pressure at the top of the column |
| $\dot{Q}$ | Heat transfer rate |
| R | Ratio of volumetric flow rates, $\frac{G_d}{G_c}$ |

| | |
|---|---|
| $r$ | Radial coordinate |
| $Rw$ | Radius of each droplet |
| $Rwo$ | Radius of a droplet at injection point |
| $ReD$ | Droplet Reynolds number |
| $t$ | Time |
| $t_l$ | Time for a droplet to rise through the heat exchanger |
| $Tb$ | Temperature of brine |
| $Tb_{in}$ | Incoming temperature of brine |
| $Tw$ | Temperature of working fluid droplets |
| $Tw_{in}$ | Incoming temperature of working fluid |
| $Two$ | Temperature of working fluid droplets at the injection point |
| $Uv$ | Interphase volumetric heat transfer coefficient |
| $Vb$ | Vertical velocity of brine |
| $Vw$ | Vertical velocity of working fluid droplets |
| $x$ | Vertical coordinate measured from the bottom |
| $\varepsilon$ | Void fraction of brine |
| $\phi$ | Void fraction of working fluid droplets |
| $\rho b$ | Density of brine |
| $\rho w$ | Density of working fluid droplets |
| $\rho wo$ | Density of working fluid droplets at injection point |
| $\mu b$ | Dynamic viscosity of brine |
| $\alpha w$ | Thermal diffusivity of working fluid |

ACKNOWLEDGEMENTS

I would like to take this opportunity to thank God for all the guidance, motivation and encouragement that he has given me in life, without which my life would have been meaningless.

This dissertation is dedicated to my wonderful wife, Tahmineh Riahi, for her support and dedication to me during the time of my entire graduate studies.

I express my deep appreciation to my advisor, Dr. Harold R. Jacobs, for his considerable help and suggestions during this research. My gratitude to Dr. Jacobs goes beyond what I could ever express because he has constantly helped me through the years at the University of Utah. I would also like to express my indebtedness to Dr. Robert F. Boehm for his considerable help.

I also like to thank my father and mother for their patience and encouragement during the past ten years which I have been away from my homeland.

Again, I express my sincere gratitude to my good and beautiful wife who made it all possible for me to pursue my graduate work and to be more dedicated to accomplishing it.

# CHAPTER 1

## INTRODUCTION

The shortage of potable water in many of the developing nations stimulated interest in the application of direct contact heat exchange in the 1960s [1] for use in water desalination systems. More recently a dwindling supply of conventional energy resources such as oil, coal and natural gas, coupled with an increasing need for energy in all areas of society prompted a search for economical alternate energy resources. One such alternative is geothermal energy. Geothermal energy is available in limited amounts in the form of dry steam. Low and moderate temperature geothermal brines are more than twenty times as prevalent. This abundance has led researchers to consider the use of these liquid brines as a source of heat to produce electricity [2, 3, 4] as well as for process heat.

The systems of utilization of the liquid dominated resources are technologically more complex than the systems necessary for the utilization of dry steam reservoirs, where filtered steam can be directly expanded through a low pressure turbine. The binary cycle has been developed to eliminate the inefficiencies inherent in steam flashing with low temperature liquid dominated resources. In this

cycle, the production well may be pumped in order to prevent steam flashing at the surface. Heat is transferred from the hot water to a secondary fluid that has a lower boiling point. High pressure vapor produced in the secondary fluid boiler is expanded through a turbine which drives a generator. The turbine exhaust vapor is then condensed and pumped back to the heat exchanger to complete the secondary fluid cycle.

Direct contact heat exchangers have received considerable attention in recent years for application in alternate energy systems, such as geothermal and solar pond power plants. The primary reasons for this interest are the advantages of these direct contact heat exchangers over the the conventional processes using metallic transfer surfaces. These advantages are:

(1) Simple design, compactness and relatively inexpensive equipment;

(2) Low maintenance due to absence, or reduction of scale formation on solid surfaces;

(3) The obtainable close temperature approaches. These advantages can lend themselves to producing economical process systems in instances where the use of conventional heat exchangers would make the process economically infeasible. It should be mentioned that in geothermal application of direct contact heat exchangers, the only disadvantage is the loss of working fluid due to dissolution into the brine.

There are basically several types of direct contact counter current heat exchangers. They include spray towers, baffle towers, perforated plate towers, packed towers and wetted wall towers. All of the first four bring into contact a higher temperature fluid with a cooler immiscible liquid. The immiscible cooler liquid can be injected as a system of discrete drops. If the fluid to be heated is of lower density than the high temperature fluid, it is injected at the bottom of the column and the drops rise due to gravity. The fifth keeps the phases separated except at cylindrical interface. The advantage of the former is a high heat transfer area within the contacting volume, while the advantage of the latter is in maintaining separation and perhaps eliminating or reducing the need for the separation system.

The device which has received the most attention as a direct contact heat exchanger for geothermal power application is the spray tower. One big advantage of a spray tower over the previously mentioned towers is that it is free from heat transfer enhancement devices which are subject to scaling. A typical spray tower is depicted in Figure 1. It consists of a vertical column, an injection nozzle for each fluid and exit ports. This device has been used both as a preheater and as a boiler. Recent designs of spray columns as heat exchangers have incorporated both a preheating section and a boiling section when applied to energy systems.

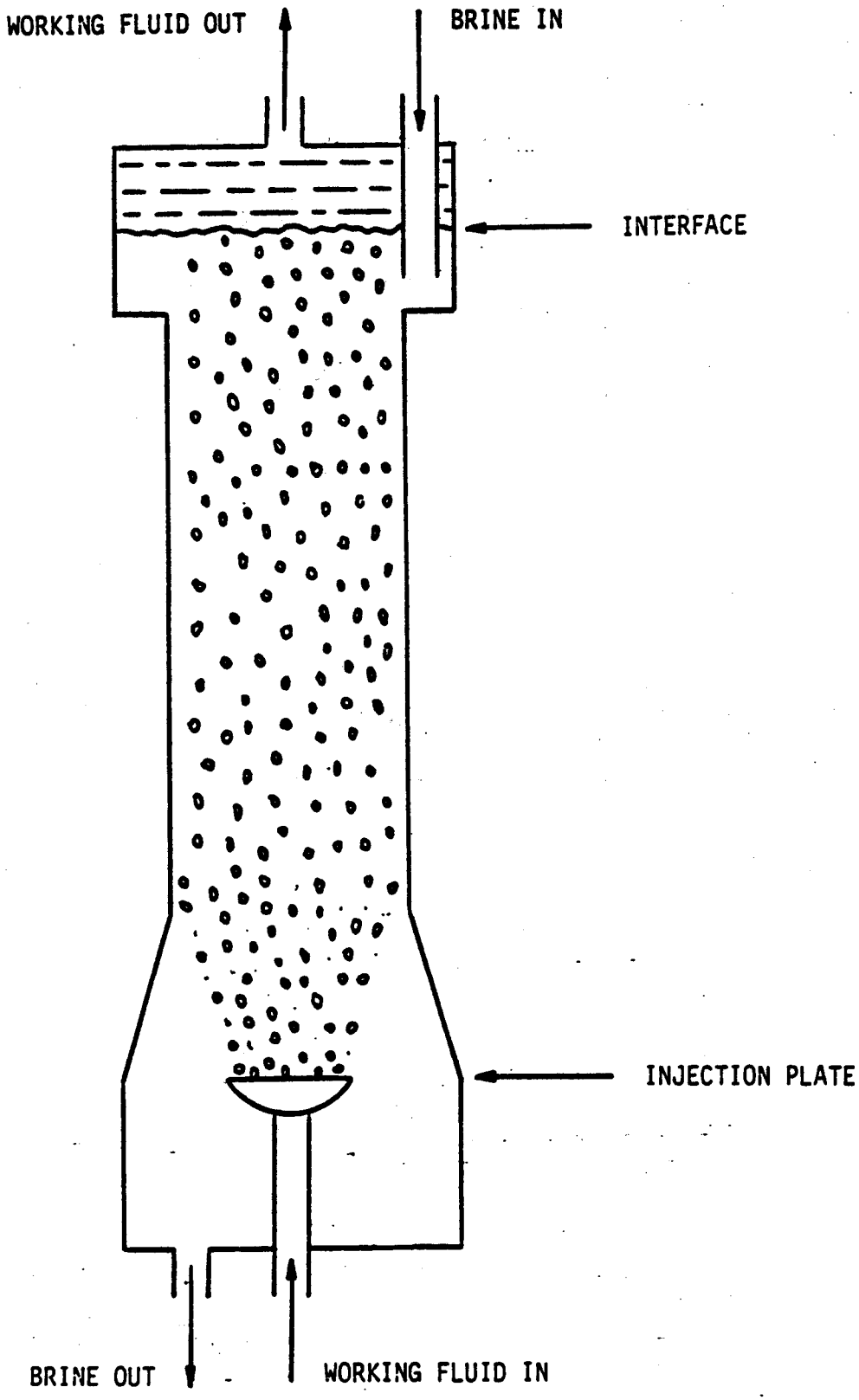


Figure 1. Schematic of a counter current spray column heat exchanger.

Some designs of spray tower liquid-liquid heat exchangers have been carried out by the method proposed by Letan [5]. Letan's work is based on the supposed hydrodynamics of the spray column. The design method requires only that the Reynolds number for the drops be less than 2300. For Reynolds numbers greater than 2300, the flow is turbulent and scaling of the size is not possible.

Spray column direct contact heat exchangers are designed to operate near the flooding point; i.e., where it is possible that the injected medium may be swept out the bottom of the column by the downward flowing heavier medium. The reason for operating near the flooding point is that the heat transfer has been shown experimentally to be highest under these conditions. Fluctuations in input characteristics of the heating fluid, for example, in geothermal applications fluctuations in pressure, dissolved gas, flow rates, salinity, etc., can upset the operation of the column and can induce localized flooding at some point along the column height. This behavior can adversely affect the overall system design. Thus, it is necessary to develop a numerical model to describe the phenomena and to investigate what the practical limitations of approach to flooding are, based on assessments of the types of disturbances that might be encountered.

In actual direct contact heat exchangers, heat transfer data are normally reported in terms of volumetric heat transfer coefficient, defined as

$$Uv = \frac{\dot{Q}}{\text{volume} \cdot \text{LMTD}} \quad . \tag{10}$$

Spray column liquid-liquid heat exchanger experiments have been conducted for the following fluids as the dispersed phase with water as the continuous phase: benzene [6], toluene [7], $CCl_4$ [8], Shell Oil A and spray base [9], gas-oil [8], kerosene [9], mercury [10], isobutane [11], and also pentane in recent design for the Solar Energy Research Institute (SERI) at the University of Utah.

The volumetric heat transfer data from these experiments have, in general, been presented as a function of holdup. For example, Garwin and Smith's [6] data for a benzene dispersed in water system can be treated statistically to show

$$Uv = 1.09 \times 10^4 \, \phi \quad \text{BTU/hr ft}^3 \, ^\circ\text{F}$$
(hot water to benzene) (1)

$$Uv = 1.67 \times 10^4 \, \phi \quad \text{BTU/hr ft}^3 \, ^\circ\text{F}$$
(hot benzene to water) . (2)

The difference seems to correlate with drop diameter as the average drop size was 7.34 mm for the hot water runs and 6.71 mm for the hot benzene runs.

Rosenthal's [7] work dealt with the toluene drops emitted from orifices 7.2 mm and 3.0 mm in diameter. These data were reduced in terms of the volumetric flow ratio and the volumetric flow rate of the continuous phase

as

$$Uv = 4.28\ G_c^{1.13}\ \left(\frac{Gd}{G_c}\right)^{1.17} \text{ BTU/hr ft}^3\ ^\circ\text{F} \qquad (4)$$

(7.2 mm orifice)

$$Uv = 5.25\ G_c^{1.17}\ \left(\frac{G_d}{G_c}\right)^{1.13} \text{ BTU/hr ft}^3\ ^\circ\text{F} \qquad (5)$$

(3 mm orifice) .

For this system it was recommended that the best performance was obtained with $G_d/G_c = 2.87$.

Woodward's [9] data are reported primarily at a single volumetric flow ratio, $G_d/G_c = 2.5$. For this condition, the data correlate as

$$Uv = 1.2 \times 10^4\ \phi \text{ BTU/hr ft}^3\ ^\circ\text{F} \quad . \qquad (6)$$

In 1979, Jacobs et al. [12] carried out a study of liquid-liquid heat transfer characteristics for a 6 ft x 6 in diameter spray column using water as the continuous phase and insulating oil as the dispersed phase. Heat transfer results were presented as a function of the ratio of the volumetric flow rates and holdup and a correlation of the data was proposed in the form of

$$Uv = 45000\ (\phi - 0.05)\ e^{-0.57\ \frac{G_d}{G_c}} + 600 \text{ BTU/hr ft}^3\ ^\circ\text{F}$$

(for $\phi > 0.05$) (7)

and

$$Uv = 12000 \quad \phi \quad \text{BTU/hr ft}^3\ ^\circ\text{F}$$

$$(\text{for } \phi < 0.05) \quad . \qquad (8)$$

In Equations (2) - (6), $\phi$ represents the dispersed phase holdup and $G_d$ and $G_c$ represent volumetric flow rate of dispersed phase and continuous phase respectively.

Of all the heat transfer coefficients represented by Equations (2) - (8), Equations (7) and (8) best represent the actual heat transfer characteristics of the heat exchanger over a wide range of parameters. This is due to the fact that the correlation was based on all of the then existing data.

It is now realized that each of the above correlations has its own limitation and as of now there is not a single unified model to describe the mechanism of heat transfer in a spray type direct contact heat exchanger. Thus, one of the objectives of this dissertation is to achieve a reliable and accurate means of predicting the heat transfer coefficient between the two immiscible liquids.

The second objective of this dissertation is to formulate the two-phase flow and heat transfer equations to describe the preheater dynamics, so that the instabilities of such devices could be better investigated. Although similar types of governing equations have been employed to investigate nuclear reactor thermal hydraulics, which is a concurrent two-phase flow problem, no attempt has been made in the past to use the same principles for direct contact

heat exchanger dynamics.

The main characteristics of such flows, and the ones which create the special difficulties which the numerical analyst must overcome, are:

(1) Two fluids are dispersed within the column and so, "share," the same space. Each thus denies to the other the volume which it occupies itself;

(2) These fluids engage in frictional, thermal and mass-transfer interactions with each other, at rates which depend upon the local relative velocity, temperature differences, etc.;

(3) There are twice the usual number of equations to solve for momentum and for temperature, and the volume fraction of the two phases must also be computed at each point within the field.

The increase in the number of equations affects the difficulty of solution; for it ruins solution algorithms which are satisfactory for single-phase flows. In fact in early stages of numerical development, it was thought that these problems were inherently intractable, and many publications during the period 1974-1979 discussed the so called "ill-posed" nature of the problem presented by the governing differential equations. Later, it was demonstrated that the equations do present "well-posed" problems, the solutions do exist and can be found numerically. The final task of this dissertation is to put together a reliable

numerical technique for solving these nonlinear transient equations.

# CHAPTER 2

# MATHEMATICAL MODELING

## 2.1. Nature of Multiphase Flows

A multiphase system consists of a fluid phase or fluid medium and a particulate phase of any number of chemical components. When the fluid medium is a gas, the particulate phase may consist of solid particles or liquid droplets or both. When the fluid medium is a liquid, the particulate phase may consist of solid particles, gas bubbles, or liquid droplets immiscible to the fluid phase.

The dynamics of multiphase systems include momentum, energy, mass and charge transfers between the phases, depending on whether or not the process is influenced by the presence of a potential field.

Multiphase systems are of frequent occurrence in nature and among engineering equipment and processes. Some examples from nature include rainfall, snowdrifts, sandstorms and silted rivers. The list of multiphase systems which appear in engineering equipment and processes is immensely long. Here are a few examples [16]:

(1) Gas-solid particle systems: pneumatic conveyors, dust collectors, fluidized beds, heterogeneous reactors, metallized propellant rockets, aerodynamic ablation, xero-

graphy, cosmic dusts, nuclear fallout problems.

(2) Gas-liquid droplet systems: atomizers, scrubbers, dryers, absorbers, combustors, agglomeration, air pollution, gas cooling, evaporation, cryopumping.

(3) Liquid-gas bubble systems: absorbers, evaporators, heat exchangers, scrubbers, air lift pump, cavitation, flotation, aeration.

(4) Liquid-liquid droplet systems: heat exchangers, settling tanks, emulsifiers, extraction, homogenizing.

(5) Liquid-solid particle systems: fluidized beds, flotation, sedimentation.

A multiphase flow, in the context of this dissertation, is one which requires for its definition more than one set of velocities, temperatures, masses per unit volume, etc., at each location in the calculation domain. The material associated with each set of variables is what is meant by a "phase," in this connection.

## 2.2. Necessity of One-Dimensional Two-phase Flow Modeling for Spray Column Preheater

As mentioned previously, multiphase flow and heat transfer phenomena occur in many kinds of engineering equipment. Spray columns are typical of such equipment. They have received, recently, considerable attention for use as direct contact heat exchangers for geothermal power application. The ability to predict the detailed flow

fields in such equipment, as influenced by geometrical configuration and both normal and abnormal operating conditions, would assist both designers and operators of the equipment.

A one-dimensional two-phase flow model has been developed which allows various aspects of spray column preheater operation to be studied. One-dimensional two-phase flow models are useful tools, but only if the assumption of negligible variation of phase properties across the plane normal to the flow direction can be maintained. Virtually no theoretical results can be found which predict the transient behavior of a spray column. Although there are some experimental results on the heat transfer characteristics of spray column [6-12], there is not a single unified theoretical model to describe the mechanism of heat transfer in a spray column direct contact heat exchanger. Part of the reason for the lack of theoretical studies is due to the relatively short time that spray columns have been considered as primary heat exchangers. The one-dimensional two-phase flow model is a first step for studying the transient behavior and the mechanism of heat transfer in such a device.

## 2.3. One-Dimensional Two-phase Flow

### Governing Equations Formulation

The governing equations for one-dimensional two-phase flow are presented in this section in the primitive variable form. This allows the boundary conditions to be formulated

in a fairly simple form. A typical spray column preheater for geothermal application was shown in Figure 1 in which working fluid droplets are injected from a series of orifices at the bottom and brine (essentially water) is injected at the top. Thus, the two phases are the working fluid droplets and brine.

The main features and assumptions of the present formulation are as follows:

(1) The flow is one-dimensional and transient.

(2) The cross sectional area and periphery of the column are taken as independent of both distance and time.

(3) The dependent variables are velocity, void fraction, temperature and density for each phase, and the pressure, which is taken as common to both phases.

(4) The interphase friction is accounted for according to a linear law, whereas the frictional force exerted by the solid wall is neglected due to the large diameter of the column.

(5) The momentum diffusion terms representing the viscous force exerted by neighboring fluid elements have been neglected, because they are, at least in this situation, of much smaller magnitudes than those representing the pressure, gravity and interfluid frictional forces. However, if desired, they could be included.

(6) The conversion of mechanical and potential energy to thermal energy is neglected due to their small magnitude.

(7) Agglomeration of the working fluid droplets is ne-

glected due to existence of impurities.

For each phase, we have one equation of continuity which gives the conservation of mass of that phase. The continuity equation for the brine is

$$\frac{\partial}{\partial t}(\varepsilon\ \rho b) + \frac{\partial}{\partial x}(\varepsilon\ \rho b\ Vb\ ) = 0 \tag{9}$$

where

$t$ = time

$x$ = vertical coordinate measured from the bottom

$Vb$ = vertical velocity of brine

$\rho b$ = density of brine

$\varepsilon$ = void fraction of brine .

Similarly, the continuity equation for the working fluid droplets is

$$\frac{\partial}{\partial t}(\phi\ \rho w) + \frac{\partial}{\partial x}(\phi\ \rho w\ Vw) = 0 \tag{10}$$

where

$Vw$ = vertical velocity of working fluid droplets

$\rho w$ = density of working fluid droplets

$\phi$ = void fraction of working fluid droplets.

For each phase, the conservation of momentum gives the corresponding equations of motion for that phase. The equation of motion for the brine is

$$\frac{\partial}{\partial t}(\varepsilon\ \rho b\ Vb) + \frac{\partial}{\partial x}(\varepsilon\ \rho b\ Vb^2) = -\ \varepsilon\ \frac{\partial P}{\partial x}$$

$$-\ \overline{\underline{K}}\ (Vb - Vw) - \varepsilon\ \rho b\ g \qquad (11)$$

where

P = pressure

$\overline{\underline{K}}$ = interphase friction factor

g = vertical field acceleration,

and the equation of motion for the working fluid droplets is

$$\frac{\partial}{\partial t}(\phi\ \rho w\ Vw) + \frac{\partial}{\partial x}(\phi\ \rho w\ Vw^2) = -\ \phi\ \frac{\partial P}{\partial x}$$

$$-\ \overline{\underline{K}}\ (Vw - Vb) - \phi\ \rho w\ g. \qquad (12)$$

If we add Equations (11) and (12), we obtain the equation of motion for the mixture as a whole:

$$\frac{\partial}{\partial t}(\varepsilon\ \rho b\ Vb) + \frac{\partial}{\partial x}(\varepsilon\ \rho b\ Vb^2)$$

$$+\ \frac{\partial}{\partial t}(\phi\ \rho w\ Vw) + \frac{\partial}{\partial x}(\phi\ \rho w\ Vw^2) =$$

$$-\ (\varepsilon + \phi)\ \frac{\partial P}{\partial x} - (\varepsilon\ \rho b + \phi\ \rho w)\ g\ . \qquad (13)$$

Note that the interphase friction force has disappeared since it acts with equal magnitude to both phases.

Again, for each phase the conservation of energy gives the corresponding equation of energy of that phase. The equation of energy for the brine is

$$\frac{\partial}{\partial t}(\varepsilon\ \rho b\ Hb) + \frac{\partial}{\partial x}(\varepsilon\ \rho b\ Vb\ Hb)$$

$$= \frac{\partial}{\partial t}(\varepsilon\ P) - Uv\ (Tb - Tw) \qquad (14)$$

where

Hb = thermodynamic enthalpy of brine

Uv = interphase volumetric heat transfer coefficient

Tb = temperature of brine

Tw = temperature of working fluid droplets.

The corresponding equation of energy for working fluid droplets is

$$\frac{\partial}{\partial t}(\phi\ \rho w\ Hw) + \frac{\partial}{\partial x}(\phi\ \rho w\ Vw\ Hw)$$

$$= \frac{\partial}{\partial t}(\phi\ P) - Uv\ (Tw - Tb) \qquad (15)$$

where

Hw = thermodynamic enthalpy of working fluid droplets.

Once again, from the addition of Equation (14) and (15) we obtain the equation of energy for the mixture as a whole which does not include the interphase heat transfer term:

$$\frac{\partial}{\partial t}(\varepsilon\ \rho b\ Hb) + \frac{\partial}{\partial x}(\varepsilon\ \rho b\ Vb\ Hb)$$

$$+ \frac{\partial}{\partial t}(\phi\ \rho w\ Hw) + \frac{\partial}{\partial x}(\phi\ \rho w\ Vw\ Hw)$$

$$= \frac{\partial}{\partial t}((\varepsilon + \phi\ )P) \ . \qquad (16)$$

## 2.4. Auxiliary Relations

The set of partial differential equations presented in the previous section ordinarily has to be solved in conjunction with observance of constraints on the values of the variables represented by algebraic relations. These auxiliary relations express physical laws of various kinds. The auxiliary relations which are necessary for solution of the problem at hand are as follows:

(1) The two phases together occupy the whole of the space, thus

$$\varepsilon + \phi\ = 1 \ . \qquad (17)$$

(2) For each phase we require one equation of state which relates the density to thermodynamic enthalpy and pressure, that is

$$\rho b = f\ (Hb,\ P) \qquad (18)$$

and

$$\rho w = f\ (Hw,\ P) \ . \qquad (19)$$

(3) In addition we require for each fluid an equation which relates the temperature to thermodynamic enthalpy and pressure

$$Tb = f\ (Hb,\ P) \tag{20}$$

$$Tw = f\ (Hw,\ P) \tag{21}$$

(4) A suitable relation for interphase friction is

$$\overline{K} = Nw\ \pi\ Rw^2\ Cd\ 1/2\ \rho b\ |Vw - Vb| \tag{22}$$

where

Nw = number of working fluid droplets per unit volume

Rw = radius of each droplet

Cd = drag coefficient

$|Vw - Vb|$ = relative velocity between the two phases.

Nw is related to the void fraction and radius of working fluid droplets as

$$Nw = \frac{\phi}{\frac{4\pi}{3}\ Rw^3} \ . \tag{23}$$

Substituting Equation (23) into (22), we obtain the following expression for the interphase friction coefficient

$$\overline{k} = \frac{3\ \phi}{8\ Rw}\ Cd\ \rho b\ |Vw - Vb| . \tag{24}$$

The drag coefficient is in general a function of the Rey-

nolds number of the droplet, which in turn is a function of the droplet radius, brine kinematic viscosity and the relative velocity between the phases. However, in the present analysis the drag coefficient is assigned a constant value of 0.4 which is approximately valid for a Reynolds number range of $10^3$ - $10^5$. This range is typical of that calculated for the rise of hydrocarbon liquid droplets in water or geothermal brine.

(5) There are several ways of establishing the interphase volumetric heat transfer coefficient. One approach is to use the volumetric heat transfer coefficient obtained experimentally by Jacobs et al. [12], which is

$$Uv = 45000(C_1 - 0.05)e^{-0.57R} + 600 \quad (C_1>0.05)$$

$$Uv = 12000\ C_1 \quad (C_1<0.05) \qquad (25)$$

where

R = the ratio of volumetric flow rates equal to

$\phi$ Vw/$\varepsilon$ Vb

$C_1$ = experimentally determined constant .

The expression for the determination of $C_1$ is

$$(m+1)\ (1-R)\ (0.9\ C_1)^2 + (m+2)\ R\ (0.9\ C_1) - R = 0 \qquad (26)$$

where

m = constant equal to 1.39 for droplet Reynolds number greater than 500.

The second method for evaluation of Uv is to use a similar expression to Equation (25), except that $C_1$ is replaced by the actual void fraction of the working fluid droplets

$$U_v = 45000(\phi - 0.05)e^{-0.57R} + 600 \quad (\phi > 0.05)$$
$$U_v = 12000\,\phi \quad (\phi < 0.05). \qquad (27)$$

The third possible way for evaluation of Uv is to assume that the heat transfer to working fluid droplets is due to convection on the outside of the fluid spheres and that the internal resistance is negligible (i.e., the temperature inside the fluid sphere is uniform). For this method the volumetric heat transfer coefficient is

$$Uv = 4\,Nw\,\pi\,Rw^2\,\bar{h}m \qquad (28)$$

where

$\bar{h}m$ = mean heat transfer coefficient .

The mean heat transfer coefficient is related to droplet local average Nusselt number as

$$\bar{h}m = \frac{\overline{NuD}\,Kb}{2\,Rw} \qquad (29)$$

where

Kb = thermal conductivity of brine, temperature dependent

$\overline{NuD}$ = average Nusselt number .

Substituting Equations (29) and (23) into Equation (28) would result in

$$Uv = \frac{3}{2}\frac{\phi}{Rw^2} \; kb \; \overline{NuD} \; . \tag{30}$$

A suitable empirical relation for average Nusselt number is given by [1]

$$\overline{NuD} = 2.0 + 0.6 \; ReD^{1/2} \; Prb^{1/3} \tag{31}$$

where

ReD = droplet Reynolds number equal to

$$\frac{2 \; Rw \; \rho b \; |Vw - Vb|}{\mu b}$$

Prb = Prandtl number of brine equal to $\frac{Cpb \; \mu b}{kb}$

Cpb = specific heat of brine, temperature dependent

$\mu_b$ = dynamic viscosity of brine, temperature dependent .

The final method for establishing the mechanism of heat transfer between the phases is to assume that the outside heat transfer coefficient is very large and that conduction inside the fluid sphere is the dominating mechanism of heat transfer. In order to faciliate the use of this idea, one could use the one-dimensional transient spherical conduction equation with time dependent boundary condition. This equation is

$$\frac{\partial Tw}{\partial t_1} = \frac{\alpha w}{r^2} \frac{\partial}{\partial r}\left(r^2 \frac{\partial Tw}{\partial r}\right) \tag{32}$$

where

r = radial coordinate

αw = thermal diffusivity of working fluid, which is almost constant

$t_1$ = elapsed time from injection point equal to x/Vw.

The associated initial and boundary conditions are

$$Tw = Two \text{ at } t_1 = 0$$
$$Tw = \text{finite at } r = 0$$
$$Tw = Tb \text{ at } r = Rw \tag{33}$$

where

Two = temperature of working fluid droplets at the injection point.

When the time comes for solving Equation (32) subject to conditions (33), one may use two different approaches. The first is to assume that the radius of the working fluid droplets does not change significantly (Rw remains constant throughout the column). For this an analytical solution of Equations (32) and (33) is possible by using the method of Duhamel's superposition integral. This solution turns out to be

$$Tw = Two + \frac{2}{r\ Rw} \sum_{n=1}^{\infty} e^{-\frac{\alpha w\ n^2\ \pi^2}{Rw^2} t_1} \cdot$$

$$\sin \frac{n\ \pi\ r}{Rw} \left\{ -n\ \pi\ \alpha w\ (-1)^n \int_o^{t_1} e^{\frac{\alpha w\ n^2\ \pi^2}{Rw^2} s} \right.$$

$$\left. (Tb - Two)\ ds \right\} . \qquad (34)$$

Now, the mean temperature of the droplet is

$$Twm = \frac{1}{\frac{4\pi}{3} Rw^3} \int_o^{Rw} 4\ \pi\ r^2\ Tw\ dr . \qquad (35)$$

When Equation (34) is substituted into (35) and the integration is carried out, one obtains

$$Twm = Two + \frac{6\ \alpha w}{Rw^2} \sum_{n=1}^{\infty} e^{-\frac{\alpha w\ n^2\ \pi^2}{Rw^2}} \cdot$$

$$\int_o^{t_1} e^{\frac{\alpha w\ n^2\ \pi^2}{Rw^2} s} : (Tb - Two)\ ds. \qquad (36)$$

If, the integration in Equation (36) is done along small steps in time, Tb (brine temperature) could then be considered constant during this interval and the resulting expression for Twm would be

$$Twm = Two + \frac{6}{\pi^2} \cdot \sum_{n=1}^{\infty} \frac{1}{n^2} e^{-\frac{\alpha w\, n^2\, \pi^2}{Rw^2} t_1} \sum_{i=1}^{M} (Tb_i - Two) \cdot \left(e^{\frac{\alpha w\, n^2 \pi^2}{Rw^2} (\Delta t_i - \Delta t_{i-1})}\right) \quad (37)$$

where

$\Delta t$ = time step equal to $\Delta x/Vw$

M = number of time steps required to reach time $t_1$.

The second method for solving Equations (32) and (33) is to account for the change of the working fluid droplets radius through the column. Since no mass transfer is taking place in the column, the radius of a droplet is governed by

$$Rw = Rwo \left(\frac{\rho wo}{\rho w}\right)^{1/3} \quad (38)$$

where

Rwo = radius of droplet at injection point

$\rho wo$ = density of droplet at injection point.

For this method, there is no analytical solution. Thus, the solution of Equation (32) and (33) and the calculation of the mean temperature of droplets have to be performed numerically.

Once the mean temperature of the droplets is calcu-

lated, a temperature-pressure equation is used to find the corresponding enthalpy of the working fluid droplets, which in turn is used to find the enthalpy of the brine from Equation (16).

## 2.5. Solution of the Governing Equations

In Sections 2.3. and 2.4., the governing partial differential equations and required auxiliary relations were discussed. In order to represent a complete mathematical problem, the partial differential equations and auxiliary relations must be supplemented by initial and boundary conditions, expressing the particular situation to be investigated.

The first step in the solution is to convert the governing equations into a set of algebraic equations. This is accomplished by an implicit, upwind differencing technique. The resulting finite difference equations are strongly coupled and nonlinear. They, therefore, have to be solved by means of an iterative, guess and correct technique. A scheme has been devised which is similiar to the procedure of References [13-15].

An outline of this procedure, representing what must be done to advance the solution by a single time intervals is provided below:

(1) Determine the boundary conditions at the upper and lower limits of the solution domain.

(2) Select appropriate guesses to all the dependent

variables.

(3) Determine the pressure distribution which is appropriate to the finite difference equation of the equation of motion of the mixture as a whole.

(4) Solve for the equations of energy of the two phases, after which the densities are updated using the equations of state.

(5) Using the pressure distribution, solve for the velocity of the working fluid droplets.

(6) The error in the continuity equation for the two phases added together is computed, and thus the "source term" in the pressure-correction equation is generated.

(7) The pressure corrections are solved by a tridiagonal algorithm and the resulting corrections, proportional to pressure-correction differences are applied to the velocities and densities.

(8) The void fraction of the working fluid droplets is calculated using the equation of continuity for the working fluid droplets and the necessary correction is applied so as to insure that this value does not exceed the range from zero to unity (this limitation is necessary when the solution is far from convergence).

(9) The void fraction of the brine is obtained from Equation (17).

(10) A second phase of correction is introduced by finding the velocity of the brine from its continuity equation.

(11) Return to Step (3) and repeat the cycle of compu-

tations until the continuity errors computed at Step (6) are sufficiently small.

This concludes the description of the solution routine implemented in the one-dimensional modeling of a spray column preheater. The next chapter outlines these topics in detail as well as discussing the grid assignment and the boundary conditions.

# CHAPTER 3

## NUMERICAL MODELING

A finite difference numerical method will be used to obtain a solution to Equations (9)-(16) along with the appropriate auxiliary relations described in Section 2.4. The flow field is discretized into a finite number of computational cells suitable to the boundaries under consideration. The governing equations are then cast in discrete form to conform to the mesh. Appropriate boundary conditions are specified on all free fluid surfaces. The algorithm advances in time using an initial condition which is obtained through the solution of the steady state version of the governing equations until the desired time limit has been obtained.

Section 2.5 outlined the solution procedure, which will be the guide for the development of the finite difference equations presented here. A variety of methods are available for solving the governing equations, but as stated earlier, the method employed here is similar to that of References [13-15].

The relatively simple geometry of the flow domain is easily approximated with a rectangular grid as shown in Figure 2. With the exception of the velocities, all the dependent variables (i.e., pressure, void fraction, density,

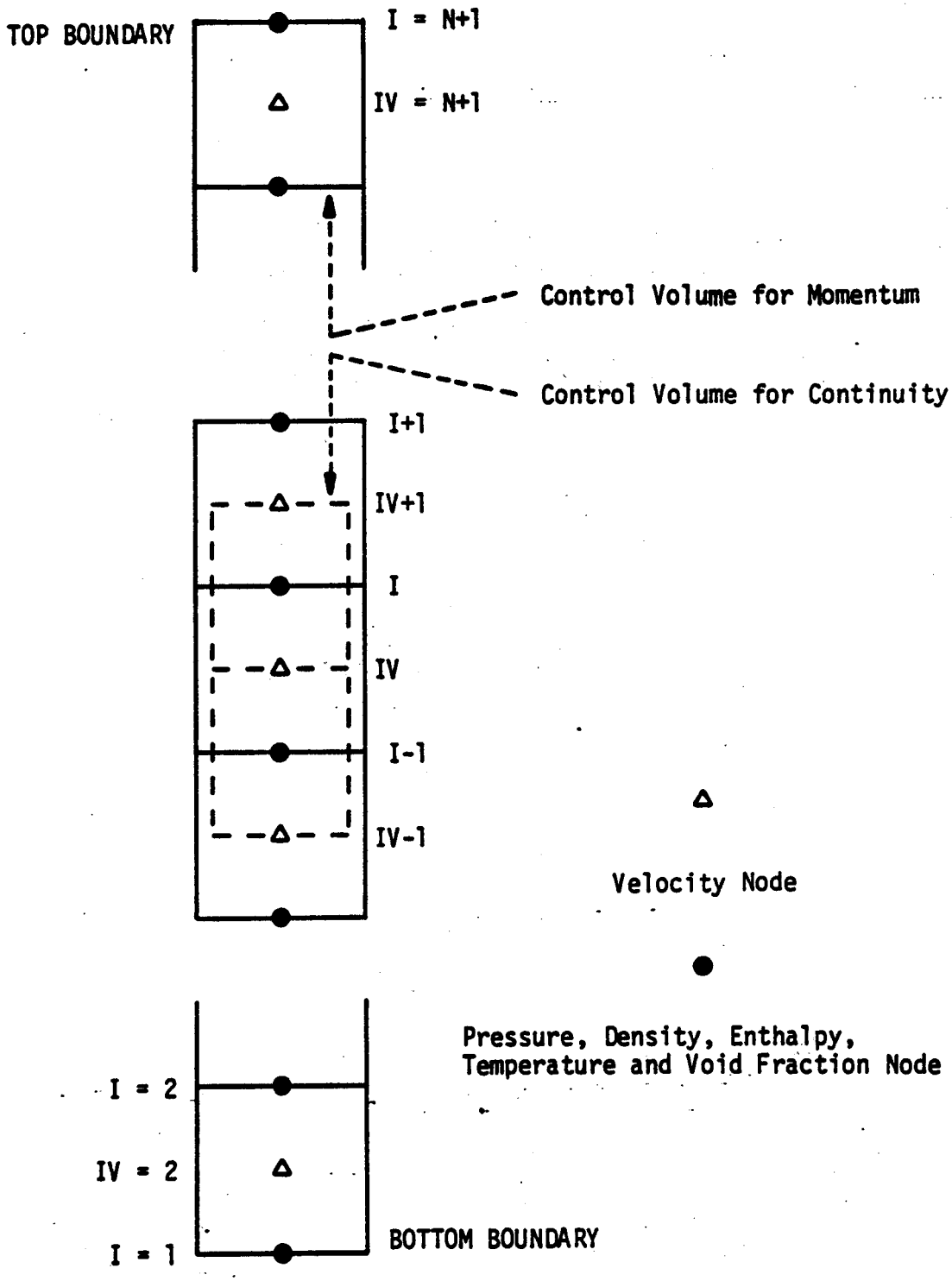


Figure 2. Schematic of finite difference nodes and control volumes.

temperature and enthalpy) are located at the grid nodes indicated by index "I." The velocities, however, are staggered in their own direction and lie midway between grid nodes. These velocity nodes are indicated by index "IV." It should be mentioned that index "N" represents the number of finite difference cells. This staggered grid system has two main advantages:

(1) The calculation of convection fluxes for a variable stationed at the grid nodes is simplified;

(2) The pressure gradients which drive the velocities can be evaluated more easily.

The formulation of the finite difference equations which will be discussed employs an implicit, upwind differencing technique. This technique has two main advantages:

(1) It is inherently more stable for this type of problem;

(2) A relatively large time step could be employed for studying the transient behavior.

## 3.1. Mass Conservation Equations

Consider the continuity control volume shown in Figure 2, which encloses a typical node (I). The continuity equation for flow of both phases through this control volume can be expressed as

$$G_{out} - G_{in} + \frac{\partial}{\partial t}(m) = 0 \qquad (39)$$

where

$G_{out}$ = mass flux out of the control volume

$G_{in}$ = mass flux into the control volume

$\frac{\partial}{\partial t}(m)$ = rate of mass accumulation within the control volume.

For the brine phase, the corresponding terms in Equations (39) are

$$G_{out} = A\, \varepsilon_I\, \rho b_I \left| Vb_{IV} \right| \tag{40}$$

$$G_{in} = A\, \varepsilon_{I+1}\, \rho b_{I+1} \left| Vb_{IV+1} \right| \tag{41}$$

$$\frac{\partial}{\partial t}(m) = \frac{A\Delta x}{\Delta t} \left( \varepsilon_I\, \rho b_I - \varepsilon_I^{\ominus}\, \rho b_I^{\ominus} \right) \tag{42}$$

where

$A$ = cross sectional area of the cell

$\Delta x$ = vertical node spacing

$\Delta t$ = time increment

$\ominus$ = signifies the previous time values.

Substituting the finite-difference equations for mass flux and mass accumulation (i.e., Equations (40) - (42)) into Equation (39) yields the following finite difference equation for the brine:

$$\left( \frac{\Delta x}{\Delta t}\, \rho b_I + \rho b_I \left| Vb_{IV} \right| \right) \varepsilon_I$$

$$-(\rho b_{I+1} |Vb_{IV+1}|)\ \epsilon_{I+1}$$

$$= \frac{\Delta x}{\Delta t}\ (\epsilon_I^{\ominus}\ \rho b_I^{\ominus}). \tag{43}$$

The finite difference equations for mass flux and mass accumulation of the working fluid droplets are

$$G_{out} = A\ \phi_I\ \rho w_I\ Vw_{IV+1} \tag{44}$$

$$G_{in} = A\ \phi_{I-1}\ \rho w_{I-1}\ Vw_{IV} \tag{45}$$

$$\frac{\partial}{\partial t}\ (m) = \frac{A\Delta x}{\Delta t}\ (\phi_I\ \rho w_I - \phi_I^{\ominus}\ \rho w_I^{\ominus}) . \tag{46}$$

Substituting these equations into Equation (39) gives the finite difference equation for the mass conservation of the working fluid droplets

$$(\frac{\Delta x}{\Delta t}\ \rho w_I + \rho w_I\ Vw_{IV+1})\ \phi_I$$

$$-(\rho w_{I-1}\ Vw_{Iv})\ \phi_{I-1} = \frac{\Delta x}{\Delta t}\ (\phi_I^{\ominus}\ \rho w_I^{\ominus}) . \tag{47}$$

Equations (43) and (47) are valid for a general interior node. Separate expressions must be obtained for the boundary nodes (i.e., node (I=1) and node (I=N+1)). At the inlet port for each phase, the mass flux is a known quantity and as a result, the finite difference form of the continuity equa-

tion for nodes representing the inlet port of each phase becomes simple. For the brine phase one obtains

$$\left(\frac{\Delta x}{2\Delta t}\,\rho b_{N+1} + \rho b_{N+1}\,|Vb_{N+1}|\right)\,\varepsilon_{N+1}$$

$$= \frac{\dot{mb}}{A} + \frac{\Delta x}{2\Delta t}\,(\varepsilon^{\ominus}_{N+1}\;\rho b^{\ominus}_{N+1}) \qquad (48)$$

where

$\dot{mb}$ = inlet mass flux of the brine.

Similarly, for the working fluid droplets, we have

$$\left(\frac{\Delta x}{2\Delta t}\,\rho w_1 + \rho w_1\;Vw_2\right)\,\phi_1$$

$$= \frac{\dot{mw}}{A} + \frac{\Delta x}{2\Delta t}\,(\phi^{\ominus}_1\;\rho w^{\ominus}_1) \qquad (49)$$

where

$\dot{mw}$ = inlet mass flux of the working fluid droplets.

The nodes representing the exit port of each phase contain only one velocity node and therefore, the ingoing and outgoing fluxes have a common velocity. With this observation, the mass conservation equation of the brine at its exit node is

$$\left(\frac{\Delta x}{2\Delta t}\,\rho b_1 + \rho b_1\,|Vb_2|\right)\,\varepsilon_1$$

$$-(\rho b_2\,|Vb_2|)\,\varepsilon_2 = \frac{\Delta x}{2\Delta t}\left(\varepsilon_1^{\ominus}\,\rho b_1^{\ominus}\right) \quad . \tag{50}$$

The corresponding equation for the working fluid becomes

$$\left(\frac{\Delta x}{2\Delta t}\,\rho w_{N+1} + \rho w_{N+1}\,Vw_{N+1}\right)\,\phi_{N+1}$$

$$-(\rho w_N\,Vw_{N+1})\,\phi_N = \frac{\Delta x}{2\Delta t}\left(\phi_{N+1}^{\ominus}\,\rho w_{N+1}^{\ominus}\right) \quad . \tag{51}$$

## 3.2 Momentum Equations

The cells for the continuity equations are located so as to enclose the nodal point; however, the cells for the momentum equations must be located between the nodes. Referring to Figure 2, one notes that the velocity in the continuity equation is not the velocity at the nodal point but the velocity halfway between nodes. Thus, the control volume used to solve for velocity is displaced from that used for the continuity equation and lies between grid lines (I) and (I-1).

The momentum equation for flow of both phases through this control volume requires that

$$M_{out} - M_{in} + \frac{\partial}{\partial t}(mo) = \Sigma\, F \tag{52}$$

where

$M_{out}$ = momentum flux out of the control volume

$M_{in}$ = momentum flux into the control volume

$\frac{\partial}{\partial t}(mo)$ = rate of momentum accumulation within the control volume

$\Sigma F$ = sum of the forces acting on the control volume.

The forces acting on the control volume consist of the forces due to pressure, gravity and the drag. With this in mind the corresponding terms in Equation (52) for the brine phase are:

$$M_{out} = \{ A \varepsilon_{I-1} \rho b_{I-1} |Vb_{I-1}| \} Vb_{IV} \tag{53}$$

$$M_{in} = \{ A \varepsilon_{I} \rho b_{I} |Vb_{I}| \} Vb_{IV+1} \tag{54}$$

$$\frac{\partial}{\partial t}(mo) = \frac{A\Delta x}{\Delta t}(\varepsilon_{IV} \rho_{IV} Vb_{IV} - \varepsilon^{\ominus}_{IV} \rho b^{\ominus}_{IV} Vb^{\ominus}_{IV}\} \tag{55}$$

$$\Sigma F = A \varepsilon_{IV} (P_{I-1} - P_{I}) - A\Delta x g \varepsilon_{IV} \rho b_{IV} + A \Delta x \bar{K}_{IV} (Vw_{IV} - Vb_{IV}) \tag{56}$$

where

$\bar{k}_{IV}$ = interphase friction.

Some of the properties and velocities in the finite difference relations presented were stated at off-location points. That is $\varepsilon_{IV}$, $\rho b_{IV}$ and $Vb_I$, for example, are not exactly defined at these identical locations. This will occur also for the other finite difference equations to be presented later (i.e., $\phi_{IV}$, $\rho w_{IV}$ and $Vw_I$). The method of handling these quantities is shown below and is readily seen to be a simple averaging across the desired location from locations that have been exactly defined.

$$\varepsilon_{IV} = \frac{1}{2}(\varepsilon_{I-1} + \varepsilon_I) \tag{57}$$

$$\phi_{IV} = \frac{1}{2}(\phi_{I-1} + \phi_I) \tag{58}$$

$$\rho b_{IV} = \frac{1}{2}(\rho b_{I-1} + \rho b_I) \tag{59}$$

$$\rho w_{IV} = \frac{1}{2}(\rho w_{I-1} + \rho w_I) \tag{60}$$

$$Vb_I = \frac{1}{2}(Vb_{IV} + Vb_{IV+1}) \tag{61}$$

$$Vw_I = \frac{1}{2}(Vw_{IV} + Vw_{IV+1}) \tag{62}$$

Substituting the finite difference equations for momentum flux, momentum accumulation and forces into Equation (52) yields

$$\left(\frac{\Delta x}{\Delta t}\,\varepsilon_{IV}\,\rho b_{IV} + \varepsilon_{I-1}\,\rho b_{I-1}\,|Vb_{I-1}| + \Delta x\,\bar{\bar{K}}_{IV}\right) Vb_{IV}$$

$$- \left(\varepsilon_{I}\,\rho b_{I}\,|Vb_{I}|\right) Vb_{IV+1} = \frac{\Delta x}{\Delta t}\left(\varepsilon^{\ominus}_{IV}\,\rho b^{\ominus}_{IV}\,Vb^{\ominus}_{IV}\right)$$

$$+ \varepsilon_{IV}\,(P_{I-1} - P_{I}) - \Delta x g\,\varepsilon_{IV}\,\rho b_{IV} + \Delta x\,\bar{\bar{K}}_{IV}\,Vw_{IV}. \quad (63)$$

For the working fluid phase, the corresponding expressions for terms in Equation (52) are

$$M_{out} = (A\,\phi_{I}\,\rho w_{I}\,Vw_{I})\,Vw_{IV} \quad (64)$$

$$M_{in} = (A\,\phi_{I-1}\,\rho w_{I-1}\,Vw_{I-1})\,Vw_{IV-1} \quad (65)$$

$$\frac{\partial}{\partial t}(mo) = \frac{A\Delta x}{\Delta t}\left(\phi_{IV}\rho w_{IV}\,Vw_{IV} - \phi^{\ominus}_{IV}\rho w^{\ominus}_{IV}\,Vw^{\ominus}_{IV}\right) \quad (66)$$

$$\Sigma F = A\,\phi_{IV}\,(P_{I-1} - P_{I}) - A\,\Delta x g\,\phi_{IV}\,\rho w_{IV}$$

$$+ A\,\Delta x\,\bar{\bar{K}}_{IV}\,(Vb_{IV} - Vw_{IV}). \quad (67)$$

Substitution of these expressions into Equation (52) yields the finite difference equation for the momentum conservation of the working fluid droplets.

$$\left(\frac{\Delta x}{\Delta t}\,\phi_{IV}\,\rho w_{IV} + \phi_{IV}\,\rho w_{IV}\,Vw_{I} + \Delta x\,\bar{\bar{K}}_{IV}\right) Vw_{IV}$$

$$- \left(\phi_{I-1}\rho w_{I-1}\,Vw_{I-1}\right) Vw_{IV-1} = \frac{\Delta x}{\Delta t}\,\phi^{\ominus}_{IV}\,\rho w^{\ominus}_{IV}\,Vw^{\ominus}_{IV})$$

$$+ \phi_{IV} (P_{I-1} - P_I) - \Delta x g \phi_{IV} \rho w_{IV} + \Delta x \bar{K}_{IV} Vb_{IV}. \quad (68)$$

Equations (63) and (68) are valid for a general interior velocity node as well as the velocity node that represents the exit port of each phase. At the inlet port of each phase, once again, the mass flux is a known quantity and the finite difference form of the momentum equation is simplified. For the brine, we will have

$$\left(\frac{\Delta x}{\Delta t} \varepsilon_{IV=N+1} \rho b_{IV=N+1} + \varepsilon_{I=N} \rho b_{I=N} |Vb_{I=N}| + \Delta x \bar{K}_{IV=N+1} - \frac{\dot{m}b}{A}\right) Vb_{IV=N+1}$$

$$= \frac{\Delta x}{\Delta t}(\varepsilon^{\ominus}_{IV=N+1} \rho b^{\ominus}_{IV=N+1} Vb^{\ominus}_{IV=N+1}) + \varepsilon_{IV=N+1} (P_{I=N} - P_{I=N+1}) - \Delta x g \varepsilon_{IV=N+1} \rho b_{IV=N+1} + \Delta x \bar{K}_{IV=N+1} Vw_{IV=N+1}. \quad (69)$$

For the working fluid, one obtains

$$\left(\frac{\Delta x}{\Delta t} \phi_{IV=2} \rho_{IV=2} + \phi_{I=2} \rho_{I=2} Vw_{I=2} + \Delta x \bar{K}_{IV=2} - \frac{\dot{m}w}{A}\right) Vw_{IV=2} = \frac{\Delta x}{\Delta t} (\phi^{\ominus}_{IV=2} \rho^{\ominus}_{IV=2} Vw^{\ominus}_{IV=2}) + \phi_{IV=2} (P_{I=1} - P_{I=2}) - \Delta x g \phi_{IV=2} \rho w_{IV=2} + \Delta x \bar{K}_{IV=2} Vb_{IV=2}. \quad (70)$$

During the course of computation, Equations (63), (68), (69) and (70) could be used to obtain the velocity of each phase. However, the recommended procedure is to use only one of the phases' momentum equations and the combined momentum equation of the mixture of the two phases. In this way, the interphase friction would only appear in one of these equations and the stability of the numerical scheme is enhanced. The combined momentum equation is obtained by simply adding the two momentum equation and noting that the sum of the two void fractions add to unity (i.e., $\varepsilon + \phi = 1$).

## 3.3 Energy Equations

In order to obtain finite difference equations for the conservation of energy, one must, first, establish which cells to use. These cells are the same as the ones used for derivation of the continuity finite difference equations. Depending on which method of heat transfer is employed, the corresponding energy equation would appear to be different. But, what is common to all the methods is the combined energy equation, which is always valid regardless of the nature of the heat transfer mechanism. Thus, this relation is derived first. Once again, reference is made to a typical continuity control volume which encloses a typical node (I). The energy equation for flow of both phases through this cell requires that

$$E_{out} - E_{in} + \frac{\partial}{\partial t}(E) = \dot{Q} \tag{71}$$

where

$E_{out}$ = energy flux out of the control volume

$E_{in}$ = energy flux into the control volume

$\frac{\partial}{\partial t}(E)$ = rate of energy accumulation within the control volume

$\dot{Q}$ = heat transfer rate into each phase .

As stated earlier, the heat transfer is from one phase to the other. Thus, when Equation (71) is used to obtain the energy equation of the mixture, the $\dot{Q}$ term will disappear. For the mixture, the corresponding terms in Equation (71) are

$$E_{out} = (A\ \varepsilon_I\ \rho b_I\ |Vb_{IV}|)\ Hb_I + (A\ \phi_I\ \rho w_I\ Vw_{IV+1})\ Hw_I \tag{72}$$

$$E_{in} = (A\ \varepsilon_{I+1}\ \rho b_{I+1}\ |Vb_{IV+1}|)\ Hb_{I+1} + (A\ \phi_{I-1}\ \rho w_{I-1}\ Vw_{IV})\ Hw_{I-1} \tag{73}$$

$$\frac{\partial}{\partial t}(E) = \frac{A\Delta x}{\Delta t}(\varepsilon_I\ \rho b_I\ Ub_I - \varepsilon_I^{\ominus}\ \rho b_I^{\ominus}\ Ub_I^{\ominus}) + \frac{A\Delta x}{\Delta t}(\phi_I\ \rho w_I\ Uw_I - \phi_I^{\ominus}\ \rho w_I^{\ominus}\ Uw_I^{\ominus}) . \tag{74}$$

In Equation (74) Ub and Uw are the internal energy of the brine and the working fluid respectively. The internal energy could be related to enthalpy and pressure as

$$Uw = Hw - \frac{P}{\rho w} \tag{75}$$

$$Ub = Hb - \frac{P}{\rho_b} . \tag{76}$$

Substitution of Equations (72) - (76) into Equation (71) will yield the finite difference equation for the conservation of energy of the mixture in the form

$$\begin{aligned}
&\left(\frac{\Delta x}{\Delta t}\ \varepsilon_I\ \rho b_I + \varepsilon_I\ \rho b_I\ |Vb_{IV}|\right)\ Hb_I \\
&- \left(\varepsilon_{I+1}\ \rho b_{I+1} |Vb_{IV+1}|\right)\ Hb_{I+1} \\
&+ \left(\frac{\Delta x}{\Delta t}\ \phi_I\ \rho w_I + \phi_I\ \rho w_I\ Vw_{IV+1}\right)\ Hw_I \\
&- \left(\phi_{I-1}\ \rho w_{I-1}\ Vw_{IV}\right)\ Hw_{I-1} \\
&= \frac{\Delta x}{\Delta t}\left(\varepsilon_I^{\ominus}\ \rho b_I^{\ominus}\ Hb_I^{\ominus} + \phi_I^{\ominus}\ \rho w_I^{\ominus}\ Hw_I^{\ominus}\right) \\
&+ \frac{\Delta x}{\Delta t}\left(\varepsilon_I\ P_I + \phi_I\ P_I - \varepsilon_I^{\ominus}\ P_I^{\ominus} - \phi_I^{\ominus}\ P_I^{\ominus}\right) .
\end{aligned} \tag{77}$$

Once again, this equation is valid for a general interior node. The boundary conditions for this equation are that the enthalpy of the brine is fixed at its incoming lo-

cation (i.e., node (I = N+1)) and the enthalpy of the working fluid is known at its respective incoming location (i.e., node (I = 1)). At the outlet port of the brine, zero gradient is assumed for the enthalpy of the brine.

We now have to turn our attention to the second enthalpy equation, which as stated earlier, would have a different look depending upon the method chosen to evaluate the heat transfer coefficient. If the interphase heat transfer is assumed to be either described by the experimentally determined volumetric heat transfer coefficient or where the heat transfer is limited by outside convection, all that is needed is an enthalpy equation for the brine phase alone. In this connection, the appropriate terms in Equation (71) are

$$E_{out} = (A\ \varepsilon_I\ \rho b_I\ |Vb_{IV}|)\ Hb_I \tag{78}$$

$$E_{in} = (A\ \varepsilon_{I+1}\ \rho b_{I+1}\ |Vb_{IV+1}|)\ Hb_{I+1} \tag{79}$$

$$\frac{\partial}{\partial t}(E) = \frac{A\Delta x}{\Delta t}(\varepsilon_I\ \rho b_I\ Ub_I - \varepsilon_I^{\ominus}\ \rho b_I^{\ominus}\ Ub_I^{\ominus}) \tag{80}$$

$$\dot{Q} = A\Delta x\ Uv_I\ (Tb_I - Tw_I) \tag{81}$$

where depending on the method employed for heat transfer, the expression for $Uv_I$ is obtained from one of the equations (25) - (31). Substitution of Equations (76) and (78) - (81) into Equation (71) will yield the brine's finite dif-

ference form of the energy equation, which is

$$\left(\frac{\Delta x}{\Delta t}\,\varepsilon_I\,\rho_I + \varepsilon_I\,\rho b_I\,|Vb_{IV}|\right)Hb_I$$

$$- \left(\varepsilon_{I+1}\,\rho b_{I+1}\,|Vb_{IV+1}|\right)\,Hb_{I+1}$$

$$= \frac{\Delta x}{\Delta t}\left(\varepsilon_I^{\ominus}\,\rho b_I^{\ominus}\,Hb_I^{\ominus}\right) - \Delta x\;Uv_I\left(Tb_I - Tw_I\right)$$

$$+ \frac{\Delta x}{\Delta t}\left(\varepsilon_I\,P_I - \varepsilon_I^{\ominus}\,P_I^{\ominus}\right) \quad . \tag{82}$$

For the case where heat transfer is controlled by conduction within the drops, assuming no change in the drop radius, Equation (37) is solved for the mean temperature of the droplets in the column. Once this temperature is found, use is made of the temperature - enthalpy relation to obtain the enthalpy of the working fluid droplets, after which Equation (77) is used to give the enthalpy of the brine.

## 3.4 Finite Difference Formulation for the Solution of the Conduction Equation for the Expanding Droplet

The expression for the heat diffusion within the droplets, Equations (32), (33) and (38), is in the form of a partial differential equation, and has to be solved numerically using finite differences. This is done by dividing

the radius into small increments $\Delta r_{IR}$, with a nodal point at the beginning and end of each increment. Fourier's law of heat conduction and conservation of energy are applied to the incremental volume around each nodal point. A schematic of a few nodal points is shown in Figure 3.

Applying the law of conservation of energy on the volume surrounding the central node in Figure 3 gives

$$q_{in} - q_{out} = \frac{\partial}{\partial t} (E) \tag{83}$$

where

$q_{in}$ = heat flux into the control volume

$q_{out}$ = heat flux out of the control volume.

The expression for the heat flux into the control volume is

$$q_{in} = Kw\ 4\ \pi\ (r - \frac{1}{2}\ \Delta r_{IR-1})^2\ (\frac{Tw_{IR-1} - Tw_{IR}}{\Delta r_{IR-1}}) \tag{84}$$

whereas, the expression for the heat flux out of the control volume would be

$$q_{out} = Kw\ 4\ \pi\ (r + \frac{1}{2}\ \Delta r_{IR})^2\ (\frac{Tw_{IR} - Tw_{IR+1}}{\Delta r_{IR}}) \tag{85}$$

where

Kw = thermal conductivity of the working fluid.

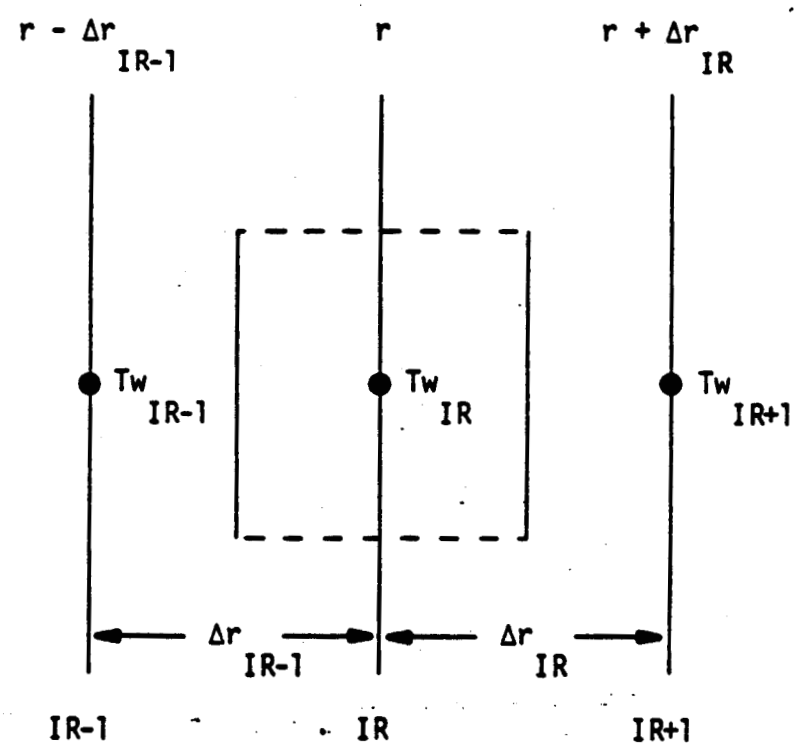


Figure 3. Schematic of nodes for finite difference solution of the transient spherical heat conduction equation within an expanding droplet.

The expression for the rate of energy accumulation is

$$\frac{\partial}{\partial t}(E) = \rho w \, Cpw \, 4 \pi r^2 \left(\frac{1}{2} \Delta r_{IR-1} + \frac{1}{2} \Delta r_{IR}\right) \cdot \left(\frac{Tw_{IR} - Tw^{\ominus}_{IR}}{\Delta t_1}\right) \tag{86}$$

where

Cpw = specific heat of the working fluid

$\Delta t_1$ = time increment based on $t_1$.

In deriving Equations (84) - (85), central differencing is used for the heat flux terms; however, upwind differencing is employed for the energy storage rate. Substituting Equation (84) - (86) into Equation (83) yields the finite difference equation for the heat diffusion within the droplet

$$\left\{\left(r - \frac{1}{2} \Delta r_{IR-1}\right)^2 \frac{1}{\Delta r_{IR-1}}\right\} Tw_{IR-1}$$

$$- \left\{\left(r - \frac{1}{2} \Delta r_{IR-1}\right)^2 \frac{1}{\Delta r_{IR-1}} + \left(r + \frac{1}{2} \Delta r_{IR}\right)^2 \frac{1}{\Delta r_{IR}}\right.$$

$$\left. + \frac{1}{\alpha w} r^2 \left(\frac{1}{2} \Delta r_{IR-1} + \frac{1}{2} \Delta r_{IR}\right) \frac{1}{\Delta t_1}\right\} Tw_{IR}$$

$$+ \left\{\left(r + \frac{1}{2} \Delta r_{IR}\right)^2 \frac{1}{\Delta r_{IR}}\right\} Tw_{IR+1}$$

$$= - \left\{\frac{1}{\alpha w} r^2 \left(\frac{1}{2} \Delta r_{IR-1} + \frac{1}{2} \Delta r_{IR}\right) \frac{1}{\Delta t_1}\right\} Tw^{\ominus}_{IR} . \tag{87}$$

This equation is valid for every interior node. At the droplet center, the condition is simply

$$Tw_{IR=1} = Tw_{IR=2} . \quad (88)$$

At the droplet surface

$$Tw_{IR=NIR+1} = Tb_{IV} \quad (89)$$

where index "NIR" represents the number of increments between r = 0 and r = Rw, which is increasing along the column due to expansion of the droplet radius.

At this point attention is turned to the way in which these equations are solved. The solution always starts at the bottom of the column where the temperature and radius are known. The solution is then advanced to a new location in the column. Once this is done, the mean temperature of the droplets is obtained from numerical integration of Equation (35). The radius is expanded by an amount equal to $Rw_{IV} - Rw_{IV-1}$ (these values are obtained from Equation (38) based on a guessed density field) and the temperature values of each node is shifted outward to the previous node. The value at the center of the droplet is assumed to be the old value which existed at the center.

## 3.5 The Pressure-correction Equation

The pressure-correction procedure adopted in this work is a very important part of the whole solution routine. After a cycle of calculation, there is found to be a net accumulation or loss of mass from each cell. Thus, a technique must be developed to eliminate these errors as the solution advances. Once these errors are eliminated, the solution to the problem is assumed to be complete. The first step in devising the pressure-correction equation is to add the two continuity equations (i.e., Equation (43) and (47). Thus

$$\left\{ \frac{\Delta x}{\Delta t} \rho b_I + \rho b_I \left(-Vb_{IV}\right)\right\} \varepsilon_I - \left\{ \rho b_{I+1} \left(-Vb_{IV+1}\right)\right\}\varepsilon_{I+1}$$

$$+ \left(\frac{\Delta x}{\Delta t} \rho w_I + \rho w_I \, Vw_{IV+1}\right) \phi_I - \left\{\rho w_{I-1} \, Vw_{IV}\right) \phi_{I-1}$$

$$- \frac{\Delta x}{\Delta t} \left\{\varepsilon_I^{\ominus} \rho b_I^{\ominus} + \phi_I^{\ominus} \rho w_I^{\ominus}\right) = 0 \, . \qquad (90)$$

Since the brine velocity is negative with respect to the coordinate chosen, the absolute values appearing in the brine continuity equation are replaced by a negative sign multiplied by the velocity of the brine. After each cycle of calculation, the values of the density, velocity and volume fraction are inserted into this equation to find the resulting error in each continuity cell. This error is denoted by the symbol $ER_I$. It is now assumed that all the pressures in the field will be modified so as to change the

densities and the velocities, and thereby to bring about the elimination of the errors. Thus, from Equation (90) the corrections to the densities and velocities resulting from the corrections to the pressures are governed by

$$\left\{ \frac{\Delta x}{\Delta t} \rho b'_I + \rho b_I \left(-Vb'_{IV}\right)\right\}\varepsilon_I$$

$$- \left\{\rho b_{I+1} \left(-Vb'_{IV+1}\right) \right\}\varepsilon_{I+1} + \left(\frac{\Delta x}{\Delta t} \rho w'_I + \rho w_I \, Vw'_{IV+1}\right)\phi_I$$

$$- \left\{\rho w_{I-1} \, Vw'_{IV}\right\} \phi_{I-1} = - ER_I \qquad (91)$$

where the primed quantities are the corrections that have to be made to the stored values. These primed quantities can all be expressed linearly in terms of the pressure corrections at in cell and neighbor grid points. Thus, for example

$$Vw'_{IV} = \frac{\partial Vw_{IV}}{\partial P_{I-1}} P'_{I-1} + \frac{\partial Vw_{IV}}{\partial P_I} P'_I + \frac{\partial Vw_{IV}}{\partial Vb_{IV}} Vb'_{IV} \qquad (92)$$

$$Vb'_{IV} = \frac{\partial Vb_{IV}}{\partial P_{I-1}} P'_{I-1} + \frac{\partial Vb_{IV}}{\partial P_I} P'_I + \frac{\partial Vb_{IV}}{\partial Vw_{IV}} Vw'_{IV} \qquad (93)$$

$$\rho b'_I = \frac{\partial \rho b_I}{\partial P_I} P'_I \qquad (94)$$

$$\rho w'_I = \frac{\partial \rho w_I}{\partial P_I} P'_I . \qquad (95)$$

The differential coefficients associated with the velocity changes result from differentiation of the finite difference momentum equations and the ones associated with the density changes are obtained from a least square curve fit to the tabulated values of density versus pressure in the pressure region of interest. The result of combining Equations (91) - (95) is a system of simultaneous equations for the p''s, the solution of which could be used to find the corrections to the densities and the velocities, which in turn could be added to the stored values of these quantities. The result is a set of densities and velocities which satisfy overall continuity at every point. The final note is to remember that one has to combine Equations (92) and (93) so that $Vw'_{IV}$ and $Vb'_{IV}$ each appear separately. It is these resulting expressions for $Vw'_{IV}$ and $Vb'_{IV}$ which should be employed in the derivation of the pressure-correction equation.

The changes to the velocities and the densities which have resulted from the pressure corrections, though they have satisfied overall continuity, will have thrown most of the other equations out of balance. It is therefore necessary to repeat the cycle, so as to undo the damage. As stated earlier, what is to be hoped is that, at each repetition of the cycle, the errors which are to be corrected become smaller and smaller.

## 3.6 Outline of the Procedure

The task, for a typical problem, is to determine sets of values, for all the points of the grid, for all the time instants considered. The finite difference equations, together with the auxiliary relations are equal to the number of unknowns.

Because of the high degree of nonlinearity and interphase coupling of the equations, the task must be performed by iterative means. As stated earlier, the procedure adopted in this dissertation is similar to that of References [13-15]. This procedure was outlined in Section 2.5.

Finally, it should be mentioned that all the thermodynamic properties are evaluated using the subroutines of References [18-19].

# CHAPTER 4

# RESULTS AND DISCUSSION

## 4.1. Steady State Solution

Prior to evaluating the transient behavior of a direct contact heat exchanger, it is necessary to ascertain what type of heat transfer model best describes the actual performance of such a device. Steady state or at least quasi-steady state data are available for the operation of the 500 kWe direct contact heat exchanger constructed by Barber Nichols for the U.S. Department of Energy [17]. Thus, a data base exists for comparison with various models.

The 500 kWe direct contact heat exchanger is a 40 inch (1 meter) diameter spray column type direct contact heat exchanger. It is shown schematically in Figure 4. It was operated as a combined preheater, boiler and used East Mesa geothermal brine as the continuous phase and isobutane as the dispersed phase. Inlet and outlet temperatures for the two fluids as well as flow rates and pressure are reported. In addition, temperatures are recorded along the length of the column. An adequate heat transfer model should be able to predict these temperatures as well as the heights of the column using only the inlet parameters. In all the temperature versus height figures to be presented in this sec-

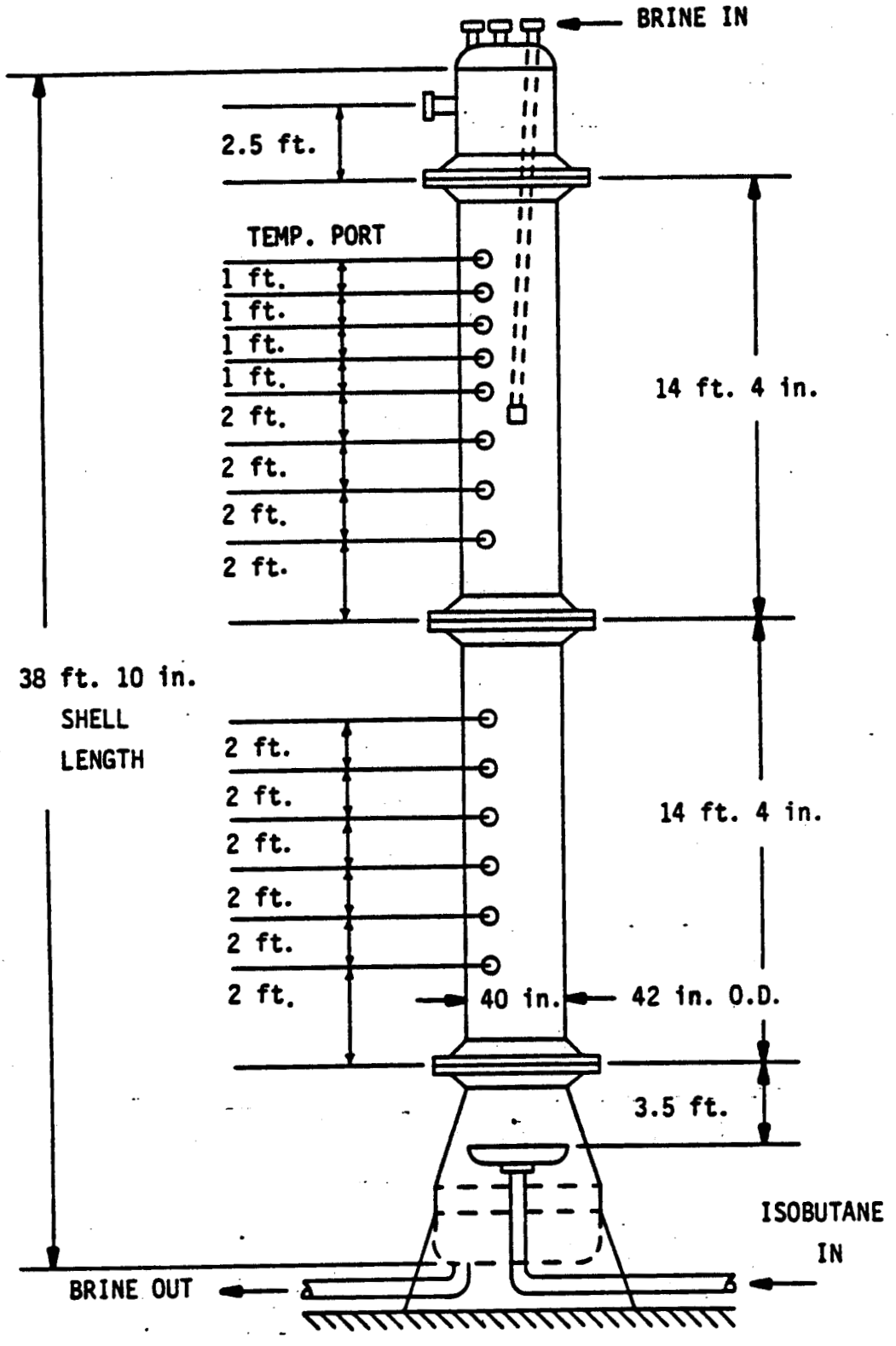


Figure 4. Schematic of 500 kWe direct contact heat exchanger.

tion, the curves with higher temperature profile belong to the brine while the curves with lower temperature profile belong to the working fluid.

Figures 5 through 8 show data from four different operating conditions of the 500 kWe direct contact heat exchanger. Figure 5 compares the first three possible methods for describing the heat transfer discussed in Chapter 2. Method I utilizes the correlation of Plass, Jacobs, and Boehm [12] and an empirical equation for holdup (see Equation (25)). Method II utilizes the same correlation, but uses local holdup values calculated from the two-phase flow equations developed herein. Method III uses Equation (31) which describes the external heat transfer to a totally mixed drop. It is clear from Figure 5 that the latter model is unacceptable as it overpredicts the heat transfer, that is, it predicts far too short of a preheater. Thus, Model III was eliminated from further consideration.

If one looked only at Figures 5 and 6, one would think that the empirical Model I would best describe the heat transfer; however, Figures 7 and 8 indicate that Model II best fits the data. The primary difference between the operating conditions for Figures 5 and 6 and Figures 7 and 8 is in the flow rate.

As the heat transfer was clearly not governed by the external heat transfer coefficients, at least as described by Method III, and neither Methods I nor II gave totally acceptable results, a fourth model was introduced. If one

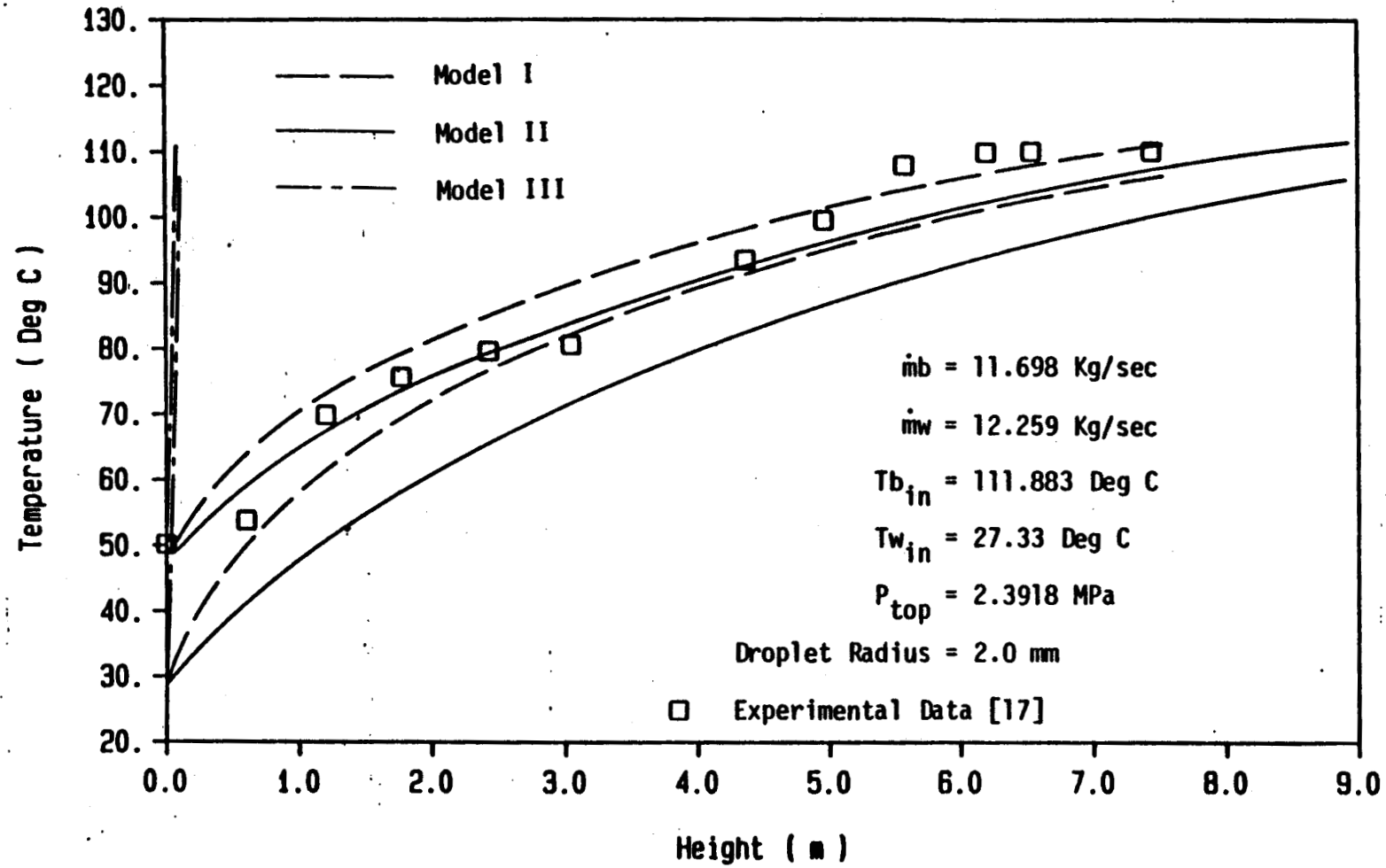


Figure 5. Temperature profile of the brine and the working fluid along the length of the column for comparison of models I, II and III.

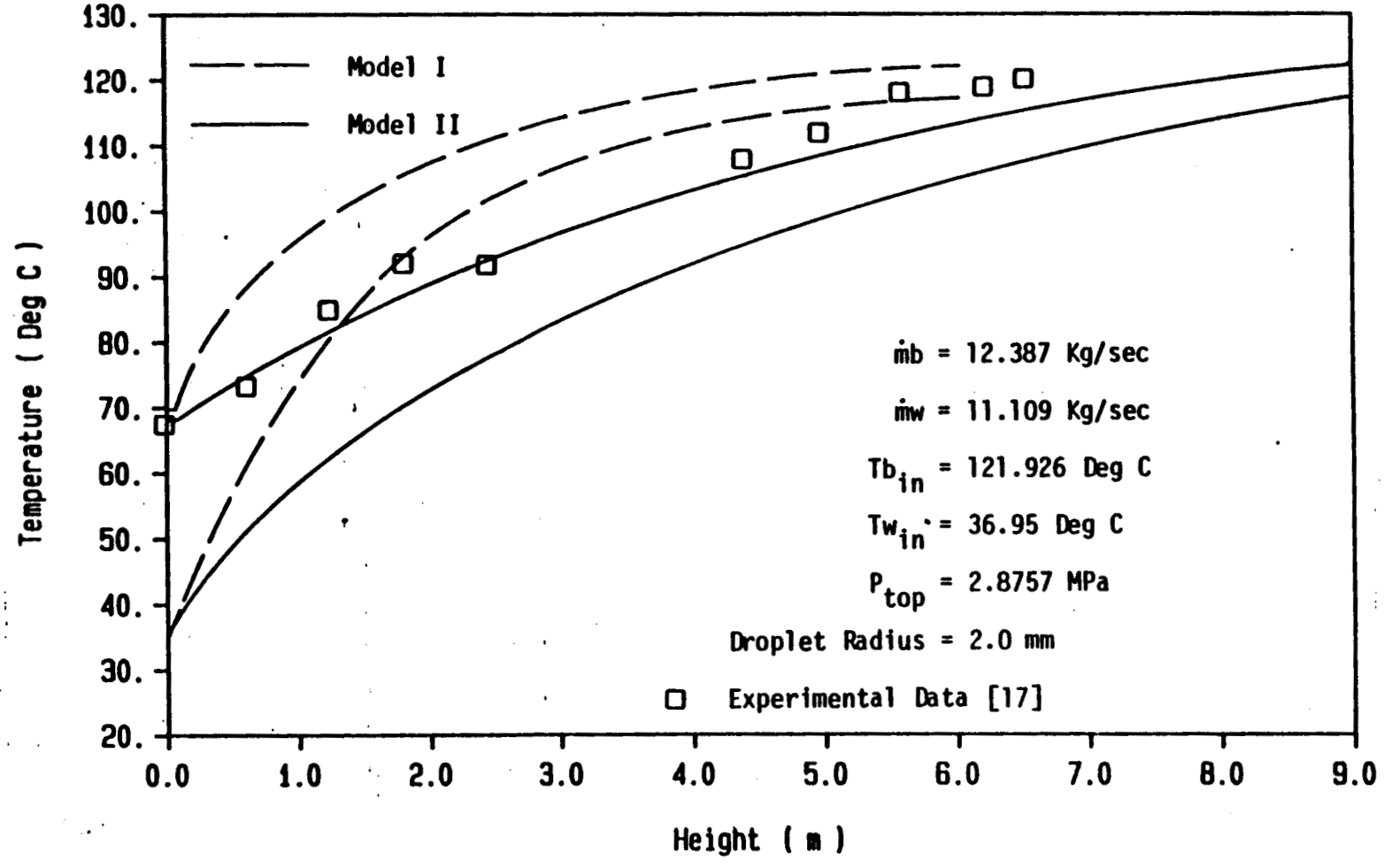


Figure 6. Temperature profile of the brine and the working fluid along the length of the column for comparing models I and II, $\dot{m}b$ = 12.387 Kg/sec, $\dot{m}w$ = 11.109 Kg/sec.

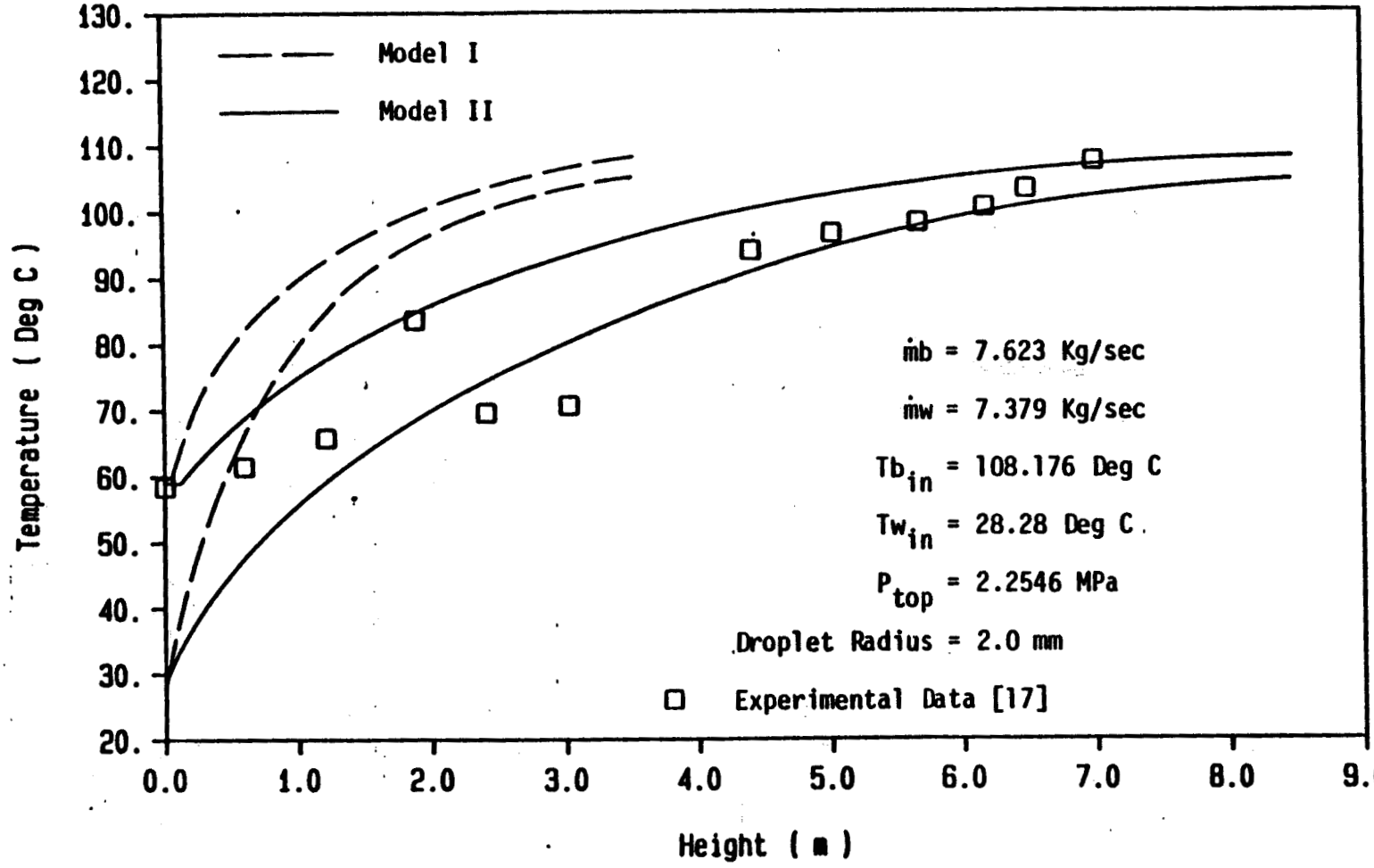


Figure 7. Temperature profile of the brine and the working fluid along the length of the column for comparing models I and II, $\dot{m}b$ = 7.623 Kg/sec, $\dot{m}w$ = 7.379 Kg/sec.

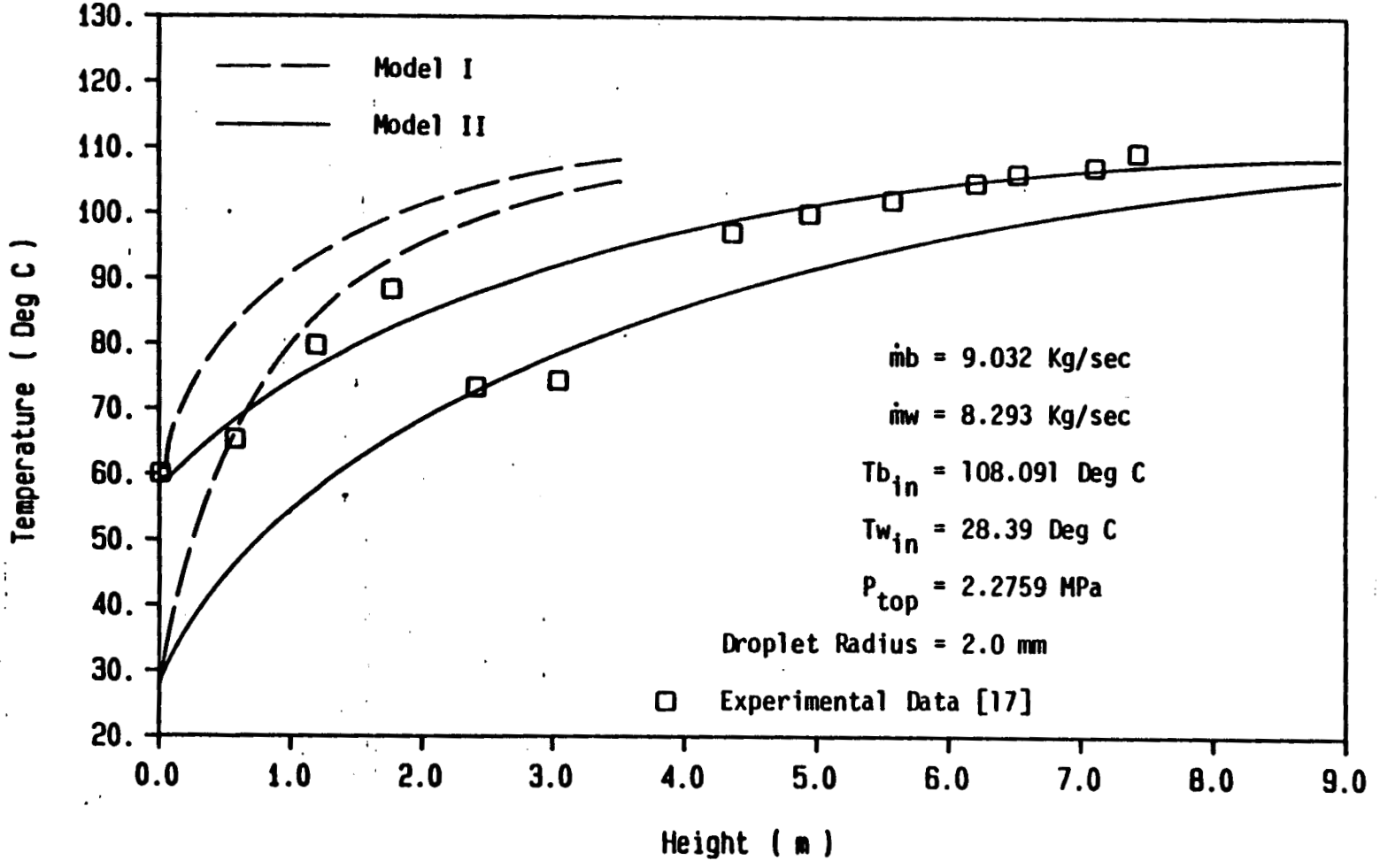


Figure 8. Temperature profile of the brine and the working fluid along the length of the column for comparing models I and II, $\dot{m}b$ = 9.032 Kg/sec, $\dot{m}w$ = 8.293 Kg/sec.

postulated that the dispersed phase was made up of drops which had no internal circulation, then the heat transfer could be dominated by internal conduction. The heat transfer would then be described by a transient conduction model such as the one described by Equation (32). Initially such a model was developed by assuming the drops would be of constant diameter even though it was known that a considerable change in density would occur for the operating conditions of the 500 kWe direct contact heat exchanger. The reason for this assumption was to cut down on the computer time of the solution, since as stated earlier, an analytical solution was available for this particular case. Figures 9 through 18 show results calculated for the constant diameter model for ten different operating conditions assuming drop radii of 1.6 and 2.0 mm. The 1.6 mm dimension was the supposed design condition for the inlet nozzle of the 500 kWe direct contact heat exchanger. It is clear for Figures 9 through 17 that sometimes the data are best fit by the 1.6 mm dimension and sometimes by the 2.0 mm dimension. On Figure 18 the bottom half of the column is best fit by the smaller drop size while the top of the column is best described by the larger size. It would, thus, seem that the change in drop diameter that could occur is important. Further, it is clear that the internal resistance to heat transfer is dominating the response of the column.

Figures 19 through 28 were obtained using a variable

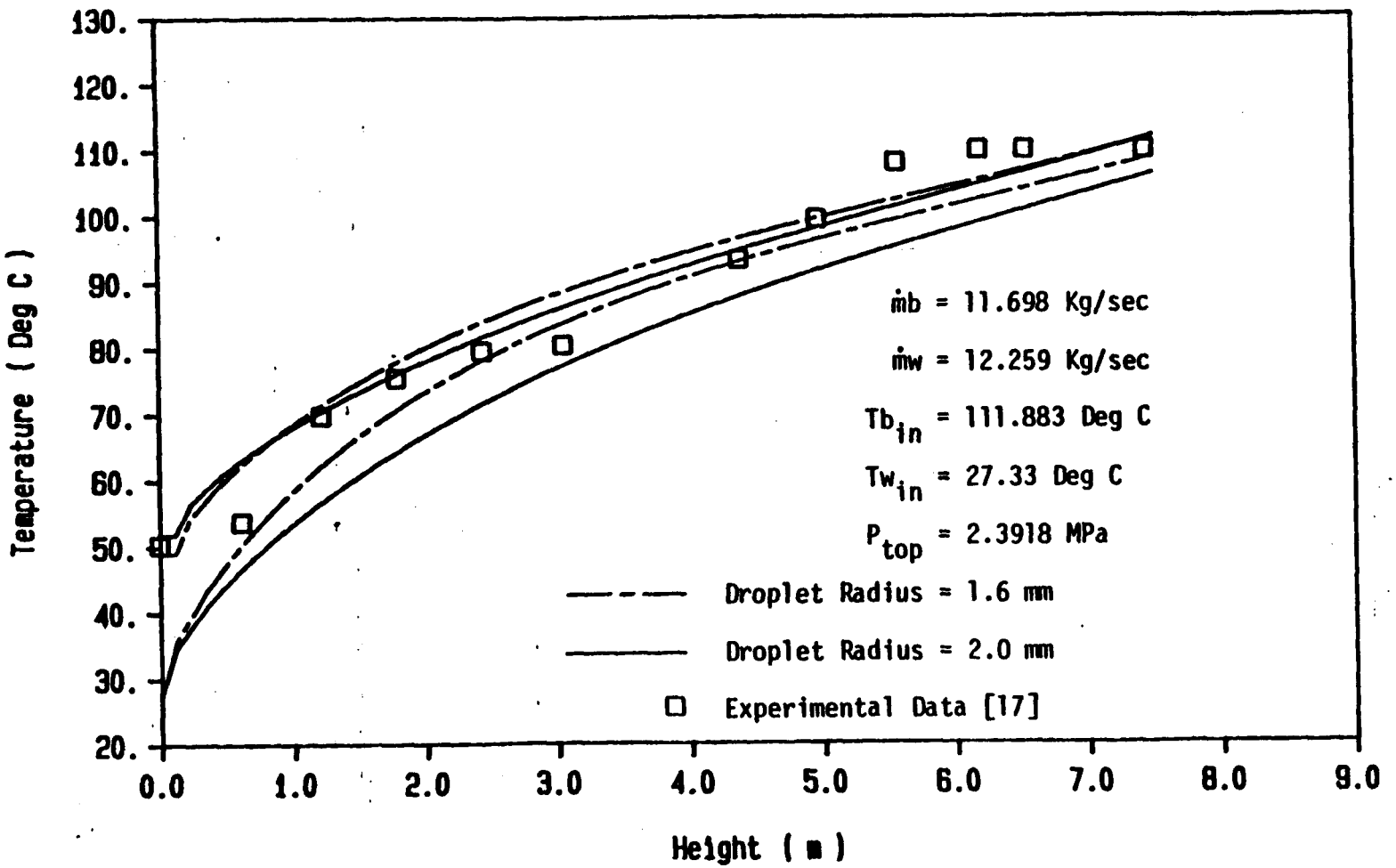


Figure 9. Temperature profile of the brine and the working fluid along the length of the column using constant diameter model, $\dot{m}b$ = 11.698 Kg/sec, $\dot{m}w$ = 12.259 Kg/sec.

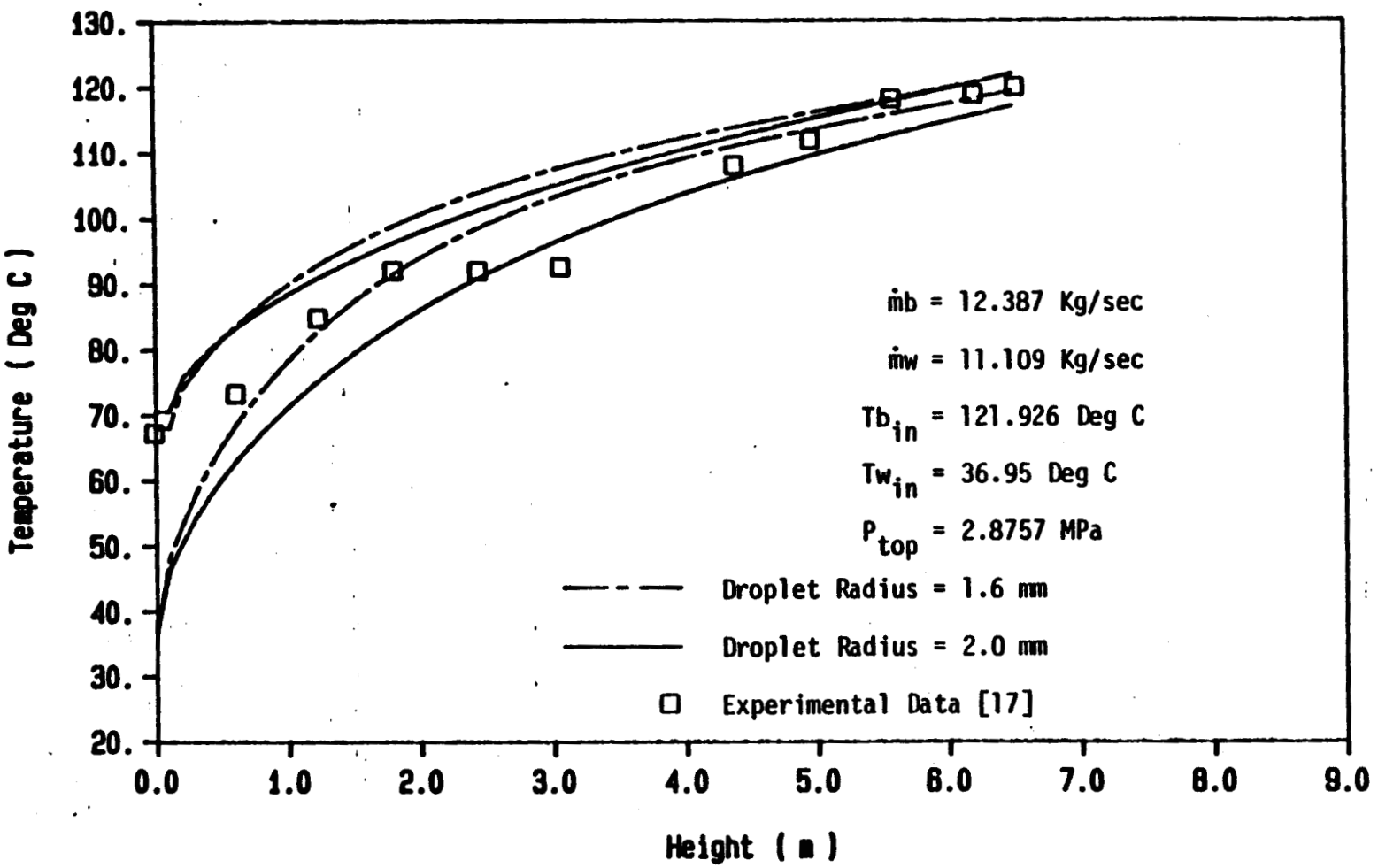


Figure 10. Temperature profile of the brine and the working fluid along the length of the column using constant diameter model, $\dot{m}b$ = 12.387 Kg/sec, $\dot{m}w$ = 11.109 Kg/sec.

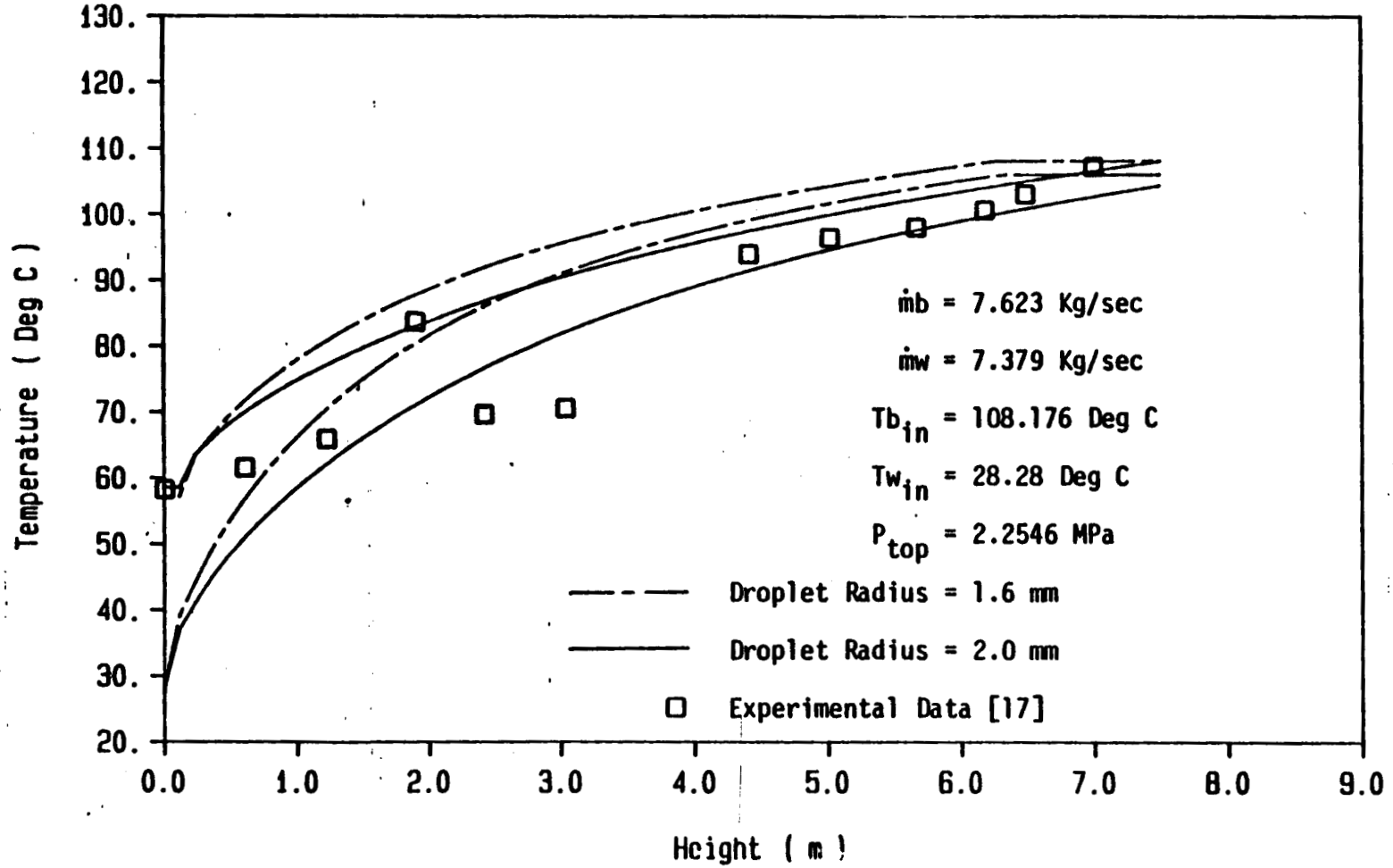


Figure 11. Temperature profile of the brine and the working fluid along the length of the column using constant diameter model, $\dot{m}b$ = 7.623 Kg/sec, $\dot{m}w$ = 7.379 Kg/sec.

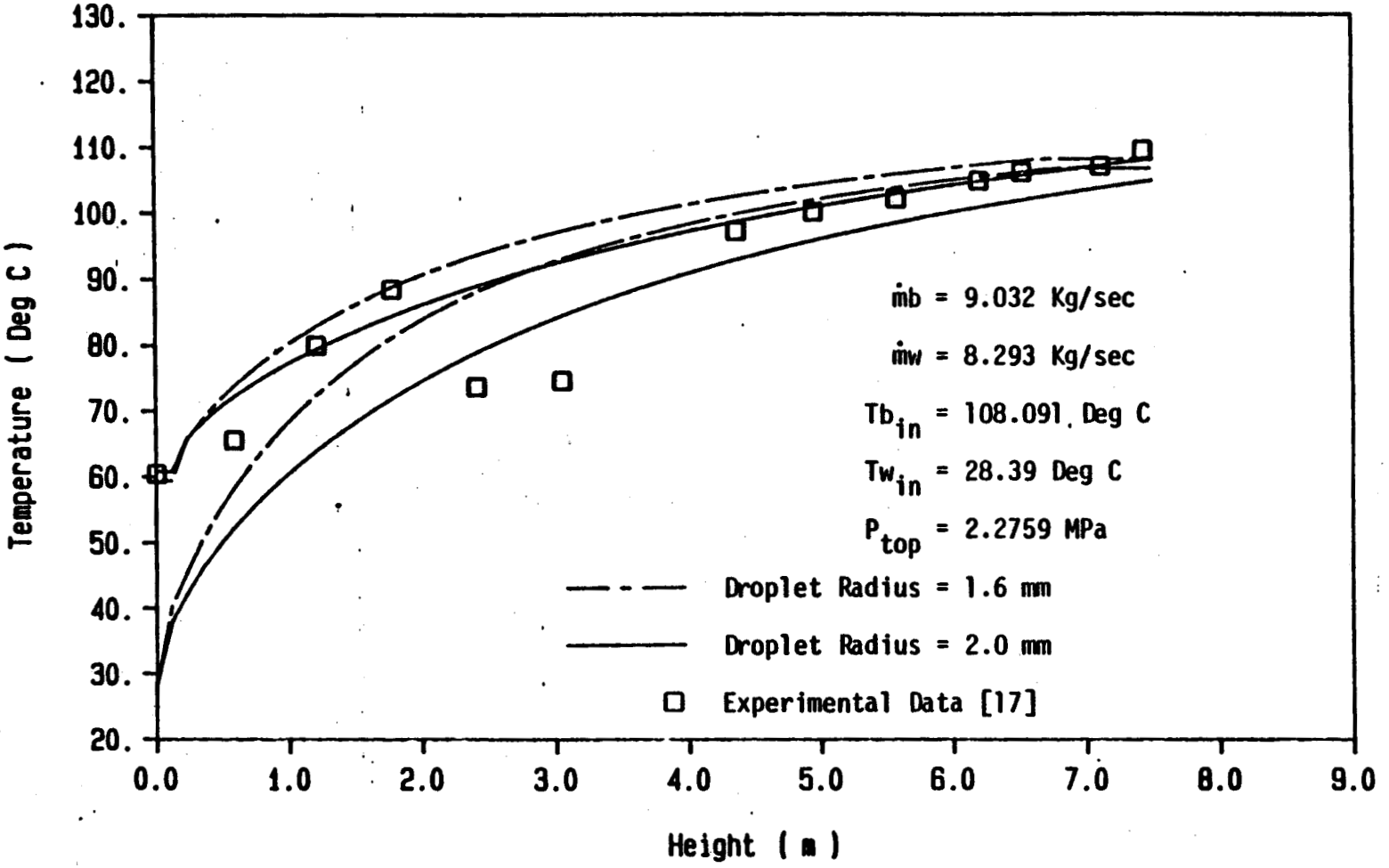


Figure 12. Temperature profile of the brine and the working fluid along the length of the column using constant diameter model, $\dot{m}b$ = 9.032 Kg/sec, $\dot{m}w$ = 8.293 Kg/sec.

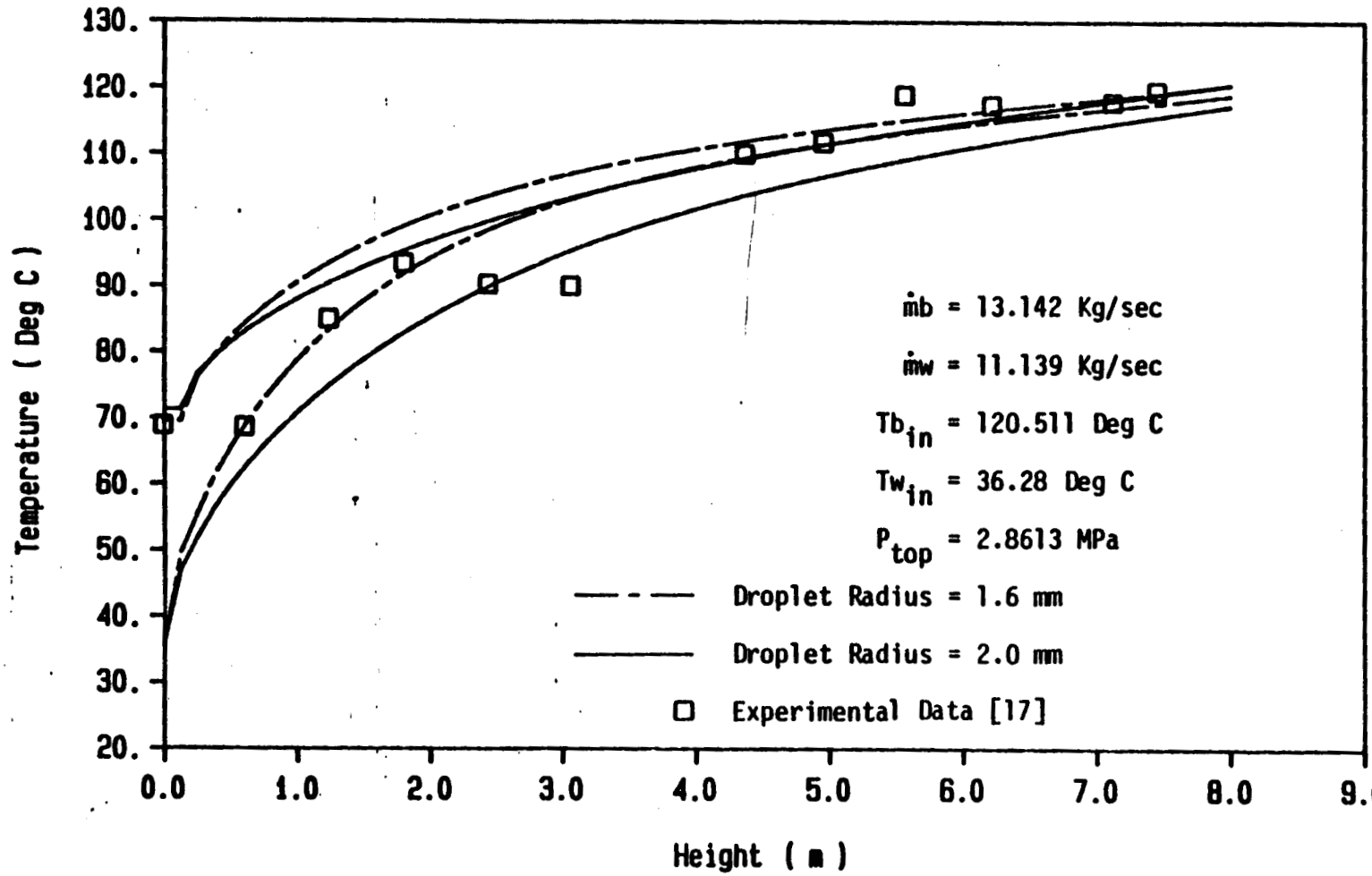


Figure 13. Temperature profile of the brine and the working fluid along the length of the column using constant diameter model, $\dot{m}b$ = 13.142 Kg/sec, $\dot{m}w$ = 11.139 Kg/sec.

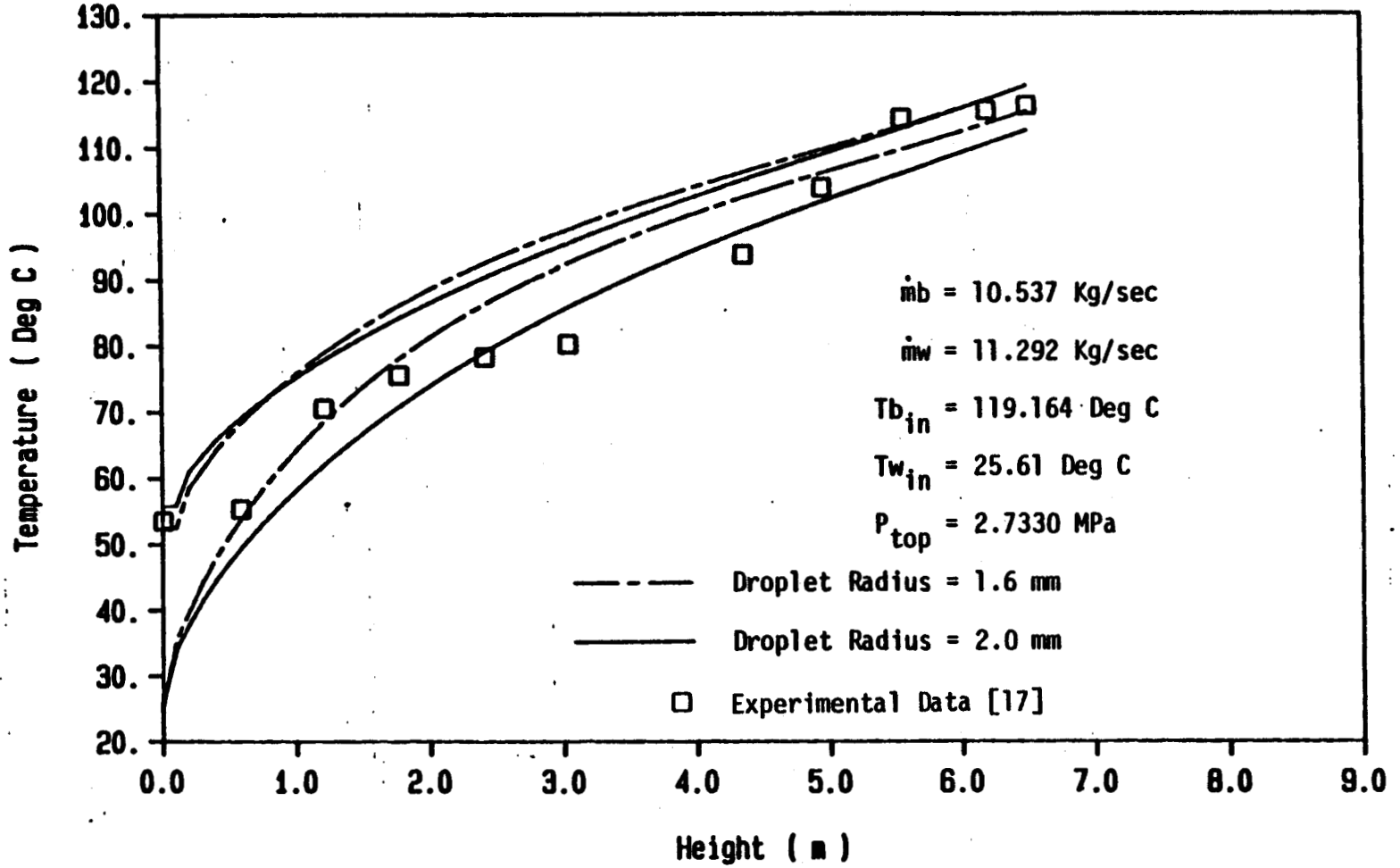


Figure 14. Temperature profile of the brine and the working fluid along the length of the column using constant diameter model, $\dot{m}b$ = 10.537 Kg/sec, $\dot{m}w$ = 11.292 Kg/sec.

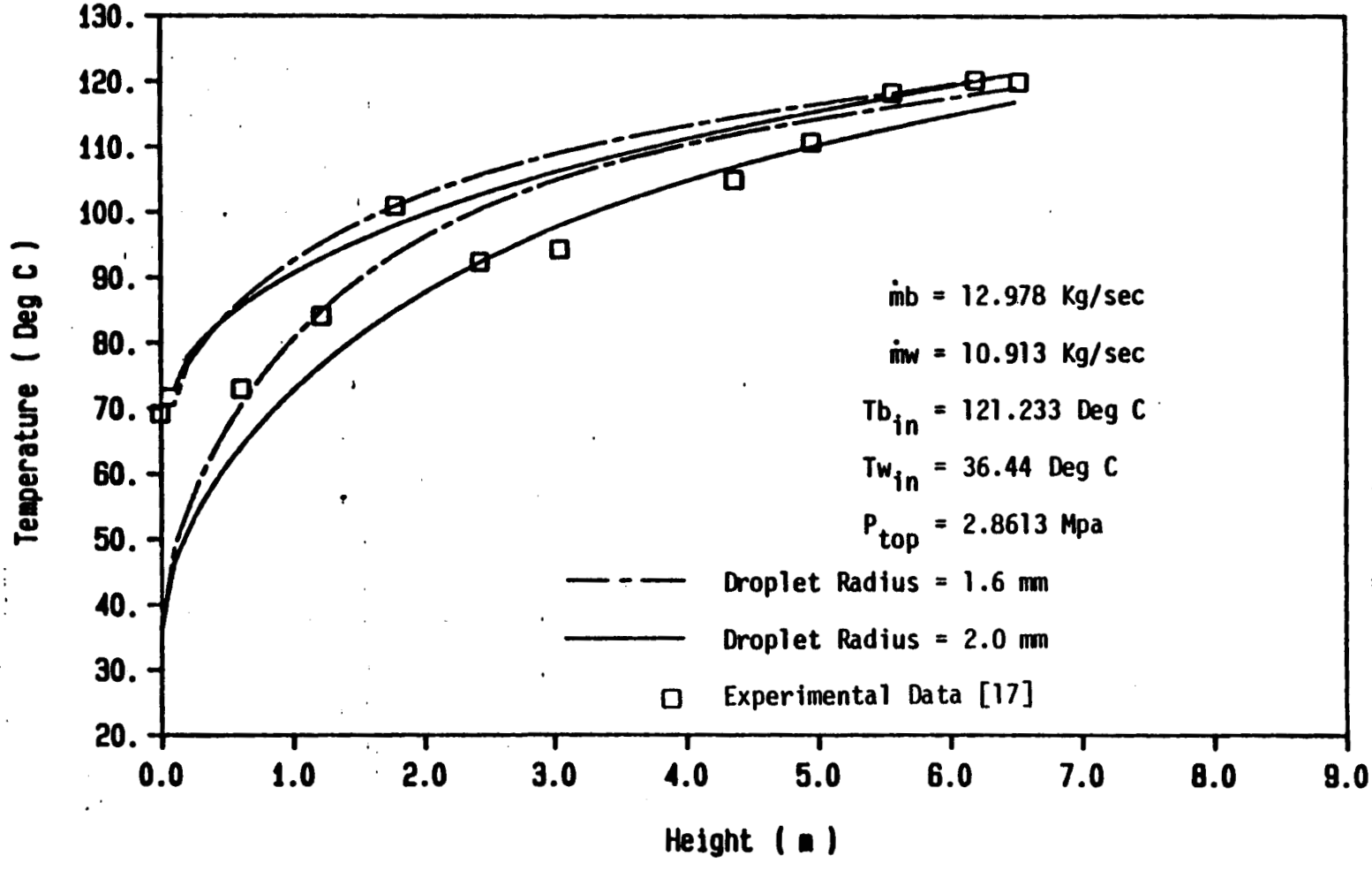


Figure 15. Temperature profile of the brine and the working fluid along the length of the column using constant diameter model, $\dot{m}b$ = 12.978 Kg/sec, $\dot{m}w$ = 10.913 Kg/sec.

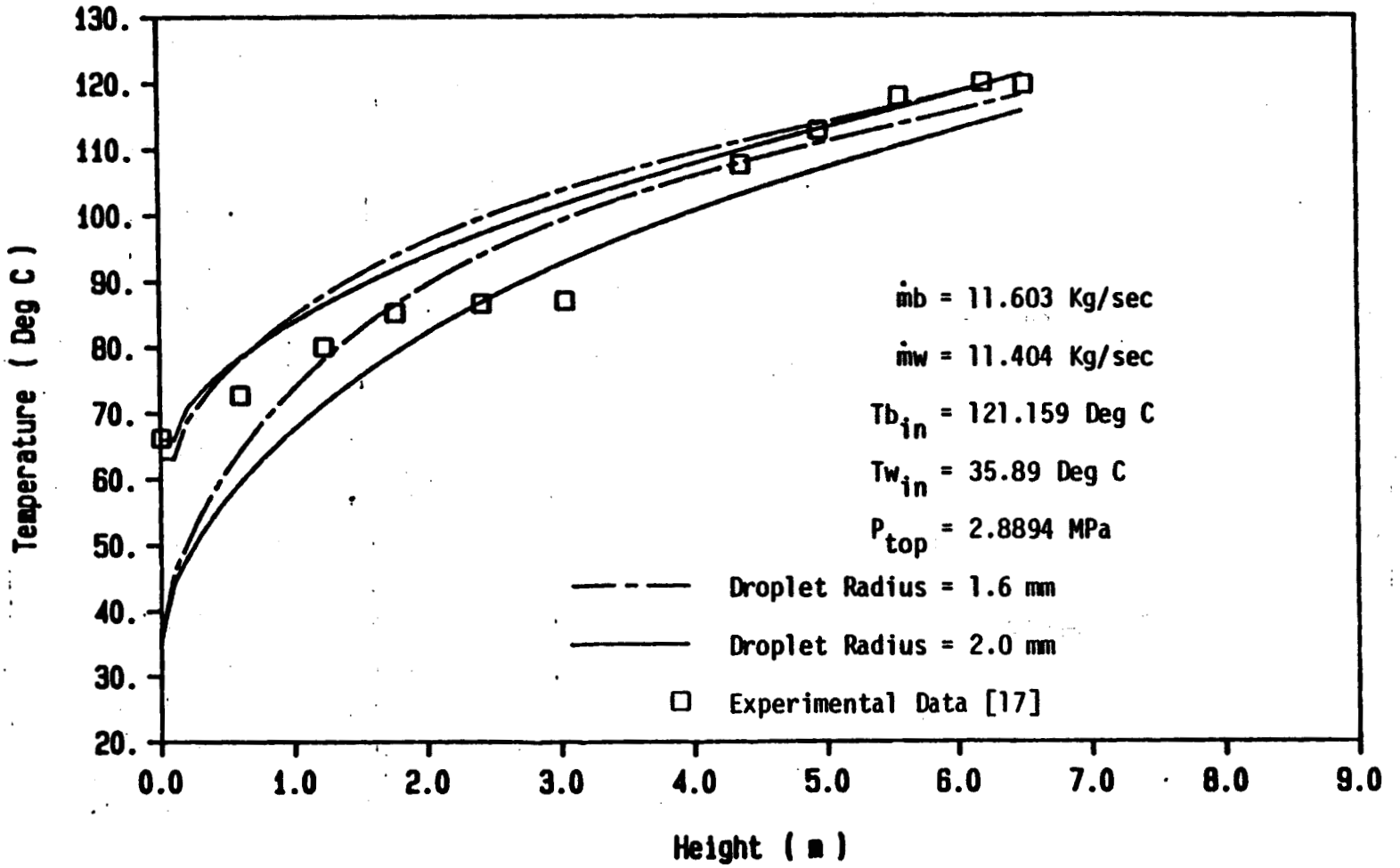


Figure 16. Temperature profile of the brine and the working fluid along the length of the column using constant diameter model, $\dot{m}b$ = 11.603 Kg/sec, $\dot{m}w$ = 11.404 Kg/sec.

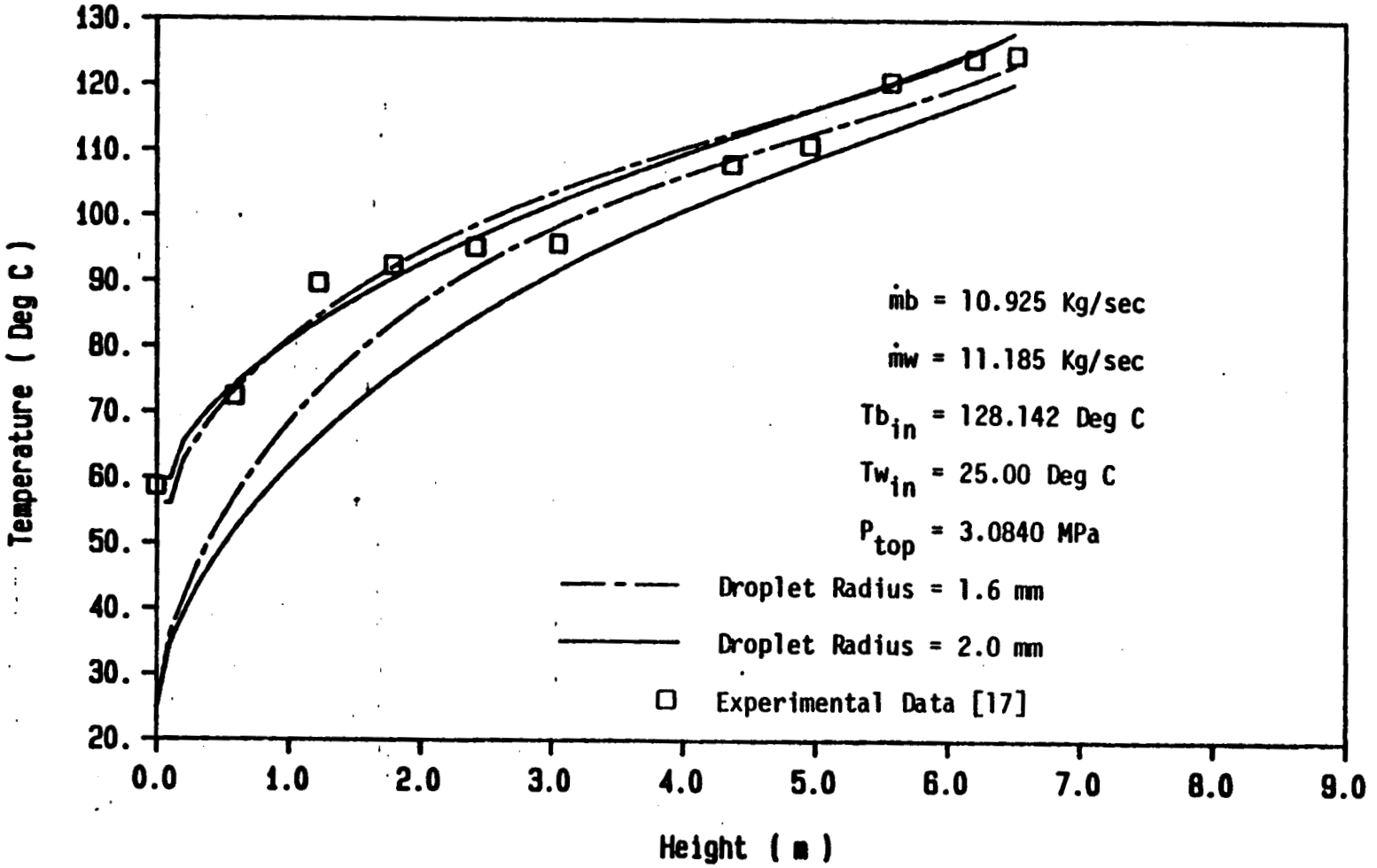


Figure 17. Temperature profile of the brine and the working fluid along the length of the column using constant diameter model, $\dot{m}b$ = 10.925 Kg/sec, $\dot{m}w$ = 11.185 Kg/sec.

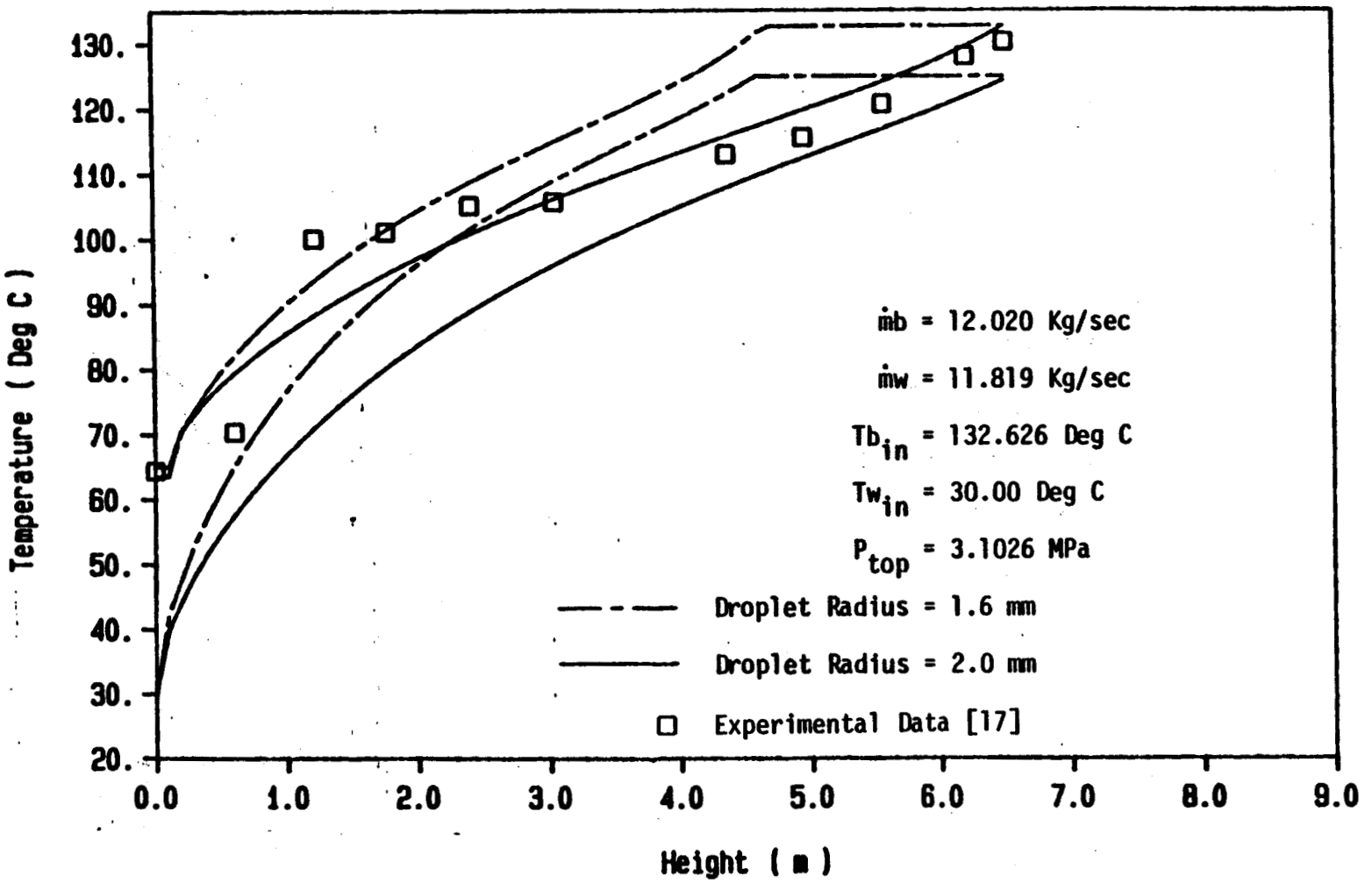


Figure 18. Temperature profile of the brine and the working fluid along the length of the column using constant diameter model, $\dot{m}b$ = 12.02 Kg/sec, $\dot{m}w$ = 11.819 Kg/sec.

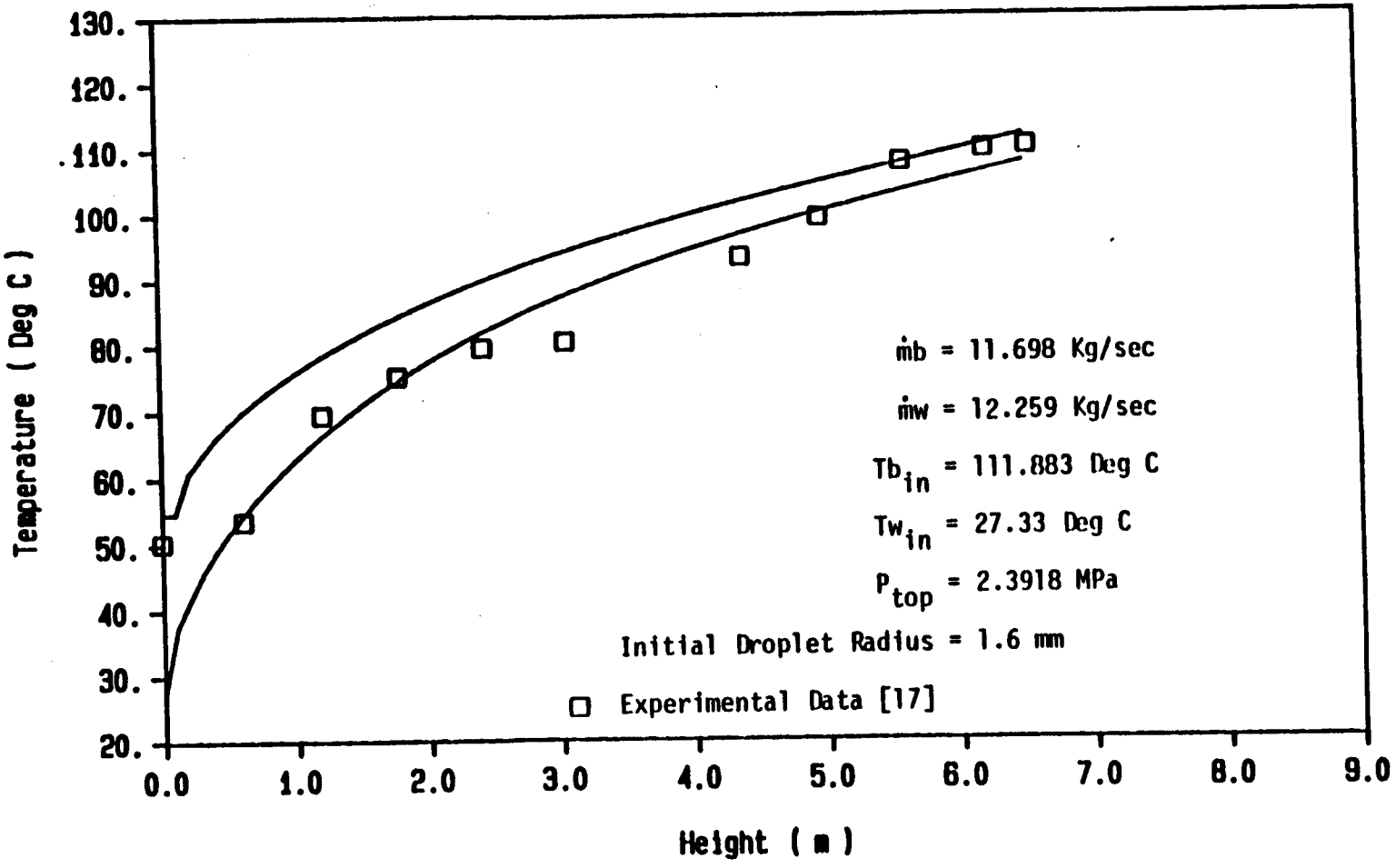


Figure 19. Temperature profile of the brine and the working fluid along the length of the column using variable radius model, $\dot{m}b$ = 11.698 Kg/sec, $\dot{m}w$ = 12.259 Kg/sec.

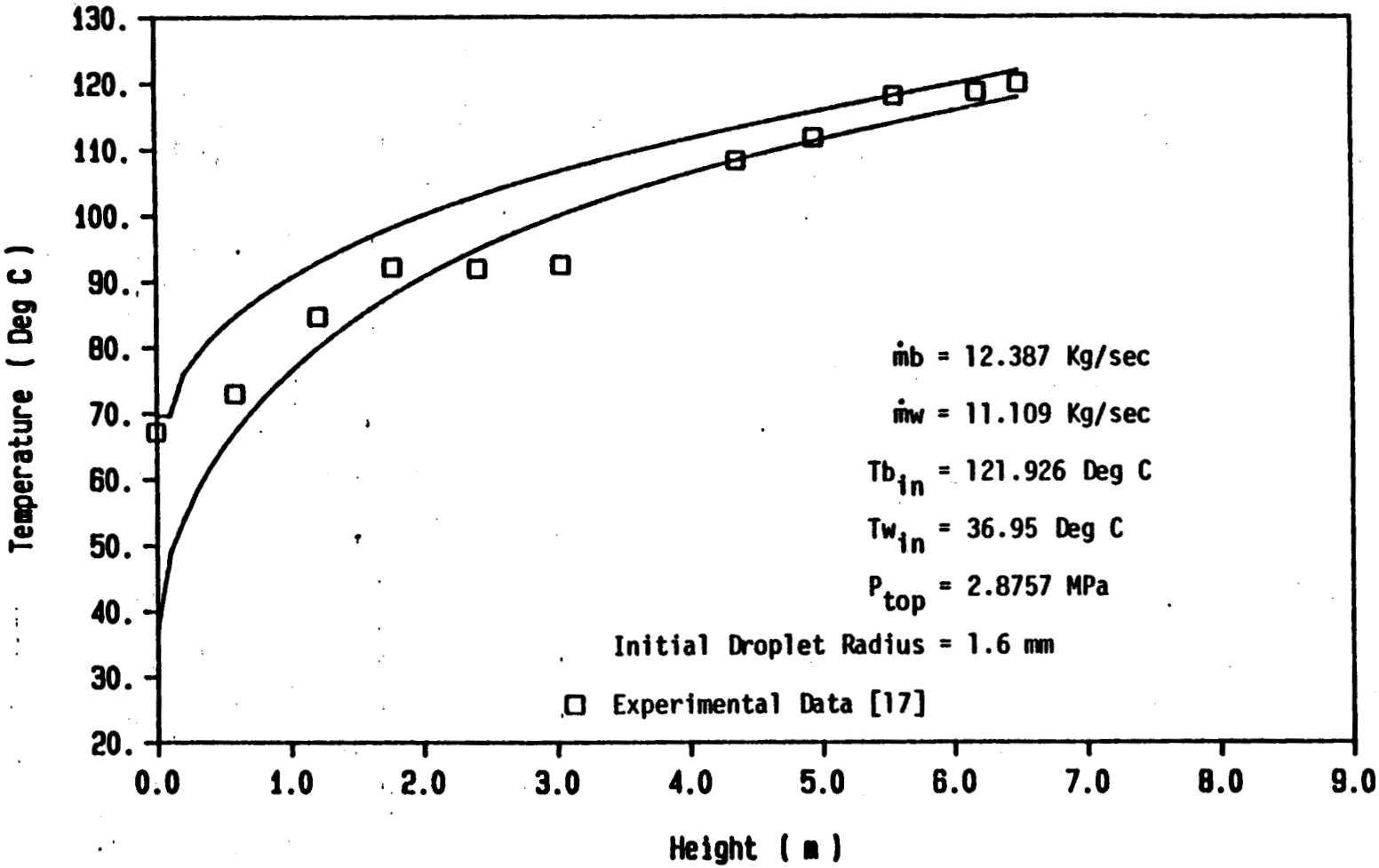


Figure 20. Temperature profile of the brine and the working fluid along the length of the column using variable radius model, $\dot{m}b$ = 12.387 Kg/sec, $\dot{m}w$ = 11.109 Kg/sec.

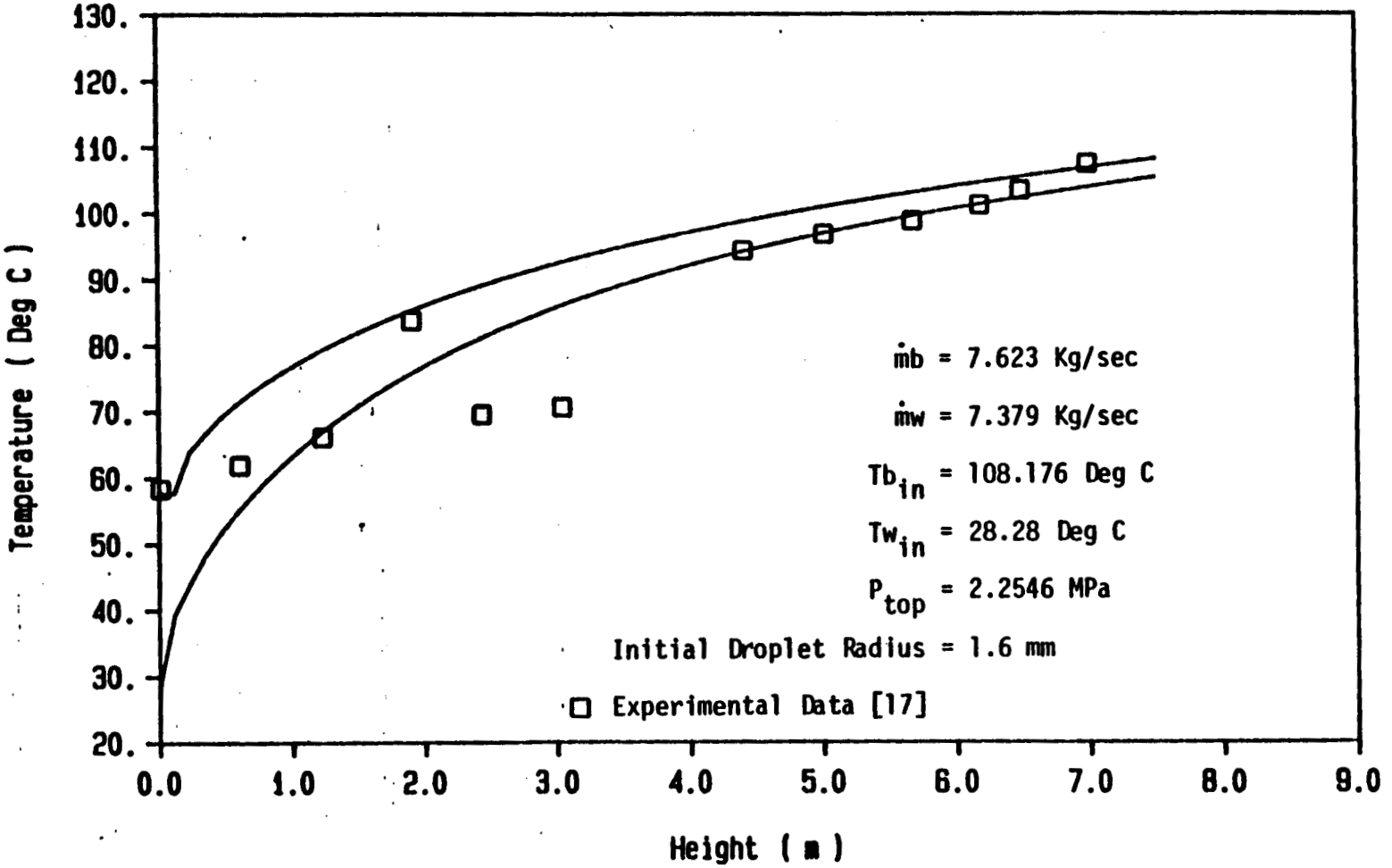


Figure 21. Temperature profile of the brine and the working fluid along the length of the column using variable radius model, $\dot{m}b$ = 7.623 Kg/sec, $\dot{m}w$ = 7.379 Kg/sec.

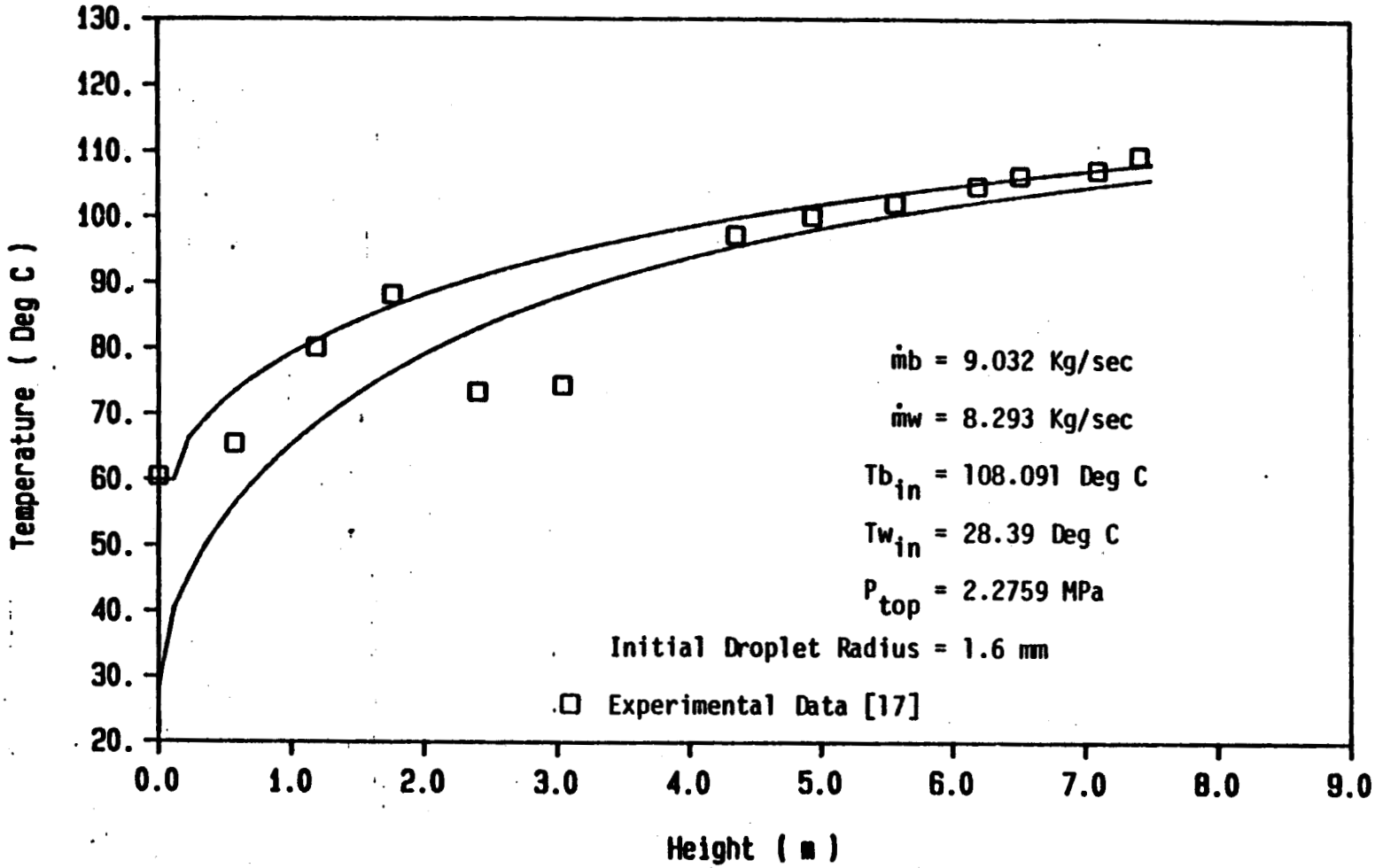


Figure 22. Temperature profile of the brine and the working fluid along the length of the column using variable radius model, $\dot{m}b$ = 9.032 Kg/sec, $\dot{m}w$ = 8.293 Kg/sec.

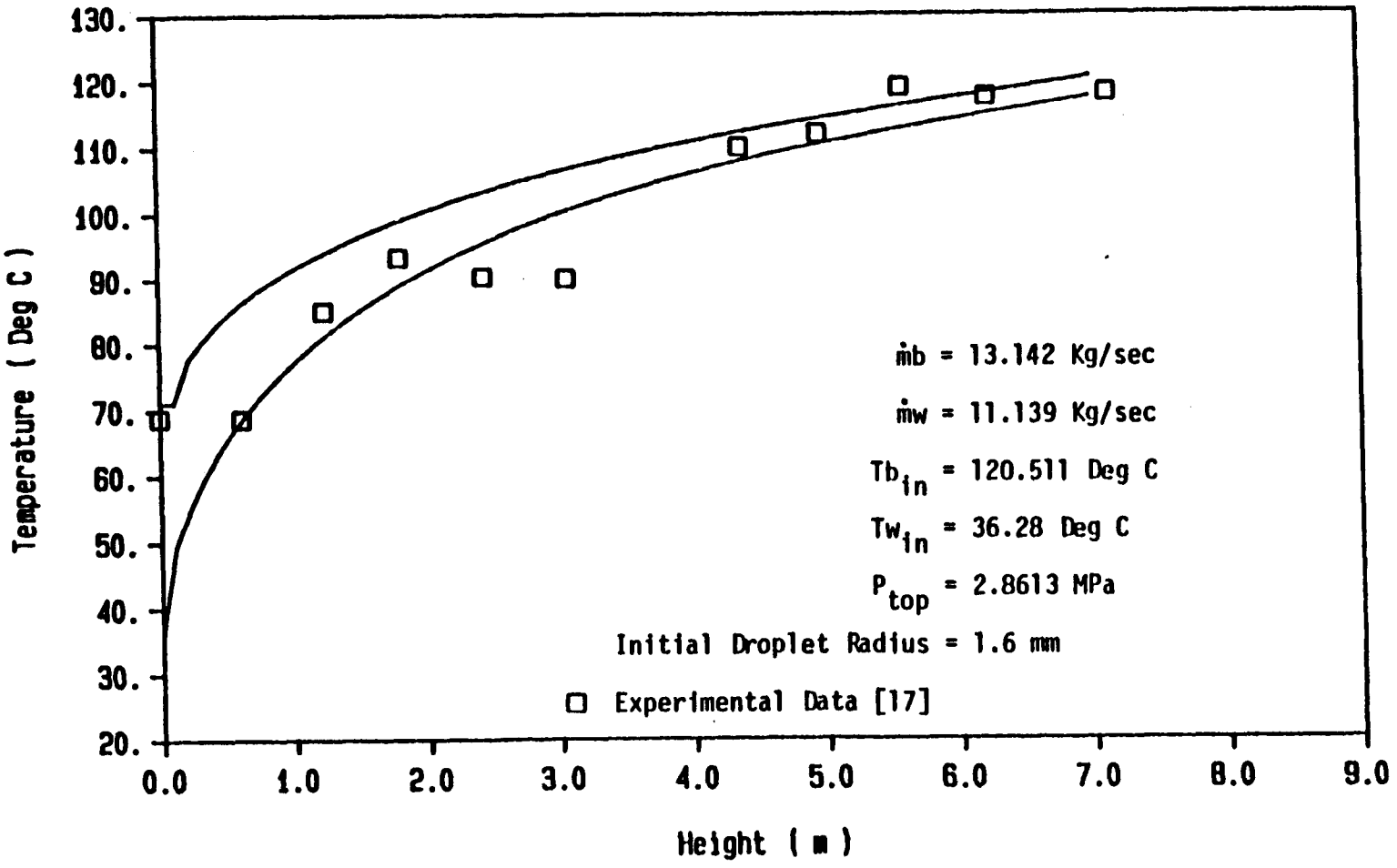


Figure 23. Temperature profile of the brine and the working fluid along the length of the column using variable radius model, $\dot{m}b$ = 13.142 Kg/sec, $\dot{m}w$ = 11.139 Kg/sec.

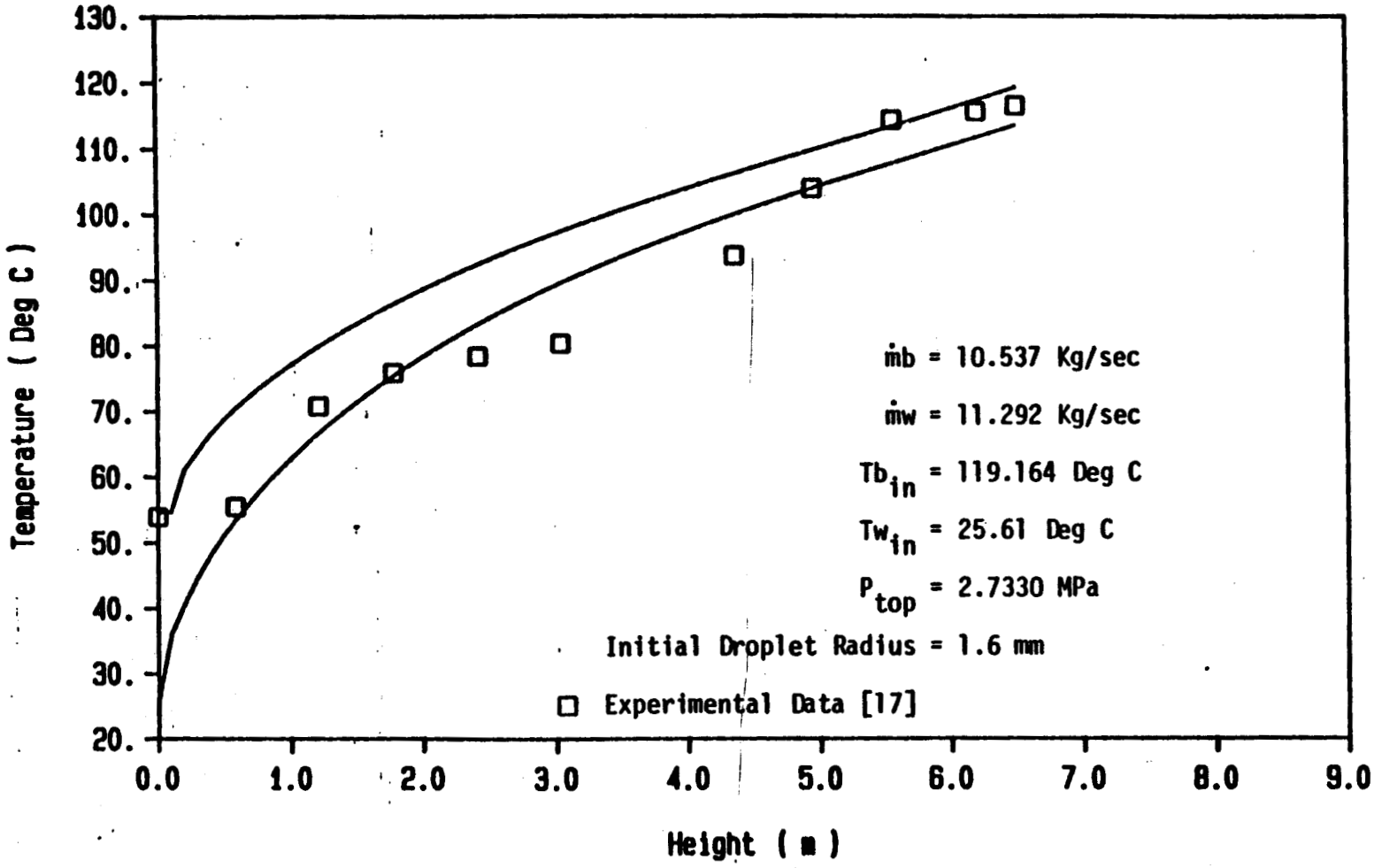


Figure 24. Temperature profile of the brine and the working fluid along the length of the column using variable radius model, $\dot{m}b$ = 10.537 Kg/sec, $\dot{m}w$ = 11.292 Kg/sec.

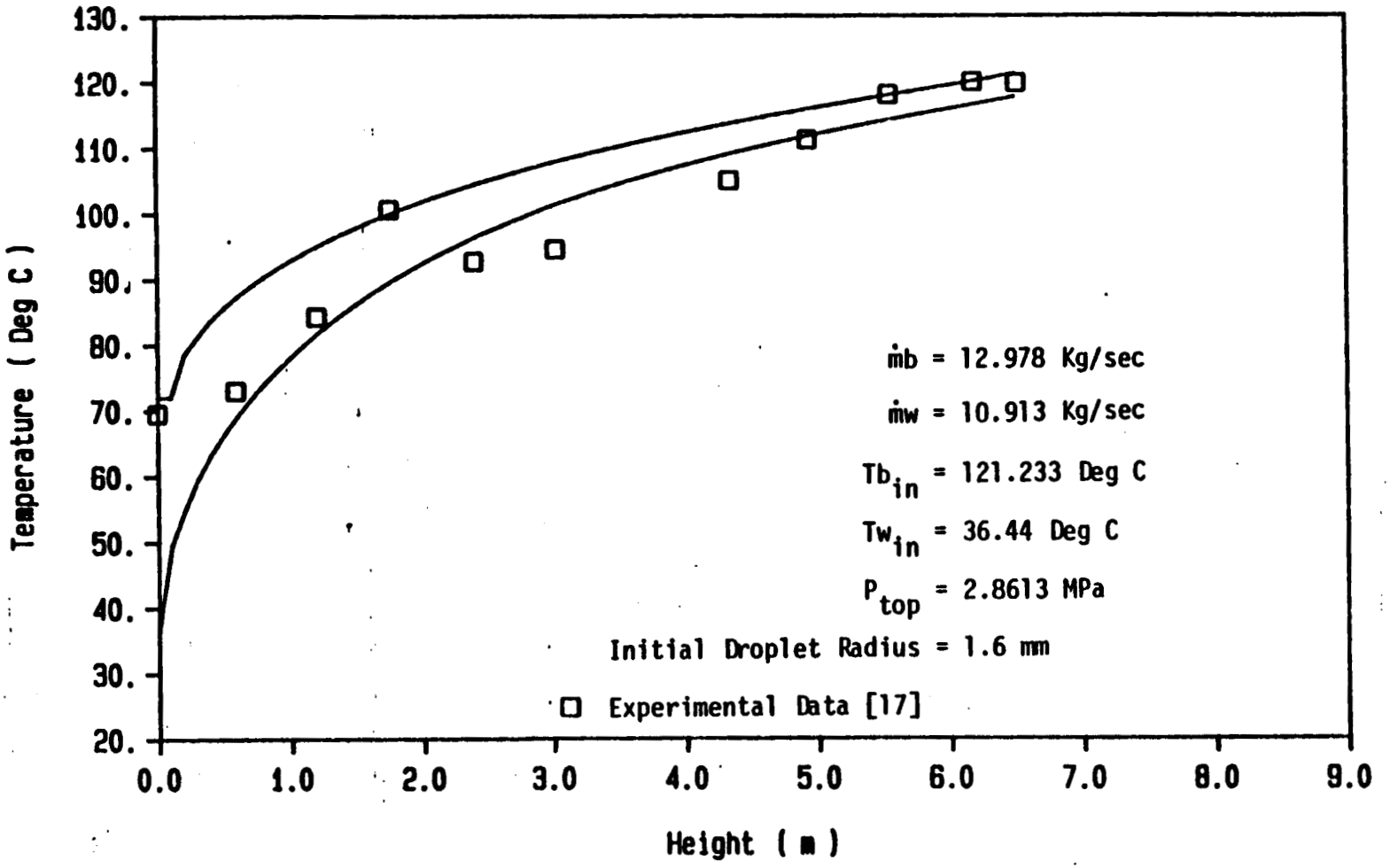


Figure 25. Temperature profile of the brine and the working fluid along the length of the column using variable radius model, $\dot{m}b$ = 12.978 Kg/sec, $\dot{m}w$ = 10.913 Kg/sec.

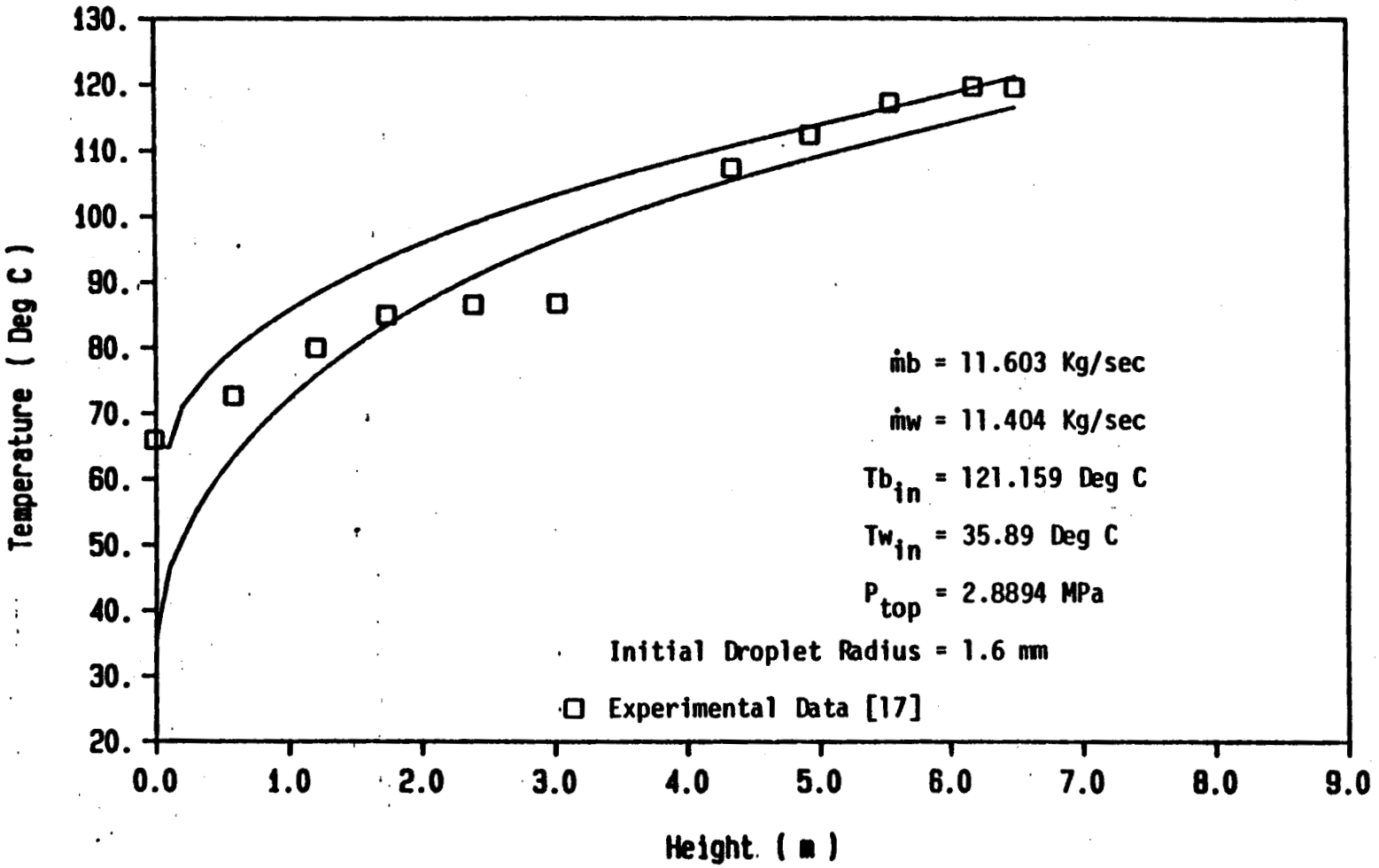


Figure 26. Temperature profile of the brine and the working fluid along the length of the column using variable radius model, $\dot{m}b$ = 11.603 Kg/sec, $\dot{m}w$ = 11.404 Kg/sec.

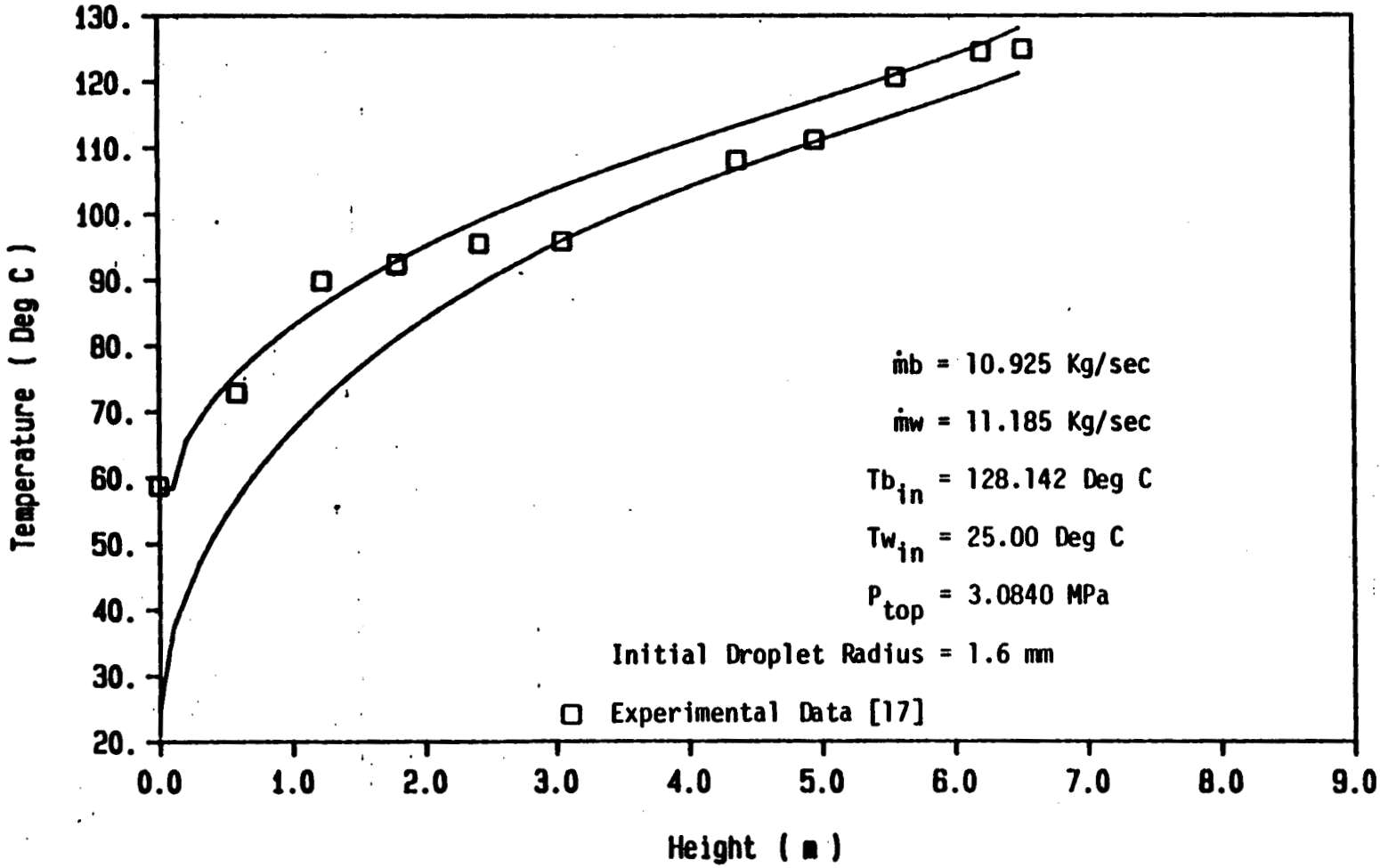


Figure 27. Temperature profile of the brine and the working fluid along the length of the column using variable radius model, $\dot{m}b$ = 10.925 Kg/sec, $\dot{m}w$ = 11.185 Kg/sec.

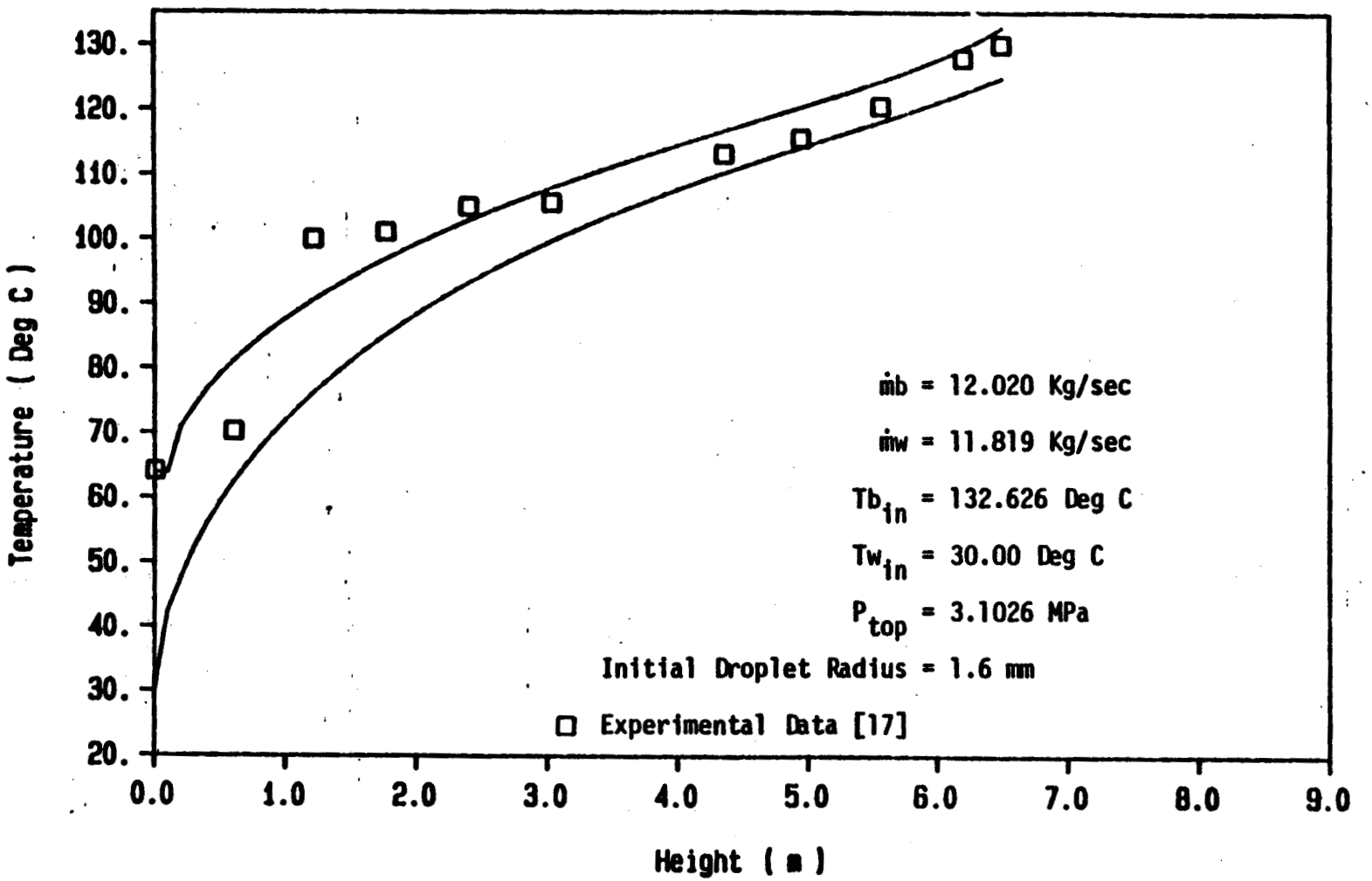


Figure 28. Temperature profile of the brine and the working fluid along the length of the column using variable radius model, $\dot{m}b$ = 12.02 Kg/sec, $\dot{m}w$ = 11.819 Kg/sec.

radius conduction model for the same ten conditions given for the constant diameter conduction model. The curves show excellent agreement with the data except at approximately 3 meters. At this location the column's two major halves (see Figure 4) are joined by massive flanges. The thermocouple at 3.2 meters is just below the flange and that at 4.3 meters is just above it. It is possible that the existence of this mass of material suppresses the temperatures by acting as both a heat sink and as an extended heat transfer surface. As the current state of two-phase flow analyses does not at this time allow for an accurate computational evaluation of transient multi-dimensional flows (although some have been tried), the other possibility of back mixing cannot be assessed.

Figures 29 and 30 show additional output that can be obtained from the two-phase model developed herein. They correspond to the temperature profiles shown in Figures 19 and 20, respectively. These figures show the change in velocities of the phases as well as the holdup. It is clear that the dispersed phase accelerates as it moves up the column, while the brine's velocity remains nearly constant. The combination of increasing drop velocity and increasing drop diameter leads to the increased holdup.

Figure 31 corresponds to the case shown in Figure 23. Here are presented the velocity of the two phases, the holdup and the increase in drop radii predicted by the model.

It is seen that the drops increased from 1.6 to 1.8

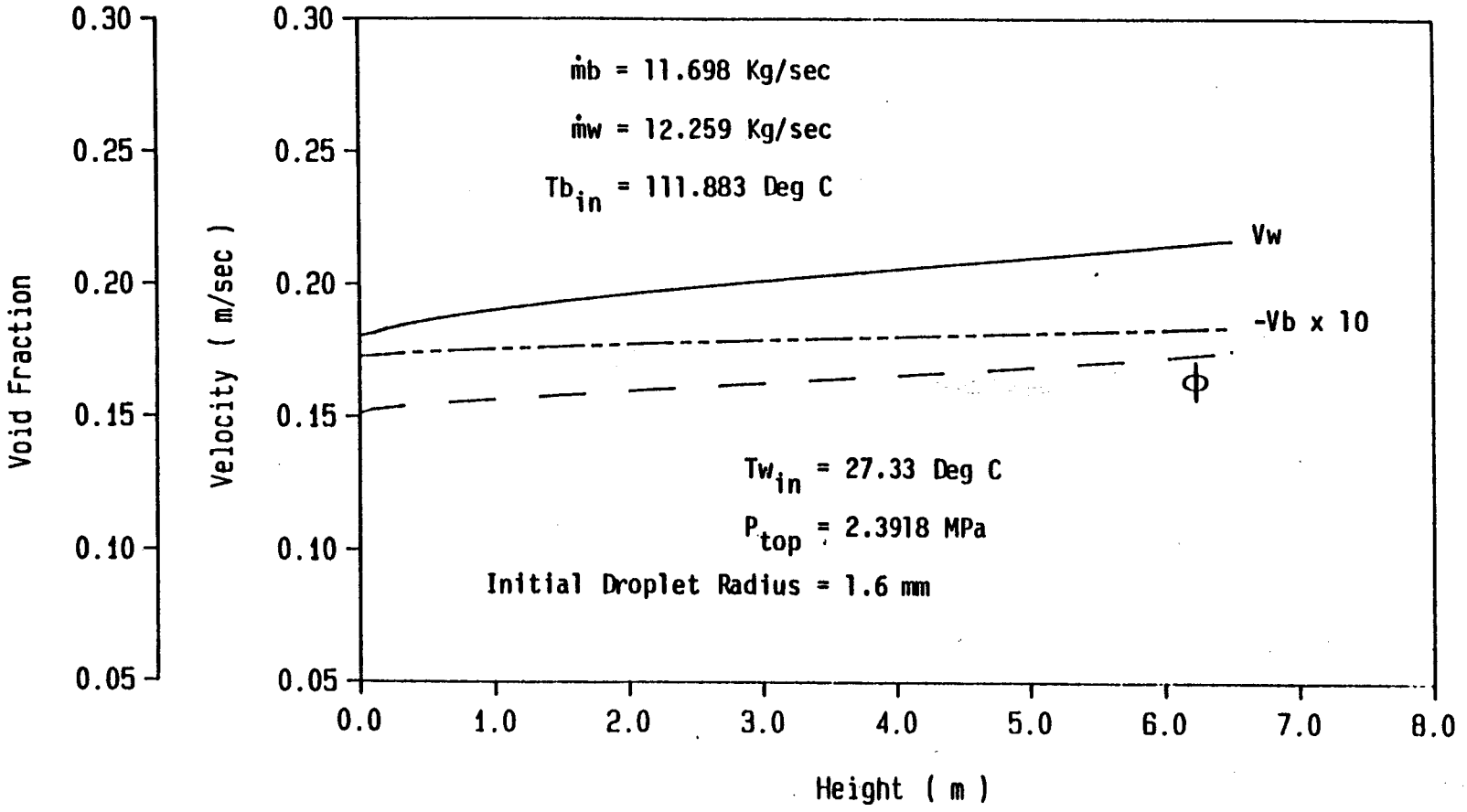


Figure 29. Variation of velocity of the brine and the working fluid as well as holdup along the length of the column, $\dot{m}b$ = 11.698 Kg/sec, $\dot{m}w$ = 12.259 Kg/sec.

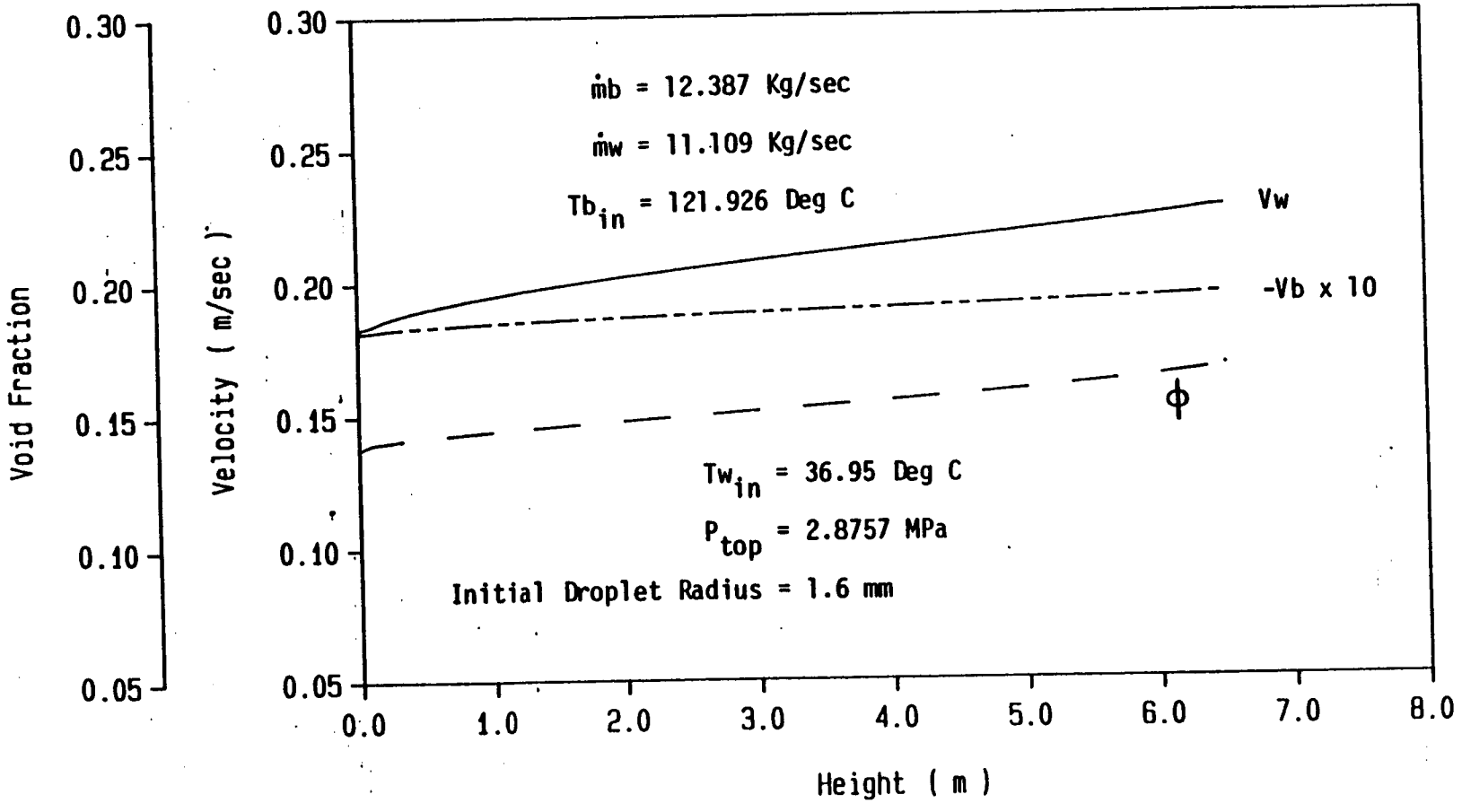


Figure 30. Variation of velocity of the brine and the working fluid as well as holdup along the length of the column, $\dot{m}b$ = 12.387 Kg/sec, $\dot{m}w$ = 11.109 Kg/sec.

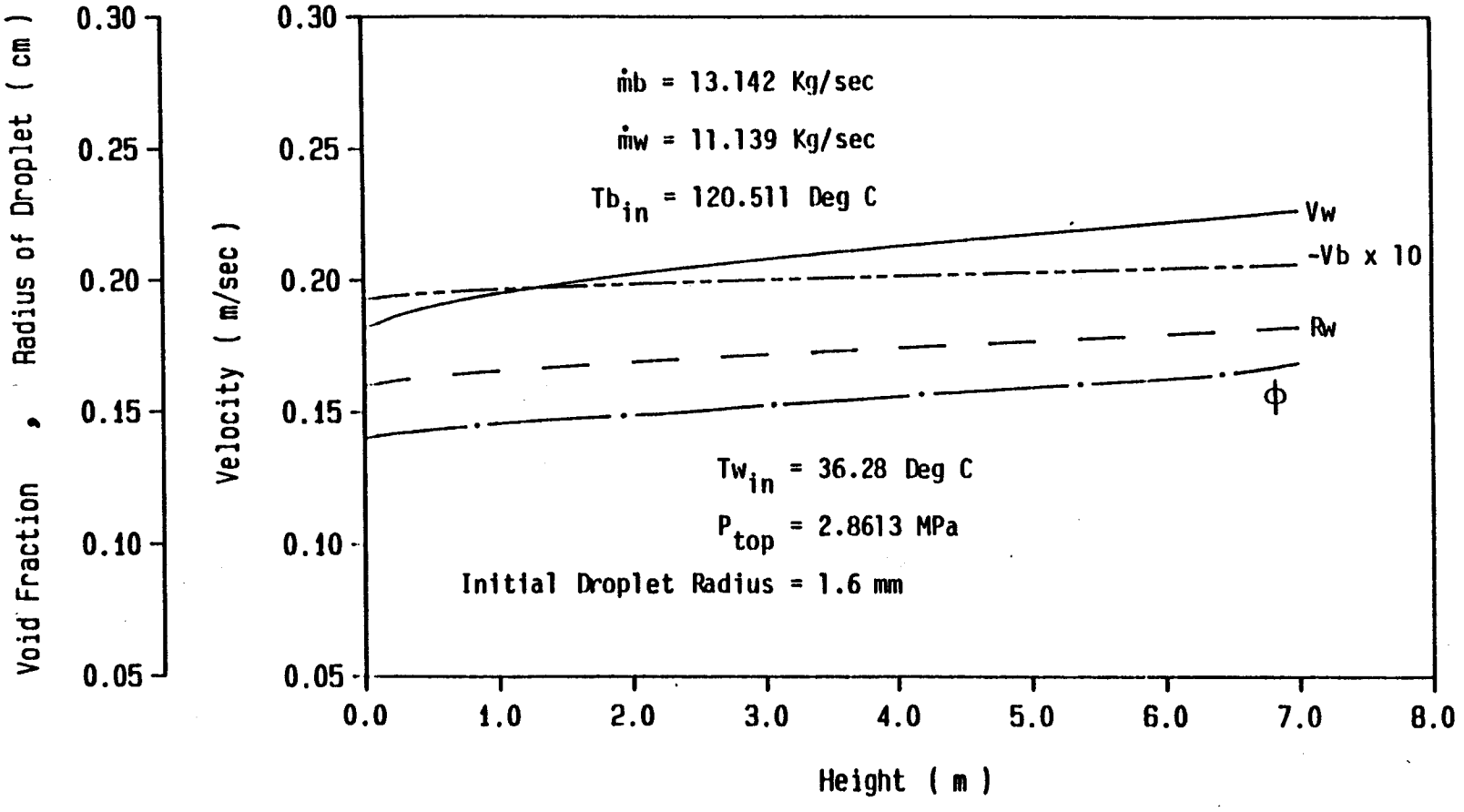


Figure 31. Variation of velocity of the brine and the working fluid as well as holdup and drop radius along the length of the column.

mm in radius. The velocity of the drops increased from 0.18 to 0.23 m/sec. The corresponding increase in holdup was from 0.14 to 0.165.

## 4.2. Transient Solution

As a result of the steady state analyses, it was decided to carry out all transient analyses utilizing the varying radius conduction model for investigating the transient response of a direct contact heat exchanger. The analyses that were conducted were carried for the isobutane-water system corresponding to the Barber Nichols 500 kWe unit.

In considering the transient response of the column, studies were first conducted to find the effect of changing the flow rate for one of the two fluid streams. Both increases and decreases were considered. Also considered was a change in the pressure at the top of the column and a decrease in the temperature of the incoming brine.

Figures 32-34 show the results obtained from changes in the flow rates by 1 kg/sec and in column pressure by 5%. Figure 32 indicates the change from the steady state brine temperature; Figure 33 indicates the change from the steady state working fluid temperature; and Figure 34 indicates the change in holdup after the column has approximately reached the new quasi-steady state conditions. These changes require approximately 180 seconds. Note that the steady state conditions prior to the assumed changes were those shown in Figure 21. It is seen that a decrease in brine flow

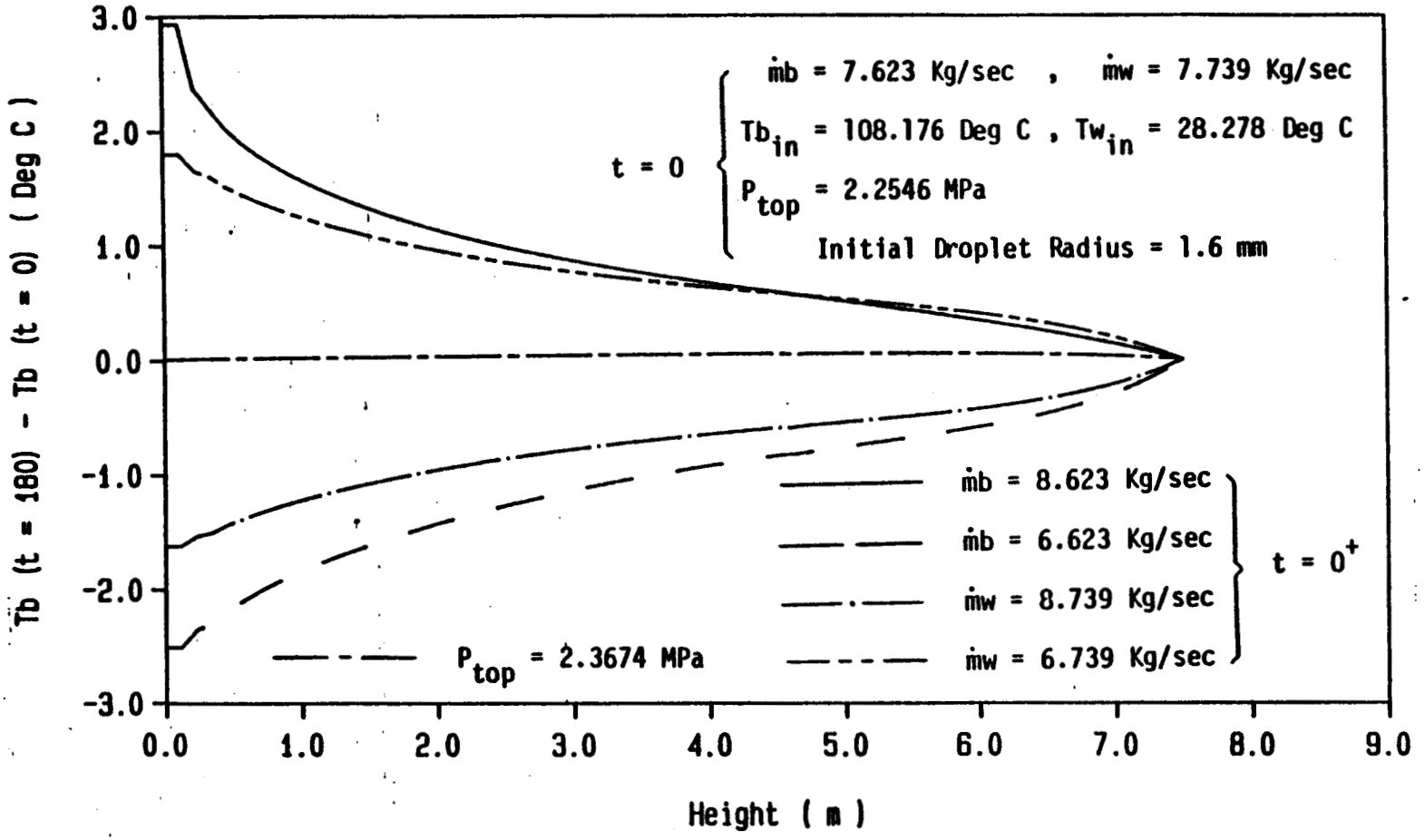


Figure 32. Effect of change in mass flow rate and column pressure on the brine temperature.

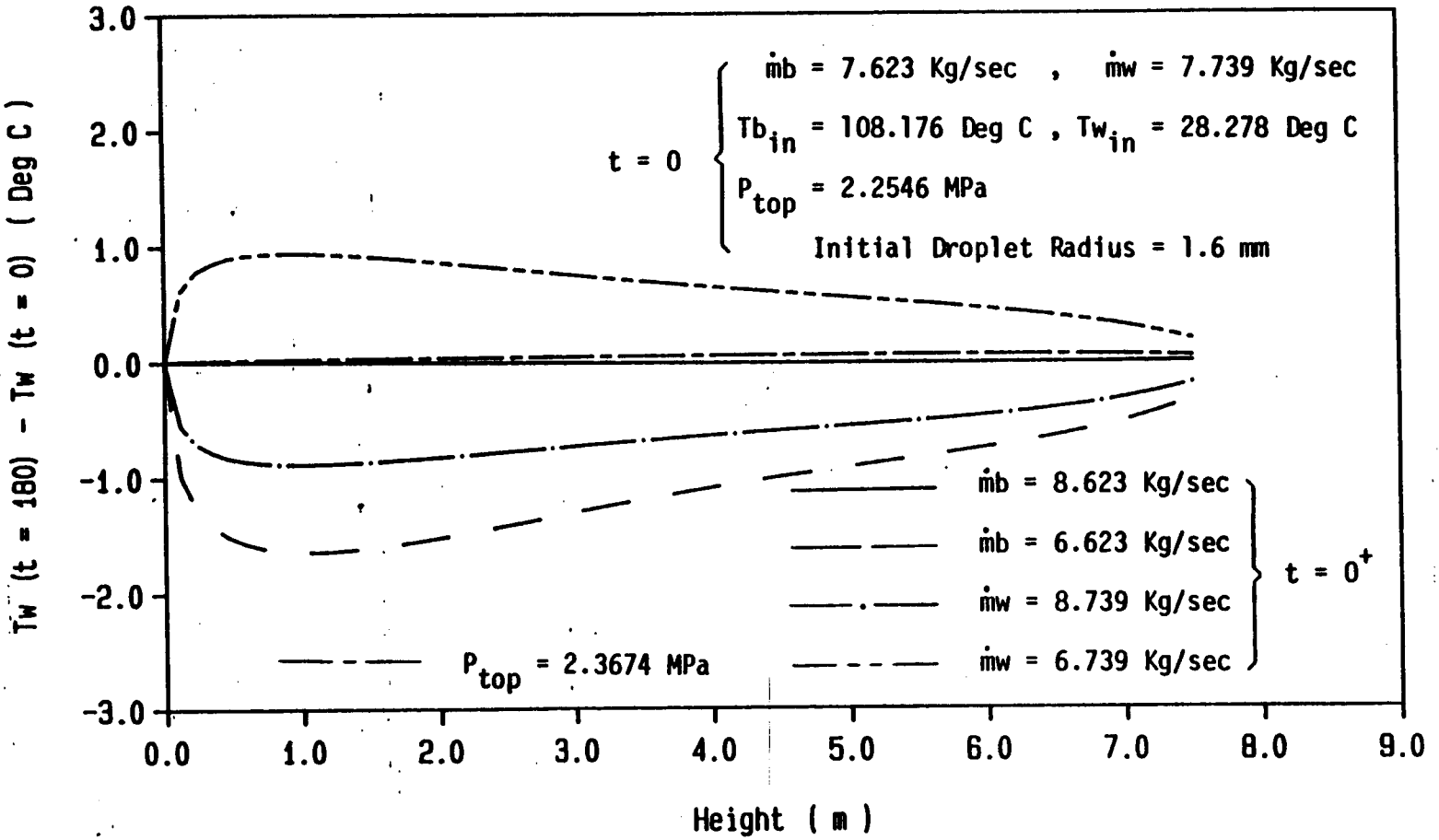


Figure 33. Effect of change in mass flow rate and column pressure on the working fluid temperature.

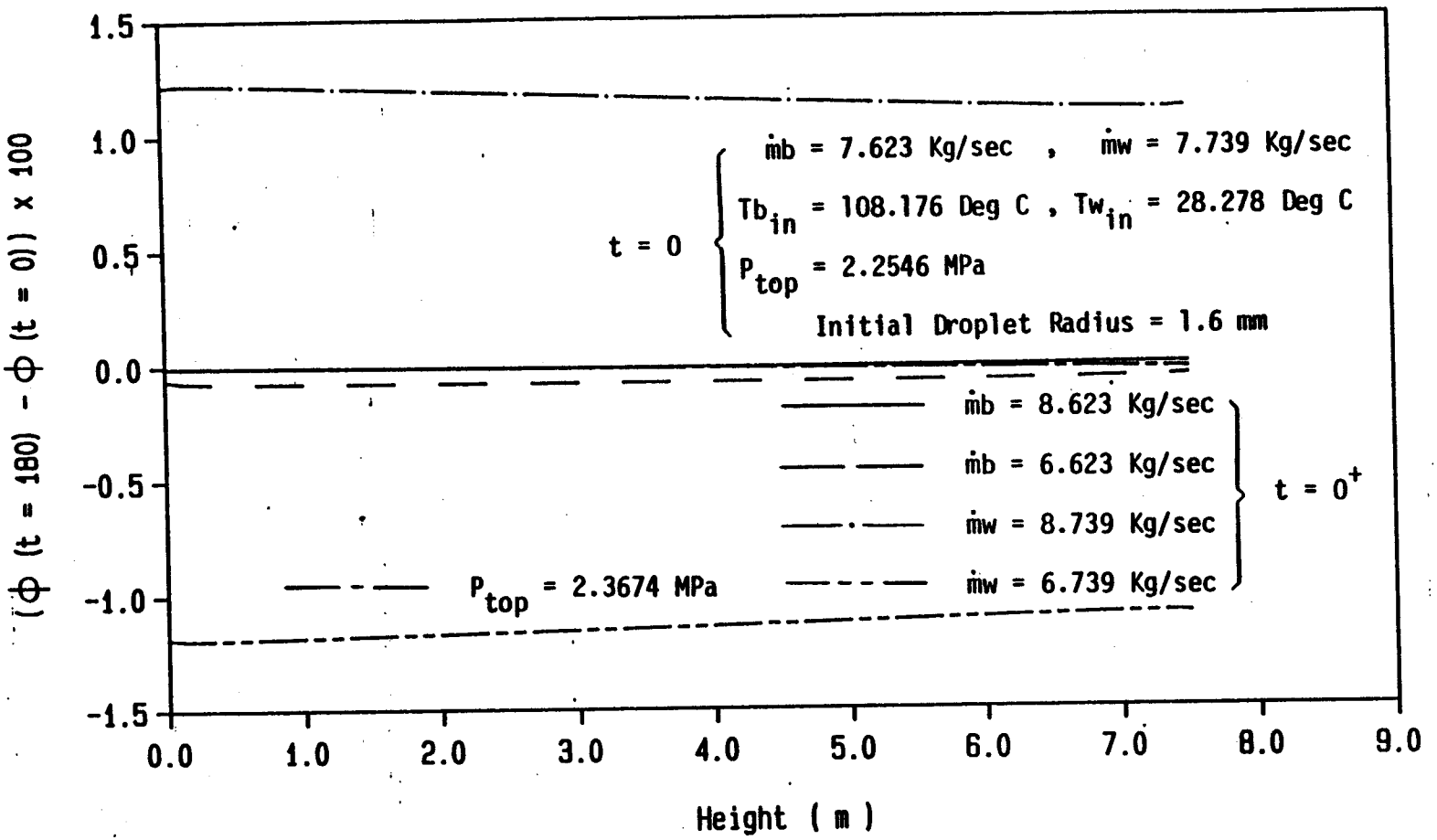


Figure 34. Effect of change in mass flow rate and column pressure on holdup.

rate decreases the working fluid temperature throughout the column while an increase in brine flow rate has negligible effect. A decrease in working fluid flow rate leads to an increase in working fluid temperature which would shorten the preheater section. An increase in working fluid flow rate increases the preheater length. An increase in system pressure by 5% requires a higher preheater working fluid exit temperature. For no change in the flow rates this results in a required increase in the preheater length of approximately 1 meter or 13%. Hold-up changes are only about 0.01; however, operation close to the flooding limits could cause complete unstabilization of the column if larger changes in flow rates or pressure occurred. The resulting preheater length changes corresponding to the cases studied in Figures 32-34 are given in Table 1.

Figure 35 illustrates the effect of a 5°C decrease in brine inlet temperature from the conditions for Figure 21. It is seen that this results in a change in the working fluid temperature of -3°C at the top of the preheater and would result in a corresponding decrease in pressure. The time constant to reach a new quasi-equilibrium state is again about 180 seconds.

Figures 36 through 39 illustrate the effects of the same type of changes that were shown in Figures 32-35; however, the initial conditions correspond to the higher flow rates for the steady state case of Figure 19.

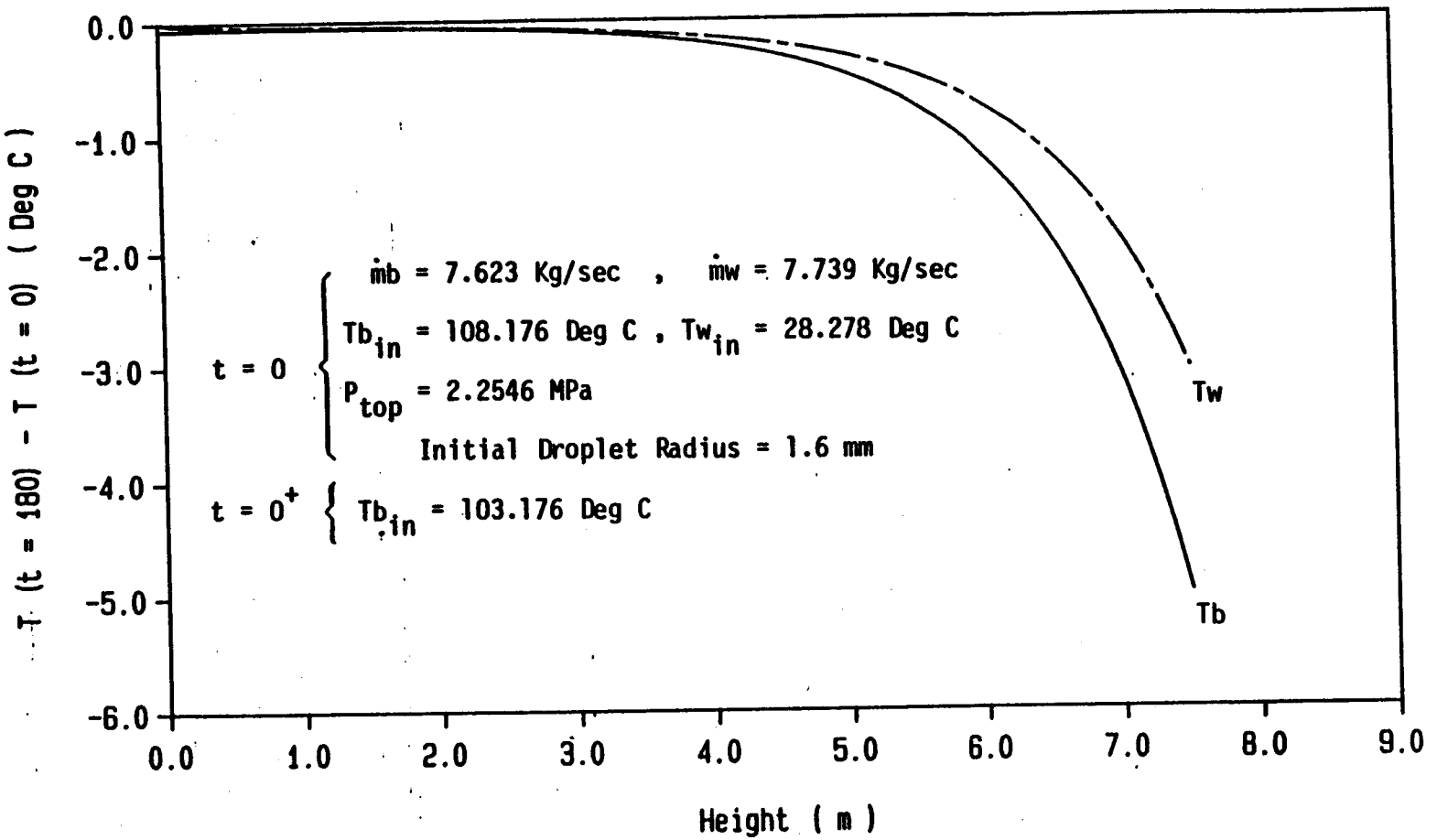


Figure 35. Effect of change in the brine inlet temperature on temperature profile of the brine and the working fluid.

Table 1

Changes in column height after a sudden change in input characteristic of the column. Steady state conditions are: $\dot{m}b$ = 7.623 kg/sec, $\dot{m}w$ = 2.379 kg/sec, $Tb_{in}$ = 108.176 Deg C, $Tw_{in}$ = 28.28 Deg C, $P_{top}$ = 2.2546 Mpa and initial droplet radius = 1.6 mm.

| change in Input characteristic | H(t=180) - H(t=0) (m) |
|---|---|
| $\dot{m}b$ increased by 1 kg/sec | -.02 |
| $\dot{m}b$ decreased by 1 kg/sec | 0.087 |
| $\dot{m}w$ increased by 2 kg/sec | 0.047 |
| $\dot{m}w$ decreased by 2 kg/sec | -0.04 |
| $P_{top}$ increased by 5% | 1.0 m |
| $Tb_{in}$ decreased by 5 Deg C | 0.81 m |

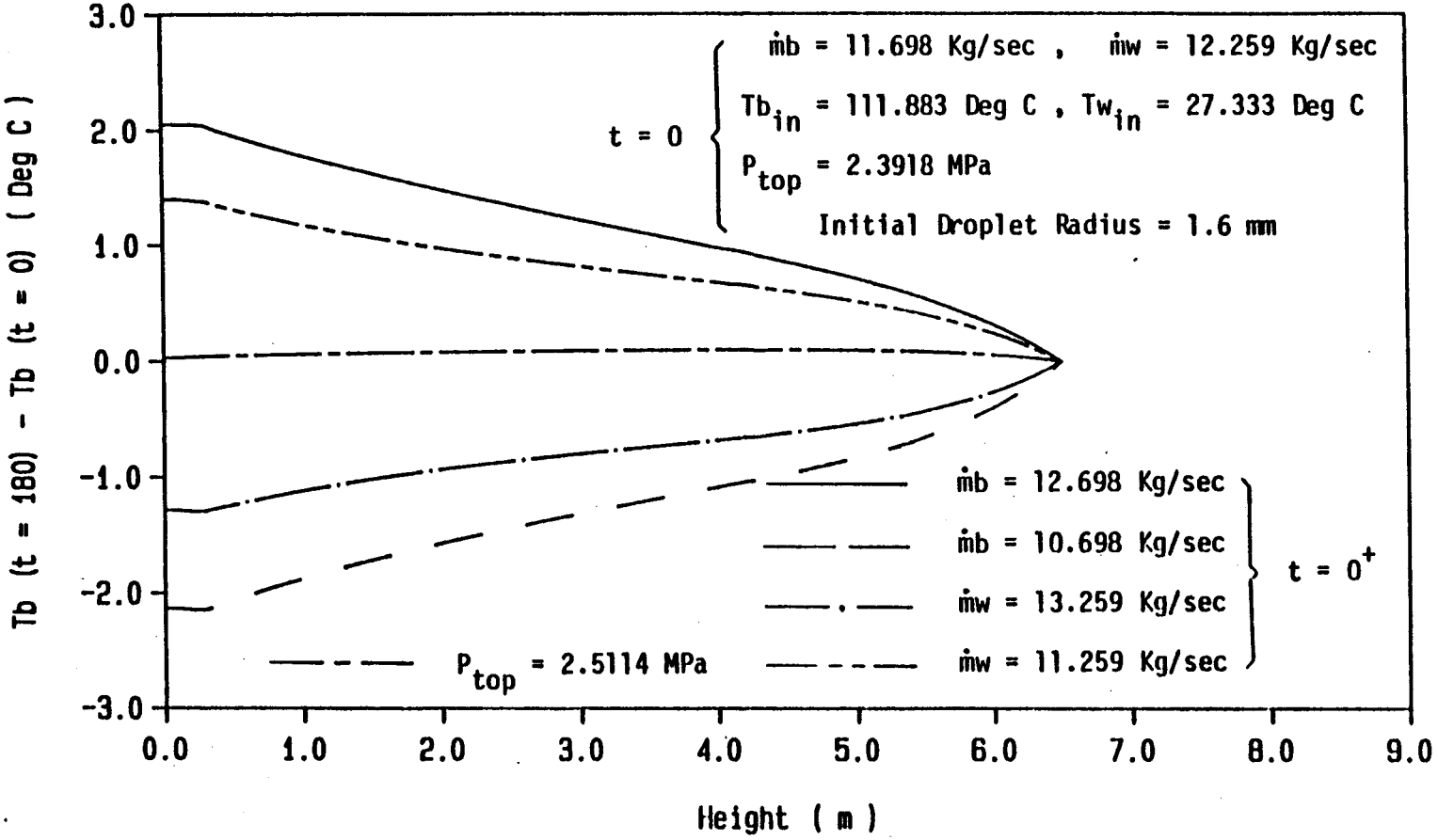


Figure 36. Effect of change in mass flow rate and column pressure on the brine temperature $\dot{m}b$ = 11.698 Kg/sec, $\dot{m}w$ = 12.259 Kg/sec.

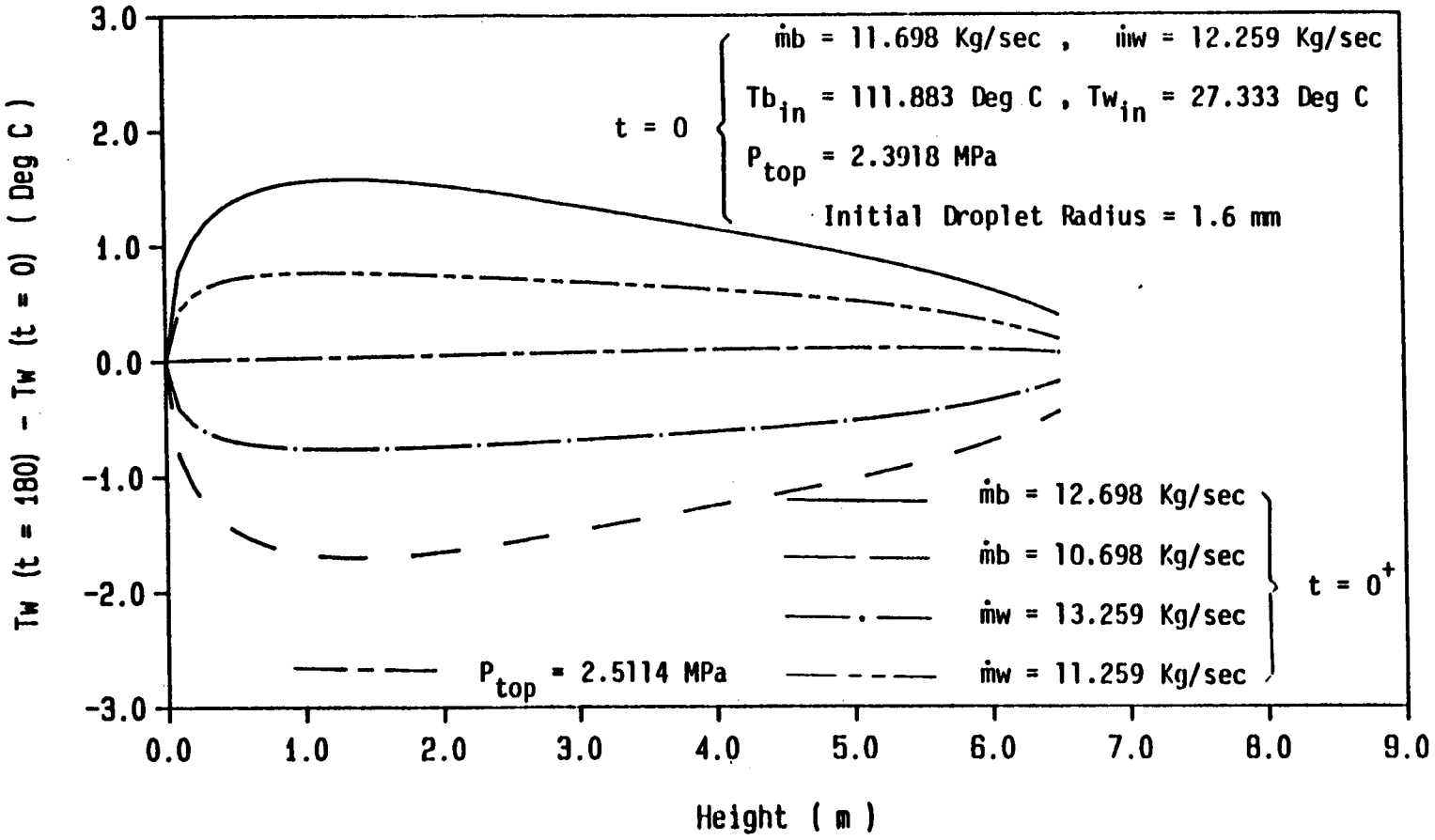


Figure 37. Effect of change in mass flow rate and column pressure on the working fluid temperature $\dot{m}b$ = 11.698 Kg/sec, $\dot{m}w$ = 12.259 Kg/sec.

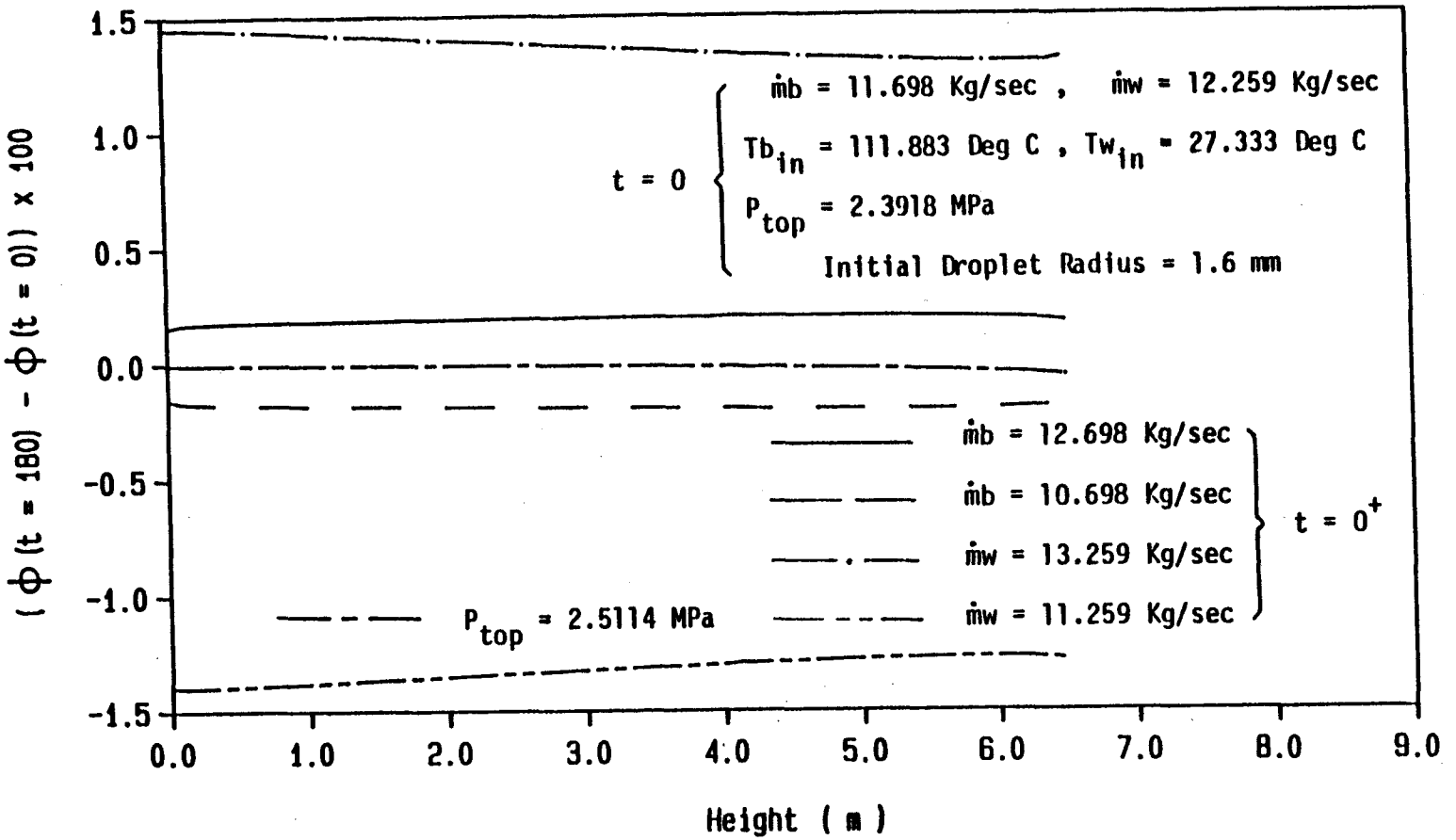


Figure 38. Effect of change in mass flow rate and column pressure on holdup ṁb = 11.698 Kg/sec, ṁw = 12.259 Kg/sec.

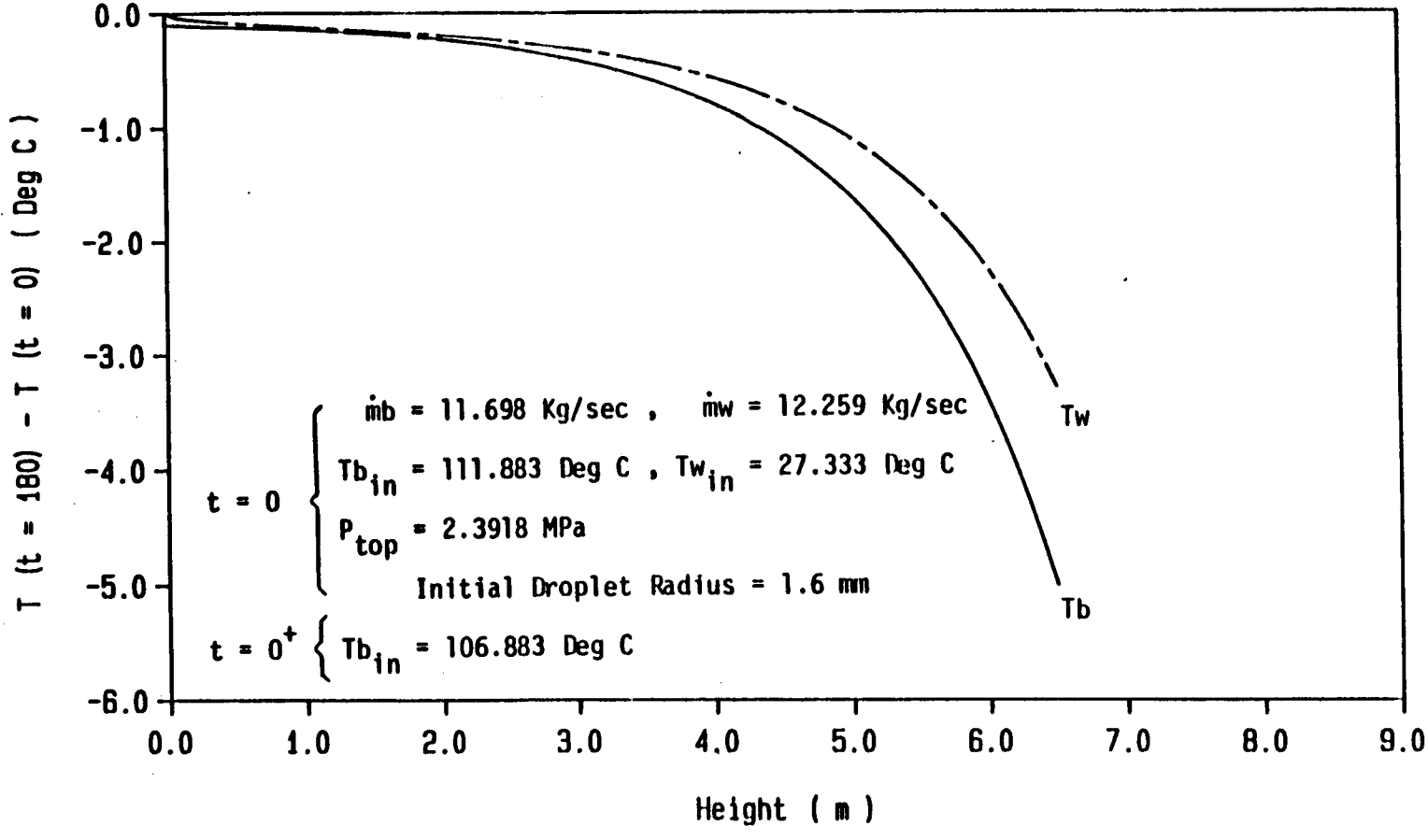


Figure 39. Effect of change in the brine inlet temperature on temperature profile at the brine and the working fluid, ṁb = 11.698 Kg/sec, ṁw = 12.259 Kg/sec.

Table 2 shows the corresponding changes in the height of the preheater.

Figures 40 through 44 illustrate the transient response of a preheater at discrete times after a change in either $\dot{m}b$, $\dot{m}w$ or Tb. The shapes of the curves, Tw (t) - Tw (t=0), remain similar for changes in $\dot{m}b$ or Tb but are variable in shape for changes in $\dot{m}w$ as viewed with respect to time.

In order to understand better the effects of changing the flow rates, Figures 45 through 52 were generated. Figures 45-48 represent the effect of a decrease in $\dot{m}b$ and Figures 49-52, an increase in $\dot{m}w$. When the brine flow rate is decreased, the working fluid drops at first increase in velocity throughout the entire column as the superficial velocity of the brine decreases. This leads to a shorter contact time and smaller heat transfer. This in turn leads to a smaller density change in the working fluid making the drops being less buoyant. Thus, the working fluid momentum through the brine is decreased as shown in Figure 46. This increase in density and the necessity of a longer column to reach the boiling point is also seen in terms of a higher pressure throughout the length of the preheater as illustrated in Figure 47. The change in velocity of the drops as they move through the column leads to a gradual decrease in holdup as shown in Figure 48.

An increase in working fluid flow rate slows the drops, at first, drastically near the bottom of the column, which

TABLE 2

Changes in column height after a sudden change in input characteristic of the column. Steady state conditions are: $\dot{m}b$ = 11.698 kg/sec, $\dot{m}w$ = 12.259 kg/sec, $Tb_{in}$ = 111.883 Deg C, $Tw_{in}$ = 27.33 Deg C, $P_{top}$ = 2.3918 Mpa and initial droplet radius = 1.6 mm.

| Change in Input Characteristic | H(t=180) - H(t=0) (m) |
|---|---|
| $\dot{m}b$ increased by 1 kg/sec | -0.87 |
| $\dot{m}b$ decreased by 1 kg/sec | 0.1 |
| $\dot{m}w$ increased by 1 kg/sec | 0.04 |
| $\dot{m}w$ decreased by 1 kg/sec | -0.04 |
| $P_{top}$ increased by 5% | 0.9 |
| $Tb_{in}$ decreased by 5 Deg C | 1.037 |

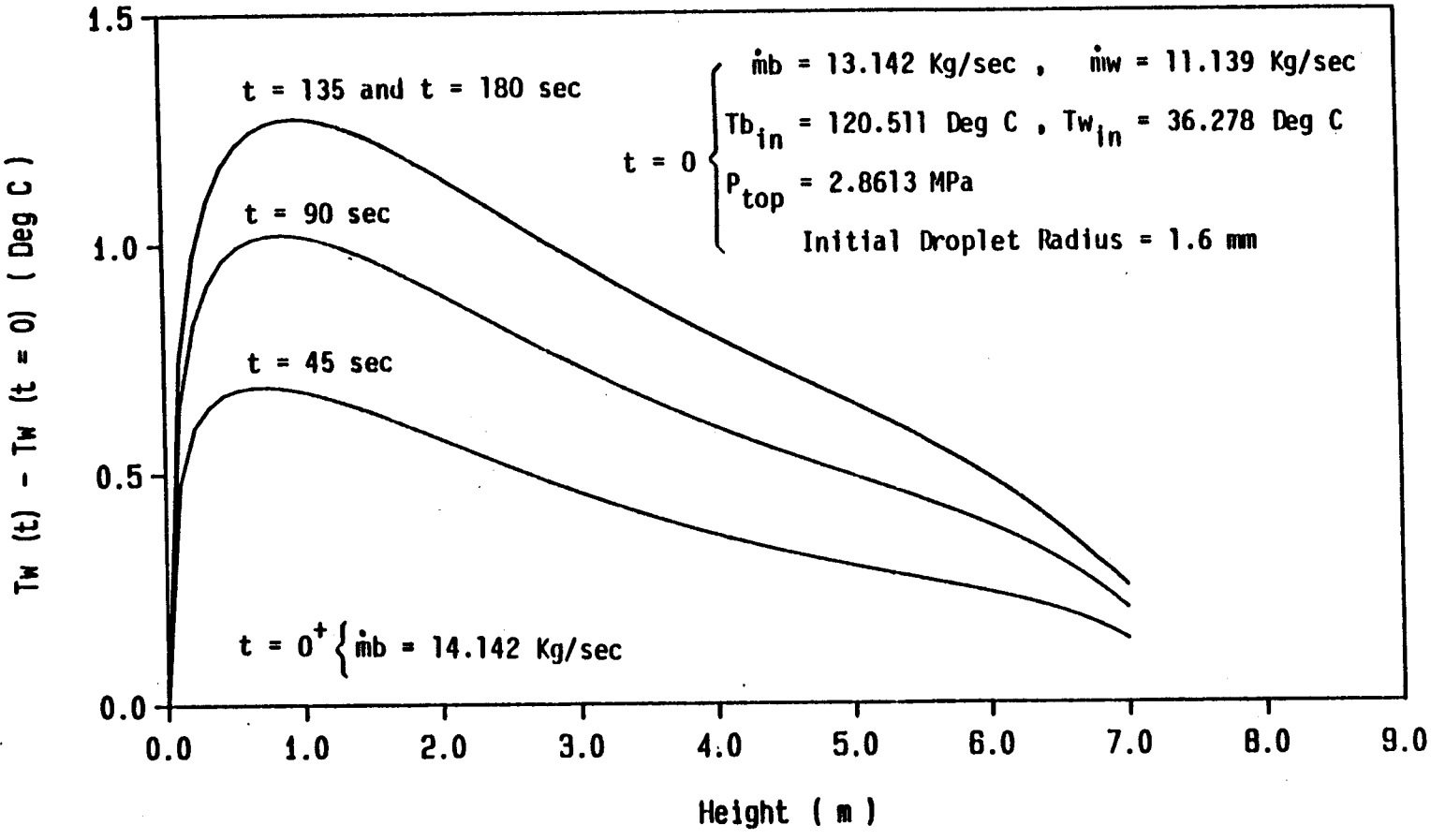


Figure 40. Transient response of the working fluid temperature after an increase in mass flow rate of the brine.

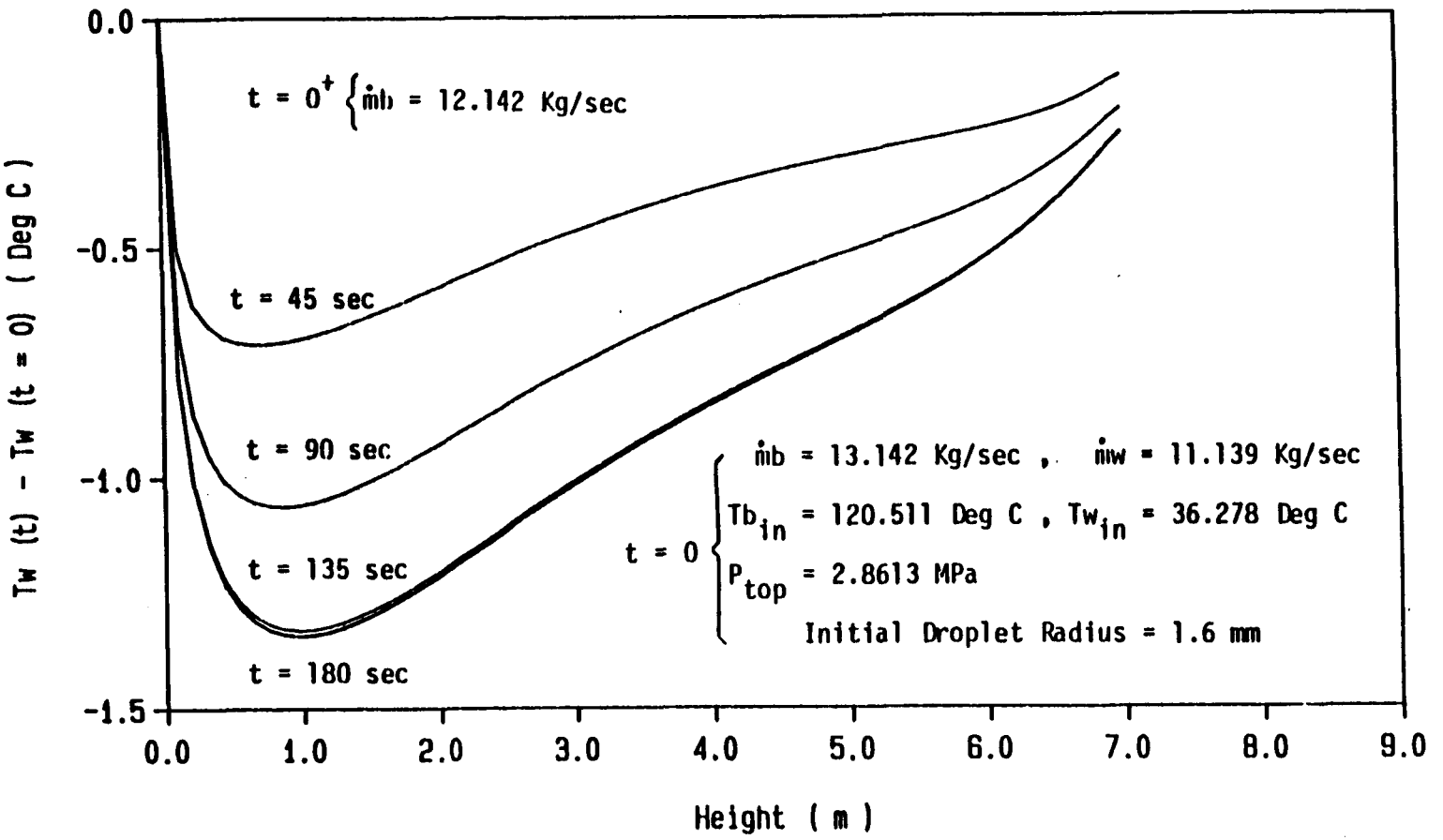


Figure 41. Transient response of the working fluid temperature after a decrease in mass flow rate of the brine.

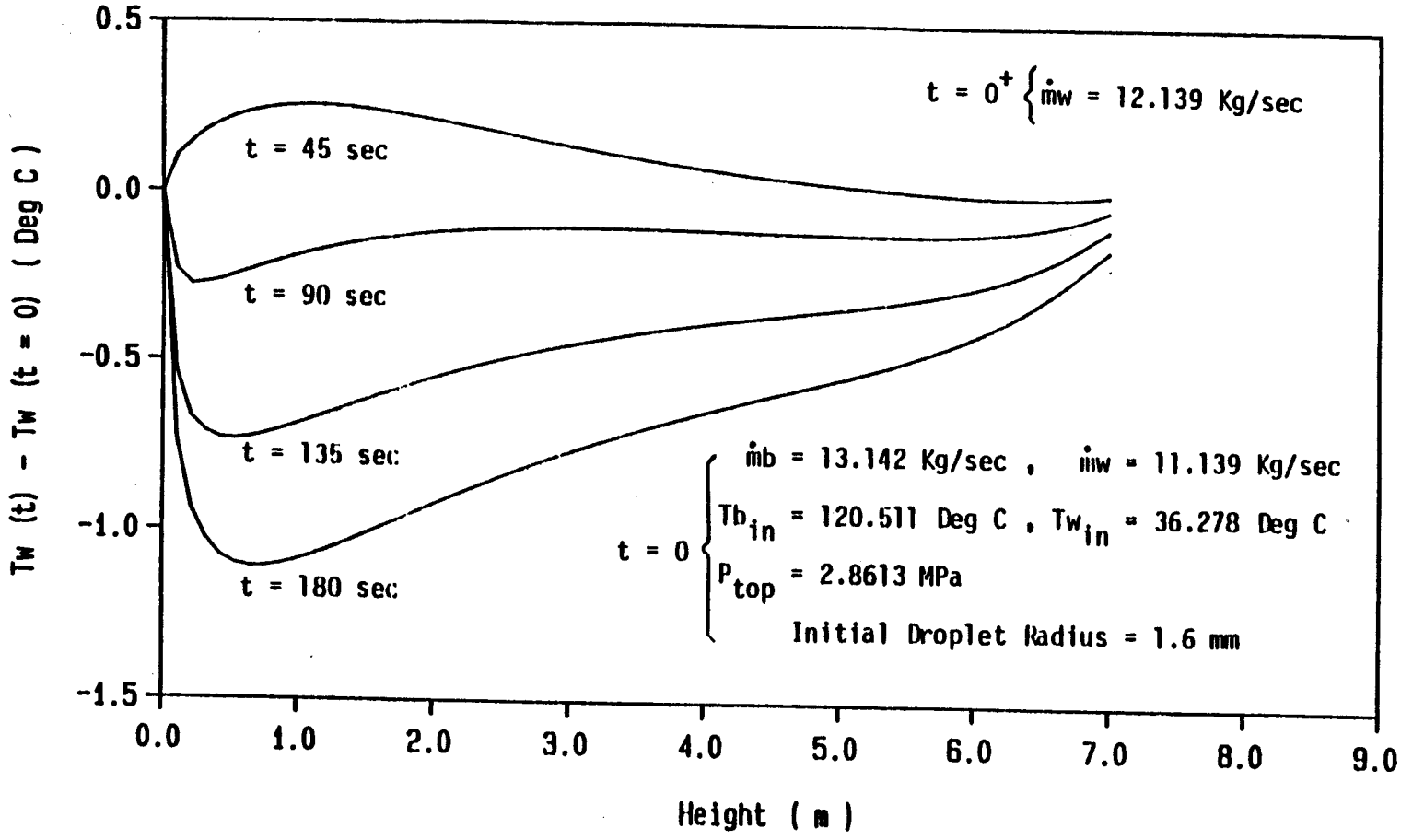


Figure 42. Transient response of the working fluid temperature after an increase in mass flow rate of the working fluid.

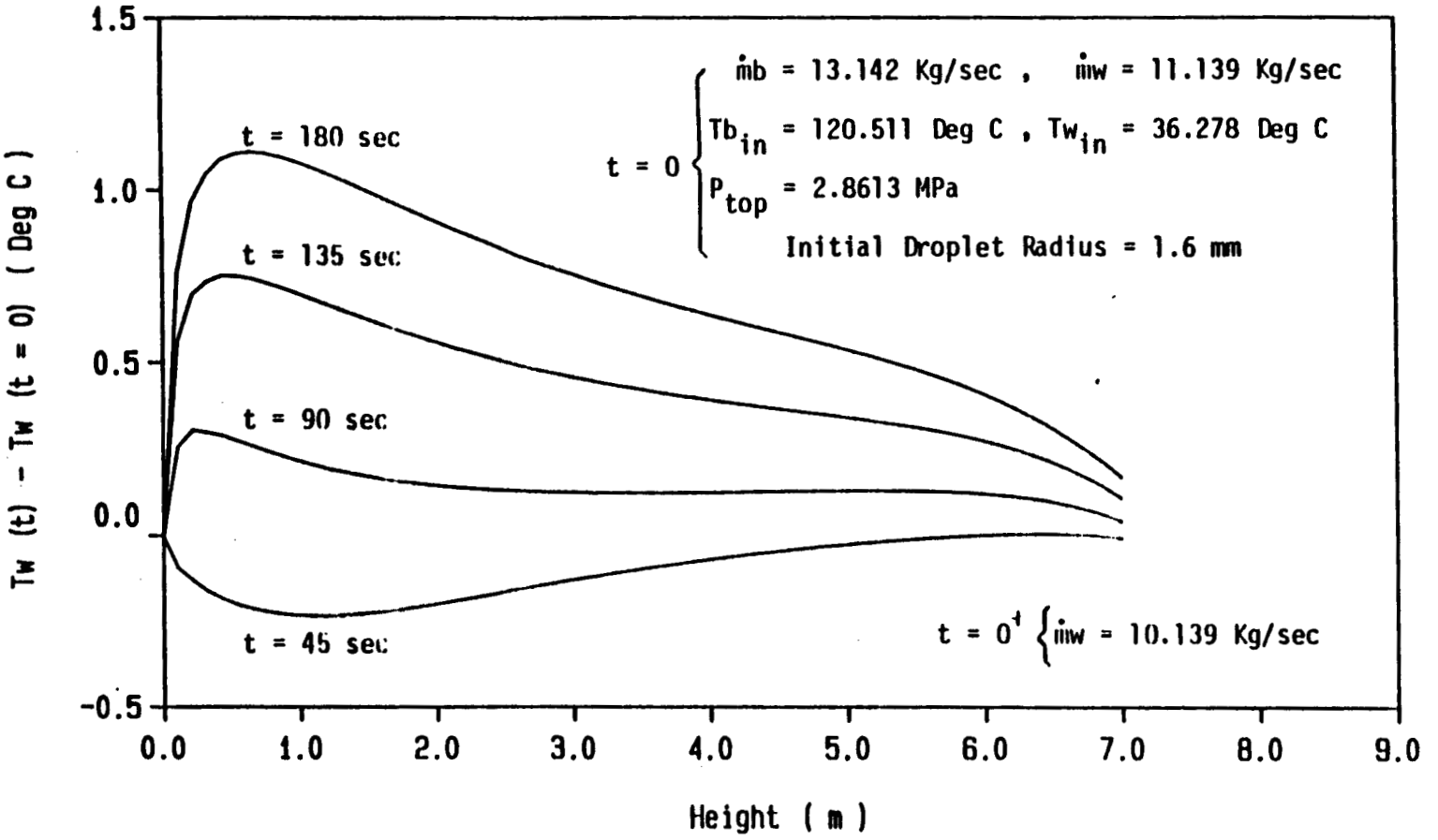


Figure 43. Transient response of the working fluid temperature after a decrease in mass flow rate of the working fluid.

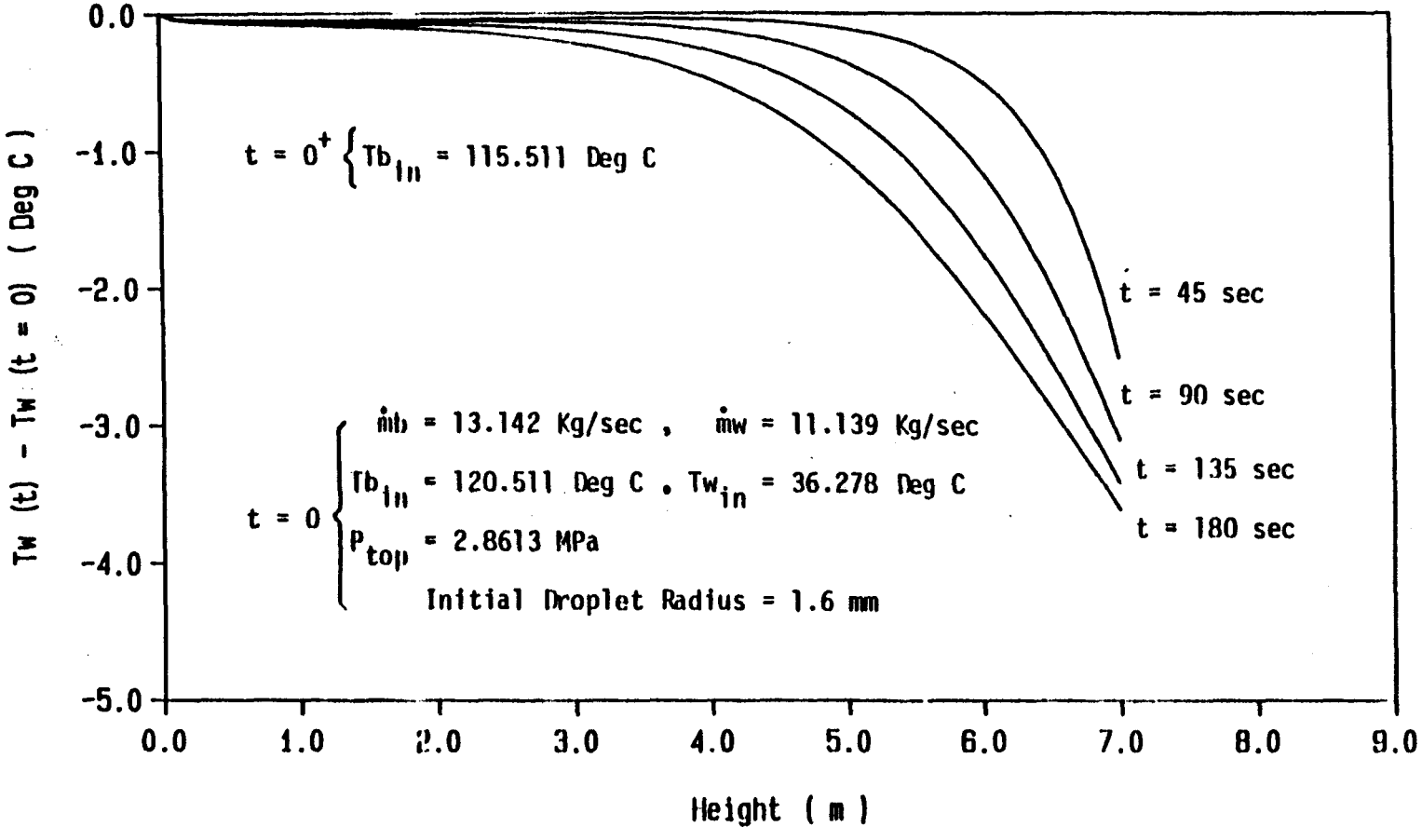


Figure 44. Transient response of the working fluid temperature after a decrease in the brine inlet temperature.

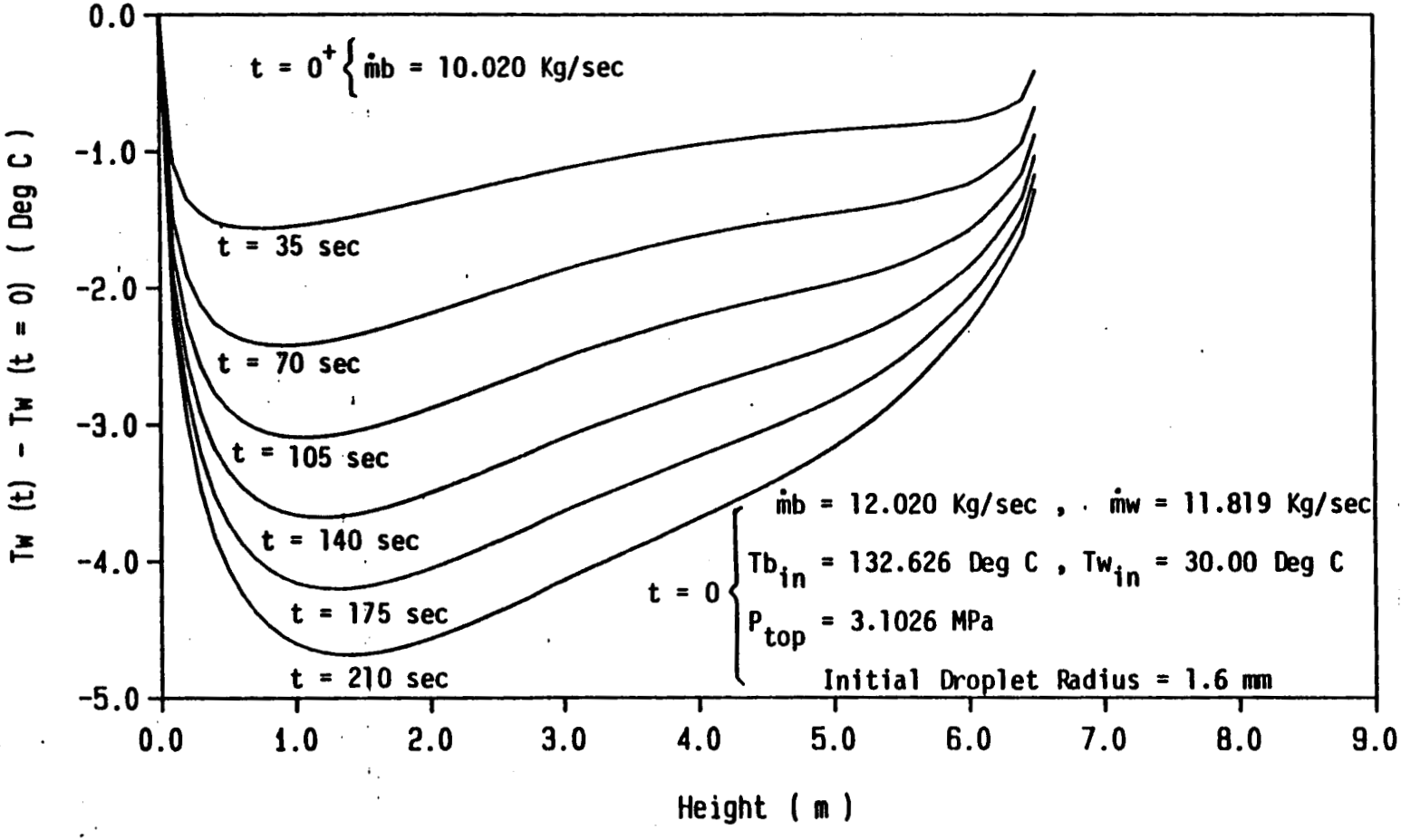


Figure 45. Transient response of the working fluid temperature after a decrease in mass flow rate of the brine, $\dot{m}b$ = 12.02 Kg/sec, $\dot{m}w$ = 11.819 Kg/sec.

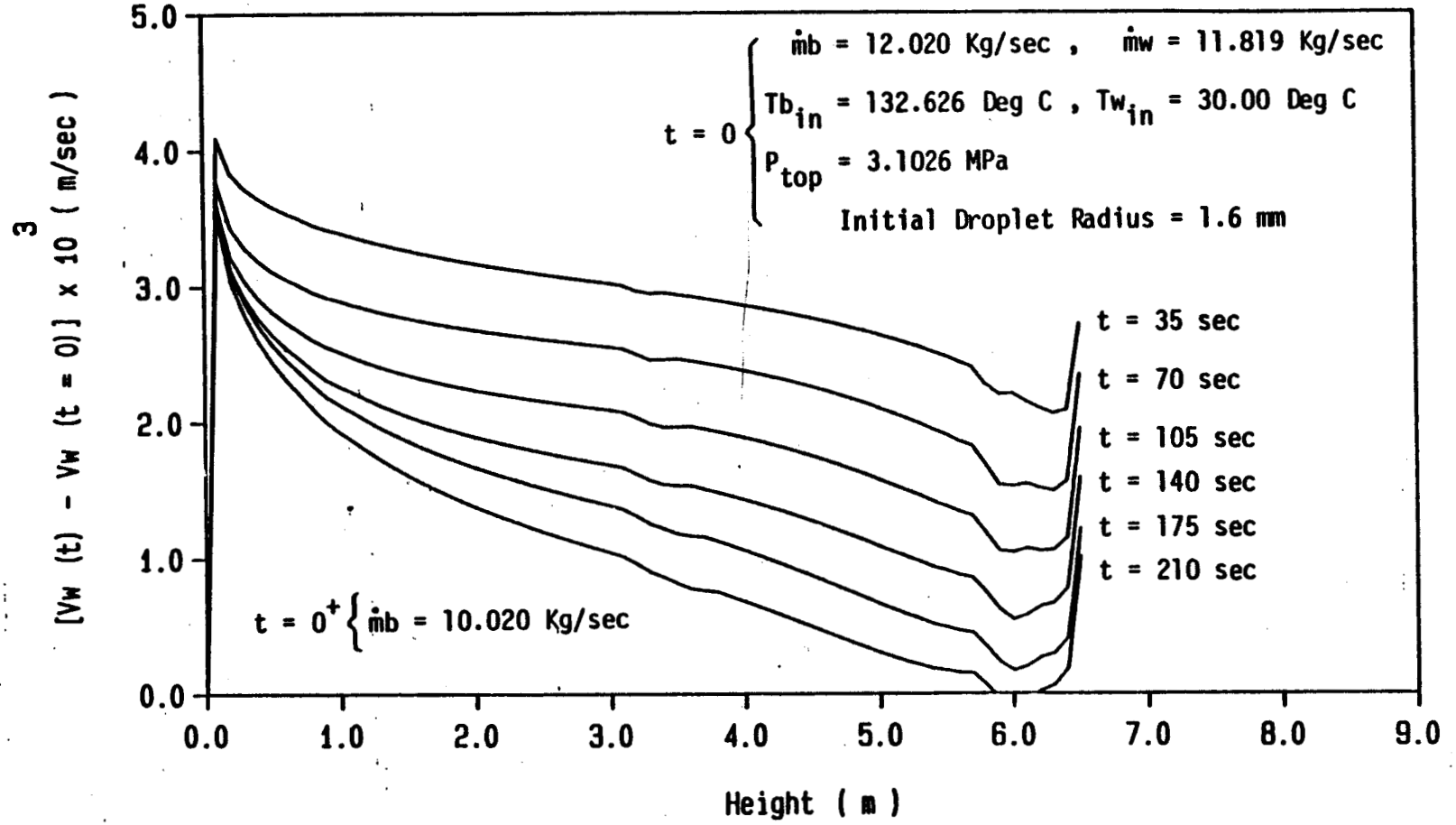


Figure 46. Transient response of the droplet velocity after a decrease in mass flow rate of the brine.

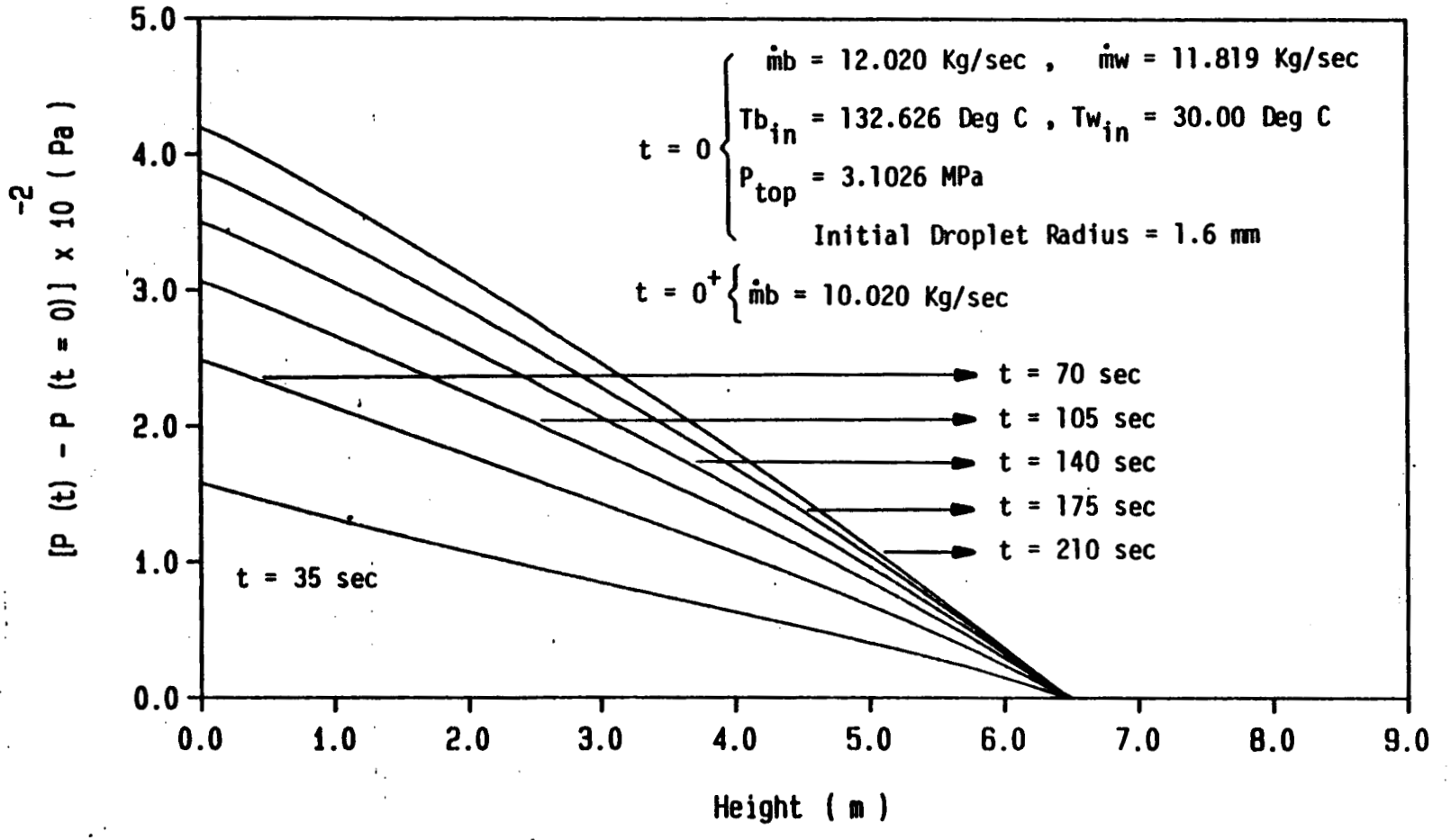


Figure 47. Transient response of the pressure after a decrease in mass flow rate of the brine.

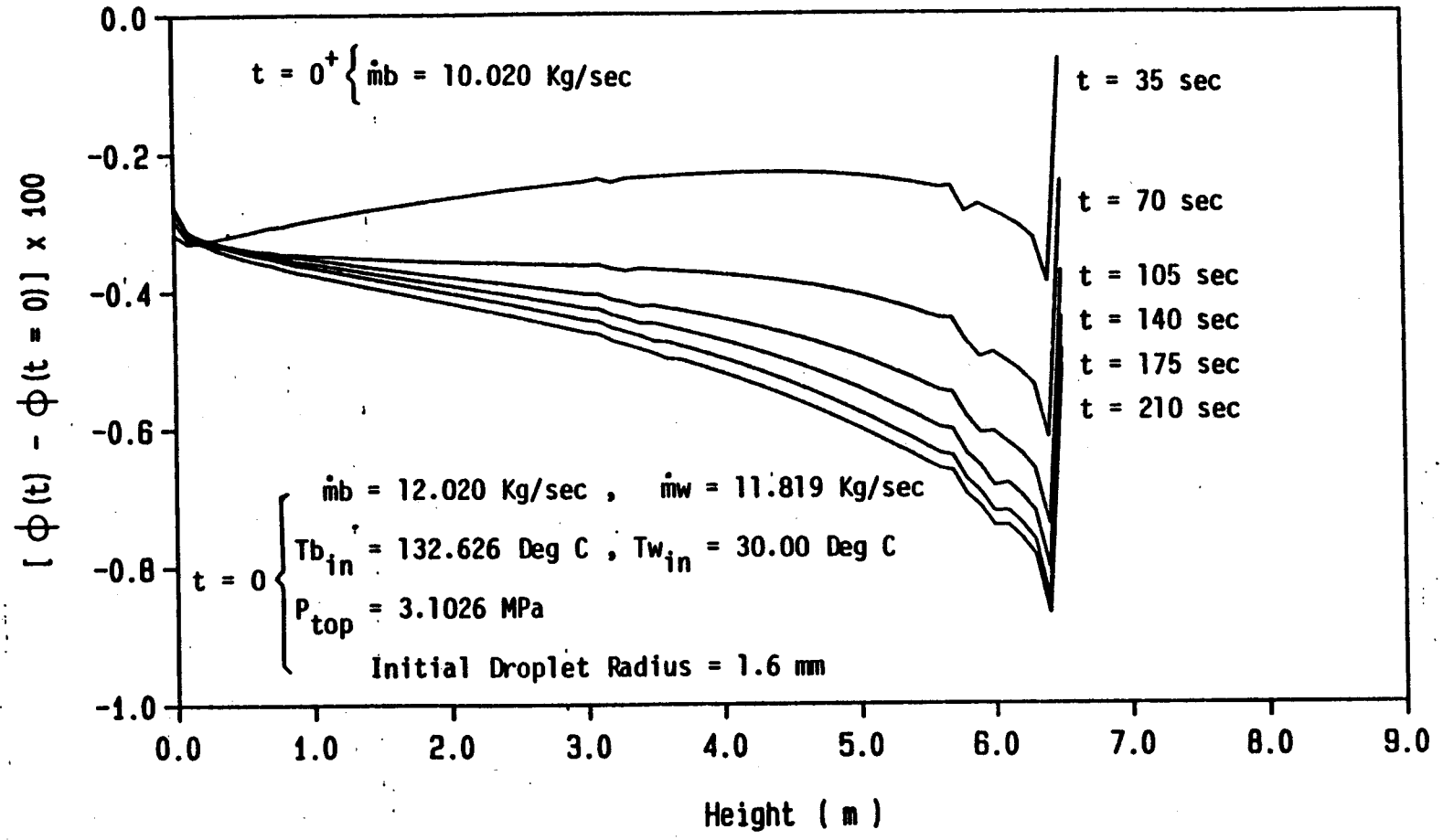


Figure 48. Transient response of the holdup after a decrease in mass flow rate of the brine.

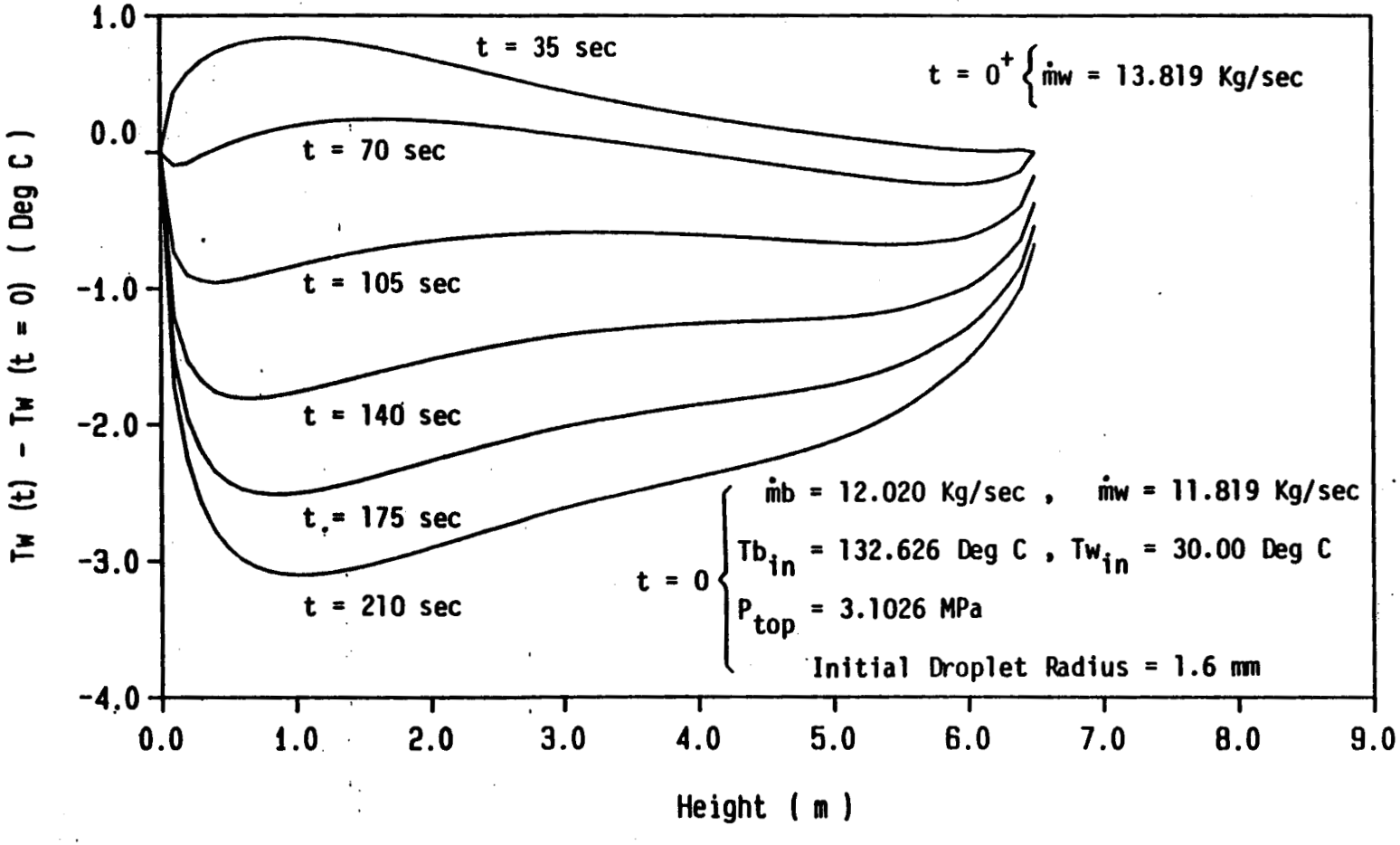


Figure 49. Transient response of the working fluid temperature after an increase in mass flow rate of the working fluid, $\dot{m}b$ = 12.02 Kg/sec, $\dot{m}w$ = 11.819 Kg/sec.

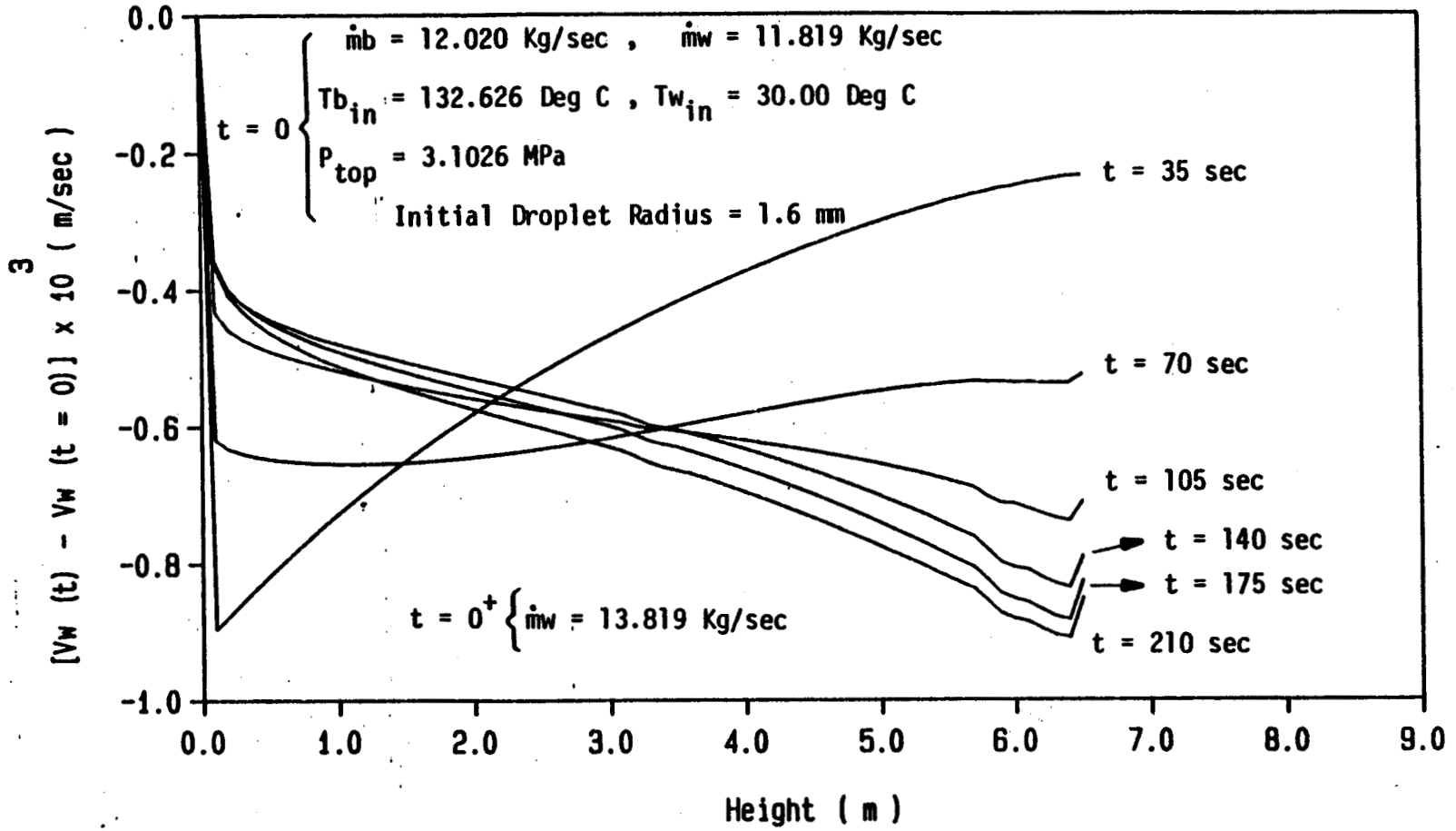


Figure 50. Transient response of the droplet velocity after an increase in mass flow rate of the working fluid.

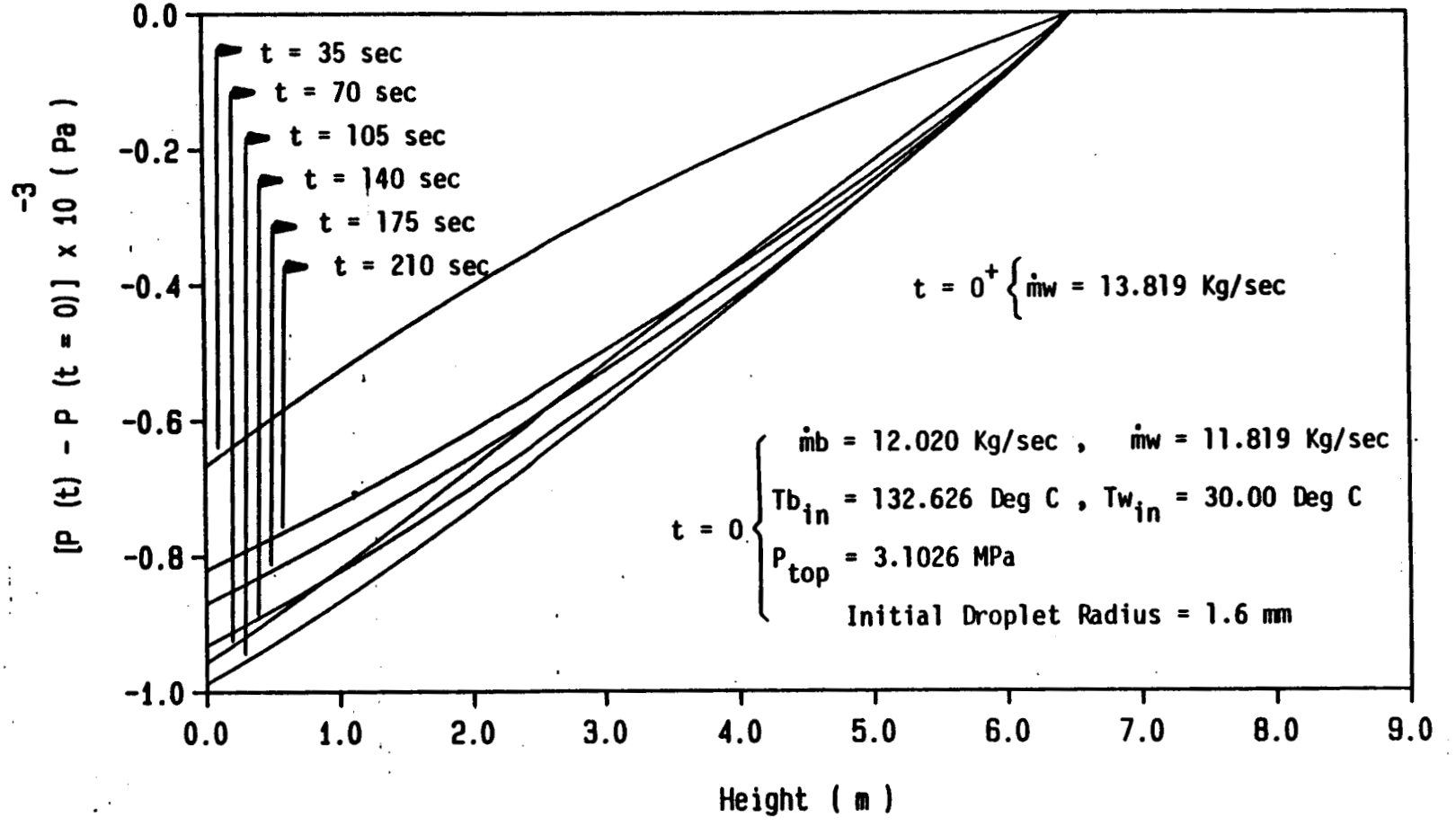


Figure 51. Transient response of the pressure after an increase in mass flow rate of the working fluid.

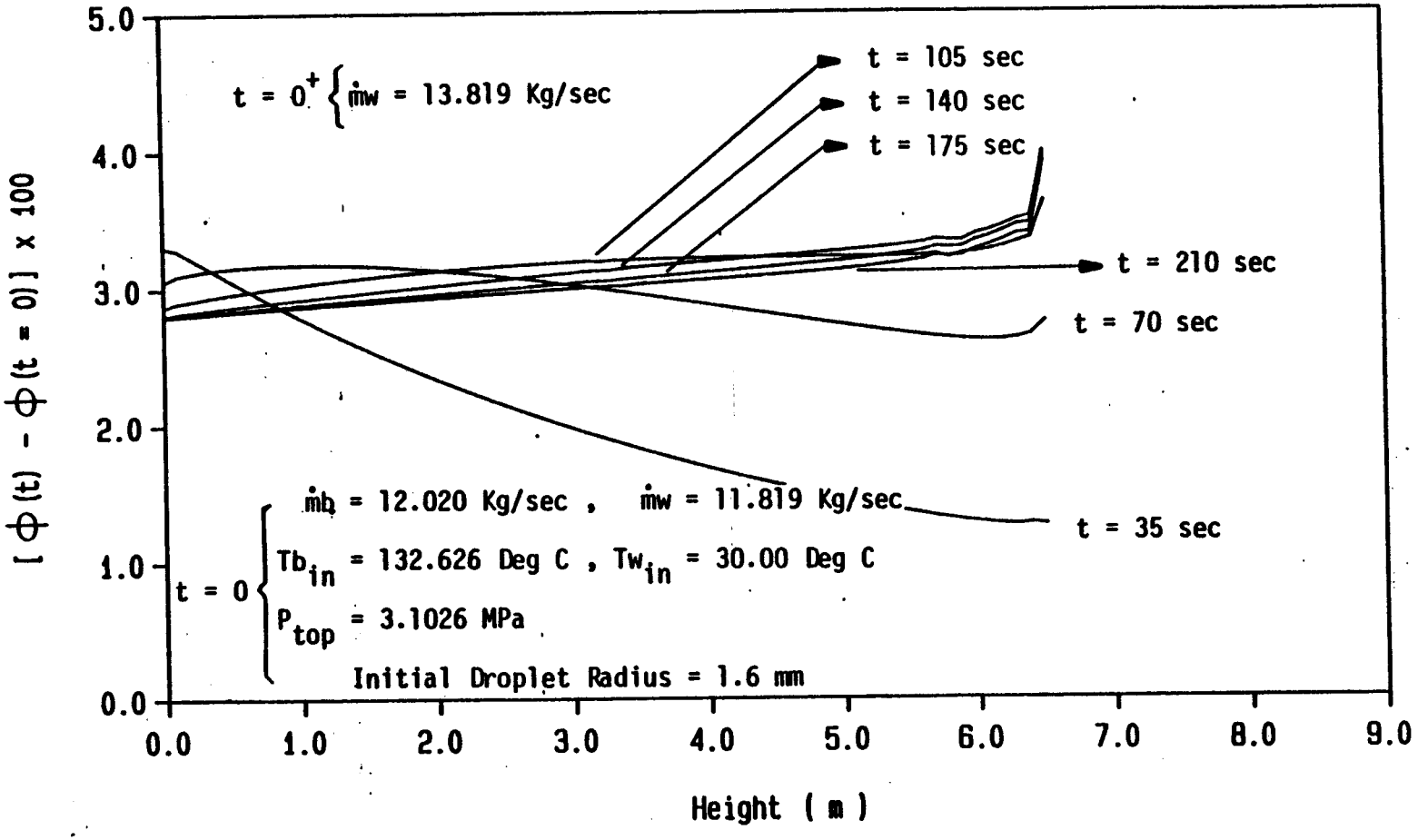


Figure 52. Transient response of the holdup after an increase in mass flow rate of the working fluid.

allows for longer heating times. Thus, as shown in Figures 49 and 50, there is at first an increase in temperature near the bottom of the column. As time increases the brine coming down is cooled and there is lower potential for heat transfer; thus, as shown in Figure 49, the working fluid at the bottom of the column gradually cools. The drops remain smaller in size and their resulting reduced drag allows for an increase in velocity, but not as high as the original values. Attempting to get a higher flow rate of working fluid through the column leads to lower pressures in the column, since the column contains more working fluid and correspondingly higher holdup as seen in Figures 51 and 52.

Figures 53 and 54 illustrate the transient effect of a decrease in brine inlet temperature. The droplets gradually cool increasing their density and thus reducing the drag due to shrinkage in size. This leads to a decrease in holdup at the top of the column and would, of course, cause an increase in the column preheater height.

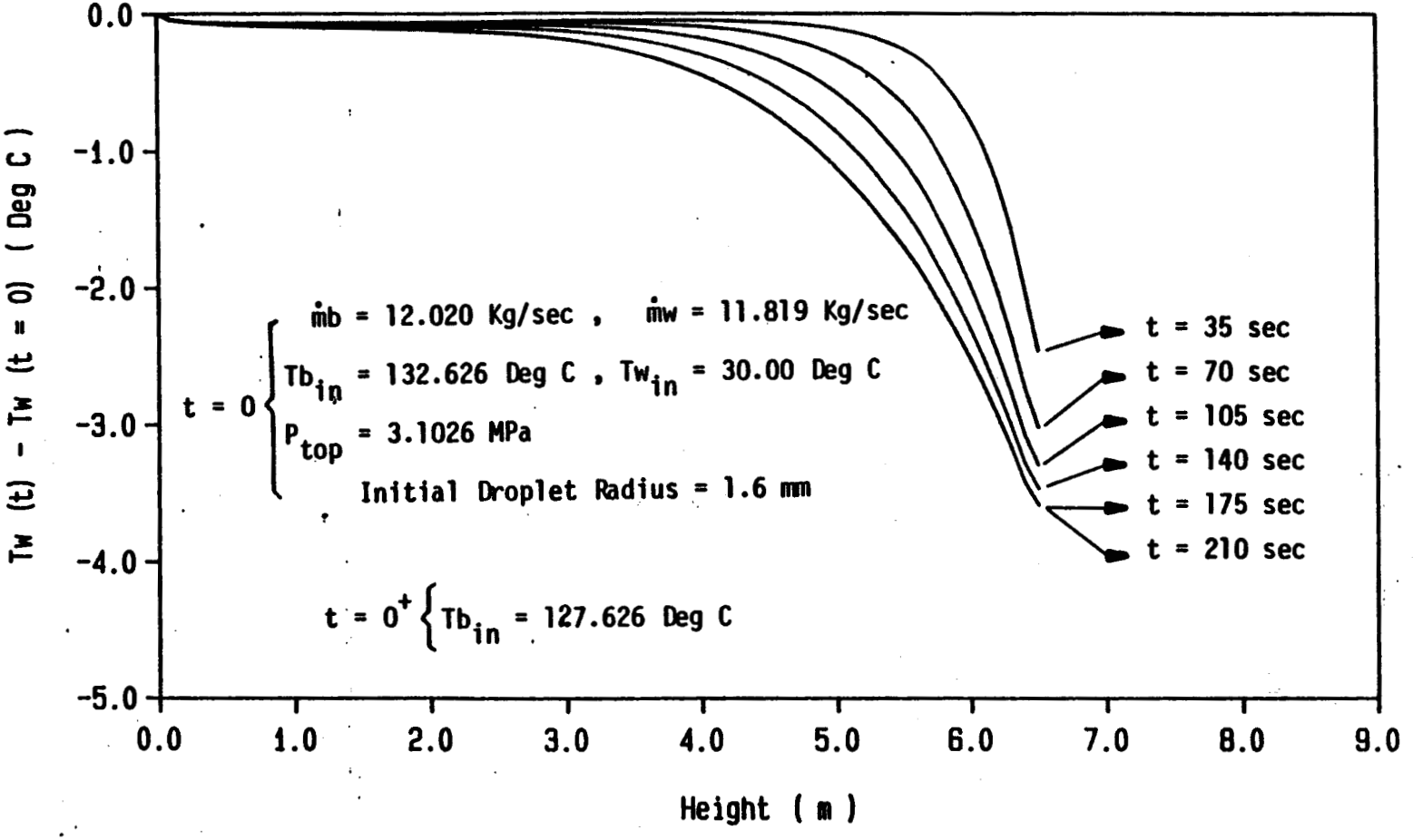


Figure 53. Transient response of the working fluid temperature after a decrease in the brine inlet temperature.

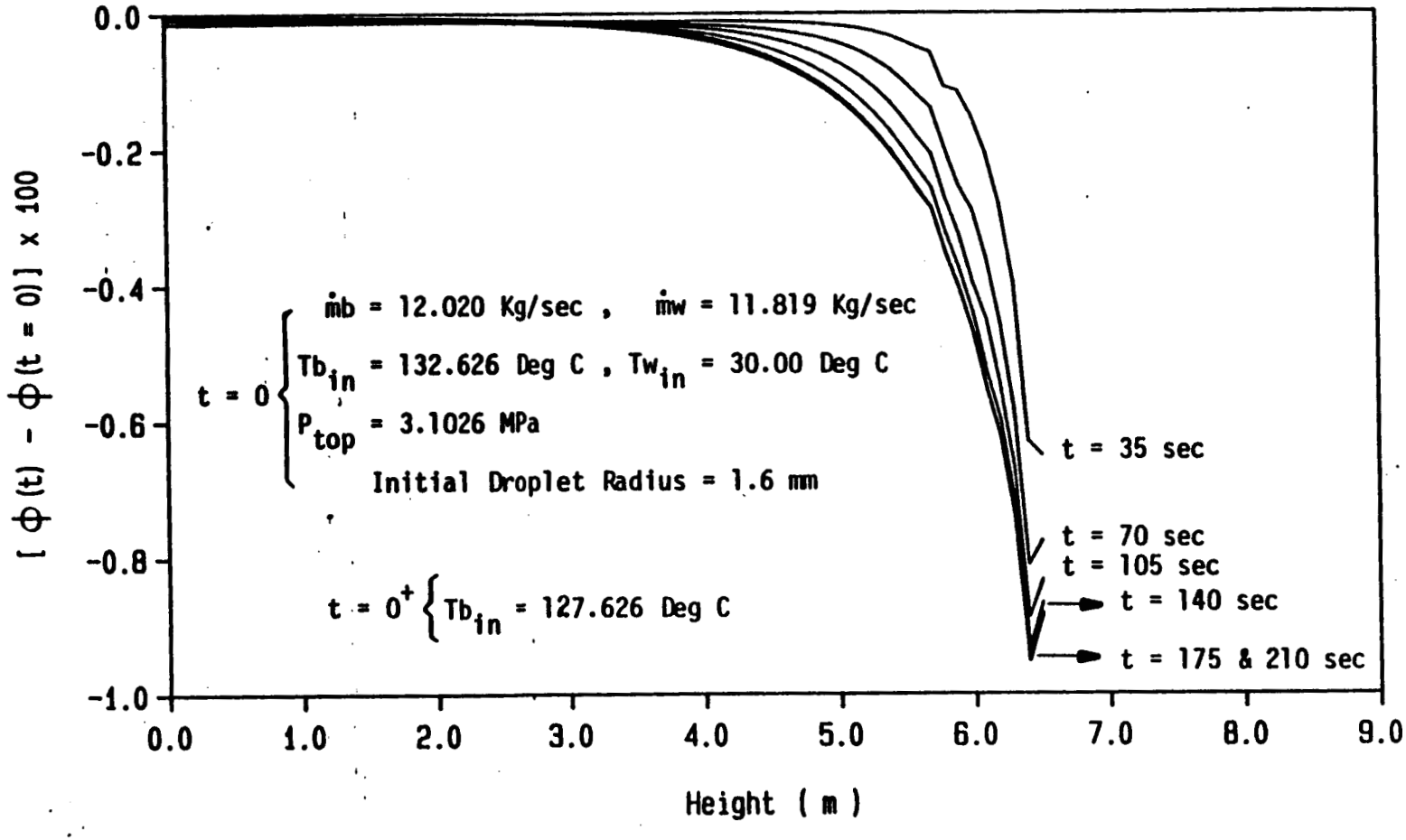


Figure 54. Transient response of the holdup after a decrease in the brine inlet temperature.

# CHAPTER 5

## CONCLUSIONS AND RECOMMENDATIONS

The operational characteristic of a spray column heat exchanger was studied using a one-dimensional transient two-phase flow and heat transfer model. A finite difference scheme was successfully applied so as to solve for the local variation of properties along the length of the column. This allowed for thorough examination of the behavior of the column in steady state as well as the transient mode of operation. The solution scheme provided a means whereby mass, momentum and energy coupling between phases could be adequately treated.

Various models of heat transfer were incorporated into the solution routine and the validity of each model was examined by comparison to experimental data. Further, the solution routine was developed which could handle the changes in droplet size. The solution clearly demonstrated the effects of mass flow rate, pressure and incoming brine temperature on the overall performance of the column.

Base on this study, which is the first to utilize the two-phase model for studying the behavior of the spray column direct contact heat exchanger, the following conclusions are made:

(1) Comparison of the present study and available experimental data suggests that conduction inside the working fluid droplet is the dominating heat transfer mechanism.

(2) Variation in flow rates of either stream, pressure and incoming brine temperature can adversely affect the operation of the column.

(3) The time constant for the transient response can be assessed. For the 500 kWe Barber-Nichols direct contactor is about 3-4 minutes.

(4) Two phase modeling provides a more accurate description of flow and temperature fields and therefore should be employed in future designs of spray type direct contact heat exchangers.

(5) For the 500 kWe Barber-Nichols direct contactor, it appears that at the point where the two major sections of the column are joined, some circulation or extended surface effect is taking place.

As far as the future is concerned, there is a lot to be done in the area of multiphase flow and heat transfer. However, as an extension to the problem studied herein, the following recommendations are made:

(1) This type of modeling should be applied to other types of direct contact heat exchangers as described in Chapter 1.

(2) A thorough investigation should be made into the mechanism of heat transfer in the boiler section of the spray column which would then allow one to utilize this

model for complete study of the boiler section or perhaps the combined preheater-boiler unit.

(3) The model should be made multidimensional so that the wall effects may be examined.

# APPENDIX A

# PROGRAM DETAILS

## A.1. Subroutines

The TOSC program is a computer code capable of analyzing the steady state or transient operation of a spray column preheater. The program can be used for studying the effects of change in mass flow rate of brine, mass flow rate of working fluid, pressure at top of the column and incoming brine temperature on operation of the column. The program is written in subroutine form such that each subroutine performs a specific task. Each subroutine is listed here with a brief description of its major function.

TOSC (main program)

(1) contains the calling sequences to the other subroutine and thus provides cyclic control over the calculation.

(2) t = t + DT.

(3) provides a shutdown procedure in the event that a solution cannot be obtained that satisfies mass conservation.

BRENT (BRine ENThalpy)

(1) Calculates the enthalpy of the brine.

BRPRO (BRine PROperty)

(1) Finds the density and temperature of the brine using its pressure and enthalpy.

BRVOI (BRine VOId)

(1) Calculates the corrected velocity of the brine based on its calculated void fraction.

COEFF (COEFFicient)

(1) Performs a least square curve fit in the pressure range of interest to find the coefficients of a linear relation for density of each phase as a function of pressure.

ERROR (continuity ERROR)

(1) Finds the continuity error for each cell.

FPRIN (Final PRINt out)

(1) Outputs data.

KDRAG (interphase friction coeffcient)

(1) Finds the interphase drag coefficient.

PCORR (Pressure CORRection)

(1) Finds the pressure correction so that the continuity equation is satisfied.

PRESS (PRESSure)

(1) Finds the pressure distribution throughout the column using the mixture's momentum equation.

SETPR (SETup the PRogram)

(1) Reads the input data.

(2) Assigns initial guess to all variables.

TRIDA (TRIDiAgonal matrix solver)

(1) Solves a tridiagonal system of linear equations.

VCORR (Velocity CORRection)

(1) Finds the velocity correction to both phases based on pressure correction to satisfy the continuity equation.

VELVA (VELocity VAriations)

(1) Calculates the velocity variation of each phase with respect to pressure.

WFPRO (Working Fluid PROperty)

(1) Finds the enthalpy and density of the working fluid using its temperature and pressure.

WFTEM (Working Fluid TEMperature)

(1) Calculates the temperature distribution within an expanding droplet subject to variable surface temperature.

WFVEL (Working Fluid VELocity)

(1) Finds the velocity of the working fluid.

WFVOI (Working Fluid VOId fraction)

(1) Finds the void fraction of the working fluid.

## A.s. Basic Input Variables

The following is a list of all the input variables and a description of each.

| | |
|---|---|
| ALPG | Guessed value of working fluid void fraction |
| ALPHA | Thermal diffusivity of working fluid |
| DIAM | Diameter of the column |
| DT | Time step |
| FTIME | Problem time to end calculation |
| FTYPE | Working fluid type |
| HEIG | Height of the column |
| N | Number of finite difference cells |
| NPRIN | Computer unit number for output |
| PTOP | Pressure at top of the column |
| PTYPE | Mode of operation (i.e., transient or steady) |
| RMDB | Steady state value of brine mass flow rate |
| RMDW | Steady state value of wroking fluid mass flow rate |

| | |
|---|---|
| RWI | Initial radius of working fluid droplets |
| TBIN | Incoming temperature of brine |
| TMDB | Transient value of brine mass flow rate |
| TMDW | Transient value of working fluid mass flow rate |
| TOL | Pressure iteration convergence criterion |
| TPTOP | Transient value of pressure at top of the column |
| TTBT | Transient value of incoming brine temperature |
| TWIN | Incoming temperature of working fluid |

## A.3. Variables and Arrays Listed in COMMON Blocks

The variables and arrays contained in COMMON blocks are given below with a brief description of each one. Variables already defined in the inputs are omitted from this list.

| | |
|---|---|
| AB | $\partial\rho b/\partial P$ |
| ALP(I) | Void fraction of working fluid at present time level |
| ALPO(I) | Void fraction of working fluid at previous time level |
| AREA | Area of the column |
| Aw | $\partial\rho w/\partial P$ |
| DCON | English-metric converison for density |
| DX | Vertical node spacing |
| E(I) | Continuity error for each cell |
| EPS(I) | Void fraction of brine at present time level |
| EPSO(I) | Void fraction of brine at previous time level |

| | |
|---|---|
| HB(I) | Enthalpy of brine at present time level |
| HBO(I) | Enthalpy of brine at previous time level |
| HCON | English-metric conversion for enthalpy |
| HW(I) | Enthalpy of working fluid at present time level |
| HWO(I) | Enthalpy of working fluid at previous time level |
| P(I) | Pressure at present time level |
| PCON | English-metric conversion for pressure |
| PO(I) | Pressure at previous time level |
| PP(I) | Correction to pressure |
| RI(I) | Radius of working fluid droplets |
| RK(I) | Interphase friction coefficient |
| ROB(I) | Density of brine at present time level |
| ROBO(I) | Density of brine at previous time level |
| ROW(I) | Density of working fluid at present time level |
| ROWO(I) | Density of working fluid at previous time level |
| TB(I) | Temperature of brine |
| TBO(I) | An array for temporary storage of brine temperature |
| TSATNW | Transient value of working fluid saturation temperature |
| TW(I) | Temperagure of working fluid |
| VB(I) | Velocity of brine at present time value |
| VBH(I) | Off-location velocity of brine |
| VBPC(I) | $\partial Vb/\partial P$ |
| VBO(I) | Velocity of brine at previous time level |
| VW(I) | Velocity of working fluid at present time level |
| VWC(I) | Correction to working fluid velocity |
| VWH(I) | Off-location velocity of working fluid |

VWPC(I) $\partial Vw/\partial p$

VWO(I) Velocity of working fluid at previous time level

## A.4. Comments on Coding, Stability and Execution of the Program

The TOSC program is written in Fortran 77. In writing the program, a repetitious coding style has been used for clarity of logic. The program is free from any numerical instability due to employment of implicit upwind differencing technique. For efficient execution of the program, the following guidelines must be observed:

(1) The number of finite difference cells should be restricted to 65 or less.

(2) The convergence tolerance for pressure iteration should be of the order of $10^{-3}$.

(3) The time step for transient calculation should be about 30 seconds or more. Thirty seconds is the approximate time required for the working fluid droplets to travel from bottom to top of the column.

All computer runs were performed using 65 finite difference cells with a convergence tolerance equal to 0.001 (i.e., N = 65 and TOL = 0.001). Under these conditions, the steady state calculations required about 1 hour of CPU time on a VAX 11/750 computer. The solution required 40-50 iterations to converge. A major portion of the CPU time was required for calculation of the properties of the phases.

## A.5. Sample Test Problem

To help the user of the TOSC code, this section contains a listing from a simple test problem. The problem is to study the transient behavior of the column when sudden changes occur in mass flow rate of brine, mass flow rate of the working fluid, pressure at top of the column and brine inlet temperature. The column is initially operating at steady state. A complete list of input parameter is:

PTYPE = TRANSIENT, FTYPE = ISOB

NPRIN = 6, ALPG = 0.1, TWIN = 20.0, TBIN = 90.0

RMDB = 9.0, RMDW = 7.0

PTOP = 2300000.0, HEIG = 1.5, DIAM = 1.0

N = 15, TOL = 0.001, ALPHA = 7.0 E-08, RWI = 0.0016

DT = 35.0, FTIME = 70.0

TMDB = 8.5, TMDW = 7.5, TPTOP = 2100000.0, TTBT = 110.0

The output from the computer program is presented in the following pages.

<<<< ANALYSIS OF THE OPERATION OF A SPRAY COLUMN PREHEATER >>>>

| | |
|---|---|
| MODE OF OPERATION | = TRANSIENT |
| TYPE OF WORKING FLUID | = ISOB |
| COLUMN PRESSURE OUT | = 2300000.000 (Pa) |
| BRINE MASS FLOW RATE | = 9.000 (Kg/s) |
| WORKING FLUID MASS FLOW RATE | = 7.000 (Kg/s) |
| BRINE TEMPERATURE IN | = 90.000 (Deg C) |
| WORKING FLUID TEMPERATURE IN | = 20.000 (Deg C) |
| WORKING FLUID SATURATION TEMPERATURE AT COLUMN PRESSURE OUT | = 107.255 (Deg C) |
| PREHEATER HEIGHT | = 1.500 (m) |
| PREHEATER DIAMETER | = 1.0000 (m) |
| RADIUS OF WORKING FLUID DROPLETS (INITIAL) | = 0.00160 (m) |
| NUMBER OF FINITE DIFFERENCE CELLS | = 15 |
| TIME STEP VALUE | = 35.000 (Seconds) |

<<<< TRANSIENT VALUES OF THE PRESSURE, MASS FLOW RATES AND INCOMING BRINE TEMPERATURE ARE AS FOLLOWS >>>>

| | |
|---|---|
| TRANSIENT VALUE OF THE COLUMN PRESSURE OUT | = 2100000.000 (Pa) |
| TRANSIENT VALUE OF THE BRINE MASS FLOW RATE | = 8.500 (Kg/s) |
| TRANSIENT VALUE OF THE WORKING FLUID MASS FLOW RATE | = 7.500 (Kg/s) |
| TRANSIENT VALUE OF THE INCOMING BRINE TEMPERATURE | = 110.000 (Deg C) |
| NEW SATURATION TEMPERATURE | = 102.208 (Deg C) |

TIME = 0.000 (Seconds)

| HEIGHT (m) | BRINE VOID FRACTION | WORKING FLUID VOID FRACTION | BRINE DENSITY (Kg/m3) | WORKING FLUID DENSITY (Kg/m3) | BRINE TEMPERATURE (Deg C) | WORKING FLUID TEMPERATURE (Deg C) | BRINE VELOCITY (m/s) | WORKING FLUID VELOCITY (m/s) | PRESSURE (MPa) |
|---|---|---|---|---|---|---|---|---|---|
| 1.50 | 0.9124 | 0.0876 | 966.26 | 484.62 | 90.00 | 75.54 | -0.01300 | 0.20948 | 2.3000 |
| 1.40 | 0.9129 | 0.0871 | 966.82 | 487.46 | 89.16 | 74.03 | -0.01299 | 0.20911 | 2.3009 |
| 1.30 | 0.9131 | 0.0869 | 967.41 | 490.40 | 88.27 | 72.44 | -0.01298 | 0.20833 | 2.3018 |
| 1.20 | 0.9133 | 0.0867 | 968.03 | 493.45 | 87.34 | 70.74 | -0.01297 | 0.20750 | 2.3027 |
| 1.10 | 0.9135 | 0.0865 | 968.67 | 496.62 | 86.35 | 68.93 | -0.01296 | 0.20665 | 2.3036 |
| 1.00 | 0.9137 | 0.0863 | 969.36 | 499.93 | 85.30 | 67.00 | -0.01294 | 0.20576 | 2.3045 |
| 0.90 | 0.9139 | 0.0861 | 970.08 | 503.40 | 84.17 | 64.93 | -0.01293 | 0.20483 | 2.3055 |
| 0.80 | 0.9141 | 0.0859 | 970.86 | 507.06 | 82.95 | 62.69 | -0.01292 | 0.20385 | 2.3064 |
| 0.70 | 0.9144 | 0.0856 | 971.70 | 510.99 | 81.63 | 60.24 | -0.01290 | 0.20280 | 2.3073 |
| 0.60 | 0.9146 | 0.0854 | 972.62 | 515.14 | 80.16 | 57.54 | -0.01289 | 0.20169 | 2.3082 |
| 0.50 | 0.9149 | 0.0851 | 973.65 | 519.66 | 78.49 | 54.53 | -0.01287 | 0.20049 | 2.3091 |
| 0.40 | 0.9151 | 0.0849 | 974.83 | 524.68 | 76.56 | 51.07 | -0.01285 | 0.19916 | 2.3100 |
| 0.30 | 0.9155 | 0.0845 | 976.29 | 530.39 | 74.12 | 47.01 | -0.01283 | 0.19762 | 2.3110 |
| 0.20 | 0.9159 | 0.0841 | 977.95 | 537.47 | 71.29 | 41.77 | -0.01281 | 0.19585 | 2.3119 |
| 0.10 | 0.9163 | 0.0837 | 981.84 | 545.44 | 64.33 | 35.61 | -0.01277 | 0.19315 | 2.3128 |
| 0.00 | 0.9176 | 0.0824 | 981.84 | 564.25 | 64.33 | 20.00 | -0.01274 | 0.19139 | 2.3137 |

TIME = 35.000 (Seconds)

| HEIGHT (m) | BRINE VOID FRACTION | WORKING FLUID VOID FRACTION | BRINE DENSITY (Kg/m3) | WORKING FLUID DENSITY (Kg/m3) | BRINE TEMPERATURE (Deg C) | WORKING FLUID TEMPERATURE (Deg C) | BRINE VELOCITY (m/s) | WORKING FLUID VELOCITY (m/s) | PRESSURE (MPa) |
|---|---|---|---|---|---|---|---|---|---|
| 1.50 | 0.9047 | 0.0953 | 951.88 | 464.67 | 110.00 | 84.54 | -0.01260 | 0.21314 | 2.1000 |
| 1.40 | 0.9063 | 0.0937 | 956.04 | 472.62 | 104.43 | 80.90 | -0.01259 | 0.21230 | 2.1009 |
| 1.30 | 0.9068 | 0.0932 | 959.31 | 479.28 | 99.93 | 77.66 | -0.01257 | 0.21071 | 2.1018 |
| 1.20 | 0.9072 | 0.0928 | 961.93 | 485.07 | 96.22 | 74.69 | -0.01257 | 0.20926 | 2.1027 |
| 1.10 | 0.9075 | 0.0925 | 964.09 | 490.29 | 93.09 | 71.90 | -0.01257 | 0.20793 | 2.1036 |
| 1.00 | 0.9078 | 0.0922 | 965.92 | 495.13 | 90.39 | 69.21 | -0.01257 | 0.20669 | 2.1045 |
| 0.90 | 0.9081 | 0.0919 | 967.52 | 499.76 | 87.98 | 66.54 | -0.01257 | 0.20548 | 2.1054 |
| 0.80 | 0.9083 | 0.0917 | 968.96 | 504.30 | 85.77 | 63.84 | -0.01257 | 0.20429 | 2.1063 |
| 0.70 | 0.9085 | 0.0915 | 970.32 | 508.86 | 83.67 | 61.03 | -0.01258 | 0.20308 | 2.1072 |
| 0.60 | 0.9087 | 0.0913 | 971.64 | 513.58 | 81.59 | 58.05 | -0.01258 | 0.20182 | 2.1081 |
| 0.50 | 0.9089 | 0.0911 | 972.98 | 518.50 | 79.44 | 54.81 | -0.01258 | 0.20050 | 2.1090 |
| 0.40 | 0.9092 | 0.0908 | 974.40 | 523.85 | 77.11 | 51.17 | -0.01258 | 0.19908 | 2.1100 |
| 0.30 | 0.9094 | 0.0906 | 976.09 | 529.80 | 74.31 | 46.97 | -0.01257 | 0.19747 | 2.1109 |
| 0.20 | 0.9098 | 0.0902 | 977.91 | 537.10 | 71.21 | 41.61 | -0.01257 | 0.19564 | 2.1118 |
| 0.10 | 0.9102 | 0.0898 | 982.05 | 545.15 | 63.78 | 35.43 | -0.01254 | 0.19295 | 2.1127 |
| 0.00 | 0.9115 | 0.0885 | 982.05 | 563.83 | 63.78 | 20.00 | -0.01252 | 0.19123 | 2.1136 |

TIME = 70.000 (Seconds)

| HEIGHT (m) | BRINE VOID FRACTION | WORKING FLUID VOID FRACTION | BRINE DENSITY (Kg/m3) | WORKING FLUID DENSITY (Kg/m3) | BRINE TEMPERATURE (Deg C) | WORKING FLUID TEMPERATURE (Deg C) | BRINE VELOCITY (m/s) | WORKING FLUID VELOCITY (m/s) | PRESSURE (MPa) |
|---|---|---|---|---|---|---|---|---|---|
| 1.50 | 0.9032 | 0.0968 | 951.88 | 459.32 | 110.00 | 86.85 | -0.01259 | 0.21468 | 2.1000 |
| 1.40 | 0.9046 | 0.0954 | 953.83 | 465.89 | 107.42 | 84.00 | -0.01257 | 0.21387 | 2.1009 |
| 1.30 | 0.9052 | 0.0948 | 956.00 | 472.33 | 104.50 | 81.04 | -0.01255 | 0.21225 | 2.1018 |
| 1.20 | 0.9057 | 0.0943 | 958.22 | 478.52 | 101.45 | 78.04 | -0.01253 | 0.21067 | 2.1027 |
| 1.10 | 0.9061 | 0.0939 | 960.39 | 484.42 | 98.40 | 75.03 | -0.01251 | 0.20917 | 2.1036 |
| 1.00 | 0.9066 | 0.0934 | 962.47 | 490.08 | 95.44 | 72.02 | -0.01249 | 0.20774 | 2.1045 |
| 0.90 | 0.9070 | 0.0930 | 964.43 | 495.53 | 92.59 | 68.99 | -0.01247 | 0.20636 | 2.1054 |
| 0.80 | 0.9073 | 0.0927 | 966.29 | 500.84 | 89.84 | 65.91 | -0.01245 | 0.20502 | 2.1063 |
| 0.70 | 0.9077 | 0.0923 | 968.06 | 506.10 | 87.16 | 62.74 | -0.01243 | 0.20368 | 2.1072 |
| 0.60 | 0.9080 | 0.0920 | 969.77 | 511.41 | 84.52 | 59.42 | -0.01241 | 0.20232 | 2.1081 |
| 0.50 | 0.9084 | 0.0916 | 971.49 | 516.91 | 81.83 | 55.87 | -0.01239 | 0.20091 | 2.1090 |
| 0.40 | 0.9088 | 0.0912 | 973.25 | 522.72 | 79.00 | 51.95 | -0.01237 | 0.19942 | 2.1099 |
| 0.30 | 0.9091 | 0.0909 | 975.24 | 529.05 | 75.74 | 47.51 | -0.01235 | 0.19777 | 2.1108 |
| 0.20 | 0.9096 | 0.0904 | 977.31 | 536.67 | 72.23 | 41.93 | -0.01232 | 0.19591 | 2.1118 |
| 0.10 | 0.9101 | 0.0899 | 981.77 | 544.92 | 64.30 | 35.60 | -0.01227 | 0.19322 | 2.1127 |
| 0.00 | 0.9116 | 0.0884 | 981.77 | 563.83 | 64.30 | 20.00 | -0.01224 | 0.19149 | 2.1136 |

# APPENDIX B

# PROGRAM LISTING

```
C     ****************************************************************
C     *                                                              *
C     *                          T O S C                             *
C     *                                                              *
C     *   THIS PROGRAM IS SETUP TO DO AN ANALYSIS OF THE STEADY      *
C     * STATE OR TRANSIENT OPERATION OF A SPRAY COLUMN PREHEATER.    *
C     *   IT IS A DRIVING PROGRAM RESPONSIBLE FOR CALLING OTHER      *
C     * SUBROUTINES WHICH HANDLE DIFFERENT STAGES OF THE SOLUTION    *
C     * ROUTINE.                                                     *
C     *                                                              *
C     ****************************************************************
C
      IMPLICIT REAL*8(A-H,O-Z)
      CHARACTER FTYPE*6
      CHARACTER PTYPE*9
      COMMON/BLK0/FTYPE,PTYPE,AW,AB,PTOP,TSAT
      COMMON/BLK1/AREA,DX,N,NP1,DT,DIAM,HEIG
      COMMON/BLK2/ROB(202),ROW(202),ROBO(202),ROWO(202)
      COMMON/BLK3/RMDB,RMDW
      COMMON/BLK4/ALP(202),EPS(202),ALPO(202),EPSO(202)
      COMMON/BLK5/VB(202),VW(202),VBO(202),VWO(202)
      COMMON/BLK6/P(202),PO(202)
      COMMON/BLK7/E(202)
      COMMON/BLK8/RK(202)
      COMMON/BLK9/PP(202)
      COMMON/BLK10/NPRIN,TOL,TIME,FTIME
      COMMON/BLK11/VBC(202),VWC(202)
      COMMON/BLK12/TB(202),TW(202)
      COMMON/BLK13/HB(202),HW(202),HBO(202),HWO(202)
      COMMON/BLK14/DCON,HCON,PCON
      COMMON/BLK15/ALPHA,RWI,RI(202)
      COMMON/BLK16/VBH(202),VWH(202)
      COMMON/BLK17/TMDB,TMDW,TPTOP,TTBT,TSATNW
      COMMON/BLK18/VBPC(202),VWPC(202)
      COMMON/BLK19/TBO(202)
      DATA DCON,HCON,PCON/0.062428,4.2995E-04,1.4504E-04/
C
      CALL SETPR
C
      IF(PTYPE .EQ. 'TRANSIENT') CALL COEFF
      ICON=0
10    ICON=ICON+1
      IF(ICON.GE.150) GO TO 200
C
      CALL SBRENT
C
      CALL BRPRO
C
      CALL WFTEM
C
      CALL WFPRO
C
      DO 20 I=1,NP1
```

```
        TB(I)=TBO(I)
20    CONTINUE
C
      CALL SPRESS
C
      CALL KDRAG
C
      CALL SWFVEL
C
      CALL SERROR
C
      DO 30 I=2,N
        IF(ABS(E(I)).GT.TOL) GO TO 40
30    CONTINUE
      GO TO 70
40    CALL SVELVA
C
      CALL PCORR
C
      CALL VCORR
C
      ROWH1=(ROW(1)+ROW(2))/2
      DO 50 I=2,NP1
        ROWH=(ROW(I-1)+ROW(I))/2
        RI(I)=RWI*(ROWH1/ROWH)**(1./3.)
50    CONTINUE
C
      CALL SWFVOI
C
      DO 60 I=2,NP1
        VB(I)=-RMDB/ROB(I)/EPS(I)/AREA
60    CONTINUE
      GO TO 10
70    DO 80 I=1,NP1
        IF(I.EQ.1) THEN
          VWH(I)=VW(2)
          VBH(I)=VB(2)
        ELSE
          IF(I.EQ.NP1) THEN
            VWH(I)=VW(NP1)
            VBH(I)=VB(NP1)
          ELSE
            VWH(I)=0.5*(VW(I)+VW(I+1))
            VBH(I)=0.5*(VB(I)+VB(I+1))
          ENDIF
        ENDIF
80    CONTINUE
      IF(PTYPE .EQ. 'TRANSIENT') THEN
        TIME=0.0
        PEN=TPTOP*PCON
        CALL CARBON('PX',PEN,0.0,PTYPE,HWEN,S,VWEN,TF,PR,0,SL,HL,
     1              VL,SV,HV,VV,QUAL)
        TSATNW=(TF-32.)/1.8
```

```
        TBEN=TTBT*1.8+32.
90      CALL WATER('TP',TBEN,PEN,90,1,0,Q,S,HBEN,VBEN,U,TF,PR,SL,HL,
     1             VL,UL,SV,HV,VV,UV,NERROR)
        HB(NP1)=HBEN/HCON
      ENDIF
C
      CALL FPRIN
C
      IF(PTYPE .EQ. 'STEADY') GO TO 210
      P(NP1)=TPTOP
      TSAT=TSATNW
95    TIME=TIME+DT
      DO 100 I=1,NP1
        EPSO(I)=EPS(I)
        ALPO(I)=ALP(I)
        VBO(I)=VB(I)
        VWO(I)=VW(I)
        PO(I)=P(I)
        HBO(I)=HB(I)
        HWO(I)=HW(I)
        ROBO(I)=ROB(I)
        ROWO(I)=ROW(I)
100   CONTINUE
      ICON=0
110   ICON=ICON+1
      IF(ICON.GE.150) GO TO 200
C
      CALL WFVOI
C
      CALL BRVOI
C
      DO 120 I=1,NP1
        P(I)=P(I)+PP(I)
120   CONTINUE
      DO 130 I=NP1,1,-1
        IF(I.EQ.1) THEN
          VWH(I)=VW(I+1)
          VBH(I)=VB(I+1)
        ELSE
          IF(I.EQ.NP1) THEN
            VWH(I)=VW(I)
            VBH(I)=VB(I)
          ELSE
            VWH(I)=(VW(I)+VW(I+1))/2
            VBH(I)=(VB(I)+VB(I+1))/2
          ENDIF
        ENDIF
130   CONTINUE
C
      CALL BRENT
C
      CALL BRPRO
C
```

```
      CALL WFTEM
C
      CALL WFPRO
C
      DO 140 I=1,NP1
        TB(I)=TBO(I)
140   CONTINUE
C
      CALL PRESS
C
      CALL KDRAG
C
      CALL WFVEL
C
      CALL ERROR
C
      DO 150 I=NP1,1,-1
        IF(I.EQ.1) THEN
          VWH(I)=VW(I+1)
          VBH(I)=VB(I+1)
        ELSE
          IF(I.EQ.NP1) THEN
            VWH(I)=VW(I)
            VBH(I)=VB(I)
          ELSE
            VWH(I)=(VW(I)+VW(I+1))/2
            VBH(I)=(VB(I)+VB(I+1))/2
          ENDIF
        ENDIF
150   CONTINUE
      DO 160 I=2,N
        IF(ABS(E(I)).GT.TOL) GO TO 170
160   CONTINUE
      GO TO 190
C
170   CALL VELVA
C
      CALL PCORR
C
      CALL VCORR
C
      ROWH1=(ROW(1)+ROW(2))/2
      DO 180 I=2,NP1
        ROWH=(ROW(I-1)+ROW(I))/2
        RI(I)=RWI*(ROWH1/ROWH)**(1./3.)
180   CONTINUE
      GO TO 110
C
190   CALL TRFPR
C
      IF(TIME .GE. FTIME) GO TO 210
      GO TO 95
200   WRITE(NPRIN,1000) PTYPE
```

```
210   STOP
1000  FORMAT(10X,'SOLUTION FAILED TO CONVERGE IN 150 ITERATIONS',
     1       10X,'DURING THE ',A9,' ROUTINE')
      END
```

```
C     ****************************************************************
C     *                                                              *
C     *                          B R E N T                           *
C     *                                                              *
C     *   THIS SUBROUTINE FINDS THE ENTHALPY OF THE BRINE.           *
C     *                                                              *
C     ****************************************************************
C
      SUBROUTINE BRENT
      IMPLICIT REAL*8(A-H,O-Z)
      COMMON/BLK1/AREA,DX,N,NP1,DT,DIAM,HEIG
      COMMON/BLK2/ROB(202),ROW(202),ROBO(202),ROWO(202)
      COMMON/BLK3/RMDB,RMDW
      COMMON/BLK4/ALP(202),EPS(202),ALPO(202),EPSO(202)
      COMMON/BLK5/VB(202),VW(202),VBO(202),VWO(202)
      COMMON/BLK6/P(202),PO(202)
      COMMON/BLK13/HB(202),HW(202),HBO(202),HWO(202)
      COMMON/BLK17/TMDB,TMDW,TPTOP,TTBT,TSATNW
C
      DO 10 I=N,2,-1
        DENO=DX/DT*EPS(I)*ROB(I)+EPS(I)*ROB(I)*DABS(VB(I))
        RNUM=EPS(I+1)*ROB(I+1)*DABS(VB(I+1))*HB(I+1)
     1       -(DX/DT*ALP(I)*ROW(I)+ALP(I)*ROW(I)*VW(I+1))*HW(I)
     2       +ALP(I-1)*ROW(I-1)*VW(I)*HW(I-1)
     3       +DX/DT*(EPSO(I)*ROBO(I)*HBO(I)+ALPO(I)*ROWO(I)*HWO(I))
     4       +DX/DT*(P(I)-PO(I))
        HB(I)=RNUM/DENO
10    CONTINUE
      HB(1)=HB(2)
      RETURN
C
      ENTRY SBRENT
C
      RAMD=RMDW/RMDB
      DO 20 I=N,2,-1
        HB(I)=-RAMD*(HW(I)-HW(I-1))+HB(I+1)
20    CONTINUE
      HB(1)=HB(2)
      RETURN
      END
```

```
C     ****************************************************************
C     *                                                              *
C     *                          B R P R O                           *
C     *                                                              *
C     *   THIS SUBROUTINE CALCULATES THE TEMPERATURE AND DENSITY     *
C     * OF THE BRINE USING  ITS  ENTHALPY AND PRESSURE.              *
C     *                                                              *
C     ****************************************************************
C
      SUBROUTINE BRPRO
      IMPLICIT REAL*8(A-H,O-Z)
      COMMON/BLK1 /AREA,DX,N,NP1,DT,DIAM,HEIG
      COMMON/BLK2/ROB(202),ROW(202),ROBO(202),ROWO(202)
      COMMON/BLK6/P(202),PO(202)
      COMMON/BLK13/HB(202),HW(202),HBO(202),HWO(202)
      COMMON/BLK14/DCON,HCON,PCON
      COMMON/BLK19/TBO(202)
C
      DO 20 I=1,NP1
        HBEN=HB(I)*HCON
        PEN=P(I)*PCON
10      CALL WATER('PH',PEN,HBEN,10,1,0,Q,S,H,VBEN,U,TF,PR,SL,HL,
     1             VL,UL,SV,HV,VV,UV,NERROR)
        TBO(I)=(TF-32.)/1.8
        ROB(I)=1./VBEN/DCON
20    CONTINUE
      RETURN
      END
```

```
C     ****************************************************************
C     *                                                              *
C     *                          B R V O I                           *
C     *                                                              *
C     *   THIS SUBROUTINE FINDS THE CORRECTED VELOCITY OF THE        *
C     * BRINE BASED ON  ITS  CALCULATED VOID FRACTION.               *
C     *                                                              *
C     ****************************************************************
C
      SUBROUTINE BRVOI
      IMPLICIT REAL*8(A-H,O-Z)
      COMMON/BLK1/AREA,DX,N,NP1,DT,DIAM,HEIG
      COMMON/BLK2/ROB(202),ROW(202),ROBO(202),ROWO(202)
      COMMON/BLK4/ALP(202),EPS(202),ALPO(202),EPSO(202)
      COMMON/BLK5/VB(202),VW(202),VBO(202),VWO(202)
      COMMON/BLK17/TMDB,TMDW,TPTOP,TTBT
      DIMENSION A(202),B(202),C(202),D(202)
C
      DO 10 I=2,NP1
        A(I)=0.0
        IF(I.EQ.NP1) THEN
          B(I)=-EPS(I)*ROB(I)
          D(I)=TMDB/AREA-DX/DT/2*(EPS(I)*ROB(I)-EPSO(I)*ROBO(I))
        ELSE
          B(I)=-EPS(I)*ROB(I)
          C(I)=EPS(I+1)*ROB(I+1)
          D(I)=-DX/DT*(EPS(I)*ROB(I)-EPSO(I)*ROBO(I))
        ENDIF
10    CONTINUE
C
      CALL TRIDA(2,NP1,A,B,C,D,VB)
      RETURN
      END
```

```
C     ***************************************************************
C     *                                                             *
C     *                        C O E F F                            *
C     *                                                             *
C     *   THIS SUBROUTINE PERFORMS A LEAST SQUARE CURVE FIT IN      *
C     * THE PRESSURE RANGE OF INTEREST TO FIND THE COEFFICIENTS     *
C     * OF A LINEAR RELATION FOR DENSITIES OF THE BRINE AND THE     *
C     * WORKING FLUID AS A FUNCTION OF PRESSURE.                    *
C     *                                                             *
C     ***************************************************************
C
      SUBROUTINE COEFF
      IMPLICIT REAL*8(A-H,O-Z)
      CHARACTER FTYPE*6
      CHARACTER PTYPE*9
      COMMON/BLKO/FTYPE,PTYPE,AW,AB,PTOP,TSAT
      COMMON/BLK14/DCON,HCON,PCON
      DIMENSION ROBC(31),ROWC(31),PTEM(31)
      DATA PDIF,NC1/2.1E05,31/
      DATA SUM1W,SUM2W,SUM1B,SUM2B,SUM3,SUM4/6*0.0/
C
      DP=PDIF/(NC1-1)
      DO 20 I=1,NC1
        PTEM(I)=PTOP+(I-1)*DP
        PEN=PTEM(I)*PCON
10      CALL WATER('PX',PEN,0.0,10,1,0,Q,S,H,VBEN,U,T,PR,SL,HL,
     1           VL,UL,SV,HV,VV,UV,NERROR)
        CALL CARBON('PX',PEN,0.0,FTYPE,H,S,VWEN,T,PR,0,
     1            SL,HL,VL,SV,HV,VV,QUAL)
        ROBC(I)=1./VBEN/DCON
        ROWC(I)=1./VWEN/DCON
20    CONTINUE
      DO 30 I=1,NC1
        SUM1B=SUM1B+ROBC(I)
        SUM2B=SUM2B+ROBC(I)*PTEM(I)
        SUM1W=SUM1W+ROWC(I)
        SUM2W=SUM2W+ROWC(I)*PTEM(I)
        SUM3=SUM3+PTEM(I)
        SUM4=SUM4+PTEM(I)**2
30    CONTINUE
      COMD=NC1*SUM4-SUM3**2
      AB=(NC1*SUM2B-SUM3*SUM1B)/COMD
      AW=(NC1*SUM2W-SUM3*SUM1W)/COMD
      BB=(SUM4*SUM1B-SUM3*SUM2B)/COMD
      BW=(SUM4*SUM1W-SUM3*SUM2W)/COMD
      RETURN
      END
```

```
C     ****************************************************************
C     *                                                              *
C     *                          E R R O R                           *
C     *                                                              *
C     *   THIS SUBROUTINE CALULATES THE CONTINUITY ERROR FOR EACH    *
C     * CONTINUITY FINITE DIFFERENCE CELL.                           *
C     *                                                              *
C     ****************************************************************
C
      SUBROUTINE ERROR
      IMPLICIT REAL*8(A-H,O-Z)
      COMMON/BLK1/AREA,DX,N,NP1,DT,DIAM,HEIG
      COMMON/BLK2/ROB(202),ROW(202),ROBO(202),ROWO(202)
      COMMON/BLK4/ALP(202),EPS(202),ALPO(202),EPSO(202)
      COMMON/BLK5/VB(202),VW(202),VBO(202),VWO(202)
      COMMON/BLK7/E(202)
C
      DO 10 I=2,N
        E(I)=ALP(I)*ROW(I)*VW(I+1)-ALP(I-1)*ROW(I-1)*VW(I)+
     1       DX/DT*(ALP(I)*ROW(I)-ALPO(I)*ROWO(I))-
     2       EPS(I)*ROB(I)*VB(I)+EPS(I+1)*ROB(I+1)*VB(I+1)+
     3       DX/DT*(EPS(I)*ROB(I)-EPSO(I)*ROBO(I))
10    CONTINUE
      RETURN
C
      ENTRY SERROR
C
      DO 20 I=N,2,-1
        E(I)=(ALP(I)*ROW(I)*VW(I+1)-ALP(I-1)*ROW(I-1)*VW(I))+
     1       (-EPS(I)*ROB(I)*VB(I)+EPS(I+1)*ROB(I+1)*VB(I+1))
20    CONTINUE
      RETURN
      END
```

```
C     ****************************************************************
C     *                                                              *
C     *                          F P R I N                           *
C     *                                                              *
C     *   THIS SUBROUTINE IS IN CHARGE OF PRINTING THE VELOCITY      *
C     * AND THE PROPERTIES OF THE BRINE AND THE WORKING FLUID IN     *
C     * THE CALCULATION DOMAIN.                                      *
C     *                                                              *
C     ****************************************************************
C
      SUBROUTINE FPRIN
      IMPLICIT REAL*8(A-H,O-Z)
      CHARACTER FTYPE*6
      CHARACTER PTYPE*9
      COMMON/BLK0/FTYPE,PTYPE,AW,AB,PTOP,TSAT
      COMMON/BLK1/AREA,DX,N,NP1,DT,DIAM,HEIG
      COMMON/BLK2/ROB(202),ROW(202),ROBO(202),ROWO(202)
      COMMON/BLK3/RMDB,RMDW
      COMMON/BLK4/ALP(202),EPS(202),ALPO(202),EPSO(202)
      COMMON/BLK6/P(202),PO(202)
      COMMON/BLK10/NPRIN,TOL,TIME,FTIME
      COMMON/BLK12/TB(202),TW(202)
      COMMON/BLK14/DCON,HCON,PCON
      COMMON/BLK15/ALPHA,RWI,RI(202)
      COMMON/BLK16/VBH(202),VWH(202)
      COMMON/BLK17/TMDB,TMDW,TPTOP,TTBT,TSATNW
C
      WRITE(NPRIN,1000)
      WRITE(NPRIN,1100) PTYPE
      WRITE(NPRIN,1200) FTYPE,PTOP,RMDB,RMDW,TB(NP1),TW(1),TSAT
      WRITE(NPRIN,1300) HEIG,DIAM,RWI,N
      IF(PTYPE.EQ.'TRANSIENT') THEN
        WRITE(NPRIN,1400) DT
        WRITE(NPRIN,1500)
        WRITE(NPRIN,1600) TPTOP,TMDB,TMDW,TTBT,TSATNW
      ELSE
        WRITE(NPRIN,1800)
      ENDIF
C
      ENTRY TRFPR
C
      IF(PTYPE.EQ. 'TRANSIENT' ) THEN
        WRITE(NPRIN,1700) TIME
      ENDIF
      WRITE(NPRIN,1900)
1000  FORMAT(1H1,2X,'<<<< ANALYSIS OF THE OPERATION OF A ',
     1       'SPRAY COLUMN PREHEATER >>>>',//)
1100  FORMAT(10X,'MODE OF OPERATION                 = ',A9,/)
1200  FORMAT(10X,'TYPE OF WORKING FLUID             = ',A6,//,
     1       10X,'COLUMN PRESSURE OUT               = ',F11.3,' (Pa)',//
     2       10X,'BRINE MASS FLOW RATE              = ',F6.3,' (Kg/s)',//,
     3       10X,'WORKING FLUID MASS FLOW RATE      = ',F6.3,' (Kg/s)',//,
     4       10X,'BRINE TEMPERATURE IN              = ',F7.3,' (Deg C)',//,
```

```
     5       1OX,'WORKING FLUID TEMPERATURE IN  = ',F6.3,' (Deg C)',//,
     6       1OX,'WORKING FLUID SATURATION        ',/,
     7       1OX,'TEMPERATURE AT COLUMN           ',/,
     8       1OX,'PRESSURE OUT                  = ',F7.3,' (Deg C)',/)
1300  FORMAT(1OX,'PREHEATER HEIGHT              = ',F6.3,' (m)',//,
     1       1OX,'PREHEATER DIAMETER             = ',F6.4,' (m)',//,
     2       1OX,'RADIUS OF WORKING FLUID         ',/,
     3       1OX,'DROPLETS (INITIAL)            = ',F7.5,' (m)',//,
     4       1OX,'NUMBER OF FINITE                ',/,
     5       1OX,'DIFFERENCE CELLS              = ',I3,/)
1400  FORMAT(1OX,'TIME STEP VALUE               = ',F7.3,
     1         ' (Seconds)',//)
1500  FORMAT(2X,'<<<< TRANSIENT VALUES OF THE PRESSURE, MASS FLOW',
     1         ' RATES AND INCOMING BRINE TEMPERATURE',
     2         ' ARE AS FOLLOWS >>>>',//)
1600  FORMAT(1OX,'TRANSIENT VALUE OF THE         ',/,
     1       1OX,'COLUMN PRESSURE OUT           = ',F11.3,' (Pa)',//,
     2       1OX,'TRANSIENT VALUE OF THE          ',/,
     3       1OX,'BRINE MASS FLOW RATE          = ',F6.3,' (Kg/s)',//,
     4       1OX,'TRANSIENT VALUE OF THE          ',/,
     5       1OX,'WORKING FLUID MASS FLOW RATE  = ',F6.3,' (Kg/s)',//,
     6       1OX,'TRANSIENT VALUE OF THE          ',/,
     7       1OX,'INCOMING BRINE TEMPERATURE    = ',F7.3,' (Deg C)',//,
     8       1OX,'NEW SATURATION TEMPERATURE    = ',F7.3,' (Deg C)')
1700  FORMAT(1H1,T54,'TIME = ',F7.3,' (Seconds)',/)
1800  FORMAT(1H1)
1900  FORMAT(1X,T2,'HEIGHT',
     1       T11,'BRINE VOID',T24,'WORKING FLUID',T40,'BRINE',
     2       T50,'WORKING FLUID',T66,'BRINE',T80,'WORKING FLUID',
     3       T96,'BRINE',T107,'WORKING FLUID',T123,'PRESSURE',/,
     4       T11,'FRACTION',T24,'VOID FRACTION',T40,'DENSITY',
     5       T50,'DENSITY',
     6       T66,'TEMPERATURE',T80,'TEMPERATURE',T96,'VELOCITY',
     7       T107,'VELOCITY',/,T2,'(m)',T40,'(Kg/m3)',T50,'(Kg/m3)',
     8       T66,'(Deg C)',T80,'(Deg C)',T96,'(m/s)',T107,'(m/s)',
     9       T123,'(MPa)',//,T2,129(''),/)
      DO 10 I=NP1,1,-1
        HEIGHT=DX*(I-1)
        WRITE(NPRIN,2000) HEIGHT,EPS(I),ALP(I),ROB(I),ROW(I),
     1                    TB(I),TW(I),VBH(I),VWH(I),P(I)/1000000.
10    CONTINUE
2000  FORMAT(1X,T2,F5.2,T13,F6.4,T27,F6.4,T40,F6.2,T53,F6.2,
     1       T68,F6.2,T83,F6.2,T96,F8.5,T110,F7.5,T124,F6.4,/)
      RETURN
      END
```

```
C     ****************************************************************
C     *                                                              *
C     *                          K D R A G                           *
C     *                                                              *
C     *   THIS SUBROUTINE FINDS THE INTERPHASE  FRICTION BASED ON    *
C     * A LINEAR MODEL.                                              *
C     *                                                              *
C     ****************************************************************
C
      SUBROUTINE KDRAG
      IMPLICIT REAL*8(A-H,O-Z)
      COMMON/BLK1/AREA,DX,N,NP1,DT,DIAM,HEIG
      COMMON/BLK2/ROB(202),ROW(202),ROBO(202),ROWO(202)
      COMMON/BLK4/ALP(202),EPS(202),ALPO(202),EPSO(202)
      COMMON/BLK5/VB(202),VW(202),VBO(202),VWO(202)
      COMMON/BLK8/RK(202)
      COMMON/BLK15/ALPHA,RWI,RI(202)
      DATA CD/0.4/
C
      DO 10 I=2,NP1
        ALPH=(ALP(I-1)+ALP(I))/2
        ROBH=(ROB(I-1)+ROB(I))/2
        RK(I)=3./8.*ALPH*ROBH*CD*(DABS(VW(I)-VB(I)))/RI(I)
10    CONTINUE
      RETURN
      END
```

```
C     ****************************************************************
C     *                                                              *
C     *                          P C O R R                           *
C     *                                                              *
C     *   THIS SUBROUTINE FINDS THE PRESSURE CORRECTION BASED ON     *
C     * CONTINUITY ERROR OF EACH CELL IN ORDER TO BRING ABOUT A      *
C     * BALANCE OF CONTINUITY.                                       *
C     *                                                              *
C     ****************************************************************
C
      SUBROUTINE PCORR
      IMPLICIT REAL*8(A-H,O-Z)
      CHARACTER FTYPE*6
      CHARACTER PTYPE*9
      COMMON/BLK0/FTYPE,PTYPE,AW,AB,PTOP,TSAT
      COMMON/BLK1/AREA,DX,N,NP1,DT,DIAM,HEIG
      COMMON/BLK2/ROB(202),ROW(202),ROBO(202),ROWO(202)
      COMMON/BLK4/ALP(202),EPS(202),ALPO(202),EPSO(202)
      COMMON/BLK7/E(202)
      COMMON/BLK9/PP(202)
      COMMON/BLK18/VBPC(202),VWPC(202)
      DIMENSION A(202),B(202),C(202),D(202)
C
      PP(1)=0.0
      PP(NP1)=0.0
      DO 10 I=2,N
        B1=-ALP(I-1)*ROW(I-1)*VWPC(I)
      C1=-EPS(I)*ROB(I)*VBPC(I)
           A1=ALP(I)*ROW(I)*VWPC(I+1)
           D1=EPS(I+1)*ROB(I+1)*VBPC(I+1)
        IF(PTYPE .EQ. 'TRANSIENT') THEN
          E1=DX/DT*ALP(I)*AW
          F1=DX/DT*EPS(I)*AB
        ELSE
          E1=0.0
          F1=0.0
        ENDIF
        A(I)=B1+C1
        B(I)=A1-B1-C1+D1+E1+F1
        C(I)=-A1-D1
             D(I)=-E(I)
 10   CONTINUE
C
      CALL TRIDA(2,N,A,B,C,D,PP)
      RETURN
      END
```

```
C     ****************************************************************
C     *                                                              *
C     *                          P R E S S                           *
C     *                                                              *
C     *   THIS SUBROUTINE FINDS THE PRESSURE DISTRIBUTION FROM       *
C     * COMBINED MOMENTUM EQUATION BASED ON GUESSED VALUES OF THE    *
C     * VELOCITIES,DENSITIES AND THE VOID FRACTIONS.                 *
C     *                                                              *
C     ****************************************************************
C
      SUBROUTINE PRESS
      IMPLICIT REAL*8(A-H,O-Z)
      COMMON/BLK1/AREA,DX,N,NP1,DT,DIAM,HEIG
      COMMON/BLK2/ROB(202),ROW(202),ROBO(202),ROWO(202)
      COMMON/BLK3/RMDB,RMDW
      COMMON/BLK4/ALP(202),EPS(202),ALPO(202),EPSO(202)
      COMMON/BLK5/VB(202),VW(202),VBO(202),VWO(202)
      COMMON/BLK6/P(202),PO(202)
      COMMON/BLK16/VBH(202),VWH(202)
      COMMON/BLK17/TMDB,TMDW,TPTOP,TTBT,TSATNW
C
      DO 10 I=NP1,2,-1
        ALPPH=(ALP(I-1)+ALP(I))/2
        ROWH=(ROW(I-1)+ROW(I))/2
        ALPOH=(ALPO(I-1)+ALPO(I))/2
        ROWOH=(ROWO(I-1)+ROWO(I))/2
        EPSH=(EPS(I-1)+EPS(I))/2
        ROBH=(ROB(I-1)+ROB(I))/2
        EPSOH=(EPSO(I-1)+EPSO(I))/2
        ROBOH=(ROBO(I-1)+ROBO(I))/2
        IF(I.EQ.2) THEN
          FLUXIW=TMDW*VW(I)
          FLUXIB=AREA*EPS(I)*ROB(I)*DABS(VBH(I))*VB(I+1)
        ELSE
          IF(I.EQ.NP1) THEN
            FLUXIW=AREA*ALP(I-1)*ROW(I-1)*VWH(I-1)*VW(I-1)
            FLUXIB=TMDB*VB(I)
          ELSE
            FLUXIW=AREA*ALP(I-1)*ROW(I-1)*VWH(I-1)*VW(I-1)
            FLUXIB=AREA*EPS(I)*ROB(I)*DABS(VBH(I))*VB(I+1)
          ENDIF
        ENDIF
        FLUXOW=AREA*ALP(I)*ROW(I)*VWH(I)*VW(I)
        FLUXOB=AREA*EPS(I-1)*ROB(I-1)*DABS(VBH(I-1))*VB(I)
        STORAW=AREA*DX/DT*(ALPH*ROWH*VW(I)-ALPOH*ROWOH*VWO(I))
        STORAB=AREA*DX/DT*(EPSH*ROBH*VB(I)-EPSOH*ROBOH*VBO(I))
        TERM1=FLUXOW+FLUXOB-FLUXIW-FLUXIB+STORAW+STORAB
        TERM2=AREA*DX*9.81*(EPSH*ROBH+ALPH*ROWH)
        P(I-1)=P(I)+(TERM1+TERM2)/AREA
10    CONTINUE
      RETURN
C
      ENTRY SPRESS
```

```
C
      DO 20 I=NP1,2,-1
        IF(I.EQ.2) THEN
          FLUXOW=RMDW*VW(2)
          FLUXIW=RMDW*VW(2)
          FLUXOB=RMDB*VB(2)
          FLUXIB=RMDW*VB(3)
        ELSE
          IF(I.EQ.NP1) THEN
            FLUXOW=RMDW*VW(NP1)
            FLUXIW=RMDW*VW(N)
            FLUXOB=RMDB*VB(NP1)
            FLUXIB=RMDB*VB(NP1)
          ELSE
            FLUXOW=RMDW*VW(I)
            FLUXIW=RMDW*VW(I-1)
            FLUXOB=RMDB*VB(I)
            FLUXIB=RMDB*VB(I+1)
          ENDIF
        ENDIF
        TERM1=FLUXOW-FLUXIW+FLUXOB-FLUXIB
        TERM2=(0.5*(EPS(I-1)+EPS(I))*0.5*(ROB(I-1)+ROB(I))+
     1         0.5*(ALP(I-1)+ALP(I))*0.5*(ROW(I-1)+ROW(I)))*
     2         AREA*DX*9.81
        P(I-1)=P(I)+(TERM1+TERM2)/AREA
20    CONTINUE
      RETURN
      END
```

```
C     ****************************************************************
C     *                                                              *
C     *                        S E T P R                             *
C     *                                                              *
C     *   THIS SUBROUTINE IS IN CHARGE OF READING THE INPUT          *
C     * PARAMETERS AND SETTING UP THE INITIAL GUESSES FOR ALL THE    *
C     * VARIABLES.                                                   *
C     *                                                              *
C     ****************************************************************
C
      SUBROUTINE SETPR
      IMPLICIT REAL*8(A-H,O-Z)
      CHARACTER FTYPE*6
      CHARACTER PTYPE*9
      COMMON/BLK0/FTYPE,PTYPE,AW,AB,PTOP,TSAT
      COMMON/BLK1/AREA,DX,N,NP1,DT,DIAM,HEIG
      COMMON/BLK2/ROB(202),ROW(202),ROBO(202),ROWO(202)
      COMMON/BLK3/RMDB,RMDW
      COMMON/BLK4/ALP(202),EPS(202),ALPO(202),EPSO(202)
      COMMON/BLK5/VB(202),VW(202),VBO(202),VWO(202)
      COMMON/BLK6/P(202),PO(202)
      COMMON/BLK10/NPRIN,TOL,TIME,FTIME
      COMMON/BLK12/TB(202),TW(202)
      COMMON/BLK13/HB(202),HW(202),HBO(202),HWO(202)
      COMMON/BLK14/DCON,HCON,PCON
      COMMON/BLK15/ALPHA,RWI,RI(202)
      COMMON/BLK17/TMDB,TMDW,TPTOP,TTBT,TSATNW
C
      READ(5,1000) PTYPE,FTYPE
      READ(5,*) NPRIN,ALPG,TWIN,TBIN
      READ(5,*) RMDB,RMDW
      READ(5,*) PTOP,HEIG,DIAM
      READ(5,*) N,TOL,ALPHA,RWI
      IF(PTYPE .EQ. 'TRANSIENT') THEN
        READ(5,*) DT,FTIME
        READ(5,*) TMDB,TMDW,TPTOP,TTBT
      ENDIF
C
      NP1=N+1
      DX=HEIG/N
      AREA=4.*ATAN(1.)*(DIAM/2.)**2
      P(NP1)=PTOP
      PTEN=PTOP*PCON
      CALL CARBON('PX',PTEN,0.0,FTYPE,H,S,V,TSAT,PR,0,
     1            SL,HL,VL,SV,HV,VV,QUAL)
      TSAT=(TSAT-32)/1.8
      TB(NP1)=TBIN
      TBIN=TBIN*1.8+32
10    CALL WATER('TP',TBIN,PTEN,10,1,0,Q,S,HBEN,VBEN,U,T,PR,SL,HL,
     1           VL,UL,SV,HV,VV,UV,NERROR)
      HB(NP1)=HBEN/HCON
      ROB(NP1)=1./VBEN/DCON
      DO 20 I=1,NP1
```

```
      TW(I)=TWIN+(TSAT-TWIN-0.5)*(I-1)/N
      TWEN=TW(I)*1.8+32
      CALL CARBON('TP',TWEN,PTEN,FTYPE,HWEN,S,VWEN,T,P,O,
     1                SL,HL,VL,SV,HV,VV,QUAL)
      HW(I)=HWEN/HCON
      ROW(I)=1./VWEN/DCON
20    CONTINUE
      DO 30 I=1,NP1
      ALP(I)=0.05+DABS((ALPG-0.05))/N*(I-1)
      EPS(I)=1.-ALP(I)
      P(I)=PTOP
      ROB(I)=ROB(NP1)
30    CONTINUE
      DO 40 I=NP1,2,-1
      VB(I)=-RMDB/ROB(I)/AREA/EPS(I)
      VW(I)=RMDW/ROW(I-1)/AREA/ALP(I-1)
40    CONTINUE
      ROWH1=(ROW(1)+ROW(2))/2
      DO 50 I=2,NP1
      ROWH=(ROW(I-1)+ROW(I))/2
      RI(I)=RWI*(ROWH1/ROWH)**(1./3.)
50    CONTINUE
1000  FORMAT(A9,1X,A6)
      RETURN
      END
```

```
C     ****************************************************************
C     *                                                              *
C     *                          T R I D A                           *
C     *                                                              *
C     *   THIS SUBROUTINE FINDS THE SOLUTION TO A SET OF LINEAR      *
C     * SIMULTANEOUS ALGEBRAIC EQUATIONS WHICH ARE IN TRIDIAGONAL    *
C     * FORM.                                                        *
C     *                                                              *
C     ****************************************************************
C
      SUBROUTINE TRIDA(IF,L,A,B,C,D,V)
      IMPLICIT REAL*8(A-H,O-Z)
      DIMENSION A(L),B(L),C(L),D(L),V(L),BETA(202),GAMMA(202)
C
      BETA(IF)=B(IF)
      GAMMA(IF)=D(IF)/BETA(IF)
      IFP1=IF+1
      DO 10 I=IFP1,L
        BETA(I)=B(I)-A(I)*C(I-1)/BETA(I-1)
        GAMMA(I)=(D(I)-A(I)*GAMMA(I-1))/BETA(I)
10    CONTINUE
      V(L)=GAMMA(L)
      LAST=L-IF
      DO 20 K=1,LAST
        I=L-K
        V(I)=GAMMA(I)-C(I)*V(I+1)/BETA(I)
20    CONTINUE
      RETURN
      END
```

```
C     ****************************************************************
C     *                                                              *
C     *                          V C O R R                           *
C     *                                                              *
C     *   THIS SUBROUTINE FINDS THE CORRECTION TO VELOCITIES OF      *
C     * THE BRINE AND THE WORKING FLUID BASED ON THE PRESSURE        *
C     * CORRECTIONS TO BRING ABOUT A BALANCE IN CONTINUITY.          *
C     *                                                              *
C     ****************************************************************
C
      SUBROUTINE VCORR
      IMPLICIT REAL*8(A-H,O-Z)
      CHARACTER FTYPE*6
      CHARACTER PTYPE*9
      COMMON/BLK0/FTYPE,PTYPE,AW,AB,PTOP,TSAT
      COMMON/BLK1/AREA,DX,N,NP1,DT,DIAM,HEIG
      COMMON/BLK2/ROB(202),ROW(202),ROB0(202),ROW0(202)
      COMMON/BLK5/VB(202),VW(202),VB0(202),VW0(202)
      COMMON/BLK9/PP(202)
      COMMON/BLK11/VBC(202),VWC(202)
      COMMON/BLK18/VBPC(202),VWPC(202)
C
      DO 10 I=2,NP1
        VWC(I)=VWPC(I)*(PP(I-1)-PP(I))
     VBC(I)=VBPC(I)*(PP(I-1)-PP(I))
10    CONTINUE
      DO 20 I=2,NP1
        VW(I)=VW(I)+VWC(I)
        VB(I)=VB(I)+VBC(I)
20    CONTINUE
      IF(PTYPE .EQ. 'TRANSIENT') THEN
        DO 30 I=1,NP1
          ROB(I)=ROB(I)+AB*PP(I)
          ROW(I)=ROW(I)+AW*PP(I)
30      CONTINUE
      ENDIF
      RETURN
      END
```

```
C     ****************************************************************
C     *                                                              *
C     *                          V E L V A                           *
C     *                                                              *
C     *   THIS SUBROUTINE FINDS THE VARIATION OF VELOCITIES OF       *
C     * EACH PHASE WITH RESPECT TO PRESSURE.                         *
C     *                                                              *
C     ****************************************************************
C
      SUBROUTINE VELVA
      IMPLICIT REAL*8(A-H,O-Z)
      COMMON/BLK1/AREA,DX,N,NP1,DT,DIAM,HEIG
      COMMON/BLK2/ROB(202),ROW(202),ROBO(202),ROWO(202)
      COMMON/BLK3/RMDB,RMDW
      COMMON/BLK4/ALP(202),EPS(202),ALPO(202),EPSO(202)
      COMMON/BLK8/RK(202)
      COMMON/BLK16/VBH(202),VWH(202)
      COMMON/BLK17/TMDB,TMDW,TPTOP,TTBT
      COMMON/BLK18/VBPC(202),VWPC(202)
C
      DO 10 I=2,NP1
        ALPH=(ALP(I-1)+ALP(I))/2
        ROWH=(ROW(I-1)+ROW(I))/2
      EPSH=(EPS(I-1)+EPS(I))/2
      ROBH=(ROB(I-1)+ROB(I))/2
        IF(I.EQ.2) THEN
          VWP=1./(DX/DT*ALPH*ROWH+ALP(I)*ROW(I)*VWH(I)+DX*RK(I)-
     1          TMDW/AREA)*ALPH
          VWVB=1./(DX/DT*ALPH*ROWH+ALP(I)*ROW(I)*VWH(I)+DX*RK(I)-
     1           TMDW/AREA)*DX*RK(I)
          VBP=1./(DX/DT*EPSH*ROBH+EPS(I-1)*ROB(I-1)*DABS(VBH(I-1))+
     1          DX*RK(I))*EPSH
          VBVW=1./(DX/DT*EPSH*ROBH+EPS(I-1)*ROB(I-1)*DABS(VBH(I-1))+
     1           DX*RK(I))*DX*RK(I)
        ELSE
          IF(I.EQ.NP1) THEN
            VWP=1./(DX/DT*ALPH*ROWH+ALP(I)*ROW(I)*VWH(I)+
     1             DX*RK(I))*ALPH
            VWVB=1./(DX/DT*ALPH*ROWH+ALP(I)*ROW(I)*VWH(I)+
     1             DX*RK(I))*DX*RK(I)
            VBP=1./(DX/DT*EPSH*ROBH+EPS(I-1)*ROB(I-1)*DABS(VBH(I-1))+
     1             DX*RK(I)-TMDB/AREA)*EPSH
            VBVW=1./(DX/DT*EPSH*ROBH+EPS(I-1)*ROB(I-1)*DABS(VBH(I-1))+
     1             DX*RK(I)-TMDB/AREA)*DX*RK(I)
          ELSE
            VWP=1./(DX/DT*ALPH*ROWH+ALP(I)*ROW(I)*VWH(I)+
     1             DX*RK(I))*ALPH
            VWVB=1./(DX/DT*ALPH*ROWH+ALP(I)*ROW(I)*VWH(I)+
     1             DX*RK(I))*DX*RK(I)
            VBP=1./(DX/DT*EPSH*ROBH+EPS(I-1)*ROB(I-1)*DABS(VBH(I-1))+
     1             DX*RK(I))*EPSH
            VBVW=1./(DX/DT*EPSH*ROBH+EPS(I-1)*ROB(I-1)*DABS(VBH(I-1))+
     1             DX*RK(I))*DX*RK(I)
```

```
          ENDIF
        ENDIF
        VWPC(I)=(VWP+VWVB*VBP)/(1.-VWVB*VBVW)
        VBPC(I)=(VBP+VBVW*VWP)/(1.-VBVW*VWVB)
10    CONTINUE
      RETURN
C
      ENTRY SVELVA
C
      DO 20 I=2,NP1
        ALPH=(ALP(I-1)+ALP(I))/2
        EPSH=(EPS(I-1)+EPS(I))/2
        IF(I.EQ.2) THEN
          VWP=1./(AREA*DX*RK(I))*AREA*ALPH
          VWVB=1.0
               VBP=1./(RMDB+AREA*DX*RK(I))*AREA*EPSH
          VBVW=1./(RMDB+AREA*DX*RK(I))*AREA*DX*RK(I)
        ELSE
          IF(I.EQ.NP1) THEN
            VWP=1./(RMDW+AREA*DX*RK(I))*AREA*ALPH
            VWVB=1./(RMDW+AREA*DX*RK(I))*AREA*DX*RK(I)
            VBP=1./(AREA*DX*RK(I))*AREA*EPSH
            VBVW=1.0
          ELSE
            VWP=1./(RMDW+AREA*DX*RK(I))*AREA*ALPH
            VWVB=1./(RMDW+AREA*DX*RK(I))*AREA*DX*RK(I)
                 VBP=1./(RMDB+AREA*DX*RK(I))*AREA*EPSH
            VBVW=1./(RMDB+AREA*DX*RK(I))*AREA*DX*RK(I)
          ENDIF
        ENDIF
        VWPC(I)=(VWP+VWVB*VBP)/(1.-VWVB*VBVW)
        VBPC(I)=(VBP+VBVW*VWP)/(1.-VBVW*VWVB)
20    CONTINUE
      RETURN
      END
```

```
C     ****************************************************************
C     *                                                              *
C     *                        W F P R O                             *
C     *                                                              *
C     *   THIS SUBROUTINE CALCULATES THE ENTHALPY AND DENSITY OF     *
C     * OF THE WORKING FLUID USING ITS TEMPERATURE AND PRESSURE.     *
C     *                                                              *
C     ****************************************************************
C
      SUBROUTINE WFPRO
      IMPLICIT REAL*8(A-H,O-Z)
      CHARACTER FTYPE*6
      CHARACTER PTYPE*9
      COMMON/BLKO/FTYPE,PTYPE,AW,AB,PTOP,TSAT
      COMMON/BLK1/AREA,DX,N,NP1,DT,DIAM,HEIG
      COMMON/BLK2/ROB(202),ROW(202),ROBO(202),ROWO(202)
      COMMON/BLK6/P(202),PO(202)
      COMMON/BLK12/TB(202),TW(202)
      COMMON/BLK13/HB(202),HW(202),HBO(202),HWO(202)
      COMMON/BLK14/DCON,HCON,PCON
C
      TLIMIT=(TSAT-0.5)*1.8+32.0
      DO 10 I=1,NP1
        TWEN=TW(I)*1.8+32.
        TWEN=DMIN1(TWEN,TLIMIT)
        PEN=P(I)*PCON
        CALL CARBON('TP',TWEN,PEN,FTYPE,HWEN,S,VWEN,T,PR,O,SL,HL,
     1              VL,SV,HV,VV,QUAL)
        HW(I)=HWEN/HCON
        ROW(I)=1./VWEN/DCON
10    CONTINUE
      RETURN
      END
```

```
C     ****************************************************************
C     *                                                              *
C     *                        W F T E M                             *
C     *                                                              *
C     *   THIS SUBROUTINE FINDS THE MEAN DROPLET TEMPERATURE BE      *
C     * BASED ON THE NUMERICAL SOLUTION OF TRANSIENT SPHERICAL       *
C     * CONDUCTION EQUATION SUBJECT TO VARIABLE SURFACE              *
C     * TEMPERATURE.                                                 *
C     *                                                              *
C     ****************************************************************
C
      SUBROUTINE WFTEM
      IMPLICIT REAL*8(A-H,O-Z)
      CHARACTER FTYPE*6
      CHARACTER PTYPE*9
      COMMON/BLK0/FTYPE,PTYPE,AW,AB,PTOP,TSAT
      COMMON/BLK1/AREA,DX,N,NP1,DT,DIAM,HEIG
      COMMON/BLK5/VB(202),VW(202),VB0(202),VW0(202)
      COMMON/BLK12/TB(202),TW(202)
      COMMON/BLK15/ALPHA,RWI,RI(202)
      DIMENSION T0(202),DR(202),A(202),B(202),C(202),D(202),
     1          FAC(202),DTC(202),T(202)
C
      NIR=50
      NT=5
      NIRP1=NIR+1
      DO 5 IR=1,NIRP1
        T0(IR)=TW(1)
        DR(IR)=RWI/NIR
5     CONTINUE
      DO 10 I=2,NP1
        DTC(I-1)=DX/VW(I)
10    CONTINUE
      DO 80 I=2,NP1
        TBH=(TB(I-1)+TB(I))/2
        DTD=DTC(I-1)/NT
        DO 50 JJ=1,NT
          DO 30 IR=2,NIR
            R=0.0
            K=IR-1
            DO 20 J=1,K
              R=R+DR(J)
20          CONTINUE
            IF(JJ.EQ.NT) THEN
              FAC(1)=(DR(1)/2)**3
              FAC(IR)=(R+DR(IR)/2)**3-(R-DR(IR-1)/2)**3
            ENDIF
            A(IR)=(R-DR(IR-1)/2)**2/DR(IR-1)
            B(IR)=-(R-DR(IR-1)/2)**2/DR(IR-1)-(R+DR(IR)/2)**2/DR(IR)-
     1              (DR(IR-1)/2+DR(IR)/2)*R**2/DTD/ALPHA
            C(IR)=(R+DR(IR)/2)**2/DR(IR)
            D(IR)=-(DR(IR-1)/2+DR(IR)/2)*R**2/DTD/ALPHA*T0(IR)
30        CONTINUE
```

```
            IF(JJ.EQ.NT) THEN
              FAC(NIRP1)=RI(I)**3-(RI(I)-DR(NIR)/2)**3
            ENDIF
            D(1)=0.
            D(NIRP1)=TBH
            B(1)=-1.
            C(1)=1.
            A(NIRP1)=0.
            B(NIRP1)=1.
            CALL TRIDA(1,NIRP1,A,B,C,D,T)
            DO 40 IR=1,NIRP1
              TO(IR)=T(IR)
40          CONTINUE
50        CONTINUE
          SUMI=0.0
          DO 60 IR=1,NIRP1
            SUMI=SUMI+T(IR)*FAC(IR)
60        CONTINUE
          TW(I)=SUMI/RI(I)**3
          NIR=NIRP1
          NIRP1=NIR+1
          DO 70 IR=NIRP1,2,-1
           TO(IR)=TO(IR-1)
70        CONTINUE
          TO(1)=TO(2)
          DR(NIR)=RI(I+1)-RI(I)
80      CONTINUE
        DO 90 I=1,NP1
          TW(I)=DMIN1((TSAT-0.5),TW(I))
90      CONTINUE
        RETURN
        END
```

```
C     ****************************************************************
C     *                                                              *
C     *                          W F V E L                           *
C     *                                                              *
C     *   THIS SUBROUTINE CALCULATES THE VELOCITY OF THE WORKING     *
C     * FLUID DROPLETS.                                              *
C     *                                                              *
C     ****************************************************************
C
      SUBROUTINE WFVEL
      IMPLICIT REAL*8(A-H,O-Z)
      COMMON/BLK1/AREA,DX,N,NP1,DT,DIAM,HEIG
      COMMON/BLK2/ROB(202),ROW(202),ROBO(202),ROWO(202)
      COMMON/BLK3/RMDB,RMDW
      COMMON/BLK4/ALP(202),EPS(202),ALPO(202),EPSO(202)
      COMMON/BLK5/VB(202),VW(202),VBO(202),VWO(202)
      COMMON/BLK6/P(202),PO(202)
      COMMON/BLK8/RK(202)
      COMMON/BLK16/VBH(202),VWH(202)
      COMMON/BLK17/TMDB,TMDW,TPTOP,TTBT,TSATNW
      DIMENSION A(202),B(202),C(202),D(202)
C
      DO 10 I=2,NP1
        ALPH=(ALP(I-1)+ALP(I))/2
        ROWH=(ROW(I-1)+ROW(I))/2
        ALPOH=(ALPO(I-1)+ALPO(I))/2
        ROWOH=(ROWO(I-1)+ROWO(I))/2
     A(I)=-ALP(I-1)*ROW(I-1)*VWH(I-1)
        IF(I.EQ.2) THEN
          B(I)=DX/DT*ALPH*ROWH+ALP(I)*ROW(I)*VWH(I)+DX*RK(I)-
     1         TMDW/AREA
        ELSE
          B(I)=DX/DT*ALPH*ROWH+ALP(I)*ROW(I)*VWH(I)+DX*RK(I)
        ENDIF
        C(I)=0.0
        D(I)=DX/DT*ALPOH*ROWOH*VWO(I)+ALPH*(P(I-1)-P(I))-
     1       DX*9.81*ALPH*ROWH+DX*RK(I)*VB(I)
10    CONTINUE
      CALL TRIDA(2,NP1,A,B,C,D,VW)
      RETURN
C
      ENTRY SWFVEL
C
      DO 20 I=2,NP1
        AH=0.5*(ALP(I-1)+ALP(I))
        DH=0.5*(ROW(I-1)+ROW(I))
     A(I)=-RMDW
        IF(I.EQ.2) THEN
          B(I)=AREA*DX*RK(I)
        ELSE
          B(I)=RMDW+AREA*DX*RK(I)
        ENDIF
        C(I)=0.0
```

```
      D(I)=AREA*AH*(P(I-1)-P(I))-AREA*DX*9.81*AH*DH+
     1       AREA*DX*RK(I)*VB(I)
20    CONTINUE
      CALL TRIDA(2,NP1,A,B,C,D,VW)
      RETURN
      END
```

```
C     ****************************************************************
C     *                                                              *
C     *                          W F V O I                           *
C     *                                                              *
C     *   THIS SUBROUTINE FINDS THE VOID FRACTION OF THE WORKING     *
C     * FLUID DROPLETS BASED ON ITS  CORRECTED VELOCITY.             *
C     *                                                              *
C     ****************************************************************
C
      SUBROUTINE WFVOI
      IMPLICIT REAL*8(A-H,O-Z)
      COMMON/BLK1/AREA,DX,N,NP1,DT,DIAM,HEIG
      COMMON/BLK2/ROB(202),ROW(202),ROBO(202),ROWO(202)
      COMMON/BLK3/RMDB,RMDW
      COMMON/BLK4/ALP(202),EPS(202),ALPO(202),EPSO(202)
      COMMON/BLK5/VB(202),VW(202),VBO(202),VWO(202)
      COMMON/BLK17/TMDB,TMDW,TPTOP,TTBT,TSATNW
      DIMENSION A(202),B(202),C(202),D(202)
      DATA ALPHIG,ALPLOW/0.99,0.01/
C
      DO 10 I=1,NP1
        IF(I.EQ.1) THEN
          B(I)=DX/DT/2*ROW(I)+ROW(I)*VW(I+1)
          D(I)=DX/DT/2*ALPO(I)*ROWO(I)+TMDW/AREA
        ELSE
          IF(I.EQ.NP1) THEN
            A(I)=-ROW(I-1)*VW(I)
            B(I)=DX/DT/2*ROW(I)+ROW(I)*VW(I)
            D(I)=DX/DT/2*ALPO(I)*ROWO(I)
          ELSE
            A(I)=-ROW(I-1)*VW(I)
            B(I)=DX/DT*ROW(I)+ROW(I)*VW(I+1)
            D(I)=DX/DT*ALPO(I)*ROWO(I)
          ENDIF
        ENDIF
        C(I)=0.0
10    CONTINUE
      CALL TRIDA(1,NP1,A,B,C,D,ALP)
      DO 20 I=1,NP1
        ALP(I)=DMIN1(ALPHIG,DMAX1(ALPLOW,ALP(I)))
        EPS(I)=1.-ALP(I)
20    CONTINUE
      RETURN
C
      ENTRY SWFVOI
C
      DO 30 I=1,NP1
        C(I)=0.0
        IF(I.EQ.1) THEN
          B(I)=ROW(I)*VW(I+1)
          D(I)=RMDW/AREA
        ELSE
          IF(I.EQ.NP1) THEN
```

```
            A(I)=-ROW(I-1)*VW(I)
            B(I)=ROW(I)*VW(I)
            D(I)=0.0
          ELSE
            A(I)=-ROW(I-1)*VW(I)
            B(I)=ROW(I)*VW(I+1)
            D(I)=0.0
          ENDIF
        ENDIF
30    CONTINUE
      CALL TRIDA(1,NP1,A,B,C,D,ALP)
      DO 40 I=1,NP1
        ALP(I)=DMIN1(ALPHIG,DMAX1(ALPLOW,ALP(I)))
        EPS(I)=1.-ALP(I)
40    CONTINUE
      RETURN
      END
```

## REFERENCES


1. Sideman, S., "Direct Contact Heat Transfer Between Immiscible Liquids," Advances in Chemical Engineering, Vol. 6, Academic Press, New York (1966) pp. 207-286.

2. Boehm, R.F., Jacobs, H.R., and Coates, W., "Application of Direct Contact Heat Exchangers to Power Generating Systems Utilizing Geothermal Brines," 9th IECEC Conference Proceedings, Paper 749145 (1974).

3. Jacobs, H.R., "Evaluation and Design Considerations for Liquid-Liquid Direct Contact Heat Exchangers for Geothermal Applications," ASME Paper No. 77-HT-2, (1977).

4. Sheinbaum, I., "Direct Contact Heat Exchangers in Geothermal Power Productions," ASME Paper No. 75-HT-52, (1975).

5. Letan, R. "Design of Particulate Direct Contact Heat Exchanger: Uniform, Countercurrent Flow," ASME Paper No. 76-HT-27, 1976.

6. Garwin, L., and Smith, B.D., "Liquid-Liquid Spray Tower Operation in Heat Transfer," Chemincal Engineering Progress, Vol.49, No. 11 (1953) pp. 591-601.

7. Treybal, R.E., Liquid Extraction, (1st Edition), McGraw Hill, New York (1953).

8. Johnson, A.I., Mirand, G.W., Huang, C.J., Hansuld, J.H., and McNamara, V.M., "Spray-Extraction Tower Studies," AICHE J., Vol. 3, (1957), pp. 101110.

9. Woodward, T., "Heat Transfer in a Spray Column," Chemical Engineering Progress, Vol. 57, (1961), pp. 52-57.

10. Pierce, R.D., Dwyer, O.E., and Martin, J.J., "Heat Transfer and Fluid Dynamics in Mercury-Water Spray Columns," AICHE J. Vol. 5, (1959), pp. 257.

11. Suratt, W.B., and Hart, G.K., "Study and Testing of Direct Contact Heat Exchangers for Geothermal Brines," DDS Engineers, Fort Lauderdale, Florida, ERDA Report No. ORO-4893-1 (January 1977).

12. Plass, S.B., Jacobs, H.R. and Boehm, R.F., "Operational Characteristics of a Spray Column Type Direct Contact Preheater," AICHE Symposium Series No. 189 (1979) pp. 227-234.

13. Spalding, D.B., "The Calculation of Free-convection Phenomena in Gas-Liquid Mixtures," Lecture at ICHMT Seminar, Dubrovnik, Yogoslavia (1976).

14. Spalding D. Brian., "Numerical Computation of Multi-Phase Fluid Flow and Heat Transfer," Recent Advances in Numerical Methods in Fluids, Editors: C. Taylor and K. Morgan, Pineridge Press, Swansea, pp. 139-167.

15. Kurosaki, Y. and Spalding D. Brian, "One-Dimensional Two Phase Flows," 2nd Multi-phase Flow and Heat Transfer Symposium Workship, "Multi-phase Transport: Fundamentals, Reactor Safety, Application," Hemisphere Publishing, Washington, D.C., Vols. 1-5 (1979).

16. Soo, S.L., Fluid Dynamics of Multi-phase Systems, Blaisdell Publishing Company, Waltham, MAsssachusetts (1967).

17. Olander, R., Oshmyansku, S. Nichols, K., and Werner D., "Final Phase Testing and Evaluation of the 500 kWe Direct Contact Pilot Plant at East Mesa ERDA Report DOE/SF/11700-T1, Arvada, Colorado, (December 1983).

18. Riemer, D.H., Jacobs, H.R., Boehm, R.F., and Cook, D.S., "A Computer Program for Determining the Thermodynamic Properties of Light Hydocarbons," University of Utah. DOE Report IDO/1549.3.

19. Riemer, D.H., Jacobs, H.R., Boehm, R.F., "A Computer Program for Determining the Thermodynamic Properties of Water," University of Utah. DOE Report IDO/1549-2. (1976).